

CIVIL ENGINEERING STUDIES
STRUCTURAL RESEARCH SERIES NO. 545

PB89-197040
UILU-ENG-89-2002



ISSN: 0069-4274

EXPERIMENTAL SEISMIC INVESTIGATION OF APPENDAGES IN STRUCTURES

By

D. Segal
and
W. J. Hall

A Technical Report of Research
Supported by the
NATIONAL SCIENCE FOUNDATION
Under Grant Nos. CEE 82-03973 and DFR 84-19191
and
THE DEPARTMENT OF CIVIL ENGINEERING

DEPARTMENT OF CIVIL ENGINEERING
UNIVERSITY OF ILLINOIS
AT URBANA-CHAMPAIGN
URBANA, ILLINOIS

MAY 1989

REPRODUCED BY
U.S. DEPARTMENT OF COMMERCE
NATIONAL TECHNICAL INFORMATION SERVICE
SPRINGFIELD, VA. 22161

REPORT DOCUMENTATION PAGE	1. REPORT NO. UILU-ENG-89-2002	2.	3. Recipient's Accession No. PB89 197040/AS	
4. Title and Subtitle EXPERIMENTAL SEISMIC INVESTIGATION OF APPENDAGES IN STRUCTURES			5. Report Date May 1989	
7. Author(s) D. Segal and W. J. Hall			6.	
9. Performing Organization Name and Address University of Illinois at Urbana-Champaign Department of Civil Engineering 205 N. Mathews Avenue Urbana, Illinois 61801			8. Performing Organization Rept. No. SRS 545	
12. Sponsoring Organization Name and Address National Science Foundation Washington, D.C. 20550			10. Project/Task/Work Unit No.	
			11. Contract(C) or Grant(G) No. (C) (G)	
15. Supplementary Notes			13. Type of Report & Period Covered	
			14.	
<p>16. Abstract (Limit: 200 words) In this study, the behavior of light appendages mounted in structures that respond inelastically to earthquakes was examined experimentally and analytically.</p> <p>A simple interpretation of an elastic detuned appendage is derived. It is shown that the tuned appendage can be considered as a limiting case of the detuned appendage and that the transition can be approximated using the slightly detuned appendage. In the case of a SDOF inelastic supporting structure, the actual structure is replaced by an equivalent linear system. In the case of a MDOF inelastic supporting structure, the concept of modal ductility is used to obtain equivalent linear modes.</p> <p>A series of experiments of SDOF appendages mounted on one- and two-story structures was performed. The combined systems were subjected to earthquake motions. Good agreement was obtained between the measurements and the maximum appendages responses evaluated using the suggested procedure.</p> <p>The main conclusion of this study is that the concepts of equivalent linear system and modal ductility provide a good tool for estimating the maximum response of an appendage mounted on an inelastic supporting structure. The expected accuracy is about the same for elastic and inelastic supporting structures.</p>				
<p>17. Document Analysis a. Descriptors</p> <p>Seismic, Earthquake Resistant Design, Inelastic Systems, Dynamic Response, Secondary Systems, Experimental, Appendages</p> <p>b. Identifiers/Open-Ended Terms</p> <p>c. COSATI Field/Group</p>				
18. Availability Statement Release Unlimited			19. Security Class (This Report) Unclassified	21. No. of Pages 280
			20. Security Class (This Page) Unclassified	22. Price

EXPERIMENTAL SEISMIC INVESTIGATION
OF
APPENDAGES IN STRUCTURES

by
DAVID SEGAL
and
WILLIAM J. HALL

A Report on a Research Project Sponsored by the
NATIONAL SCIENCE FOUNDATION
Under Grant Nos. CEE 82-03973 and DFR 84-19191

and
THE DEPARTMENT OF CIVIL ENGINEERING

Department of Civil Engineering
University of Illinois
Urbana, Illinois
May 1989

ACKNOWLEDGEMENTS

This report was prepared as a doctoral dissertation by Mr. David Segal and was submitted to the Graduate College of the University of Illinois at Urbana-Champaign in partial fulfillment of the requirements for the degree of Doctor of Philosophy in Civil Engineering. The thesis was completed under the supervision of Professor William J. Hall.

The investigation was a part of a research program sponsored by the National Science Foundation under grants CEE 82-03973 "Design Studies in Earthquake Engineering" and DFR 84-19191, "Studies Towards New Seismic Design Approaches." Any findings or recommendations expressed in this dissertation are those of the authors and do not necessarily reflect the views of the National Science Foundation. Support also was received from the Jacob Karol Fellowship in Civil Engineering and the Newmark Fund, both administered by the University of Illinois Foundation.

Acknowledgement is due to the CE Shop employees, under the direction of V. J. McDonald, for making the test specimens and for their technical help.

The experiments were performed at the U.S. Army Corps of Engineers Construction Engineering Research Laboratory, Champaign, Illinois. Use of their equipment is deeply appreciated and the authors acknowledge with gratitude the help of this institution, as well as the strong support and dedicated assistance of Mr. James B. Gambill and Mr. William J. Gordon. Most importantly, the authors acknowledge the assistance of the late Dr. James Prendergast who was responsible for CERL's involvement in this study.

The numerical results and plotting were obtained using the Department of Civil Engineering Harris 800-2 computer as well as Apollo DN3000 and DN4000 computers.

The authors wish to thank Professors D. A. W. Pecknold, A. R. Robinson and M. A. Sozen for their constructive assistance, suggestions and comments. Also the authors are grateful for the contributions provided by Mrs. Susan Warsaw in the preparation of the manuscript.

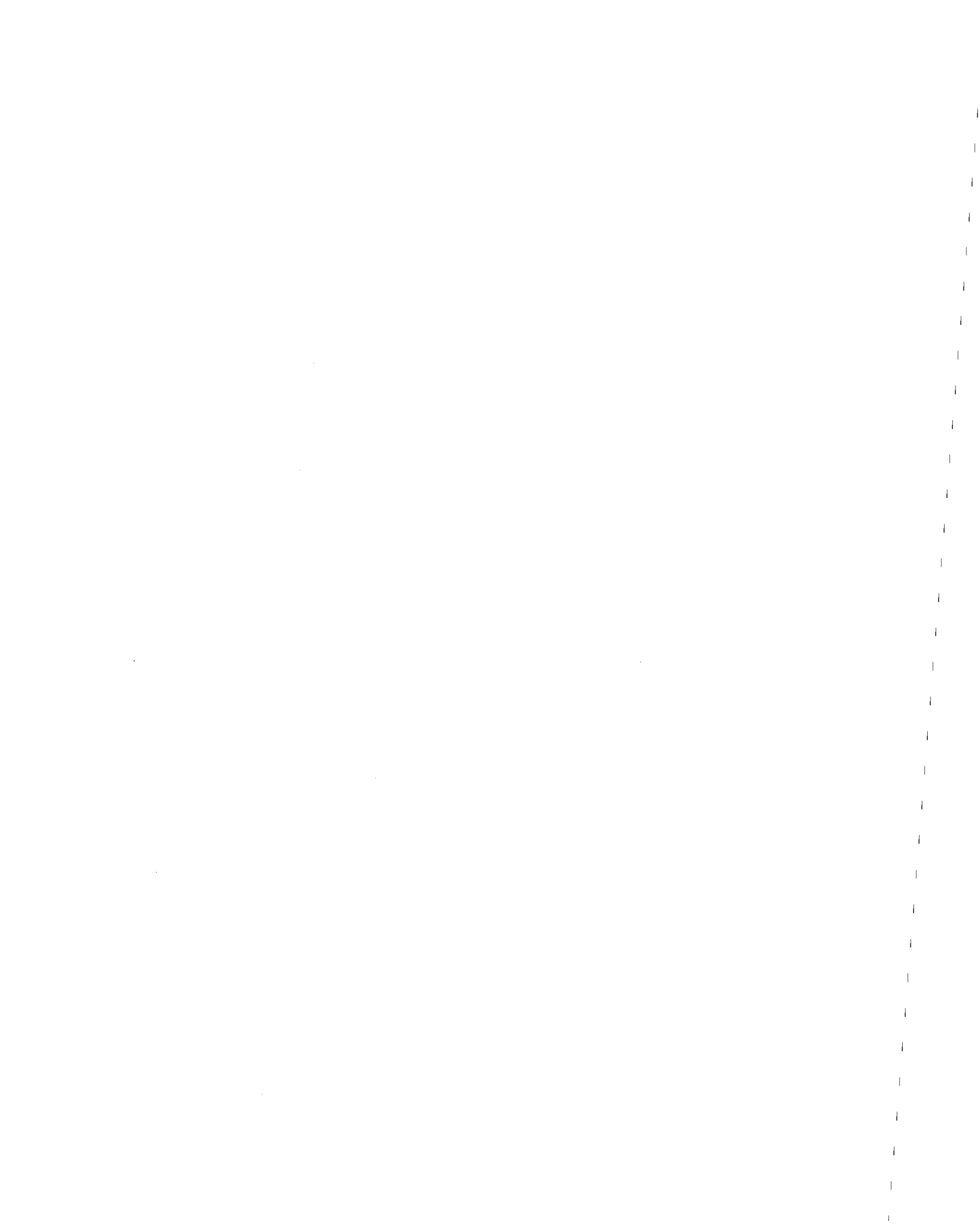


TABLE OF CONTENTS

CHAPTER		Page
1	INTRODUCTION	1
	1.1 Background	1
	1.2 Objectives of Study	3
	1.3 Scope of Work and Organization	4
	1.4 Notation	6
2	REVIEW OF RELATED WORK	12
	2.1 General	12
	2.2 Appendages on Elastic Primary Structures	14
	2.3 Appendages on Inelastic Primary Structures	17
	2.4 Experimental Studies	18
3	ANALYTICAL MODELS	20
	3.1 General	20
	3.2 Appendages on Elastic Primary Structures	20
	3.2.1 Detuned Appendages	20
	3.2.2 Tuned Appendages	31
	3.2.3 Slightly Detuned Appendages	40
	3.2.4 Total Response of an Appendage on a MDOF Structure	47
	3.3 Appendages on Inelastic Structures	48
	3.3.1 General	48
	3.3.2 Definition of Ductility	50
	3.3.3 Equivalent Linear System	51
	3.3.3.1 General	51
	3.3.3.2 SDOF Structures	52
	3.3.3.3 MDOF Structures	57
4	DESCRIPTION OF THE EXPERIMENTS	63
	4.1 Introduction	63
	4.2 Structures and Appendages Tested	63
	4.2.1 General	63
	4.2.2 Single-Story Structures	65
	4.2.2.1 Detuned and Slightly Detuned Systems	65
	4.2.2.2 Tuned Systems	65
	4.2.3 Two-Story Structures	65
	4.2.4 Appendages	65



LIST OF TABLES

Table	Page
3.1 Normalized Expressions for the Maximum Response of a Tuned Appendage	115
4.1 List of the Single-Story Structures	116
4.2 List of the Two-Story Structures	116
4.3 List of the Appendages	117
4.4 List of the Combined Systems Composed of Single-Story Structures and Appendages and the Earthquake Ground Motions Used in the Tests	118
4.5 List of the Combined Systems Composed of Two-Story Structures and Appendages and the Earthquake Ground Motions Used in the Tests	119
5.1 Measured Natural Frequencies, Masses, Stiffnesses and Equivalent Viscous Damping Ratios of the Single-Story Structures	120
5.2 Comparison of Magnifications, Measured and Calculated Using Average Viscous Damping. Elastic Single-Story Structure S1, Natural Frequency 2.89 Hz, Damping 3%, Subjected to Harmonic Excitation	121
5.3 Comparison of Acceleration Amplifications Measured and Calculated Using Average and Scaled Viscous Damping, Elastic Single-Story Structures Subjected to Earthquake Excitation . . .	122
5.4 Comparison of Displacement Amplifications Measured and Calculated Using Average and Scaled Viscous Damping, Elastic Single-Story Structures Subjected to Earthquake Excitation . . .	123
5.5a Calculated Natural Frequencies, Mode Shapes, Modal Masses, Modal Stiffnesses and Modal Viscous Damping Ratios of the Two-Story Structures	124
5.5b Comparison of Measured and Calculated Natural Frequencies and Modal Damping Ratios of the Two-Story Structures	124
5.6 Comparison of Measured and Calculated Responses of the Two-Story Structures Subjected to Earthquake Excitation	125
5.7 Masses, Measured Natural Frequencies, Stiffnesses and Damping Ratios of the Appendages	126

	Page
5.8a Comparison of Measured and Calculated Amplifications of the Decoupled Appendages Subjected to Earthquakes	127
5.8b Comparison of Amplifications Measured and Calculated Using Corrected Natural Frequencies of the Decoupled Appendages Subjected to Earthquakes	127
5.9a Measured Magnification Factors, Ductilities and Dissipated Energies. Inelastic Single-Story Structure S1, Elastic Natural Frequency 2.89 Hz, Elastic Damping 3%, Subjected to Harmonic Excitation	128
5.9b Measured Secant Stiffness, Calculated Equivalent Stiffness and Damping Ratio, and Comparison of the Calculated and Measured Magnifications. Inelastic Single-Story Structure S1, Elastic Natural Frequency 2.89 Hz, Elastic Damping 3%, Subjected to Harmonic Excitation	129
5.10a Comparison of Measured and Calculated Story and Modal Ductilities. Two Story Structure M1, With or Without Appendage, Subjected to El Centro Earthquake	130
5.10b Comparison of Measured and Calculated Story and Modal Ductilities. Two Story Structure M2, With or Without Appendage, Subjected to El Centro Earthquake	131
5.10c Comparison of Measured and Calculated Story and Modal Ductilities. Two Story Structure M1, With or Without Appendage, Subjected to Melendy Earthquake	132
5.11 Exact Undamped and Approximate Undamped Natural Frequencies and Eigenvectors and Measured Natural Frequencies of the Detuned Single-Story Structures with Appendage	133
5.12 Exact Undamped and Tuned Damped Natural Frequencies and Eigenvectors and Measured Natural Frequencies of the Tuned Single-Story Structures with Appendage	134
5.13a Exact Undamped and Approximate Undamped Natural Frequencies and Eigenvectors of the Slightly Detuned Single-Story Structures with Appendage	135
5.13b Approximate Undamped and Tuned Damped Natural Frequencies and Eigenvectors and Measured Natural Frequencies of the Slightly Detuned Single-Story Structures with Appendage	136
5.14 Comparison of Amplifications Determined from Response Spectra of the Equivalent Linear System, from Inelastic Modified Response Spectra and from Measured Floor Response of the Detuned Single-Story Structures with Appendage	137

	Page
5.15a Exact Undamped and Approximate Undamped Natural Frequencies and Eigenvectors and Measured Natural Frequencies of the Two-Story Structure M1 with Appendages AS2 and AS3	140
5.15b Exact Undamped and Approximate Undamped Natural Frequencies and Eigenvectors and Measured Natural Frequencies of the Two-Story Structure M2 with Appendages AS2 and AS3	141



LIST OF FIGURES

Figure	Page
2.1 Decoupled Systems	143
2.2 Combined System	143
3.1 Comparison of Calculated Normalized Amplifications of a Tuned Appendage, $\ddot{x}_{\max}/\ddot{x}_{\zeta}$, as a Function of $\sqrt{\gamma}/2\zeta$	144
3.2 Transfer Functions of a Detuned Appendage (SRSS) and a Slightly Detuned Appendage as a Function of the Frequency Ratio, ω_0/Ω	145
3.3 Transfer Functions of a Detuned Appendage (ABSS) and a Slightly Detuned Appendage as a Function of the Frequency Ratio, ω_0/Ω	146
3.4 Frequency Ratio, ω_0/Ω , at the Boundary Between Tuning and Detuning as a Function of the Mass Ratio, γ	147
3.5 Transfer Function Values at the Boundary Between Tuning and Detuning, Normalized to $\sqrt{\gamma}$ as a Function of the Mass Ratio, γ	147
3.6 Definition of Ductility	148
3.7 Typical Hysteresis Loop and the Ellipse of Equivalent Linear Viscous Damping	149
4.1 Typical Two-Story Structure with an Appendage Mounted on the Second Story	150
4.2 Schematic Layout of the Equipment Used for Data Acquirement	151
4.3 Ground Acceleration Records and Undamped Response Spectra of the Unfiltered and Filtered El Centro Earthquake	152
4.4 Ground Acceleration Records and Undamped Response Spectra of the Unfiltered and Filtered Melendy Earthquake	153
4.5 Ground Acceleration Records and Undamped Response Spectra of the Unfiltered and Filtered Taft Earthquake	154
4.6 Schematic Arrangement of a Static Test	155
5.1 Measured Free Vibrations, Acceleration and Displacement, of the Single-Story Structure S1	156
5.2 Measured Free Vibrations, Acceleration and Displacement, of the Single-Story Structure S4	157

	Page
5.3 Measured Free Vibrations, Acceleration and Displacement, of the Single-Story Structure S7	158
5.4 Measured Free Vibrations Acceleration of the Two-Story Structure M1	159
5.5 Measured Free Vibrations Acceleration of the Two-Story Structure M2	160
5.6 Free Vibrations Modal Acceleration of the Two-Story Structure M1	161
5.7 Free Vibrations Modal Acceleration of the Two-Story Structure M2	162
5.8 Measured Free Vibrations Acceleration of Appendage AS2	163
5.9 Measured Free Vibrations Acceleration of Appendage AL3	163
5.10 Measured Free Vibrations Acceleration of Appendage AS1	164
5.11 Measured Free Vibrations Acceleration of Appendage AT6	164
5.12 Typical Measured Static Force-Displacement Relation of a Single-Story Structure (Structure S1)	165
5.13 Typical Measured Response of a Single-Story Structure (Structure S1) Subjected to Harmonic Ground Motion	165
5.14a Comparison of Measured Amplifications with Amplifications Calculated Using Different Equivalent Linear Systems. Single-Story Structures Subjected to El Centro Earthquake	166
5.14b Comparison of Measured Amplifications with Amplifications Calculated Using Different Equivalent Linear Systems. Single-Story Structure S2 Subjected to El Centro, Melendy and Taft Earthquakes	167
5.15a Comparison of Measured Amplifications with Amplifications Calculated Using Modified Response Spectra. Single-Story Structure S2 Subjected to El Centro Earthquake	168
5.15b Comparison of Measured Amplifications with Amplifications Calculated Using Modified Response Spectra. Single-Story Structure S2 Subjected to El Centro, Melendy and Taft Earthquakes	169
5.16a Typical Measured Response of the First Story of the Two-Story Structure M1 Subjected to El Centro Earthquake	170

	Page
5.16b Typical Measured Response of the Second Story of the Two-Story Structure M1 Subjected to El Centro Earthquake	171
5.17a Typical Measured Response of the First Story of the Two-Story Structure M2 Subjected to El Centro Earthquake	172
5.17b Typical Measured Response of the Second Story of the Two-Story Structure M2 Subjected to El Centro Earthquake	173
5.18a Typical Measured Response of the First Story of the Two-Story Structure M1 Subjected to Melendy Earthquake	174
5.18b Typical Measured Response of the Second Story of the Two-Story Structure M1 Subjected to Melendy Earthquake	175
5.19 Typical Storys Hysteretic Behavior of the Two-Story Structure M1 Subjected to El Centro Earthquake	176
5.20 Typical Storys Hysteretic Behavior of the Two-Story Structure M2 Subjected to El Centro Earthquake	177
5.21 Typical Storys Hysteretic Behavior of the Two-Story Structure M1 Subjected to Melendy Earthquake	178
5.22 Typical Modal Hysteretic Behavior of the Two-Story Structure M1 Subjected to El Centro Earthquake	179
5.23 Typical Modal Hysteretic Behavior of the Two-Story Structure M2 Subjected to El Centro Earthquake	180
5.24 Typical Modal Hysteretic Behavior of the Two-Story Structure M1 Subjected to Melendy Earthquake	181
5.25a Comparison of Measured and Calculated Modal Ductility of Mode 1 of the Structure M1 subjected to El Centro Earthquake	182
5.25b Comparison of Measured and Calculated Modal Ductility of Mode 2 of the Structure M1 subjected to El Centro Earthquake	183
5.26a Comparison of Measured and Calculated Modal Ductility of Mode 1 of the Structure M2 subjected to El Centro Earthquake	184
5.26b Comparison of Measured and Calculated Modal Ductility of Mode 2 of the Structure M2 subjected to El Centro Earthquake	185
5.27a Comparison of Measured and Calculated Modal Ductility of Mode 1 of the Structure M1 subjected to Melendy Earthquake	186
5.27b Comparison of Measured and Calculated Modal Ductility of Mode 2 of the Structure M1 subjected to Melendy Earthquake	187

	Page
5.28 Typical Measured Free Vibrations Accelerations of a Combined Detuned System (Single-Story Structure S4 and Small Appendage AS4)	188
5.29 Typical Measured Free Vibrations Accelerations of a Combined Detuned System (Single-Story Structure S1 and Large Appendage AL3)	189
5.30 Typical Free Vibrations Modal Accelerations of a Combined Detuned System (Single-Story Structure S4 and Small Appendage AS4)	190
5.31 Typical Free Vibrations Modal Accelerations of a Combined Detuned System (Single-Story Structure S1 and Large Appendage AL3)	191
5.32 Typical Measured Free Vibrations Accelerations of a Combined Tuned System with Low Damping (Single-Story Structure S8 and Small Appendage AT2)	192
5.33 Typical Measured Free Vibrations Accelerations of a Combined Tuned System with Low Damping (Single-Story Structure S9 and Large Appendage AT7)	193
5.34 Typical Measured Free Vibrations Accelerations of a Combined Tuned System with High Appendage Damping (Single-Story Structure S8 and Small Appendage AT4)	194
5.35 Typical Measured Free Vibrations Accelerations of a Combined Tuned System with High Appendage and Structure Damping (Single-Story Structure S4 and Small Appendage AT6)	195
5.36 Typical Free Vibrations Modal Accelerations of a Combined Tuned System with Low Damping (Single-Story Structure S8 and Small Appendage AT2)	196
5.37 Typical Free Vibrations Modal Accelerations of a Combined Tuned System with Low Damping (Single-Story Structure S9 and Large Appendage AT7)	197
5.38 Typical Free Vibrations Modal Accelerations of a Combined Tuned System with High Appendage Damping (Single-Story Structure S8 and Small Appendage AT4)	198
5.39 Typical Free Vibrations Modal Accelerations of a Combined Tuned System with High Appendage and Structure Damping (Single-Story Structure S4 and Small Appendage AT6)	199

	Page
5.40 Typical Measured Free Vibrations Accelerations of a Combined Slightly Detuned System (Single-Story Structure S1 with Small Appendage AS2)	200
5.41 Typical Measured Free Vibrations Accelerations of a Combined Slightly Detuned System (Single-Story Structure S1 with Large Appendage AL2)	201
5.42 Typical Free Vibrations Modal Accelerations of a Combined Slightly Detuned System (Single-Story Structure S1 with Small Appendage AS2)	202
5.43 Typical Free Vibrations Modal Accelerations of a Combined Slightly Detuned System (Single-Story Structure S1 with Large Appendage AL2)	203
5.44 Comparison of Measured and Calculated Amplifications of the Detuned Appendages on Structure S1 Subjected to El Centro Earthquake	204
5.45 Comparison of Measured and Calculated Amplifications of the Detuned Appendages on Structure S2 Subjected to El Centro Earthquake	205
5.46 Comparison of Measured and Calculated Amplifications of the Detuned Appendages on Structure S4 Subjected to El Centro Earthquake	206
5.47 Comparison of Measured and Calculated Amplifications of the Detuned Appendages on Structure S5 Subjected to El Centro Earthquake	207
5.48 Comparison of Measured and Calculated Amplifications of the Detuned Appendages on Structure S2 Subjected to Melendy and Taft Earthquakes	208
5.49a Comparison of Measured and Calculated Appendage Normalized Amplifications, $\ddot{x}_{max}/\ddot{x}_G$, for the Single-Story Tuned and Slightly Detuned Systems	209
5.49b Comparison of Measured and Calculated Appendage Normalized Amplifications, $\ddot{x}_{max}/\ddot{x}_G$, of the Single-Story Tuned and Slightly Detuned Systems for Two Earthquakes	210
5.49c Comparison of Measured and Calculated Appendage Normalized Amplifications, $\ddot{x}_{max}/\ddot{x}_G$, of the Single-Story Tuned and Slightly Detuned Systems for Large and Small Appendage Mass . .	211

	Page
5.50 Comparison of Measured and Calculated Appendage Normalized Amplifications, $\ddot{x}_{max}/\ddot{x}_g$, of the Single-Story Tuned and Slightly Detuned Systems for Elastic and Inelastic Behavior of the Supporting Structure	212
5.51 Comparison of Measured and Calculated Appendage Normalized Amplifications, $\ddot{x}_{max}/\ddot{x}_g$, of the Single-Story Tuned and Slightly Detuned Structure After Correction for the Yield Resistance of the Structure	213
5.52 Comparison of Appendage Normalized Amplifications, $\ddot{x}_{max}/\ddot{x}_g$, of the Single-Story Tuned and Slightly Detuned Systems Determined Numerically for the Equivalent Linear Systems and Calculated (Eqs. 3.37, 3.43 and 3.51)	214
5.53 Comparison of Measured and Calculated Appendage Transfer Function of the Single-Story Tuned and Slightly Detuned Systems	215
5.54 Measured Response of a Single-Story Tuned System. Structure S8 and Appendage AT2 Subjected to El Centro Earthquake. Ductility = 1.00	216
5.55 Measured Response of a Single-Story Tuned System. Structure S8 and Appendage AT2 Subjected to El Centro Earthquake. Ductility = 1.10	217
5.56 Measured Response of a Single-Story Tuned System. Structure S8 and Appendage AT2 Subjected to El Centro Earthquake. Ductility = 1.43	218
5.57 Measured Response of a Single-Story Tuned System. Structure S8 and Appendage AT2 Subjected to El Centro Earthquake. Ductility = 2.55	219
5.58 Measured Response of a Single-Story Tuned System. Structure S8 and Appendage AT3 Subjected to Melendy Earthquake. Ductility = 1.08	220
5.59 Measured Response of a Single-Story Tuned System. Structure S8 and Appendage AT3 Subjected to Melendy Earthquake. Ductility = 1.33	221
5.60 Measured Response of a Single-Story Tuned System. Structure S8 and Appendage AT3 Subjected to Melendy Earthquake. Ductility = 1.83	222
5.61 Measured Response of a Single-Story Tuned System. Structure S8 and Appendage AT3 Subjected to Melendy Earthquake. Ductility = 2.76	223

	Page
5.62 Measured Response of a Single-Story Tuned System. Structure S4 and Appendage AT6 Subjected to El Centro Earthquake. Ductility = 1.00	224
5.63 Measured Response of a Single-Story Tuned System. Structure S4 and Appendage AT6 Subjected to El Centro Earthquake. Ductility = 2.30	225
5.64 Measured Response of a Single-Story Tuned System. Structure S4 and Appendage AT6 Subjected to Melendy Earthquake. Ductility = 1.20	226
5.65 Measured Response of a Single-Story Tuned System. Structure S4 and Appendage AT6 Subjected to Melendy Earthquake. Ductility = 3.68	227
5.66 Measured Response of a Single-Story Tuned System. Structure S9 and Appendage AT7 Subjected to El Centro Earthquake. Ductility = 1.00	228
5.67 Measured Response of a Single-Story Tuned System. Structure S9 and Appendage AT7 Subjected to El Centro Earthquake. Ductility = 2.16	229
5.68 Measured Response of a Single-Story Tuned System. Structure S9 and Appendage AT7 Subjected to Melendy Earthquake. Ductility = 1.21	230
5.69 Measured Response of a Single-Story Tuned System. Structure S9 and Appendage AT7 Subjected to Melendy Earthquake. Ductility = 3.18	231
5.70 Typical Measured Free Vibrations Accelerations of the Combined Two-Story Structure M1 and Appendage AS2 Mounted on the Second Story	232
5.71 Typical Measured Free Vibrations Accelerations of the Combined Two-Story Structure M1 and Appendage AS3 Mounted on the First Story	233
5.72 Typical Measured Free Vibrations Accelerations of the Combined Two-Story Structure M1 and Appendage AS3 Mounted on the Second Story	234
5.73 Typical Measured Free Vibrations Accelerations of the Combined Two-Story Structure M2 and Appendage AS2 Mounted on the Second Story	235

	Page
5.74 Typical Measured Free Vibrations Accelerations of the Combined Two-Story Structure M2 and Appendage AS3 Mounted on the First Story	236
5.75 Typical Measured Free Vibrations Accelerations of the Combined Two-Story Structure M2 and Appendage AS3 Mounted on the Second Story	237
5.76 Typical Free Vibrations Modal Accelerations of the Combined Two-Story Structure M1 and Appendage AS2 Mounted on the Second Story	238
5.77 Typical Free Vibrations Modal Accelerations of the Combined Two-Story Structure M1 and Appendage AS3 Mounted on the First Story	239
5.78 Typical Free Vibrations Modal Accelerations of the Combined Two-Story Structure M1 and Appendage AS3 Mounted on the Second Story	240
5.79 Typical Free Vibrations Modal Accelerations of the Combined Two-Story Structure M2 and Appendage AS2 Mounted on the Second Story	241
5.80 Typical Free Vibrations Modal Accelerations of the Combined Two-Story Structure M2 and Appendage AS3 Mounted on the First Story	242
5.81 Typical Free Vibrations Modal Accelerations of the Combined Two-Story Structure M2 and Appendage AS3 Mounted on the Second Story	243
5.82 Comparison of Measured and Calculated Appendage Amplifications. Appendages on Two-Story Structure M1 Subjected to El Centro Earthquake	244
5.83 Comparison of Measured and Calculated Appendage Amplifications. Appendages on Two-Story Structure M2 Subjected to El Centro Earthquake	245
5.84 Comparison of Measured and Calculated Appendage Amplifications. Appendages on Two-Story Structure M1 Subjected to Melendy Earthquake	246
5.85 Measured Response of a Combined System. Appendage AS3 Mounted on the Second Floor of Structure M1 Subjected to El Centro Earthquake. First Story Ductility = 1.00	247

	Page
5.86 Measured Response of a Combined System. Appendage AS3 Mounted on the Second Floor of Structure M1 Subjected to El Centro Earthquake. First Floor Ductility = 8.68	248
5.87 Measured Response of a Combined System. Appendage AS3 Mounted on the Second Floor of Structure M1 Subjected to Melendy Earthquake. First Floor Ductility = 1.00	249
5.88 Measured Response of a Combined System. Appendage AS3 Mounted on the Second Floor of Structure M1 Subjected to Melendy Earthquake. First Floor Ductility = 2.16	250
5.89 Measured Response of a Combined System. Appendage AS2 Mounted on the First Floor of Structure M2 Subjected to El Centro Earthquake. Second Floor Ductility = 1.00	251
5.90 Measured Response of a Combined System. Appendage AS2 Mounted on the First Floor of Structure M2 Subjected to El Centro Earthquake. Second Floor Ductility = 5.52	252
5.91 Measured Response of a Combined System. Appendage AS3 Mounted on the First Floor of Structure M2 Subjected to El Centro Earthquake. Second Floor Ductility = 1.00	253
5.92 Measured Response of a Combined System. Appendage AS3 Mounted on the First Floor of Structure M2 Subjected to El Centro Earthquake. Second Floor Ductility = 5.87	254

CHAPTER 1. INTRODUCTION

1.1 Background

The seismic behavior of appendages mounted on structures has been studied extensively in the past fifteen years, primarily because of the attention focused on equipment response as a part of the seismic resistance of nuclear power plant construction. Most of the work is based on the assumption that both structure and appendage behavior remains linearly elastic. However, during an earthquake, structures (and appendages) can undergo inelastic deformations which may have considerable influence on their response. This influence is a result of the change in the stiffness (and natural frequencies) as well as the energy dissipated during the inelastic excursions.

Inelastic behavior, even when the ductility ratios are small, can reduce the seismic loads transferred to a structure significantly. The inelastic behavior of structures (without appendages) has been studied extensively. Since modal superposition is not valid in the case of inelastic structures, usually motion time-history analyses involving step by step direct integration are performed to calculate the response. For MDOF structures these calculations are costly and modeling can become complicated. Simplified methods have been suggested to avoid these difficulties in estimating nonlinear response (42), (40), (36). Modified Response Spectra to account for inelastic behavior of SDOF systems also have been developed (31), (33). The use of these Modified Spectra to calculate the response of MDOF systems still poses some problems (33), (48), (26).

Although both the response of appendages on elastic primary structures and the inelastic behavior of primary structures were studied extensively, it is only recently that some attention has been given to the seismic response of appendages mounted on inelastic structures. Step-by-step direct integration, using motion time history of decoupled SDOF and MDOF primary systems (18), (7), (41), (24), (25) were reported. In one of these studies (24), (25), some combined systems consisting of a SDOF inelastic primary structure and SDOF elastic appendage also were studied numerically, showing that decoupling would cause overestimating the appendage response. The results of these studies were presented as changes in the floor response spectra computed for the elastic structures. These results show that appendages mounted on inelastic structures are usually subjected to lower seismic loads than those mounted on linear elastic structures, at least over some frequency range. Loading reduction for the appendage is less than for the supporting structure. Slightly higher loads can occur in the case of very flexible appendages (24) and when the appendage is tuned to one of the structure's higher frequencies (7), (41). These results have significance in the design of nuclear power plants where certain damage to the structures can be tolerated, especially if safety related equipment mounted in them remains functional.

However, the studies mentioned earlier are limited in scope and are based only on numerical computations of the decoupled structures. No analytical models or experimental verifications of the behavior of appendages on inelastic primary structures are reported. Therefore no design rules for the general case of an appendage on inelastic structures can be derived from these studies.

Although a large amount of analytical work exists about appendages on elastic primary structures, it is sometimes difficult to understand the physical behavior of detuned and tuned appendages from the results of these studies. Also the ranges in which an appendage should be considered tuned or detuned and the transition from the detuned to the tuned case is not always clear.

Also, almost no information exists about experimental tests of appendages on elastic structures with which the large amount of existing analytical or numerical work could be compared. Only three cases of experimental studies of tuned appendages on elastic supporting structures are reported (39), (19), (27). These studies which are limited in scope will be discussed briefly in Chapter 2.

Clearly, clarification of the points just noted appears needed.

1.2 Objectives of Study

The main objective of this study is to establish a better understanding of the behavior of appendages on inelastic structures by means of tests. Based on existing conventional methods for the analysis of inelastic structures as well as existing conventional methods for the analysis of appendages on elastic structures, a procedure for the design of an appendage on a structures that responds inelastically will be suggested in this study. The complexity of such a process requires making several assumptions and simplifications in the development. The results of the experiments will be used to evaluate the suggested method and to modify it empirically if necessary.

Another objective of this study, is to establish a better understanding of the behavior of appendages on elastic structures by means of simple interpretations that will be compared with previous work and with results of the experiments.

As developed herein, the procedure for the design of appendages on inelastic primary structures will be based on conventional methods. Accordingly, some testing of the response of appendages on elastic primary structures and of the behavior of inelastic primary structures (without appendages) also should be performed. The results of these experiments will be compared with results of the analytical methods that will be used in the development of the method suggested in this study. This comparison will be useful as a reference in the evaluation of the suggested method for appendages on inelastic structures.

1.3 Scope of Work and Organization

In Chapter 2 related work about appendages mounted on elastic and inelastic structures is reviewed and observations that are important for this study are made. The different methods which are in use to calculate the response of an appendage on an elastic primary structure, such as the decoupled and combined models and floor response spectra are briefly discussed and their developments are described. For inelastic primary structures, previous studies involving the numerical generation of inelastic floor response spectra are described.

In Chapter 3 a simple interpretation of a detuned appendage on an elastic primary structure is developed and is shown to be identical to the results of previous studies. This interpretation is extended to the tuned

case and compared with the results of other studies. A transition between the detuned and tuned case, which is based on the slightly detuned case (38), (37) is suggested.

The case of an inelastic primary structure is treated by modeling the structure as an equivalent linear system, which is a function of the ductility. A SDOF structure subjected to harmonic ground motion is considered and insight of the meaning of replacing the actual structure with an equivalent one is obtained. In the case of earthquakes, existing relations (42), (16), (11) are used to estimate the SDOF equivalent linear system. For MDOF primary structures a procedure to estimate modal ductility from local ductilities is suggested and is compared with other studies. Once modal ductilities are obtained equivalent linear modes can be estimated for the use in the calculation of the appendage response.

In Chapter 4 a description of the experiments is presented. The different models, such as single-story structures, two-story structures, and the appendages, are listed and described. The test equipment, including the earthquake simulator and the instrumentation used with the different models, is described and discussed. The ground motions used in this study are given and modifications such as filtering and scaling are described and explained. The tests are divided into three main series: the preliminary tests, tests of appendages on single-story structures and tests of appendages on two-story structures. For each series, the models, the test settings and equipment, the loading, the instrumentation and data collection are described.

In Chapter 5 the results of the experiments are presented and discussed. This chapter is divided into three main sections. First the

preliminary experiments are treated. These include experiments performed to determine the properties of the structures and appendages as well as experiments which were used as reference cases. Such experiments are static inelastic tests of the structures, free vibrations of the decoupled one and two story structures, free vibrations of the decoupled appendages and forced vibrations of the decoupled structures and appendages.

In the second section appendages mounted on the single-story structures are treated. This section includes a test series of tuned and some nearly tuned (slightly detuned) models. Free vibrations and earthquake excitation of the combined systems are discussed.

In the third section appendages mounted on either story of the two-story structures are treated. Free vibrations and earthquake excitation of the combined systems are discussed.

In Chapter 6 a procedure is suggested to estimate the response of appendages on inelastic primary structures, based on the discussion in Chapter 5 and the analytical considerations from Chapter 3.

The results and conclusions are summarized in Chapter 7. The main conclusion is that the response of appendages on inelastic structures can be estimated reasonably using the procedure suggested in this study. The agreement with the results of the experiments is comparable to that obtained in the case of elastic primary structures.

1.4 Notation

All terms are defined where they first appear in the text. The following notation is used in this study:

A maximum ground acceleration

AF	amplification factor
$ A(\Omega) $	Fourier amplitude spectrum at frequency Ω
c_{eq}	equivalent linear viscous damping of an inelastic system
C_{rc}^*	term of the generalized damping matrix (row r and column c)
[C]	damping matrix of the decoupled structure
d_R	detuning parameter from Ref. 37
d_S	detuning parameter from Ref. 38
D	maximum ground displacement
F_d	damping force
k	appendage stiffness
K	stiffness of a SDOF structure
K_i	stiffness of story i of a structure
K_j^*	generalized stiffness of mode j of the decoupled structure
[K]	stiffness matrix of the decoupled structure
[K*]	generalized stiffness matrix of the decoupled structure
$[K_{eq}]$	equivalent linear stiffness matrix of an inelastic MDOF system
m	appendage mass
M	mass of a SDOF structure
MF	magnification factor
M_i	mass of story i of a structure
M_j^*	generalized mass of mode j of the decoupled structure
[M]	mass matrix of the decoupled structure
[M*]	generalized mass matrix of the decoupled structure
R	resistance
R_{max}	maximum resistance
R_j	modal resistance of mode j

$\{R_i^Y\}$	vector of yield resistances of the members (or stories)
R_j^Y	modal yield resistance of mode j
$\{R_y\}$	vector of resistances R_j in the modal coordinates
$\{R_u\}$	vector of resistances in the DOF coordinates
$\{R(\{u\})\}$	vector of resistances in the DOF coordinates
$SA(\Omega, \zeta)$	pseudo-acceleration spectrum at frequency Ω and damping ratio ζ
t	time
t_d	earthquake duration
TF	transfer function defined in Eq. 3.61
u	relative displacement
u_e	elastic portion of the relative displacement
u_{max}	maximum relative displacement
\ddot{u}_g	ground acceleration
$\{u\}$	vector of relative displacements
$\{\dot{u}\}$	vector of relative velocities
$\{\ddot{u}\}$	vector of relative accelerations
$\{U\}$	vector of relative displacement amplitudes
W_d	energy dissipated in one hysteresis loop
\ddot{x}_i	acceleration of DOF i
\ddot{x}_{max}	maximum absolute appendage acceleration
\ddot{x}_ζ	reference maximum absolute appendage acceleration (Eq. 3.44)
$\{\ddot{x}\}$	vector of absolute accelerations
y_j	displacement of mode j
\ddot{y}_j	acceleration of mode j
y_j^Y	yield displacement of mode j

Y_j	amplitude of mode j
$\{y\}$	vector of the displacements y_j in the normal coordinates
$\{y^Y\}$	vector of yield displacements y_j^Y in the normal coordinates
$\{Y\}$	vector of amplitudes Y_j in the normal coordinates
α	empirical constant
γ	mass ratio
γ_m	modal mass ratio of mode m
$\gamma_R^\#$	equivalent mass ratio of a slightly detuned appendage, Ref. 37
$\gamma_S^\#$	equivalent mass ratio of a slightly detuned appendage, Ref. 38
Γ_j	participation factor of mode j of the decoupled structure
Γ_{Cj}	participation factor of a mode of the detuned combined system, when the frequency is equal to a frequency of the structure
Γ_{C0}	participation factor of a mode of the detuned combined system, when the frequency is equal to the frequency of the appendage
δ	constant defined in Eq. 3.49
ζ	damping ratio, damping ratio of a SDOF structure
ζ_{e1}	elastic viscous damping ratio
ζ_{eq}	equivalent linear viscous damping ratio of an inelastic system
ζ_{eq}^E	equivalent linear viscous damping ratio of an inelastic system for earthquake excitation
ζ_{eq}^H	equivalent linear viscous damping ratio of an inelastic system for harmonic ground motion
ζ_j	damping ratio of mode j of the decoupled structure
ζ_0	damping ratio of the decoupled appendage
ζ_B	beat envelope damping ratio

η	coefficient of hysteretic energy for curved force-deformation relation
κ	coefficient defined in Eq. 3.40
μ	ductility
μ_1	story (or member) ductility
μ_j	modal ductility of mode j
ϕ_{ij}	modal displacement of the decoupled structure, DOF i and mode j
ϕ_{0j}	modal displacement of the appendage in a mode of the combined detuned system
ϕ_{i0}	modal displacement of DOF i of the structure in a mode of the combined detuned system
$\{\phi_j\}$	mode shape j of the decoupled structure
$\{\phi_{Cj}\}$	mode shape of the combined system, when the frequency is equal to a frequency of the structure
$\{\phi_{C0}\}$	mode shape of the combined system, when the frequency is equal to the frequency of the appendage
$[\phi_{ij}]$	modal matrix of the decoupled structure
ω	tuning frequency
ω_0	natural frequency of the decoupled SDOF appendage
ω_1	lower natural frequency of the combined tuned system
ω_2	higher natural frequency of the combined tuned system
ω_{C0}	natural frequency of the detuned combined system, when the frequency is equal to the frequency of the appendage
ω_B	beat frequency of the damped combined system
$\omega_R^\#$	equivalent tuning frequency of a slightly detuned appendage, Ref. 37
$\omega_S^\#$	equivalent tuning frequency of a slightly detuned appendage, Ref. 38
$\Delta\omega$	beat frequency of the undamped combined system
Ω	natural frequency of a decoupled SDOF structure

- Ω_j natural frequency of the decoupled MDOF structure in mode j
- Ω_H harmonic forcing frequency
- Ω_{Cj} natural frequency of the detuned combined system,
when the frequency is equal to a frequency of the structure
- Ω_{eq}^E equivalent linear frequency of an inelastic system for
earthquake excitation
- Ω_{eq}^H equivalent linear frequency of an inelastic system for
harmonic ground motion

CHAPTER 2. REVIEW OF RELATED WORK

2.1 General

Over the years there have evolved, especially in connection with nuclear power plant design (1), (2), various approaches for designing appendages mounted in structures. In most cases it is assumed that both the appendage and the supporting structure are linearly elastic and one of the following analysis methods is normally used:

Decoupled models employing motion time history analysis (Figure 3.1)
The decoupled structure is subjected to the ground motion and the response at the point of attachment of the appendage as a function of time (time history) is obtained by a numerical solution of the equations of motion, either directly or by using modal superposition. Interaction between structure and appendage is usually neglected, under the assumption that the mass of the appendage is small. The appendage is then subjected to the motions calculated at the point of support. Neglect of interaction can lead to overestimating the appendage response, particularly in the case where the appendage is tuned or slightly detuned to one or more frequencies of the structure (53), (37).

Combined Model employing motion time history analysis (Figure 3.2)
The structure and appendage are included in a combined model, so that the interaction between the primary and the secondary systems is included in the analysis. This model is subjected to the ground motion and the response as a function of time is calculated usually by the method of modal superposition. Numerical difficulties may arise from the large differences in the elements of the mass and stiffness matrices, and

different damping ratios may lead to nonproportional damping. In the case of MDOF appendages on MDOF structures, the use of this method can become complicated and costly.

As a result of these difficulties, as well as the fact that the structure and appendage are designed separately, this method is seldom used in practice. The method is often considered as an exact solution and used for comparison with other methods. Recently, methods were suggested to evaluate the frequencies and mode shapes of the combined system from those of the decoupled structure and appendage, so that some of the numerical difficulties mentioned earlier could be avoided (29), (53), (37), (9), (15).

Floor response spectra -- Since the ground motion during an earthquake cannot be predicted exactly, several analyses using several different ground motions are needed when the appendage response is estimated by the decoupled or combined model. In order to avoid the need for several analyses, floor response spectra, which are plots of the maximum response of the appendage as a function of its natural frequency and damping, were developed.

Floor response spectra for the point of attachment in the structure are calculated from time-histories of ground motions or directly from the response spectra (17), (34), (39), (10). Interaction between structure and appendage is usually neglected but recently the effects of interaction, tuning and nonproportional damping also have been studied (29), (39), (53), (37).

In normal practice, floor response spectra for several earthquakes are calculated, averaged, smoothed and the peaks are widened to give floor

response spectra for the design (floor design spectra). The maximum response of the appendage is estimated from one computation involving modal analysis and response summation which replaces several computations involving step by step time integration. However, only the maximum response can be obtained.

The main difficulty in the development of floor response spectra is in the determination of the amplification of the resonant case, i.e., when the appendage is tuned or slightly detuned to a frequency of the structure.

2.2 Appendages on Elastic Primary Structures

The development of analysis methods which include interaction of appendages and elastic structures is reviewed here briefly. The purpose of this presentation is to point out some common properties that will be used in this study. Some of the references will be discussed in detail in other chapters, where they are related to the analytical model or experiments.

Biggs (4), (5) suggested estimating the amplification as a weighted Square Root of the Sum of the Squares (SRSS) of the amplification factors of each appendage normal mode with each structural normal mode. For the detuned case these amplification factors were determined assuming that the input to the appendage consists of harmonic components of the ground motion at the appendage frequency, amplified by the damped structure. For the tuned and slightly detuned case these amplification factors are determined numerically as a function of the ratio of the periods of the appendage and the structure.

Newmark (32) and Nakhata, Newmark and Hall (29), suggested a procedure to approximate the normal modes and natural frequencies of the combined system, assuming that the significant input to the appendage consists of a series of harmonic components. Amplification factors for each nonresonant appendage normal mode with each structural normal mode are calculated. Amplification for the resonant case is approximated semi-empirically as a function of the effective mass ratio and appendage damping. The total amplification is estimated by the Absolute Sum (ABSS) rule.

Villaverde and Newmark (53) developed a procedure to calculate the natural frequencies and normal modes of the combined system by decoupling the structure and appendage and applying the interaction force on both. The frequencies of the resonant case are approximated from a reduced eigenvalue problem, where only the two modes of the decoupled systems whose frequencies are close are taken into account. For the nonresonant cases the frequencies of the combined and decoupled systems are approximately the same. The eigenvectors of the combined system are calculated as linear combinations of the eigenvectors of the decoupled systems, using results derived in the first step. Then the response and amplification of the appendage can be calculated, using response spectra and the SRSS rule. The procedure was expanded to include nonproportional damping and two points of attachment.

Ruzicka and Robinson (37) used an undamped 2-DOF system to study the case where the appendage is tuned or slightly detuned to one frequency of the structure. The solution could be simplified due to the small mass and stiffness ratios and approximations were obtained for the frequencies and

mode shapes of the combined system. Two closely spaced frequencies were obtained and the free vibrations were characterized by a beat phenomenon. The response of the appendage to ground motion was obtained using Duhamel's Integral and also was characterized by the presence of beats. The appendage maximum response was then estimated, assuming that it occurs after the earthquake (short ground motion) and then extended for long ground motions. The method was then expanded to include proportionally and nonproportionally damped systems (using frequency domain analysis). Finally the method was expanded to include MDOF appendages on MDOF structures, including the response of the detuned modes.

An independent parallel study was conducted at the University of California at Berkeley by Sackman and Kelly (38), (39) and Der Kiureghian et al. (9), (8). In this study frequency domain analysis and Laplace transforms were used instead of the modal analysis procedure used in the study conducted at the University of Illinois. The results of the two studies are generally similar.

Random vibration techniques were utilized by Singh (43), (44), (45), (46) for the construction of Floor Response Spectra.

All these methods show some important common properties that will be used in this study, namely the following: the amplification of each mode of the appendage with each mode of the structure is calculated, a summation of these amplifications is performed usually by the SRSS rule, and the nonresonant case is usually simple in form (decoupled). Some problems are associated with the resonant case that require certain assumptions concerning the earthquake and/or some approximations associated with the small mass of the appendage.

2.3 Appendages on Inelastic Primary Structures

Kawakatsu et al. (18) used motion time-history step by step direct integration to calculate the response at different locations of a decoupled inelastic MDOF primary structure. Two earthquake records were used in this study. The results were used to generate floor response spectra that were compared with floor response spectra calculated for the elastic structure. These results show that appendages on inelastic structures are subjected to lower seismic loads than appendages on elastic structures when they are tuned to the fundamental frequency of the structure. Higher seismic loads can exist in the higher frequencies.

Coats (7) reports a similar study with similar results.

Sewell et al. (41) conducted an extensive numerical study, calculating the response at different locations of a decoupled MDOF primary structure. The influence of several parameters was investigated and included such items as the integration method, ground motion and structural properties (number of DOF, damping, hysteresis type, ductility) but yielding was restricted to one location in the structure. Again, the results show lower seismic loads for appendages tuned to the fundamental frequency of the structure. In higher frequencies, seismic loads can be lower or higher and the dependence on the different parameters is not always clear. Higher seismic loads also can occur in lower frequencies.

Lin and Mahin (24), (25) used motion time-history step by step direct integration to calculate the response of decoupled SDOF inelastic primary structures. Ten earthquake records and two types of hysteretic models were used in the analysis. Floor response spectra were generated and were compared with floor response spectra calculated for the elastic primary

structure. The results show lower seismic loads when the appendage is tuned or has a higher frequency than the structure. Slightly higher seismic loads can occur in lower frequencies. The influence of interaction between structure and appendage was studied by analyzing some cases of tuned combined systems, also using step-by-step direct integration. The results show that floor response spectra based on decoupled structures will overestimate the appendage response.

These studies are limited in scope and illustrate certain tendencies of behavior. Prediction of the response of the general case of an appendage mounted on inelastic structures cannot yet be derived from the results as published.

2.4 Experimental Studies

Sackman and Kelly (39) tested tuned light appendages mounted on an elastic three-story structure that was subjected to three different earthquakes. The results were used qualitatively to suggest a summation rule for the appendage maximum responses in the detuned and tuned modes.

Kelly (19) tested tuned light appendages that were mounted on an elastic five-story base-isolated structure and was subjected to three different earthquakes. The results were used to study the effect of three different base-isolation systems on structure and appendage response.

Manolis et. al (27) tested two detuned and two tuned appendages that were mounted on an elastic three-story structure and subjected to white noise and one earthquake. The results were used for system identification and were compared with numerical analyses.

These studies are limited in scope and cannot be considered as a systematic comparison of the theory with experimental results.

CHAPTER 3. ANALYTICAL MODELS

3.1 General

In this chapter, two analytical models are developed. In Section 3.2 the case of a light appendage on elastic structure is treated first. Since a large amount of analytical work already exists, emphasis is placed on simple interpretations of the behavior of detuned and tuned appendages, the transition between the detuned and the tuned case, and estimates of upper and lower bounds. A comparison of the results with previous studies gives insight into the behavior of appendages. The case of an inelastic primary structure is studied in Section 3.3. The idea is to replace the inelastic structure by an equivalent linear elastic system and estimate the appendage maximum response using procedures for an appendage on an elastic structure. The method is developed for a SDOF supporting structure and then extended for a MDOF supporting structure.

3.2 Appendages on Elastic Primary Structures3.2.1 Detuned Appendages

An appendage is detuned when its natural frequency is neither equal to nor close to a frequency of the structure. The range where an appendage should be considered detuned is discussed in Section 3.2.3. In this section a simple interpretation of the behavior of a detuned appendage is suggested and the results compared with those of other studies.

Previous studies of detuned light appendages on elastic structures, show that the natural frequencies of the combined system are approximately

equal to the natural frequencies of the decoupled structure and appendage (29), (38), (53), (37). The fact that the frequencies remain unchanged means that when either structure or appendage vibrates at one of its own natural frequencies, it applies a harmonic disturbance to the other system which vibrates at the same frequency but with negligible feedback. To see this behavior the following assumptions are made:

- I) When the circular frequency Ω_{c_j} of the combined system is equal to a frequency Ω_j of the structure, the mode shape of the combined system is composed of the unchanged mode shape of the structure and the deformed shape of the appendage subjected to the harmonic motions of its supports in the structure.

- II) When the circular frequency ω_{c_0} of the combined system is equal to a frequency ω_0 of the appendage, the mode shape of the combined system is composed of the unchanged mode shape of the appendage and the deformed shape of the structure subjected to the harmonic forces applied by the appendage at its supports.

Since this study deals with SDOF appendages, for simplicity only the case of a SDOF appendage mounted on one location (degree of freedom k) in a MDOF structure (with n DOF's) will be treated here. However, the same procedure can apply to MDOF multiply supported appendages.

Case I) $\Omega_{Cj} = \Omega_j$

The mode shape $\{\phi_{Cj}\}$ of the combined system is

$$\{\phi_{Cj}\} = \begin{Bmatrix} \phi_{1j} \\ \phi_{2j} \\ \vdots \\ \phi_{kj} \\ \vdots \\ \phi_{nj} \\ \phi_{0j} \end{Bmatrix}, \quad (3.1)$$

in which ϕ_{ij} is the displacement of DOF i in mode j of the decoupled structure and ϕ_{0j} is the displacement of the appendage (as yet unknown).

The maximum absolute displacement response ϕ_{0j} of the decoupled undamped SDOF appendage subjected to the harmonic base motion $\phi_{kj} \sin \Omega_j t$, where t is the time, is equal to (6)

$$\phi_{0j} = \phi_{kj} \frac{1}{1 - \left(\frac{\Omega_j}{\omega_0}\right)^2} = \frac{\omega_0^2}{\omega_0^2 - \Omega_j^2} \phi_{kj} \quad (3.2)$$

Substitution of Eq. 3.2 into Eq. 3.1 gives:

$$\{\phi_{Cj}\} = \begin{Bmatrix} \phi_{1j} \\ \phi_{2j} \\ \vdots \\ \phi_{kj} \\ \vdots \\ \phi_{nj} \\ \frac{\omega_0^2}{\omega_0^2 - \Omega_j^2} \phi_{kj} \end{Bmatrix} \quad (3.3)$$

Case II) $\omega_{c0} = \omega_0$

The mode shape $\{\phi_{c0}\}$ of the combined system is

$$\{\phi_{c0}\} = \begin{Bmatrix} \phi_{10} \\ \phi_{20} \\ \vdots \\ \phi_{k0} \\ \vdots \\ \phi_{n0} \\ 1 \end{Bmatrix} = \begin{Bmatrix} \left\{ \begin{matrix} \vdots \\ U \\ \vdots \end{matrix} \right\} \\ 1 \end{Bmatrix}, \quad (3.4)$$

in which ϕ_{i0} is the displacement of the structure DOF i (yet unknown) and $\{U\}$ is the vector of the unknown relative displacement amplitudes ϕ_{i0} , where $i=1,2,\dots,n$.

The appendage with mass m , vibrating with a displacement amplitude of 1, applies a harmonic force $m\omega_0^2 \sin\omega_0 t$ to the structure at the point of support k . The equation of motion of the decoupled undamped MDOF structure subjected to this harmonic force is given by

$$[M]\{\ddot{u}\} + [K]\{u\} = \begin{Bmatrix} 0 \\ 0 \\ \vdots \\ 0 \\ 1 \\ 0 \\ \vdots \\ 0 \end{Bmatrix} m\omega_0^2 \sin\omega_0 t, \quad (3.5)$$

in which:

$\{u\}$ is the vector of unknown displacements

$\{\ddot{u}\}$ is the vector of unknown accelerations

$[M]$ is the mass matrix of the decoupled structure

$[K]$ is the stiffness matrix of the decoupled structure.

Using the transformation

$$\{u\} = [\Phi_{i,j}]\{y\} \quad , \quad (3.6)$$

assuming harmonic response of the structure

$$\{u\} = \{U\}\sin\omega_0 t \quad (3.7a)$$

$$\{y\} = \{Y\}\sin\omega_0 t \quad , \quad (3.7b)$$

in which:

$[\Phi_{i,j}]$ is the modal matrix of the structure (DOF i and mode j)

$\{y\}$ is the vector of displacements in the normal coordinates

$\{Y\}$ is the vector of the amplitudes Y_j in the normal coordinates

and premultiplying both sides by $[\Phi_{i,j}]^T$, Eq. 3.5 becomes

$$-[\Phi_{i,j}]^T [M] [\Phi_{i,j}] \{Y\} \omega_0^2 \sin\omega_0 t + [\Phi_{i,j}]^T [K] [\Phi_{i,j}] \{Y\} \sin\omega_0 t - [\Phi_{i,j}]^T \begin{Bmatrix} 0 \\ 0 \\ \vdots \\ 0 \\ 1 \\ 0 \\ \vdots \\ 0 \end{Bmatrix} m\omega_0^2 \sin\omega_0 t \quad (3.8)$$

or

$$\left[-[M^*] \omega_0^2 + [K^*] \right] \{Y\} = m\omega_0^2 \begin{Bmatrix} \phi_{k1} \\ \phi_{k2} \\ \vdots \\ \vdots \\ \vdots \\ \vdots \\ \phi_{kn} \end{Bmatrix} \quad , \quad (3.9a)$$

in which:

$$[M^*] = [\Phi_{i,j}]^T [M] [\Phi_{i,j}] \quad (3.9b)$$

$$[K^*] = [\Phi_{i,j}]^T [K] [\Phi_{i,j}] \quad (3.9c)$$

are respectively, the diagonal generalized mass and stiffness matrices of the decoupled structure.

Equation 3.9a can be uncoupled to obtain

$$\left[-\omega_0^2 M_j^* + K_j^* \right] Y_j = m \omega_0^2 \phi_{kj} \quad , \quad (3.10)$$

in which M_j^* and K_j^* are respectively, the generalized mass and stiffness of mode j of the decoupled structure (terms of the diagonal matrices $[M^*]$ and $[K^*]$).

Solving for the amplitudes gives

$$Y_j = \left(\frac{m}{M_j^*} \right) \left(\frac{\omega_0^2}{\Omega_j^2 - \omega_0^2} \right) \phi_{kj} \quad . \quad (3.11)$$

Equation 3.6 can be written in the form

$$\{U\} = \sum_{j=1}^n \{\phi_j\} Y_j \quad (3.12)$$

in which $\{\phi_j\}$ is a mode shape of the decoupled structure, $j = 1, 2, \dots, n$.

Substitution of Eq. 3.11 into Eq. 3.12 gives

$$\{U\} = \sum_{j=1}^n \left(\frac{m}{M_j^*} \right) \left(\frac{\omega_0^2}{\Omega_j^2 - \omega_0^2} \right) \phi_{kj} \{\phi_j\} \quad (3.13)$$

and after substitution of Eq. 3.13 into Eq. 3.4, the eigenvector becomes

$$\{\phi_{C0}\} = \left\{ \begin{array}{c} \sum_{j=1}^n \left(\frac{m}{M_j^*} \right) \left(\frac{\omega_0^2}{\Omega_j^2 - \omega_0^2} \right) \phi_{kj} \phi_{1j} \\ \sum_{j=1}^n \left(\frac{m}{M_j^*} \right) \left(\frac{\omega_0^2}{\Omega_j^2 - \omega_0^2} \right) \phi_{kj} \phi_{2j} \\ \cdot \\ \cdot \\ \sum_{j=1}^n \left(\frac{m}{M_j^*} \right) \left(\frac{\omega_0^2}{\Omega_j^2 - \omega_0^2} \right) \phi_{kj} \phi_{nj} \\ 1 \end{array} \right\} \quad (3.14)$$

The participation factors of the combined system can now be calculated for the two cases:

Case I) $\Omega_{Cj} = \Omega_j$

$$\Gamma_{Cj} = \frac{\sum_{i=1}^n \phi_{ij} M_i + \left(\frac{\omega_0^2}{\omega_0^2 - \Omega_j^2} \phi_{kj} \right) m}{\sum_{i=1}^n \phi_{ij}^2 M_i + \left(\frac{\omega_0^2}{\omega_0^2 - \Omega_j^2} \phi_{ki} \right)^2 m} \quad (3.15)$$

The terms containing the appendage mass m are small compared to the summations and will be neglected in both the numerator and denominator.

Equation 3.15 becomes

$$\Gamma_{Cj} = \frac{\sum_{i=1}^n \phi_{ij} M_i}{\sum_{i=1}^n \phi_{ij}^2 M_i} = \frac{\sum_{i=1}^n \phi_{ij} M_i}{M_j^*} = \Gamma_j \quad (3.16)$$

The participation factors, Γ_{Cj} , of the combined system are, in this case, approximately the same as the participation factors, Γ_j , of the decoupled structure.

Case II) $\omega_{C0} = \omega_0$

$$\Gamma_{C0} = \frac{\sum_{i=1}^n \left\{ M_i \left[\sum_{j=1}^n \frac{m}{M_j^*} \frac{\omega_0^2}{\Omega_j^2 - \omega_0^2} \phi_{kj} \phi_{ij} \right] \right\} + m}{\sum_{i=1}^n \left\{ M_i \left[\sum_{j=1}^n \frac{m}{M_j^*} \frac{\omega_0^2}{\Omega_j^2 - \omega_0^2} \phi_{kj} \phi_{ij} \right]^2 \right\} + m} \quad (3.17)$$

Using the orthogonality of the modes of the decoupled structure in the denominator, Equation 3.17 can be rewritten as

$$\Gamma_{C0} = \frac{\sum_{j=1}^n \left\{ \frac{\omega_0^2}{\Omega_j^2 - \omega_0^2} \phi_{kj} \frac{\sum_{i=1}^n M_i \phi_{ij}}{M_j^*} \right\} + 1}{\sum_{j=1}^n \left\{ \frac{m}{M_j^*} \left[\frac{\omega_0^2}{\Omega_j^2 - \omega_0^2} \phi_{kj} \right]^2 \frac{\sum_{i=1}^n M_i \phi_{ij}^2}{M_j^*} \right\} + 1} \quad (3.18)$$

The summation containing the small mass m of the appendage in the denominator will now be neglected. Each term of this summation contains three factors. The first factor (mass ratio) becomes very small for low Ω_j ; the second becomes very small for high Ω_j ; and the third is equal to unity.

Substitution of Eq. 3.16 into Eq. 3.18 gives

$$\Gamma_{c0} = 1 + \sum_{j=1}^n \frac{\omega_0^2}{\Omega_j^2 - \omega_0^2} \Gamma_j \phi_{kj} \quad (3.19)$$

Using the SRSS rule, the maximum absolute acceleration response of a detuned appendage \ddot{x}_{max} can be estimated as:

$$\ddot{x}_{max} = \left\{ \sum_{j=1}^n \left[\frac{\omega_0^2}{\omega_0^2 - \Omega_j^2} \Gamma_j \phi_{kj} SA(\Omega_j, \zeta_j) \right]^2 + \left[\left(1 + \sum_{j=1}^n \frac{\omega_0^2}{\Omega_j^2 - \omega_0^2} \Gamma_j \phi_{kj} \right) SA(\omega_0, \zeta_0) \right]^2 \right\}^{\frac{1}{2}}, \quad (3.20)$$

in which $SA(\Omega_j, \zeta_j)$ is the acceleration response spectrum at frequency Ω_j and damping ratio ζ_j of the decoupled structure and $SA(\omega_0, \zeta_0)$ is the acceleration response spectrum at frequency ω_0 and damping ratio ζ_0 of the decoupled appendage.

The results will now be compared with other studies.

Using frequency domain and Laplace Transforms to solve the equations of motion directly and dropping negligible terms associated with the small mass, Sackman and Kelly (38) obtained the following expression for the maximum acceleration response of a detuned SDOF appendage with a single support, on a MDOF structure:

$$\ddot{x}_{\max} = \left\{ \sum_{j=1}^n \left[\frac{\omega_0^2}{\omega_0^2 - \Omega_j^2} \Gamma_j \phi_{kj} SA(\Omega_j, \zeta_j) \right]^2 + \left[\left(\sum_{j=1}^n \frac{\Omega_j^2}{\Omega_j^2 - \omega_0^2} \Gamma_j \phi_{kj} \right) SA(\omega_0, \zeta_0) \right]^2 \right\}^{\frac{1}{2}} \quad (3.21)$$

It is possible to show that Eqs 3.20 and 3.21 are identical.

Using the equality $\sum_{j=1}^n \Gamma_j \phi_{kj} = 1$, the second term of Eq. 3.20 becomes

$$\left(\sum_{j=1}^n \Gamma_j \phi_{kj} + \sum_{j=1}^n \frac{\omega_0^2}{\Omega_j^2 - \omega_0^2} \Gamma_j \phi_{kj} \right) SA(\omega_0, \zeta_0) \quad (3.22)$$

and after combining the terms into a single summation

$$\left(\sum_{j=1}^n \frac{\Omega_j^2}{\Omega_j^2 - \omega_0^2} \Gamma_j \phi_{kj} \right) SA(\omega_0, \zeta_0) \quad (3.23)$$

which is the second term in Eq. 3.21. In the following Eq. 3.21 will be used instead of Eq. 3.20.

In the case of SDOF detuned appendage on a SDOF structure, Eq. 3.21 becomes

$$\ddot{x}_{\max} = \left\{ \left[\frac{\omega_0^2}{\omega_0^2 - \Omega^2} SA(\Omega, \zeta) \right]^2 + \left[\frac{\Omega^2}{\Omega^2 - \omega_0^2} SA(\omega_0, \zeta_0) \right]^2 \right\}^{\frac{1}{2}} \quad (3.24)$$

in which Ω and ζ are the frequency and damping ratio of the SDOF decoupled structure, respectively.

The two terms in Eq. 3.24 are symmetrical. Since the first is the result of a structure with a frequency Ω driving an appendage with a frequency ω_0 , the second can be interpreted as the result of a structure

with a frequency ω_0 driving an appendage with a frequency Ω . This observation will be useful in the interpretation of the tuned case.

Using time domain solution of the equations of motion and also dropping negligible terms associated with the small appendage mass, Ruzicka and Robinson (37) obtained an expression for the displacements relative to the ground, of a detuned MDOF appendage multiply supported on a MDOF structure (Eq. 199 in Ref. 37). It is possible to bring their expression to a form similar to Eq. 3.21, assuming a SDOF appendage and a single support. With recognition that the two integrals in their expression are the relative displacement responses of damped SDOF systems, the maximum responses can be estimated from the displacement response spectra. Using the SRSS rule, an expression similar to Eq. 3.21 but for displacements relative to the ground, is obtained.

It is also interesting to compare the expressions obtained by Villaverde and Newmark (53) for the relative displacements (distortions) of a detuned MDOF appendage with a single support on a MDOF structure (Eqs. 3.42 to 3.45 in Ref. 53). These expressions were obtained by modal analysis and compatibility conditions at the support of the appendage. Assuming a SDOF appendage, these expressions also can be brought to a form similar to Eq. 3.21, by making the same assumption that led from Eq. 3.18 to Eq. 3.19. After some manipulations and the use of the SRSS rule, an equation for displacements relative to the ground, which is similar to Eq. 3.21, is obtained.

From these comparisons it is concluded that the simple interpretation suggested in this study leads to response estimates of detuned appendages that are identical to the results obtained using different, usually more

involved, approaches. A better understanding of the physical behavior of detuned appendages is obtained, namely that each of the decoupled systems vibrates in its own natural frequencies and forces the other system to vibrate in the same frequencies with negligible feedback. This behavior was confirmed from observations that were made during the free vibrations experiments of the combined structure-appendage systems (Sections 5.2.1 and 5.3.1).

3.2.2 Tuned Appendages

An appendage is tuned when its natural frequency is equal (or close) to a frequency of the structure. The range of a tuned (or nearly tuned) appendage is discussed in Section 3.2.3. In this section the simple interpretation of the detuned case from Section 3.2.1, is extended to the tuned case and the results compared with those of previous studies.

An approximate solution of the response of a tuned (or slightly detuned) appendage is presented by Ruzicka and Robinson (37). Their solution is based on the equation of motion of the undamped 2DOF tuned structure-appendage system, assuming that the mass of the appendage is small and characterized by the mass ratio

$$\gamma = \frac{m}{M} = \frac{k}{K} \ll 1 \quad (3.25)$$

in which m and k are the appendage mass and stiffness and M and K are the structure mass and stiffness. These mass and stiffness terms are related by:

$$\frac{K}{M} = \frac{k}{m} = \omega^2 \quad (3.26)$$

in which ω is the tuning circular frequency.

The eigenvalue problem of the 2-DOF system was solved and small terms resulting from powers of γ were neglected to obtain approximate eigenvalues. Two close frequencies ω_1 and ω_2 were obtained (Ruzicka1980):

$$\omega_1 \approx \omega \left(1 - \frac{\sqrt{\gamma}}{2} \right) = \omega - \Delta\omega \quad (3.27a)$$

$$\omega_2 \approx \omega \left(1 + \frac{\sqrt{\gamma}}{2} \right) = \omega + \Delta\omega \quad (3.27b)$$

and the free vibrations of the combined system were characterized by a beat with frequency $\Delta\omega$.

The same approximate results were obtained by Sackman and Kelly (38) who used time domain solution and Laplace Transforms to solve the equations of motion directly; and by Villaverde and Newmark (53) who used modal analysis and compatibility conditions at the support of the appendage.

The fact that two distinct frequencies were obtained suggests that the response of the tuned case could be estimated as a limiting case of the detuned case. However, since small differences in the eigenvalues are associated with large differences in the eigenvectors, it is not expected that the procedure used in Section 3.2.1 to calculate the eigenvectors and participation factors will give useful results, even if the feedback between the two systems is accounted for. Instead, Eq. 3.24 will be used directly, making the following assumptions:

- I) The structure and appendage are detuned, each having a natural frequency approximately equal to one of the frequencies of the combined system:

$$\Omega \approx \omega_1 \approx \omega - \Delta\omega \quad (3.28a)$$

$$\omega_0 \approx \omega_2 \approx \omega + \Delta\omega \quad (3.28b)$$

- II) The damping ratios of the structure and appendage are identical:

$$\zeta_0 = \zeta \quad .$$

In the case of nonproportional damping, where $\zeta_0 \neq \zeta$, the average damping ratio can be used (38) (37).

- III) The absolute sum (ABSS) will be used instead of the SRSS, since the frequencies are close.

- IV) The response spectrum accelerations are approximately the same:

$$SA(\Omega, \zeta) \approx SA(\omega_0, \zeta) \approx SA(\omega, \zeta) \quad (3.29)$$

Equation 3.24 will then take the form

$$\ddot{x}_{\max} = \left| \frac{(\omega + \Delta\omega)^2}{(2\omega)(2\Delta\omega)} SA(\omega, \zeta) \right| + \left| \frac{(\omega - \Delta\omega)^2}{(2\omega)(2\Delta\omega)} SA(\omega, \zeta) \right| \quad (3.30)$$

and after neglecting the small term $(\Delta\omega)^2$

$$\ddot{x}_{\max} = \left\{ \left| \frac{\sqrt{\gamma} + 1}{2\sqrt{\gamma}} \right| + \left| \frac{\sqrt{\gamma} - 1}{2\sqrt{\gamma}} \right| \right\} SA(\omega, \zeta) \quad (3.31)$$

Since $\sqrt{\gamma} < 1$, then $|\sqrt{\gamma} - 1| = 1 - \sqrt{\gamma}$, Eq. 3.31 becomes

$$\ddot{x}_{\max} = \frac{2}{2\sqrt{\gamma}} SA(\omega, \zeta) = \frac{SA(\omega, \zeta)}{\sqrt{\gamma}} \quad (3.32)$$

An identical amplification factor of $\frac{1}{\sqrt{\gamma}}$, was obtained for an undamped tuned appendage in previous studies, using different approaches (29), (38), (37). With recognition that the expressions in Eqs. 3.21 and 3.24 were developed by using approximate eigenvectors of the undamped combined system for the detuned case, it is concluded that Eq. 3.32 will give a good approximation only in the case of an undamped tuned appendage and will be rewritten as

$$\ddot{x}_{\max} = \frac{SA(\omega, 0)}{\sqrt{\gamma}} \quad (3.33)$$

It is also concluded that the response of an undamped tuned appendage can be estimated as a limiting case of the detuned appendage by using the two frequencies of the combined system.

To obtain an expression for the damped case, Eq. 3.32 is written as

$$\ddot{x}_{\max} = \frac{SA(\omega, \zeta)}{\frac{2\Delta\omega}{\omega}} \quad (3.34)$$

Ruzicka and Robinson (37) defined the damped beat frequency ω_B and the beat damping ζ_B as

$$\omega_B = \left[(\Delta\omega)^2 + (\zeta\omega)^2 \right]^{1/2} \quad (3.35)$$

and

$$\zeta_B = \frac{2\zeta}{\left[(2\zeta)^2 + \gamma \right]^{1/2}} \quad (3.36)$$

When the undamped beat frequency $\Delta\omega$ is replaced by Eq. 3.35, Eq. 3.34 will give the following approximation for the damped case:

$$\ddot{x}_{\max} = \frac{SA(\omega, \zeta)}{\left[\gamma + (2\zeta)^2\right]^{1/2}} \quad (3.37)$$

Eq. 3.37 will now be compared with the results of previous studies.

Ruzicka and Robinson (37) used time domain solution of the equations of motion and approximated the maximum appendage response by locating the maximum of the beat envelope. For short ground motions where the duration t_d is limited by

$$\Delta\omega t_d \ll 1 \quad (3.38)$$

and

$$\zeta\omega t_d \ll 1 \quad (3.39)$$

the maximum appendage displacement relative to the ground u_{\max} is given by

$$u_{\max} = \frac{e^{-\kappa}}{\omega \left[\gamma + (2\zeta)^2\right]^{1/2}} |A(\omega)| \quad (3.40)$$

in which:

$$\kappa = \frac{2\zeta}{\sqrt{\gamma}} \arctan\left(\frac{\sqrt{\gamma}}{2\zeta}\right) \quad (3.41)$$

and $|A(\omega)|$ is the Fourier Amplitude Spectra (FAS) at the tuning frequency ω . For long ground motions, where Eqs. 3.38 and 3.39 are not satisfied, $|A(\omega)|$ should be replaced by a corrected average value of the FAS in the region of the two frequencies of the combined system (bandpass) (37).

Sackman and Kelly (38) used frequency domain and Laplace Transforms to solve the equation of motion directly. Also, making an assumption

about short ground motions they obtained the following expression for the appendage maximum acceleration response:

$$\ddot{x}_{\max} = \frac{e^{-\kappa}}{[\gamma + (2\zeta)^2]^{\frac{1}{2}}} SA(\omega, \zeta) \quad (3.42)$$

The amplification factors in Eqs. 3.42 and 3.40 are identical. The only difference is that response spectra is used in Eq. 3.42 and Fourier Amplitude Spectra is used in Eq. 3.40.

The difference between these two methods will be discussed in Chapter 5 together with the results of the experiments. At this stage it will be assumed that the two methods are identical and Eq. 3.42 will be used for comparison with the results of other previous studies and Eq. 3.37 suggested in this study. Eq. 3.42 will be written as

$$\ddot{x}_{\max} = e^{-\kappa} \ddot{x}_{\zeta} \quad (3.43)$$

in which:

$$\ddot{x}_{\zeta} = \frac{SA(\omega, \zeta)}{[\gamma + (2\zeta)^2]^{\frac{1}{2}}} \quad (3.44)$$

will serve as a basis for the comparison and is identical to Eq. 3.37.

As mentioned earlier, the average damping can be used in the case of nonproportional damping (37), (38). However, the mass ratio γ , should also be corrected and becomes (37)

$$\gamma = (\zeta - \zeta_0)^2 \quad (3.45a)$$

The denominator will take the following form (37), (38)

$$[\gamma + 4\zeta_0\zeta]^{\frac{1}{2}} \quad (3.45b)$$

In most practical cases, Eqs. 3.38 and 3.39 are violated. Only systems that are very close to tuning and have very small mass ratio and damping will meet these requirements. Nevertheless, when the results of the experiments are evaluated in Chapter 5, it will be seen that in many cases Eq. 3.42 (or Eq. 3.40) gives a reasonable prediction of the appendage response.

Willaverde and Newmark (53) obtained an expression for the maximum relative displacements (distortions) of a MDOF appendage with a single support, tuned to one frequency of a MDOF structure (Eqs. 3.39 to 3.41 in Ref. 53). For the maximum acceleration response of a SDOF appendage their expression can be written as

$$\ddot{x}_{\max} = \frac{1}{\sqrt{2}} \frac{SA(\omega, \zeta)}{[\gamma + (2\zeta)^2]^{1/2}} \quad (3.46a)$$

or

$$\ddot{x}_{\max} = \frac{\ddot{x}_{\zeta}}{\sqrt{2}} \quad (3.46b)$$

It is also interesting to compare the semi-empirical rule obtained by Nakhata, Newmark and Hall (29) with the other previous studies. The amplification of a tuned SDOF appendage on a SDOF structure is given by

$$\frac{1}{\alpha\zeta + \sqrt{\gamma}} \quad (3.47)$$

where α is an empirical constant which is a function of $\frac{\zeta}{\sqrt{\gamma}}$ and $2 \leq \alpha \leq 3$.

The maximum acceleration response of the appendage will be

$$\ddot{x}_{\max} = \frac{SA(\omega, \zeta)}{\alpha\zeta + \sqrt{\gamma}} = \frac{SA(\omega, \zeta)}{[\gamma + (2\zeta)^2]^{\frac{1}{2}}} \frac{1}{[1 + \delta]^{\frac{1}{2}}} = \frac{1}{[1 + \delta]^{\frac{1}{2}}} \ddot{x}_{\zeta} \quad , \quad (3.48)$$

in which:

$$\delta = \frac{\alpha \frac{\sqrt{\gamma}}{\zeta} + \frac{\alpha^2 - 4}{4}}{1 + \frac{\gamma}{(2\zeta)^2}} \quad . \quad (3.49)$$

The ratio $\ddot{x}_{\max}/\ddot{x}_{\zeta}$ is plotted as a function of $\sqrt{\gamma}/2\zeta$ in Figure 3.1 for five cases, namely the three references discussed in this section, Eq. 3.37 suggested in this study, and the undamped case (Eq. 3.32). These cases are summarized in Table 3.1.

The following observations can be made:

- 1) In the case of low damping, all the equations, except Eq. 3.46, will give approximately the same maximum appendage response.
- 2) In the case of high damping, all methods, except Eq. 3.37, will result in a substantial reduction of the maximum appendage response, compared with the undamped case.
- 3) The empirical equation (Eq. 3.48) and Eq. 3.43 based on the location of the maximum of the beat envelope lead to similar results over the whole range of damping (except for very low mass ratio near zero or very large damping near infinity).
- 4) Eq. 3.37 suggested in this study will give response estimates which are higher than those obtained by the other methods. The differences will be larger for larger damping.

Based on these observations, it could be concluded that Eq. 3.43 will give a good estimate while Eq. 3.37 will give an upper bound for the maximum response of the appendage. In order to obtain a better understanding of the difference between the two equations the following assumption will be made:

$$\kappa = \zeta_B \frac{\pi}{2} \quad (3.50)$$

Eq. 3.50 is substituted in Eq. 3.43 and the result is also plotted in Fig. 3.1. It can be seen that although the results are slightly lower a good agreement is obtained with Eq. 3.43. This means that the maximum beat envelope (and maximum appendage response) should occur near the maximum of the first lobe of the free beat after the earthquake (short ground motion). This is in agreement with the assumptions made in the development of Eq. 3.43 (38), (37). However, for long ground motions, where the maximum appendage response can occur during the earthquake, the conditions for (relatively) free beats are not always possible. In such cases, it is expected that Eq. 3.37 will give a better estimate of the maximum appendage response.

On the other hand, when the beat is heavily damped, for instance in some cases of inelastic behavior, it is expected that a better estimate of the maximum appendage response will be obtained by substitution of the beat envelope damping ζ_B (Eq. 3.36) into Eq. 3.37, giving

$$\ddot{x}_{\max} = \frac{SA(\omega, \zeta_B)}{[\gamma + (2\zeta)^2]^{\frac{1}{2}}} = \frac{SA(\omega, \zeta_B)}{SA(\omega, \zeta)} \ddot{x}_{\zeta} \quad (3.51)$$

The ratio of response spectra in Eq. 3.51, can be estimated from equations for spectrum amplification factors given by Newmark and Hall (33). However, this cannot be done for a dimensionless $\sqrt{\gamma}/2\zeta$ and was therefore performed for two cases of γ , namely 0.1 and 0.01. The results are also plotted in Figure 3.1. It can be seen that Eq. 3.51 can be considered to be an estimate of the lower bound of the maximum appendage response.

It can be concluded from the results that the suggestion made in this section regarding interpretation of the tuned appendage as a limiting case of the detuned appendage (Eq. 3.37) will give a good estimate of the upper value of the appendage maximum response. The method based on the location of the maximum of the beat envelope (Eq. 3.43) provides a good estimate of the maximum response but may underestimate the response in some cases. A lower bound of the response can be obtained by using response spectra based on beat damping (Eq. 3.51) instead of damping of the combined system.

3.2.3 Slightly Detuned Appendages

An appendage is slightly detuned (or nearly tuned) when its frequency is close to a frequency of the structure. The range of a slightly detuned appendage is estimated in this section and it is shown that the case of the slightly detuned appendage can be used as a transition between the detuned case where the SRSS rule is used and the tuned case that was interpreted as a result of the ABSS rule.

Before the slightly detuned case is treated, it should be noted that if the SRSS is used in Eq. 3.30 instead of the ABSS, the response of the

tuned appendage calculated from Eqs. 3.33 and 3.37 will be reduced by a factor of $\sqrt{2}$. These two reduced values represent the upper limit of amplifications that should be calculated for the detuned undamped and damped cases, respectively.

The case of slightly detuned appendage was studied by Ruzicka and Robinson (37) and Sackman and Kelly (38). In both these studies it is suggested that the equations for tuned appendage should be used with some equivalent tuning frequency and mass ratio. Although their definition of the detuning parameter is different, it can be shown that their results are approximately identical.

Ruzicka and Robinson (37) define a detuning parameter d_R as

$$d_R = \frac{1}{\sqrt{\gamma}} \left(\frac{\omega_0^2 - \Omega^2}{\Omega^2} \right) \quad (3.52)$$

and show that the solution for tuned appendage can be used with the following equivalent tuning frequency $\omega_R^\#$ and mass ratio $\gamma_R^\#$

$$\omega_R^\# = \Omega \left(1 + \frac{d_R \sqrt{\gamma}}{4} \right) \quad (3.53a)$$

$$\gamma_R^\# = \gamma \left(1 + \frac{d_R^2}{4} \right) \quad (3.53b)$$

Sackman and Kelly (38) define the detuning parameter d_S and the equivalent tuning frequency $\omega_S^\#$ as

$$d_S = \frac{\Omega - \omega_0}{\omega_0} \quad (3.54)$$

$$\omega_S^* = \frac{\Omega + \omega_0}{2} = \frac{\Omega}{2} \left(1 + \frac{1}{d_S + 1} \right) \quad (3.55)$$

and obtain an equivalent mass ratio

$$\gamma_S^* = \gamma + d_S^2 \quad (3.56)$$

Eq. 3.52 will be expanded to

$$d_R = \frac{1}{\sqrt{\gamma}} \left(\frac{(\omega_0 - \Omega)(\omega_0 + \Omega)}{\Omega^2} \right) \quad (3.57)$$

and the assumption of slight detuning will give

$$\frac{\Omega + \omega_0}{\Omega} \approx 2 \quad (3.58a)$$

and

$$\frac{\omega_0 - \Omega}{\Omega} \approx \frac{\omega_0 - \Omega}{\omega} \approx -d_S \quad (3.58b)$$

or

$$d_S \approx \frac{-\sqrt{\gamma}}{2} d_R \quad (3.59)$$

Substitution of Eq. 3.59 in Eqs. 3.55 and 3.56 gives

$$\omega_R^* \approx \omega_S^* \quad , \quad \text{and} \quad (3.60a)$$

$$\gamma_R^* \approx \gamma_S^* \quad (3.60b)$$

To see the transition between the detuned and tuned cases, a transfer function TF is defined as

$$TF = \left| \frac{\ddot{x}_{max}}{SA\left(\frac{\Omega + \omega_0}{2}, \zeta\right)} \right| \quad (3.61)$$

Similar to the tuned case, it will be assumed that the damping ratios of the structure and appendage are identical ($\zeta_0 = \zeta$) or that the average value can be used.

For the detuned case, Eq. 3.24 will be used. Since detuning is slight and damping is identical, the following approximation can be made, namely

$$SA(\Omega, \zeta) \approx SA(\omega_0, \zeta_0) \approx SA\left(\frac{\Omega + \omega_0}{2}, \zeta\right) \quad (3.62)$$

Substitution of Eqs. 3.24 and 3.62 into Eq. 3.61 gives

$$TF = \left| \frac{[\omega_0^4 + \Omega^4]^{1/2}}{\omega_0^2 - \Omega^2} \right| \quad (3.63a)$$

A plot of TF as a function of the frequency ratio $\frac{\omega_0}{\Omega}$ (Eq. 3.63a) is given in Figure 3.2.

If ABSS is used instead of SRSS in Eq. 3.24 the transfer function becomes

$$TF = \left| \frac{\omega_0^2 + \Omega^2}{\omega_0^2 - \Omega^2} \right| \quad (3.63b)$$

Eq. 3.63b is plotted in Figure 3.3 for comparison.

For the tuned case, Eq. 3.37 will be used. The damping term $(2\zeta)^2$ in the denominator will be ignored. This term is a constant that can be added to γ and the sum $\gamma + (2\zeta)^2$ can be interpreted as an effective γ .

The equivalent mass ratio defined in Eq. 3.56 will then replace γ and substitution of Eqs. 3.37 and 3.62 into Eq. 3.61 gives

$$TF = \frac{1}{\left[\gamma + \left(\frac{\Omega - \omega_0}{\omega_0} \right)^2 \right]^{\frac{1}{2}}} \quad (3.64)$$

Equation 3.64 is also plotted in Figures 3.2 and 3.3 for different values of γ between 0.001 and 0.1. It can be seen in Figure 3.3 that the ABSS detuned case and the slightly detuned case will give very close results over a certain frequency range, depending on γ . This is in agreement with the suggestion made in this study, to interpret the tuned case as limiting case of the detuned case. In Figure 3.2 it can be seen that the curves of Eq. 3.64 give relatively smooth transitions from the detuned to the tuned case. The intersection points in Figure 3.2 were determined numerically. The curves of Eq. 3.64 for $\gamma > 0.04$ approach but do not intersect the curve of Eq. 3.63a for frequency ratios smaller than one (left branch of curve). In these cases, the points where the distances between the curves were minimum were chosen to replace the intersections. These points will have different symbols in the next figures.

The frequency ratios at the intersections are presented in Figure 3.4 as a function of γ . The relation can be approximated by

$$\frac{\omega_0}{\Omega} = 1 \pm 1.1\sqrt{\gamma} \quad (3.65)$$

Eq. 3.65 is also plotted in Figure 3.4. The agreement with the calculated intersection points is very good except where there is no intersection of the curves of the transfer functions in Figure 3.2.

Eq. 3.65 defines the range where the appendage should be considered tuned or slightly detuned as

$$1 - 1.1\sqrt{\gamma} \leq \frac{\omega_0}{\Omega} \leq 1 + 1.1\sqrt{\gamma} \quad (3.66a)$$

In the remaining range

$$\frac{\omega_0}{\Omega} \leq 1 - 1.1\sqrt{\gamma} \quad (3.66b)$$

and

$$\frac{\omega_0}{\Omega} \geq 1 + 1.1\sqrt{\gamma} \quad (3.66c)$$

the appendage should be considered detuned.

The values of the transfer function at the intersection points, each normalized to the maximum amplification at tuning, $\frac{1}{\sqrt{\gamma}}$, for the same γ , are given in Figure 3.5 as a function of γ . It is noted that there is only a slight change in these values which are close to $\frac{1}{\sqrt{2}}$. Therefore it can be concluded that the slightly detuned case gives a reasonable transition between the detuned and tuned cases.

If Eq. 3.42 is used instead of Eq. 3.37 in the calculation of the ranges, the range where the appendage should be considered tuned, will be larger than the range defined by Eq. 3.66a. This may lead to underestimates of the appendage maximum response in some cases.

It is interesting to compare the results with the following ranges suggested for a detuned appendage by Villaverde and Newmark (53):

$$\left| \frac{\omega_0^2 - \Omega^2}{\Omega^2} \right| \geq \sqrt{\gamma} \quad , \text{ and} \quad (3.67)$$

$$\left| \frac{\Omega^2 - \omega_0^2}{\omega_0^2} \right| \geq \sqrt{\gamma} \quad . \quad (3.68)$$

Eqs. 3.67 and 3.68 will give four values for the ranges of the detuned case, which after some manipulations and neglect of higher powers of $\sqrt{\gamma}$, will reduce to the following two expressions,

$$\frac{\omega_0}{\Omega} \leq 1 - \frac{\sqrt{\gamma}}{2} \quad , \text{ and} \quad (3.69a)$$

$$\frac{\omega_0}{\Omega} \geq 1 + \frac{\sqrt{\gamma}}{2} \quad . \quad (3.69b)$$

Eq. 3.69 is also plotted in Figure 3.4 for comparison. It is noted that the range of the detuned case starts closer to tuning than the range defined in Eq. 3.66 in this study. The difference is the result of the method which is used in Ref. 53 to set the limit of the amplification for each term of the detuned appendage, directly as the amplification of the tuned appendage without considering the SRSS rule. It is expected that the use of the equation for the detuned case, in the range between Eq. 3.66 and Eq. 3.69 will result in appendage responses higher than the slightly detuned or even the tuned case. This can be seen by substitution of Eq. 3.69 in Eq. 3.63a, expansion of Eq. 3.63a, and neglect of powers of $\sqrt{\gamma}$, which will lead to

$$TF \approx \frac{\sqrt{2}}{\sqrt{\gamma}} \quad . \quad (3.70)$$

This transfer function value is larger than the amplification of the tuned case, by a factor of $\sqrt{2}$. The exact values of TF at the intersections of Eqs. 3.69 and 3.63a, were determined numerically and also are presented in Figure 3.5. A good agreement with the approximate value of Eq. 3.70 is obtained.

In this section, it was shown that the case of a slightly detuned appendage could be used as a transition between the detuned case and the tuned case. The ranges of the detuned and slightly detuned cases are given in Eq. 3.66.

3.2.4 Total Response of an Appendage on a MDOF Structure

An inspection of Eq. 3.21, shows that the maximum response of a detuned appendage is calculated as a summation of amplifications of the ground motion evaluated at the frequencies of the decoupled structure and appendage. Each of these terms depends on the frequency ratio, the location of the appendage in the structure, and the acceleration response spectrum, which in turn is a function of the frequency and damping. These observations will be useful when the case of an inelastic supporting structure will be treated.

When the appendage is tuned or nearly tuned to a frequency Ω_m of the structure, the amplification at this particular frequency cannot be determined from Eq. 3.21. This amplification is determined separately from Eq. 3.42, which has to include the following modifications:

- 1) The modal mass ratio γ_m should be determined assuming that the modal mass of the structure is concentrated at the point of support k , or

$$\gamma_m = \frac{m}{M_m^* / \phi_{km}^2} = \frac{m \phi_{km}^2}{M_m^*} \quad (3.71)$$

- 2) Eq. 3.42 should be multiplied by the modal displacement of mode m at the point of support k . This term vanished when Eq. 3.24 for the SDOF structure was derived from Eq. 3.21. The value of $\Gamma_m \phi_{km}$ (38) will be used in this study, although as a result of the interaction with the appendage this is only an approximation (37).

Eq. 3.42 becomes

$$\ddot{x}_{max} = \frac{e^{-\kappa}}{\left[\gamma_m + (2\zeta)^2 \right]^{1/2}} \Gamma_m \phi_{km} SA(\omega, \zeta) \quad (3.72)$$

Inspection of Eq. 3.72 shows the analogy with Eq. 3.21. The term containing the frequency ratio was replaced by a term containing the mass ratio and damping. In the case of slight detuning, the frequency ratio is included in the mass ratio (Eq. 3.56).

The total amplification is obtained by adding the response calculated from Eq. 3.72 to the result of Eq. 3.21, using the SRSS rule (39).

3.3 Appendages on Inelastic Structures

3.3.1 General

One of the methods employed to evaluate the response of an inelastic structure (without an appendage) centers on replacing the actual structure with an equivalent linear structure and by determining the frequency shift and additional damping as a result of yielding (42), (48), (16).

In Section 3.2.4 it was observed that the maximum response of an appendage mounted in an elastic structure can be estimated as a summation

of amplifications of the ground motion. Also was it noted that these amplifications are functions of the following parameters:

detuned case:	frequency ratio and acceleration response spectrum
slightly detuned case:	frequency ratio, mass ratio, damping and acceleration response spectra
tuned case:	mass ratio, damping and acceleration response spectrum.

It is noted that the acceleration response spectra also are a function of frequency and damping.

It seems therefore reasonable that in the case of an inelastic supporting structure the appendage response could be estimated by using the procedures for the elastic supporting structure by taking into account the frequency shift and additional damping.

In the case of a SDOF supporting structure, the definition of ductility is simple and the frequency shift and damping can be determined empirically (16), (11). However, different definitions of ductility exist in the case of a MDOF supporting structure, such as member or story ductilities, overall (average) ductility (33), and modal ductilities (48), (54), (25). It seems that the concept of modal ductility is the most suitable for use in this study.

In normal practice, the response of a MDOF inelastic structure is determined numerically and member ductilities are obtained. A method to estimate modal ductilities from member ductilities will be suggested and compared with other studies in this section and with the results of the experiments in Chapter 5. Simplified methods also are available for

design. Such methods include the use of a global value of design ductility for all modes (33), simplifying the structure as a SDOF inelastic system (40), (36) and estimating frequencies shifts and modal damping ratios from member ductilities (42). In such cases, modal ductilities have to be estimated either directly or from member ductilities.

3.3.2 Definition of Ductility

In this study the following standard definition of ductility, μ , will be used

$$\mu = \frac{u_{max}}{u_e} = \frac{K u_{max}}{R_{max}} \quad (3.73)$$

in which K is the elastic stiffness, u_{max} is the maximum relative displacement (distortion), u_e is the elastic portion of the relative displacement and R_{max} is the maximum resistance. This definition is shown in Figure 3.6. Although this choice does not represent the inelastic hysteretic energy exactly, it has been used in other studies (21) and has the following characteristics:

- 1) The stiffness in Eq. 3.73 is identical to the linear elastic stiffness of the structure.
- 2) The maximum resistance in Eq. 3.73 is identical to the resistance of the structure.
- 3) The yield deformation is equal to the deformation of an elastic unloading.

- 4) The chosen ductility lies between two values that represent the inelastic hysteretic energy exactly, one where the elastic stiffness, and the other where the maximum resistance, is conserved. These two values also are shown in Figure 3.6.
- 5) The error in the energy is small especially for large ductilities.
- 6) During an earthquake, the inelastic hysteretic loops are not identical and there is no unique relation between the ductility and the dissipated energy.

3.3.3 Equivalent Linear System

3.3.3.1 General

The concept of an equivalent linear system consists of replacing the nonlinear system with a linear system that has similar energy dissipation and response characteristics. A good overview, as well as comparison, of several studies is given by Hadjian (11). Usually an equivalent elastic stiffness (or natural frequency) and an equivalent viscous damping ratio are estimated as functions of the ductility (11). The equivalent stiffness and damping are different for the cases of harmonic and earthquake ground motion, but certain correlations exist between these two cases (48) (11).

The method of equivalent linearization has been previously used to estimate the response of inelastic SDOF and MODF structures. In this study an attempt is made to use this concept to estimate the response of appendages on inelastic primary structures. Different methods will be

reviewed here and will be compared with the results of the experiments in Chapter 5.

The case of harmonic ground motion will be studied first. The purpose is to explain the meaning and demonstrate the validity of replacing the actual structure with an equivalent one. Also, as mentioned earlier, certain correlations with earthquake excitations exist.

3.3.3.2 SDOF Structures

Harmonic Ground Motion -- A typical single hysteresis loop of the response of a single-story structure to harmonic ground motions is given in Figure 3.7. The energy W_D , dissipated in one inelastic hysteresis loop, is equal to the area enclosed by the loop. For elasto-plastic systems this area is equal to

$$W_D = 4R_{\max} \left(1 - \frac{1}{\mu} \right) u_{\max} = 4K \left(\frac{\mu - 1}{\mu^2} \right) u_{\max}^2 \quad (3.74)$$

For the curved force-displacement relations and the ductility defined in this study, the dissipated energy will be calculated numerically and can be expressed as

$$W_D = \eta R_{\max} \left(1 - \frac{1}{\mu} \right) u_{\max} = \eta K \left(\frac{\mu - 1}{\mu^2} \right) u_{\max}^2 \quad (3.75)$$

in which η is a constant smaller than 4.

The equivalent viscous damping will be defined as having an elliptical force-displacement loop with the same area W_D and the same maximum displacement u_{\max} as the inelastic hysteresis loop (6), (49).

The equation of this ellipse is

$$F_D = \pm c_{eq} \Omega_H \left[u_{max}^2 - u^2 \right]^{1/2} \quad (3.76)$$

in which F_D is the damping force, c_{eq} is the equivalent viscous damping factor, Ω_H is the harmonic forcing frequency and u is the relative displacement. Such an elliptical loop is shown as a dashed line in Figure 3.7, together with the inelastic loop having the same area.

The equivalent viscous damping factor is calculated from the area of the ellipse as

$$c_{eq} = \frac{W_D}{\pi \Omega_H u_{max}^2} \quad (3.77)$$

and after substitution of Eq. (3.73) becomes

$$c_{eq} = \frac{\eta K \left(\frac{\mu - 1}{\mu^2} \right)}{\pi \Omega_H} \quad (3.78)$$

The equivalent damping is a function of the frequency of the motion.

It remains to define the equivalent stiffness, which means that the abscissa of the ellipse has to be rotated. Since the equivalent viscous damping is based on equal areas of the loops, it seems logical that the best equivalency of the two systems will be obtained when maximum overlapping between the two areas is reached. The slope of the rotated ellipse in this position will be defined as the equivalent stiffness, K_{eq} . The equation of the rotated ellipse becomes

$$R = K_{eq}u + F_D \quad (3.79)$$

in which R is the resistance of the equivalent linear system. This rotated position can be determined numerically and also is shown in Figure 3.7.

The equivalent damping ratio, ζ_{eq} , is calculated from

$$\zeta_{eq} = \frac{\eta K \left(\frac{\mu - 1}{\mu^2} \right)}{2\pi\Omega_H [K_{eq}M]^{1/2}} \quad (3.80)$$

in which M is the mass of the structure.

The equivalent damping ratio is also a function of the frequency. In the case of resonance, where the forcing frequency is equal to the (equivalent) natural frequency, Eq. 3.80 simplifies to

$$\zeta_{eq} = \frac{\eta K \left(\frac{\mu - 1}{\mu^2} \right)}{2\pi K_{eq}} \quad (3.81)$$

If the equivalent stiffness, K_{eq} , is assumed to be equal to the secant stiffness, $\frac{K}{\mu}$, a further simplification is obtained

$$\zeta_{eq} = \frac{\eta(\mu - 1)}{2\pi\mu} \quad (3.82)$$

Earthquake -- The main difference between the inelastic response to harmonic and to earthquake excitation is that the response cycles are not identical and the maximum response is normally attained only once during

an earthquake. However, computed time histories of the energy dissipated in damping and inelastic hysteresis during earthquakes, are similar (58) (28). These studies were performed on elastoplastic systems where yield was concentrated in a few cycles. In the case of a curved force deformation relation, which characterizes most structures (and the models used in this study), yield is more evenly distributed and a better agreement between the dissipated energies is expected. Frequency shift also will be more evenly distributed in this case.

Attempts have been made to estimate the equivalent stiffness and damping (11). Results of some of these studies will be compared with the experiments in Chapter 5. These studies will be reviewed here briefly.

Shibata and Sozen (42) suggested a design procedure based on a series of studies on the seismic response of concrete structures. In their method, the actual inelastic MDOF structure is replaced by a "Substitute Structure" with linear stiffnesses and damping ratios. The stiffness can be interpreted as the secant stiffness

$$K_{eq} = \frac{K}{\mu} \quad (3.83a)$$

and the damping ratio is given by

$$\zeta = \zeta_{e1} + 0.2 \left[1 - \frac{1}{\sqrt{\mu}} \right] \quad (3.83b)$$

in which ζ_{e1} is the elastic viscous damping ratio. It seems that this method overestimates the reduction in the natural frequency (11), (47). This may have negligible effect on the design of structures using smoothed design spectra, in particular concrete structures where softening is

permanent. However, the effect on the amplifications between structure and appendage (Eq. 3.21) may be more substantial.

Iwan (16) proposed empirical expressions for period shift and effective damping of SDOF systems, based on numerical studies performed on several hysteretic models and earthquakes. By minimizing the root mean square average error between the maximum response of the inelastic and the equivalent systems the following expressions were obtained

$$K_{e_q} = \frac{K}{\left[1 + 0.121(\mu - 1)^{0.939}\right]^2} \quad (3.84a)$$

$$\zeta_{e_q} = \zeta_{e1} + 0.0587(\mu - 1)^{0.371} \quad (3.84b)$$

Iwan's method was recently extended to MDOF structures (47).

It should be noted that there is a good agreement between the expressions given in Eqs. 3.83b and 3.84b for the equivalent damping (11).

In his review, Hadjian (11) proposed the following simple ratios to relate the frequency shift and equivalent damping in the cases of earthquake and harmonic excitations:

$$\Omega_{e_q}^E \approx 2\Omega_{e_q}^H \quad (3.85a)$$

$$\zeta_{e_q}^E \approx 0.2\zeta_{e_q}^H \quad (3.85b)$$

in which $\Omega_{e_q}^E$ and $\zeta_{e_q}^E$ are the equivalent linear frequency and damping ratio for earthquake and $\Omega_{e_q}^H$ and $\zeta_{e_q}^H$ are the equivalent linear frequency and damping ratio for harmonic excitation, which are based on secant stiffness.

However, Eq. 3.85a does not give useful results for ductilities less than approximately 5. Therefore, from Fig. 5 of Hadjian's work (11) the following linear interpolation will be used in this study, namely

$$\Omega_{e\tau}^E = \frac{\mu + 3}{4} \Omega_{e\tau}^H \quad \text{for} \quad 1.0 \leq \mu \leq 5.0 \quad , \quad (3.86a)$$

and

$$\Omega_{e\tau}^E = 2\Omega_{e\tau}^H \quad \text{for} \quad 5.0 \leq \mu \quad . \quad (3.86b)$$

It should be noted that structures subjected to broad band excitations like earthquakes, vibrate essentially at their natural frequencies with variable amplitudes. Therefore the correlations of Eqs. 3.86a and 3.86b should be based on harmonic excitation at or near resonance.

Tansirikongkol and Pecknold (48) introduced a correlation which relates the earthquake maximum response to a steady state maximum, for bilinear systems. Two values of pseudo-steady-state ductilities are calculated from the expected ductility. These ductilities are used to calculate the equivalent frequency and damping respectively, for use in earthquake response. The procedure is iterative and will not be used in this study.

3.3.3.3 MDOF Structures

General -- The equation of motion of a MDOF inelastic structure, subjected to a ground acceleration \ddot{u}_g is (25)

$$[M]\{\ddot{u}\} + [C]\{\dot{u}\} + \{R(\{u\})\} = -[M]\{1\}\ddot{u}_g \quad (3.87)$$

in which $\{R(\{u\})\}$ is the vector of resistances and $\{1\}$ is a vector relating the ground motion to the structural degrees of freedom.

The elastic mode shapes constitute a basis for all the vectors of the deformed shape of the structure. Therefore, although modal superposition is not valid, the response can be expressed as a linear combination of the elastic mode shapes

$$\{u\} = [\phi_{ij}]\{y\} \quad (3.88)$$

Substitution of Eq. 3.88 into Eq. 3.87, and premultiplication of Eq. 3.87 by $[\phi_{ij}]^T$, leads to a transformation that does not uncouple the equations of motion. Coupling remains in the term of the inelastic resistance

$$\{R_y\} = [\phi_{ij}]^T \{R(\{u\})\} - [\phi_{ij}]^T \{R_u\} \quad (3.89)$$

in which $\{R_y\}$ is the vector of resistances R_j in the modal coordinates (modal resistance vector) and $\{R_u\}$ is the vector of resistances in the DOF coordinates.

It is sometimes convenient to lump the damping forces together with the resistances. Eq. 3.89 can be written as

$$\{R_y\} = [\phi_{ij}]^T \left\{ \{R(\{u\})\} + [C]\{\dot{y}\} \right\} \quad (3.90a)$$

or

$$\{R_y\} = -[\phi_{ij}]^T [M]\{\ddot{x}\} \quad (3.90b)$$

in which $\{\ddot{x}\}$ is the vector of absolute accelerations.

Eqs. 3.88 and 3.90b can be used to calculate the vectors $\{y\}$ and $\{R_y\}$ from the results of experiments or numerical analyses of the response of inelastic structures.

When each modal resistance, R_j , is plotted as a function of the relevant modal displacement, y_j , inelastic force-deformation hysteresis

curves are obtained. The general behavior is similar to the force-deformation curves of SDOF inelastic systems, but irregularities can be observed (25). These observations will be confirmed in the results of the experiments in Chapter 5. Using a modified version of the ductility defined in Section 3.3.2, it will be possible to derive in Chapter 5 approximate modal ductilities for each mode from these curves.

The main difficulty in relating the modal ductilities to local (story or member) ductilities arises because the maximum local and modal deformations do not occur simultaneously. Only a few attempts to obtain such relations are known (48), (54), (25). The limitations will be discussed briefly in the next two sections.

Harmonic Ground Motion -- The steady state response of a MDOF undamped elastic structure subjected to harmonic ground motion is in phase (or 180° out of phase) with the ground motion. Therefore, maximum modal and member displacements occur simultaneously. In the case of a damped structure there is a different phase shift for each mode and maximum modal and member displacements will not occur at the same time. The situation is much more complicated in the case of an inelastic structure. However, due to the steady state conditions, large portions of the inelastic excursions are simultaneous and the difference will be neglected.

Eq. (3.89) can now be written in the following two forms:

$$\{R_y\} = [\phi_{ij}]^T [K_{eq}] [\phi_{ij}] \{y\} \quad (3.91a)$$

in which $[K_{eq}]$ is an equivalent linear stiffness matrix and

$$\{R_y\} = [\phi_{ij}]^T [K] [\phi_{ij}] \{y^y\} \quad (3.91b)$$

in which $\{y^y\}$ is the vector of the modal yield displacements.

It is not possible to uncouple Eq. 3.91a by using the elastic mode shapes. Mode shapes of the equivalent system should be used instead (48). However, in the same study (48), it was found that the actual changes in the mode shapes are small. Also, the concept of modal ductilities which is used in this study implies that the mode shapes remain unchanged. Therefore, Eqs. 3.91a and 3.91b will be combined and "uncoupled", giving

$$\{\phi_j\}^T [K_{eq}] \{\phi_j\} y_j = \{\phi_j\}^T [K] \{\phi_j\} y_j^y \quad (3.92)$$

in which y_j^y is the yield deformation of mode j .

If the member (or story) secant stiffnesses are used in $[K_{eq}]$ and if y_j^y is compatible with the ductility defined in this study, modal ductilities μ_j are obtained as

$$\mu_j = \frac{y_j}{y_j^y} = \frac{\{\phi_j\}^T [K] \{\phi_j\}}{\{\phi_j\}^T \left[\frac{K_i}{\mu_i} \right] \{\phi_j\}} \quad (3.93)$$

in which $\left[\frac{K_i}{\mu_i} \right]$ is the stiffness matrix assembled from secant stiffnesses $\frac{K_i}{\mu_i}$ of all members (42) and K_i and μ_i are member elastic stiffness and ductility, respectively.

It is interesting to compare Eq. 3.93 with an expression derived by Tansirikongkol and Pecknold (48) for the modal ductility of a MDOF structure with bilinear elements subjected to harmonic ground motion. Their expression is based on minimizing the modal mean square error over one cycle and then simplified for secant stiffness. For an elastoplastic system, it can be written as

$$\mu_j = \frac{(\phi_j)^T \left[K_1 \left(1 - \frac{1}{\mu_1} \right) \right] (\phi_j)}{(\phi_j)^T \left[\frac{K_1}{\mu_1} \left(1 - \frac{1}{\mu_1} \right) \right] (\phi_j)} \quad (3.94)$$

in which $\left[K_1 \left(1 - \frac{1}{\mu_1} \right) \right]$ is the stiffness matrix assembled from the products of stiffness and the term in parenthesis for each member and $\left[\frac{K_1}{\mu_1} \left(1 - \frac{1}{\mu_1} \right) \right]$ is the stiffness matrix assembled from the products of the secant stiffness and the term in parenthesis for each member.

It should be noted that Eq. 3.94 was derived for an iterative procedure and should be used with the equivalent mode shapes in each iteration. As mentioned earlier the difference between the equivalent and elastic mode shapes will be neglected. It is also noted that for large member ductilities Eqs. 3.94 and 3.93 will give identical results.

Earthquake Ground Motion -- Although the peaks of the story drifts (or member deformations) do not occur simultaneously, most of the distortions take place during the large inelastic excursions. Therefore, Eq. 3.93 will be used to relate modal and story (or member) ductilities in the case of earthquakes as well. The equivalent linear frequencies and damping ratios can then be determined from the relations given in Section 3.3.3.2. It should be noted that the results of Eq. 3.94 were also used to determine equivalent linear frequencies and damping ratios (48).

Villaverde (54) used an analogy between expressions of SDOF and MDOF systems to derive approximate modal ductilities as a function of story ductilities for elastoplastic chain structures, subjected to earthquake. His expression is written as

$$\mu_j = 1 + \left| \frac{\{\phi_j\}^T [\mu_1 - 1] \{R_1^Y\}}{\Gamma_j R_j^Y} \right| \quad (3.95)$$

in which, $\{R_1^Y\}$ is the vector of member yield resistances, R_j^Y yield resistance of mode j and $[\mu_1 - 1]$ is a matrix assembled from member ductilities, depending on member connectivity (54). For two-story structures it takes the form

$$[\mu_1 - 1] = \begin{bmatrix} (\mu_1 - 1) & -(\mu_2 - 1) \\ 0 & (\mu_2 - 1) \end{bmatrix} \quad (3.96)$$

In Chapter 5, Eqs. 3.93, 3.94 and 3.95 will be compared with the results of the experiments.

It is interesting to mention that Lin and Mahin (25) used the SRSS rule to express member ductilities as a function of modal ductilities, thus taking into consideration that peaks do not occur simultaneously. Their expression will be used in this study (Chapter 5) for comparison.

Once the modal ductilities are known, the procedure described in Section 3.3.3.2 can be used to determine modal equivalent linear stiffnesses and damping ratios which in turn can be used to determine the response of appendages.

CHAPTER 4. DESCRIPTION OF THE EXPERIMENTS

4.1 Introduction

As a part of this investigation a series of experiments were performed. These experiments can be divided into three main groups:

- 1) Preliminary experiments designed to determine the elastic and inelastic properties of the structures, and the elastic properties of the appendages. These experiments are described in Section 4.5.
- 2) Tests of appendages mounted on SDOF (single-story) structures, subjected to free vibrations and earthquakes. This group included tuned and slightly detuned systems. The description of the combined systems and the experiments follows in Section 4.6.
- 3) Tests of appendages mounted on either story of two-story structures, subjected to free vibrations and earthquake motions. These tests included some cases where the appendage was slightly detuned to one mode of the structure. The description of the combined systems and the experiments follows in Section 4.7.

4.2 Structures and Appendages Tested4.2.1 General

The models of structures and appendages tested in this study were designed to simulate real inelastic structures and elastic appendages in the frequency range of the constant acceleration amplification. This frequency range is typical for structures and components of nuclear power plants (20). The models do not represent scale models of real structures and appendages.

Single-story and two-story structures with SDOF appendages were tested in this study. Single-story structures were used with the purpose of studying the basic behavior of an appendage, while the two-story structures were employed to get some insight into the behavior of an appendage on a MDOF structure.

Shear beam type structures were chosen where each story consists of a statically determinant one bay frame in the direction of the motion. The stiffness (and capacity) of each story was obtained by restraining the upper end of one column in the much stiffer floor plate. Structural steel was used for the structure and the cross section of the columns was reduced near the point of restraint so that yielding was restricted locally. The other ends of the columns were hinged. Different natural frequencies and yield strengths were achieved by changing the length of the columns and the cross section of the reduced section.

The two-story structures were composed of single-story structures mounted on top of each other. A typical two-story structure is shown in Figure 4.1.

The appendages were modelled as small one bay one story frames (shear beam type). Spring steel was used for the columns so that the required natural frequencies and capacities could be obtained at the same time. The appendages were designed to remain elastic during the testing and were hung from the floors to avoid buckling. A typical mounted appendage is also shown schematically in Figure 4.1. In the actual tests the appendages were mounted at the center front edge of the floor plate between the hinged columns.

4.2.2 Single-Story Structures

4.2.2.1 Detuned and Slightly Detuned Systems

Two series of single-story structures were used in the tests of the detuned and slightly detuned systems. One series of three structures was designed to have natural frequencies of approximately 3 Hz but different yield strengths. A second series of two structures was designed to have natural frequencies of approximately 6 Hz, but different yield strengths. These structures are listed in Table 4.1.

4.2.2.2 Tuned Systems

This series was composed of four different single-story structures. In order to bring the structures as close as possible to tuning with the appendages it was necessary to remove or add masses on the floor and restrain all the ends of all the columns in some cases. Restraining all columns also served to reduce the damping in some of the structures. These structures are also listed in Table 4.1.

4.2.3 Two-Story Structures

Two configurations of two-story structures were tested. Structure M1 was designed so that most of the yielding would take place in the first story and structure M2 was designed so that most of the yielding will take place in the second story. These structures are listed in Table 4.2.

4.2.4 Appendages

The appendages were composed of three series. The two series tested in the detuned and slightly detuned systems consisted each of four appendages with frequencies between 1.5 Hz and 9 Hz. The appendage weight

was 3.30 lbs and 26.09 lbs for the first and second series, respectively. One appendage of the second (heavier) series was used to test the influence of appendage damping on the appendage response. An adjustable damper was mounted and testing was performed at different levels of damping. The damper increased the weight of the appendage and caused some changes in the frequency.

The third series was used in the tests of the tuned systems and consisted of seven different appendages, six with small mass and one with the large mass. Two configurations were tested with the damper. In order to bring the appendages as close as possible to tuning it was necessary to add or remove mass from them. The appendages are listed in Table 4.3.

4.3 Test Equipment and Instrumentation

4.3.1 General

The experiments were performed at the U.S. Army Corps of Engineers Construction Engineering Research Laboratory (CERL) in Champaign, Illinois. The CERL Biaxial Shock Test Machine (BSTM) was used as an earthquake simulator to generate the ground motions described in Section 4.4 and harmonic ground motions.

The tested model was mounted on a thick steel base plate. A small auxiliary column was mounted permanently on the base plate which thus formed an independent platform for static and free vibration tests (see Sections 4.5.2 and 4.5.3). When earthquake and harmonic ground motion tests were to be performed the base plate was mounted on the BSTM.

4.3.2 Earthquake Simulator

The BSTM is a large machine capable of shaking large specimens with an acceleration of up to approximately 30g and velocity of 30 in/sec in both the horizontal and vertical directions. However, the maximum horizontal displacement (stroke) is limited to 2.75 inches. Vertical motions were not used in this study.

Six hydraulic actuators provide controlled horizontal motion to a table that supports the model. Table response is measured, fed back into the control systems and the input to the actuators is modified, thus ensuring accurate reproduction of the input ground motion time history.

4.3.3 Instrumentation

Piezoresistive accelerometers were used to measure the accelerations of the models. Two accelerometers were mounted in the direction of the shaking on the one-story structures. The accelerometers were placed symmetrically as far apart as possible from each other so that any torsional motion could be detected. In the case of the two-story structures one accelerometer was placed in the centerline of the first story and two accelerometers were placed on the second story. Appendage horizontal acceleration was measured using an accelerometer mounted on the axis of the appendage. Vertical appendage acceleration was also measured. Table accelerations were measured with a built-in accelerometer.

Displacements of the structures were measured using an Electro-optical Auto Collimator for each floor. These optical devices measure the motion of target (optical discontinuities) that were mounted on the floors. Appendage displacements were not measured. Table displacements

were measured with a built-in linear variable differential transformer (LVDT).

The acceleration and displacement signals were fed through a signal conditioner and recorded on tape. Two channels were also sent directly from the signal conditioner to a display analyzer so the response of both the structures and appendage could be monitored (and plotted) during the testing and the next experiment could be planned accordingly. In some cases where more information was needed during the testing the tape was played back sending the signals to a second analyzer. A schematic layout of the equipment is given in Figure 4.2.

4.4 Ground Motions

The following three earthquake motions were used in this study:

Imperial Valley, Ca., May 18, 1940. - EL CENTRO station (S00E),
Bear Valley, Ca., September 4, 1972 - MELENDY Ranch station (N29W),
Kern County, Ca., July 21, 1952 - TAFT Lincoln School station (S69W).

El Centro and Taft are long-duration records with broad-band response spectra, while Melendy is a short-duration, high frequency record with narrow-band response spectra. The acceleration records and undamped response spectra of the three earthquakes are given in Figures 4.3, 4.4 and 4.5.

The models in this study represent systems in a certain frequency range and in that sense are small structures and not scale models. Therefore, the earthquake records were used without any time scaling. Accelerations were scaled to a desired level depending on the required level of inelastic response.

Since the maximum stroke of the shake table was 2.75 inches it was not possible to generate the required accelerations at low frequencies. Therefore the records had to be filtered, using a 1 Hz high pass filter. The filtered acceleration records and undamped response spectra are also shown in Figures 4.3, 4.4 and 4.5. It can be seen that filtering has almost no influence on the acceleration records. Also, no changes can be seen in the response spectra in the frequency range of interest (1 Hz to 10 Hz).

The El Centro record was used to test most decoupled and combined systems in this study. The Melendy record was used to test several systems, including most cases of tuning. The Taft record was used to test only one decoupled and one combined system.

4.5 Preliminary Tests

4.5.1 General

The preliminary tests include all experiments, static and dynamic, that were performed to determine the properties of the decoupled systems, or to serve as reference cases. These include static tests of the single-story structures as well as free and forced vibrations of the decoupled systems.

4.5.2 Static Tests of Single-Story Structures

All single-story structures that were used either as SDOF structures or as stories of the two-story structures were tested statically to obtain inelastic force-displacement relations. The tested structure was mounted on the base plate and was loaded horizontally by pulling it towards the

auxillary column and then pushing it back. At least one full cycle of loading was performed. A threaded rod and nuts were used to apply the load. The rod was hinged on both ends so that it could follow the displacements of the structure without restraint. A load cell was mounted on the rod to measure the force. An LVDT, also mounted on the auxillary column and connected to the structure, was used to measure the displacement. A test arrangement is shown in Figure 4.6.

4.5.3 Free Vibrations

All decoupled systems, were tested in free vibrations to determine their natural frequencies and damping ratios.

The structures were tested by pulling the floor (or the first floor of two stories) towards the auxillary column, using a wire connected to the threaded rod, and then cutting the wire. Floor accelerations and displacements were measured.

The decoupled appendages were pulled by hand and released. Accelerations were measured.

4.5.4 Harmonic Tests of a Single-Story Structure

The purpose of these tests was to verify experimentally that an inelastic SDOF structure can be replaced by an equivalent linear system. Structure S1 was subjected to harmonic ground motions using the shake-table. The frequency was varied between 1.0 Hz and 10.0 Hz and the input acceleration also was varied from test to test. Floor accelerations and displacements as well as input ground accelerations and displacements were

measured. Inelastic response was reached in cases where the forcing frequency was close to the natural frequency.

4.5.5 Earthquake Excitation of the Decoupled Systems

4.5.5.1 Single-Story Structures

Four decoupled single-story structures were subjected to the earthquake ground motions. Structure S1, S2, S4 and S5 were subjected to the El Centro ground motion. Structure S2 was subjected to the Melendy and Taft ground motions as well. Shaking was started at a low level so at least one experiment was performed in the elastic range. Each experiment was repeated a few times, increasing the level until substantial inelastic deformation or the capacity of the BSTM was reached.

Accelerations and displacements of the floor and the table were measured.

4.5.5.2 Two-Story Structures

Structures M1 and M2 were subjected to El Centro ground motion. Structure M1 was subjected to Melendy ground motion as well. Shaking was started at a low level and then increased. Accelerations and displacements of both floors and the table were measured.

4.5.5.3 Appendages

Two of the decoupled appendages, namely AS2 and AS3, that were used in several experiments of the combined systems were subjected to the ground motions of El Centro and Melendy earthquakes. Since the appendages were designed to remain elastic during the tests only one level of excitation was used in these cases. Appendage acceleration as well as table acceleration and displacement were measured.

4.6 Appendages on Single-Story Structures

Several different configurations of detuned systems, including some slightly detuned systems, and seven different tuned systems were tested. A list of these systems is given in Table 4.4. Also listed in Table 4.4 are the ground motions used with each configuration. All systems were tested in free vibrations and all systems (except one) were subjected to the ground motion of the El Centro earthquake. All tuned systems and two detuned systems were subjected to the ground motion of the Melendy earthquake and one detuned system was subjected to the ground motion of the Taft earthquake.

Shaking was started at low levels and then increased. Accelerations and displacements of the floor and the table as well as acceleration of the appendage were measured.

4.7 Appendages on Two-Story Structures

Eight different configurations of combined systems consisting of two-story structures with appendages were tested. These systems consisted of structures M1 and M2 and appendages AS2 and AS3 mounted on either floor. A list of these systems is given in Table 4.5. Also listed in Table 4.5 are the ground motions used with each configuration. All systems were tested in free vibrations and were subjected to the ground motion of the El Centro earthquake. The configurations where structure M1 was used were subjected to Melendy earthquake as well.

Shaking was started at low levels and then increased. Acceleration and displacements of both floors and the table as well as acceleration of the appendage were measured.

CHAPTER 5. INTERPRETATION OF THE RESULTS OF THE EXPERIMENTS

5.1 Preliminary Tests5.1.1 Elastic Properties5.1.1.1 Single-Story Structures

Typical measured free vibration displacement and acceleration records of single-story structures (without an appendage), are given in Figures 5.1, 5.2 and 5.3 for structures S1, S4 and S7, respectively. It can be seen that the structures behave as damped SDOF systems with fairly constant natural frequencies. In the hinged structures such as S1 and S4, damping is mainly a result of friction in the hinges. In the tuning structures, such as S7 where no hinges were used, damping is low.

The natural frequencies were calculated from the zero crossings of the acceleration and displacement records over several cycles and then averaged. The elastic stiffnesses were determined from the measured natural frequencies and the masses. These natural frequencies and the elastic stiffnesses are given in Table 5.1.

The method of the logarithmic decrement (6) was used to calculate an equivalent viscous damping for each system as an average over the cycles of constant natural frequency of the acceleration and displacement records in free vibration. These average values are given in Table 5.1 and the envelopes of free vibrations of the same structures but with these viscous damping ratios are also given in Figures 5.1 to 5.3. It can be seen that by using average values damping may be underestimated (and response overestimated) for low excitations.

The natural frequencies and equivalent damping ratios obtained from free vibrations were checked to verify their validity in forced vibration. This was done by comparing measured amplifications of harmonic and earthquake ground motions with amplifications calculated using these natural frequencies and damping ratios.

In the case of harmonic ground motion, the magnification factor MF, defined as the ratio between the maximum structure and maximum ground accelerations (or between absolute displacements) is equal to (6)

$$MF = \frac{\left[1 + \left(2\zeta\frac{\Omega_H}{\Omega}\right)^2\right]^{\frac{1}{2}}}{\left[\left\{1 - \left(\frac{\Omega_H}{\Omega}\right)^2\right\}^2 + \left(2\zeta\frac{\Omega_H}{\Omega}\right)^2\right]^{\frac{1}{2}}} \quad (5.1)$$

In the case of earthquake ground motion, the amplification factors AF, are defined as

$$AF = \frac{SA(\Omega, \zeta)}{A} \quad (5.2a)$$

and

$$AF = \frac{SD(\Omega, \zeta)}{D} \quad (5.2b)$$

for accelerations and relative displacements, respectively. Here, A and D are the maximum ground acceleration and displacement.

The measured acceleration and displacement magnification factors are compared in Table 5.2 with the calculated values for the case of harmonic ground motions. In the case of earthquake excitation the measured acceleration and displacement amplifications are compared with the

calculated values in Table 5.3 and Table 5.4, respectively. It is noted that the use of the average viscous damping gives a good approximation of the response except for very low earthquake excitations. Also given in Tables 5.3 and 5.4 are maximum amplifications calculated using scaled equivalent viscous damping, evaluated from the free vibrations at the same level of response as for the earthquake forced vibration. It is noted that in this case a good approximation is obtained for low earthquake excitations as well.

Since this study involves large excitations well into the inelastic range equivalent viscous damping calculated from the first cycles of free vibrations (rounded to the next 0.5%) will be used in the following. These damping values, which are somewhat lower than the average values, are also given in Table 5.1 and the envelopes of the free vibrations with these damping values are also given in Figures 5.1 to 5.3.

For large excitations associated with inelastic hysteresis energy dissipation the influence of a small error in the elastic viscous damping should have a negligible effect on the response.

5.1.1.2 Two-Story Structures

The natural frequencies and eigenvectors of the two story structures (without an appendage), were calculated from the eigenvalue problem of the 2-DOF system using the masses of the floors and the stiffnesses calculated from the results of the free vibrations of the single stories from which the two-story structure is assembled. These will be called the "calculated" frequencies in the following.

The eigenvectors were normalized so that the participation factors would be equal to unity; thereafter the diagonal generalized mass and

stiffness matrices were calculated. Since the participation factors are equal to 1.0, modal masses and stiffnesses of the equivalent two SDOF systems are obtained (13).

Damping matrices were constructed using the damping values obtained for the single-story structures from which the two-story structure is assembled. Two damping matrices were constructed for each structure, one using the average values and one using the lower values for large excitations.

The damping matrix of structure M1 which is composed of two identical stories can be diagonalized by the calculated eigenvectors; however, some coupling between the modes is expected because damping is not purely viscous. In the case of structure M2 the eigenvectors do not diagonalize the damping matrix and the off-diagonal terms of the generalized damping matrix will be neglected.

Neglecting the off-diagonal terms can be interpreted as weighing the damping according to the energy stored in the springs (35), (30), (51). This method for estimating modal damping ratios for structures with nonproportional damping was first suggested by Biggs (55), (56) and is still recommended for nuclear structures (2). Results of other studies show that the errors resulting from the use of this method are small (50) especially in cases where differences in stiffness (35) and damping (52) are not too large. It seems that the method should not be used for a combined structure-appendage system where large differences in both stiffness and damping are expected but it is recommended for estimating the damping of structures with nonproportional damping that support appendages (57). Recently, a correction of the diagonal terms was

suggested by taking into account the contributions of the neglected off diagonal terms (22). The correction factor, which is identical for both modes is

$$\left(1 - \frac{C_{12}^* C_{21}^*}{C_{11}^* C_{22}^*}\right), \quad (5.3)$$

and will be used in this study for comparison. Here C_{rc}^* is the term of the generalized damping matrix in row r and column c .

The calculated natural frequencies, eigenvectors, modal masses, modal stiffnesses and the two values (average and low) of modal damping ratios are given in Table 5.5a.

The measured free vibration acceleration records of the two-story structures (without appendage) are given in Figures 5.4 and 5.5 for structures M1 and M2, respectively. It is possible to express these accelerations as linear combinations of the two modes of the structure by using the calculated eigenvectors

$$\ddot{y}_1 \begin{Bmatrix} \phi_{11} \\ \phi_{21} \end{Bmatrix} + \ddot{y}_2 \begin{Bmatrix} \phi_{12} \\ \phi_{22} \end{Bmatrix} = \begin{Bmatrix} \ddot{x}_1 \\ \ddot{x}_2 \end{Bmatrix} \quad (5.4)$$

Here \ddot{y}_j is the modal acceleration of mode j and \ddot{x}_i is the acceleration of DOF i .

The modal accelerations \ddot{y}_j for the two-story structures calculated from Eq. 5.4, are plotted in Figures 5.6 and 5.7 for structures M1 and M2, respectively. It can be seen that similar to the single-story structures each mode behaves as a damped SDOF system with a fairly constant natural frequency and damping, which also is characterized by friction.

The natural frequencies and average equivalent viscous damping ratios were determined using the same methods that were used in Section 5.1.1.1 for the single-story structures. An equivalent viscous damping for large excitations was also determined. These values will be called the "measured" natural frequencies and damping in the following.

The measured natural frequencies and damping ratios are given in Table 5.5b and can be compared with the calculated values which are also given in Table 5.5b. The agreement between the frequencies is very good and it can be concluded that the calculated eigenvectors can be used to uncouple the results of the measurements and obtain modal responses. A reasonably good agreement is obtained in the damping considering that damping is nonproportional and that friction is represented as viscous damping. It is possible that some of the differences are caused by the differences in the level of excitation of the two modes in the free vibrations. It is interesting to try the correction of the diagonal terms, mentioned earlier (Eq. 5.3). The corrected modal damping ratios also are presented in Table 5.5b. It can be seen that a better agreement is obtained for mode 1 but agreement is less good in the case of mode 2.

Since this study involves large excitations the measured lower values of damping will be used, which is consistent with the values used for the single-story structures. The envelopes of free vibrations of the two modes, but having these measured damping ratios, are also given in Figures 5.6 and 5.7.

The natural frequencies and equivalent damping ratios obtained from free vibrations were checked to verify their validity in forced vibration. This was done by comparing in Table 5.6 measured modal amplifications of

the structures subjected to earthquake ground motions in the elastic range with modal amplifications calculated using these natural frequencies and damping ratios.

The measured modal responses were obtained by using Eq. 5.4 to transform the story accelerations into modal accelerations. The measured amplifications are defined as the ratios between the maximum values of these modal accelerations and the maximum ground acceleration. The calculated amplifications were obtained using Eq. 5.2a. It is noted that the agreement is good and it can be concluded that the measured viscous damping is a good approximation for the use in response calculations of the two-story structures.

5.1.1.3 Appendages

Typical measured free vibration acceleration records of the decoupled appendages are given in Figures 5.8 to 5.11. The response of appendages AS2 with a small mass and appendage AL3 with a large mass are given in Figures 5.8 and 5.9, respectively. It can be seen that these appendages behave as SDOF systems with very light damping. This behavior is typical in all cases where no damper was used (Table 4.3). The responses of appendages AS1 and AT6 are given in Figures 5.10 and 5.11, respectively. The behavior is typical in all cases where the damper was used.

The natural frequencies and damping ratios were calculated using the same methods that were used in Section 5.1.1.1 for the single-story structures and are given in Table 5.7. The envelopes of free vibrations with the calculated damping are also given in Figures 5.8 to 5.11.

Two of the decoupled appendages, namely AS2 and AS3 which were used in several experiments, were subjected to the ground motions of El Centro

and Melendy earthquakes. The measured amplifications are compared with the calculated amplifications in Table 5.8a. It is noted that the agreement is not as good as in the case of the single and two-story structures. A probable reason for the differences is that when damping is low small deviations in the natural frequencies may result in substantial changes in the response (Figures 4.3, 4.4 and 4.5).

The following steps were undertaken to verify the reason for the differences and suggest a correction, which could be used in the interpretation of the results of the experiments performed in this study. To see the influence of small deviations in the frequencies the standard deviations of the measured natural frequencies of the two appendages were determined. Maximum and minimum responses were calculated for this range of frequencies and are also presented in Table 5.8a. It is noted that the range of response is of the same order of magnitude as the differences between the measured and calculated responses. The procedure was then repeated for the damping, but the influence on the results was much smaller in this case. The next step was to try to obtain a more accurate value of the natural frequency during a test. This can be done by measuring the frequency at the end of the record where the response is essentially in free vibrations. Since free vibrations at the end of a record were not available in several experiments the frequency was measured in the region of maximum response. These frequencies were used to calculate corrected responses. The results are given in Table 5.8b and it is noted that a better agreement with the measurements is achieved.

5.1.2 Inelastic Properties

5.1.2.1 Single-Story Structures

A typical force-displacement plot of a static test of the single-story structures is shown in Figure 5.12 for structure S1. The behavior is characterized by a linear elastic portion and a curved portion as a transition to the plastic range.

A typical inelastic measured response of the single-story structure S1 to harmonic ground motion is given in Figure 5.13. Three inelastic hysteresis loops are shown in this case. It can be seen that static and dynamic inelastic behavior is similar. In practice the static force-deformation behavior is usually known and the dynamic behavior is taken as the same or estimated from the static behavior.

The equivalent stiffness and viscous damping ratios were calculated using the procedure based on the rotation of the viscous damping ellipse outlined in Section 3.3.3.2. The results are presented in Tables 5.9a and 5.9b. Table 5.9a contains the measured maximum ground and structure displacements, magnification factors, ductilities, as well as the energy dissipated in one cycle and the coefficient η . Table 5.9b contains the calculated secant stiffnesses, $\frac{K}{\mu}$, equivalent stiffnesses and damping ratios and the magnifications calculated using these equivalent systems. For comparison, the measured magnifications from Table 5.9a are also given. The agreement is good and it can be concluded that the method suggested in Section 3.3.3.2 is suitable for the determination of the equivalent linear system in the case of harmonic ground motion. It is also noted that the secant stiffness gives a very good approximation for

the equivalent stiffness, which is in agreement with Hadjian's conclusions (11). Therefore the secant stiffness will be used in the following.

Another approach for calculating the equivalent linear system was also tried. Replacement of the actual inelastic structure by an equivalent one means that the actual response is replaced by a harmonic response which is as close as possible to the actual. Such a harmonic response can be obtained by performing a Fourier Analysis of one cycle of the actual response and keeping only the term with the forcing frequency. This procedure was performed on both the displacement and resistance responses, giving a rotated elliptical force-displacement loop for each test. These rotated ellipses were practically identical to those obtained from the best fit with the hysteresis loops.

The maximum measured inelastic response of the single-story structures (without appendage) subjected to earthquakes is shown in Figures 5.14a and 5.14b. Also shown in these figures are the responses calculated using the equivalent linear systems of Shibata (Eqs. 3.83), Iwan (Eqs. 3.84) and Hadjian (Eqs. 3.86). The results are presented as amplifications, determined from Eq. 5.2a, as a function of ductility. It can be seen that the results are generally similar. The simplification by Hadjian gives a slightly better overall agreement with the experiments. Therefore Eqs. 3.86 will be used in this study. It should be noted that the equivalent damping ratios calculated by the three methods were very close so that most of the differences are caused by differences in the calculated equivalent linear frequency. Therefore it is expected that Eq. 3.86a will give a better estimate of the frequency shift than the other methods.

It is interesting to compare the measured amplifications with amplifications calculated using modified response spectra suggested by Newmark and Hall (33). Since the models in this study are in the frequency range of the constant acceleration amplification, Eq. 5.2a can be written as

$$AF = \frac{SA(\Omega, \zeta)}{A [2\mu - 1]^{1/2}} \quad (5.5)$$

Amplifications calculated from Eq. 5.5 are compared with the measured amplifications in Figures 5.15a and 5.15b. It can be seen that the agreement is similar to that obtained by using an equivalent system. In most cases the modified spectra underestimate the measured response but give a better description of the change in the response as a function of ductility. However the modified spectra does not provide an estimate of the change in the natural frequency, which is required for the determination of the response of an appendage.

5.1.2.2 Two-Story Structures

Three typical measured inelastic responses of the two-story structures subjected to earthquakes are shown in Figs. 5.16, 5.17 and 5.18. The three cases are: Structure M1 subjected to El Centro, structure M2 subjected to El Centro, and structure M1 subjected to Melendy ground motion. The results are presented as absolute accelerations and relative displacements (drifts) of the two stories.

Story inertia forces and story resistances (shears) were calculated from the story accelerations and masses as

$$F_1 = M_1 \ddot{x}_1 \quad , \quad (5.6a)$$

$$F_2 = M_2 \ddot{x}_2 \quad , \quad (5.6b)$$

$$R_1 = -F_1 - F_2 \quad , \quad \text{and} \quad (5.6c)$$

$$R_2 = -F_2 \quad , \quad (5.6d)$$

in which F_i is the inertia force of floor i and R_i is the resistance of story i . It should be noted that the elastic damping is included in the resistance so that Eqs. 5.6 are compatible with Eq. 3.90.

The story resistances are plotted against story relative displacements in Figures 5.19, 5.20 and 5.21, for the same three typical cases. Using the ductility definition from Section 3.3.2, story ductilities can be determined.

Modal displacements were obtained from story displacements relative to the ground by using Eq. 3.88 and modal resistances from story inertia forces using Eq. 3.90b. The modal resistances are plotted against modal displacements in Fig. 5.22, 5.23 and 5.24 for the same three typical cases. The following observations can be made:

- 1) The general behavior of both modes is similar to the force-deformation curves of SDOF inelastic systems, consisting of inelastic hysteresis loops.
- 2) Large modal inelastic excursions correspond to the large story inelastic excursions. However, the maximum modal deformations and maximum story deformation do not always occur simultaneously.
- 3) The shapes of the modal hysteresis loops is less regular than in the case of SDOF systems, particularly in the higher mode. Large irregularities can be observed in the case of Melendy ground motion.

- 4) Maximum resistances and maximum deformations do not always occur simultaneously and sometimes may occur in different cycles.
- 5) The slopes of the "elastic" parts of the modal hysteresis loops are equal to the modal elastic stiffnesses, K_j^* , which are also shown in the figures.

Modal ductility, μ_j , can be determined from the modal hysteresis loops, by using the ductility defined in Section 3.3.2. Eq. 3.73 will then take the form

$$\mu_j = \frac{K_j^* (u_j)_{\max}}{(R_j^y)_{\max}} \quad (5.7)$$

in which, $(u_j)_{\max}$ is the maximum modal displacement and $(R_j^y)_{\max}$ is the maximum modal force. However, in the case of Melendy ground motion where large irregularities exist this definition will not provide useful results. Therefore, in these cases $(R_j^y)_{\max}$ will be replaced by the maximum modal resistance that occurs during the maximum inelastic excursion $(u_j)_{\max}$.

The measured story and modal ductilities are given in Tables 5.10a, 5.10b and 5.10c for the three cases of the two-story structures (with and without appendage). Also given in these Tables are modal ductilities calculated from the measured story ductilities using the Eq. 3.93 suggested in this study and Eqs. 3.94 and 3.95 suggested by Tansirikongkol and Pecknold and by Villaverde, respectively. Story ductilities calculated from the measured modal ductilities using the method suggested by Lin and Mahin (25) are also presented in Tables 5.10a, 5.10b and 5.10c.

The measured and calculated modal ductilities are plotted as a function of the maximum ground acceleration, in Figures 5.25a, 5.25b, 5.26a, 5.26b, 5.27a and 5.27b.

Based on these tables and figures, the following observations can be made:

- 1) Both the measured and calculated results show that modal and story (local) ductilities are in the same range in general. This observation is in agreement with the results of previous studies where structures were designed assuming some average ductility which was then compared with calculated local ductilities (12), (23).
- 2) Reasonable agreement is obtained between modal ductilities measured and calculated using the three equations in cases where the modal hysteresis loops are regular (usually the first mode). Agreement deteriorates as the loops become more irregular (usually the second mode and Melendy ground motion).
- 3) Eq. 3.93 suggested in this study, tends to underestimate the modal ductility of the second mode.
- 4) Large scatter exist in the modal ductilities calculated using Eq. 3.94. This scatter is attributed to the fact that one of the story ductilities is equal or close to 1.0 in several cases.
- 5) Eq. 3.95 suggested by Villaverde gives the best overall agreement with the experiments.

In view of these observations, Eq. 3.95 will be used in this study. However, it should be remembered that Eq. 3.95 is valid for chain structures only.

5.2 Appendages on Single-Story Structures

5.2.1 Free Vibrations

5.2.1.1 Detuned Systems

The natural frequencies and eigenvectors of the combined detuned single-story structures with appendage, were calculated from the 2-DOF eigenvalue problem and are given in Table 5.11. These values will be called the "exact undamped" frequencies and eigenvectors in the following. The natural frequencies of the decoupled structures and appendages, and the approximate eigenvectors calculated from Eqs. 3.3 and 3.14 are also given in Table 5.11 for comparison. These values will be called the "approximate undamped" frequencies and eigenvectors in the following. The agreement is very good.

Typical measured free vibrations acceleration records of the combined detuned single-story structures with appendages are given in Figures 5.28 and 5.29 for the case of a small and large appendage mass, respectively. It is possible to perform a modal decomposition of these accelerations, by using Eq. 5.4 and the approximate eigenvectors.

The modal accelerations are plotted in Figures 5.30 and 5.31 for the same two cases. It can be seen that the modal responses are similar to the response of a SDOF system, meaning that a reasonable degree of uncoupling is achieved by using the approximate eigenvectors. Some coupling remains in the mode of the appendage.

The modal free vibrations of the combined systems can now be compared with the free vibrations of the decoupled systems. For example, mode 1 from Figure 5.30 is compared with Figure 5.2, mode 1 from Figure 5.31 is compared with Figure 5.1, and mode 2 from Figure 5.31 is compared with

Figure 5.9. There is a good agreement with the assumption made in Section 3.2.1, that the mode shape of the combined detuned system is composed of the unchanged mode shape of either the decoupled structure or appendage and the deformed shape of the other decoupled system. These observations will also be confirmed in Section 5.3.1, where the free vibrations of the combined two-story structures with appendages are treated.

The method described in Section 5.1.1.1 was used to determine the natural frequencies from the modal acceleration records. These values, which will be called the "measured" natural frequencies in the following, are also given in Table 5.11. The agreement with the exact and approximate undamped frequencies is good. It can be concluded that the use of approximate (decoupled) frequencies suggested in previous studies and approximate eigenvectors (Eqs. 3.3 and 3.14) is justified in the case of detuned appendages.

5.2.1.2 Tuned Systems

Typical measured free vibrations acceleration records of the combined tuned single-story structures with appendages are given for the following four cases: in Figure 5.32, for a system with low damping and small appendage mass, in Figure 5.33 for a system with low damping and large appendage mass, in Figure 5.34 for a system with a small appendage mass and larger appendage damping, and in Figure 5.35 for a system with a small appendage mass and larger structure and appendage damping.

The beat phenomenon is apparent in the cases where the appendage mass is small. The beat periods, calculated for each case using Eq. 3.35, are also given in the figures and the beat damping envelopes calculated using

Eq. 3.36 are also plotted in the figures. A good agreement between the measured and calculated beat period and damping can be observed.

Two sets of natural frequencies and eigenvectors, namely the exact undamped and the tuned damped, were calculated for the tuned systems and are given in Table 5.12. It is noted that there is a good agreement in the case of low damping. For larger damping, the agreement between the frequencies is good but some differences in the eigenvectors can be observed.

Modal decomposition was performed using the two sets of eigenvectors. The results are plotted in Figures 5.36 to 5.39 for the same four cases. It can be seen that some coupling between the modes remains after the decomposition. Both sets of eigenvectors deliver identical results except in the case of large damping where the tuned damped eigenvectors give a slightly better decomposition (Figure 5.39).

The method described in Section 5.1.1.1, was used to determine the natural frequencies from the modal acceleration records. These values which will be called the "measured" natural frequencies in the following, are also given in Table 5.12. Only the results of the tuned damped case are given in the table. The agreement with the calculated values is good.

The observations made in this section indicate that the use of the approximate natural frequencies and eigenvectors (37) is justified in the case of tuned appendages even for large appendage mass up to 10 percent of the structure mass.

5.2.1.3 Slightly Detuned Systems

When the combined system is close to tuning damping cannot be neglected in the calculations. Nevertheless, the exact undamped and

approximate undamped natural frequencies and eigenvectors were determined for the slightly detuned systems as well and are given in Table 5.13a. It is noted that some differences exist in the natural frequencies and the eigenvectors. Natural frequencies and eigenvectors were also calculated, using the expressions given by Ruzicka and Robinson (37) for the tuned case and including the influence of slight detuning and damping (38), (37). These values which will be called the "tuned damped" natural frequencies and eigenvectors in the following are given in Table 5.13b. The approximate undamped frequencies and eigenvectors from Table 5.13a are also given in Table 5.13b for comparison. It is noted that the differences in the eigenvectors are substantial, although the differences in the natural frequencies are relatively small. This is not surprising since the frequencies are either equal to the decoupled frequencies in the detuned case, or close to the decoupled frequencies in tuned case (Eq. 3.27). The differences in the eigenvectors may lead to substantial differences in the appendage response if one method is used instead of the other. This observation will be confirmed in Section 5.2.2.3 where the response of the slightly detuned system subjected to earthquake ground motions is treated.

Typical measured free vibrations acceleration records of the combined slightly detuned single-story structures with appendages are given in Figures 5.40 and 5.41. Figure 5.40 represents a boundary case that could be considered either detuned or slightly detuned, according to the range defined by Eq. 3.66.

Modal decomposition of the structure and appendage acceleration records was performed using the three pairs of eigenvectors from Table

5.13. Typical results are plotted in Figure 5.42 for the case given in Figure 5.40 and in Figure 5.43 for the case given in Figure 5.41. It can be seen that substantial coupling remains in the second mode (appendage mode) in the case where the system is at the boundary of detuning, regardless of the eigenvectors used in the decomposition (Figure 5.42). In the case of the system closer to tuning reasonable uncoupling is obtained when the exact undamped or the tuned damped eigenvectors are used in the decomposition (Figure 5.43).

The method described in Section 5.1.1.1 was used to determine the natural frequencies from the modal acceleration records. These values which will be called the "measured" natural frequencies in the following are also given in Table 5.13b. Only the results of the approximate undamped and tuned damped case are given in the table. The agreement with the calculated values is good.

The observations made in this section are compatible with the assumption made in Section 3.2.3, that the slightly detuned case can be used as a transition between the tuned and the detuned case. However, it is expected that the estimated appendage response will not be as good as in the cases of a detuned or tuned appendage, particularly in cases that are near the boundary of detuning.

5.2.2 Earthquakes

5.2.2.1 General

Amplification factors, defined as the ratio between the maximum appendage acceleration response and maximum ground acceleration are used in comparison of the experimental and analytical results:

$$AF = \frac{\ddot{x}_{max}}{A} \quad (5.8)$$

In the case of an experiment, \ddot{x}_{max} is the maximum measured appendage acceleration. In the case of an analysis an equation from Section 3.2 is substituted for \ddot{x}_{max} depending if the system is tuned or detuned. When the structure behaves inelastically the equivalent linear system from Section 3.3 is used in the calculation.

5.2.2.2 Detuned Systems

The measured amplification factors of the detuned appendages are plotted as a function of the measured ductilities for different supporting structures in Figures 5.44 to 5.48.

Amplification factors were calculated using Eq. 3.24 and are plotted in Figures 5.44 to 5.48 together with the measured values. An upper bound was estimated by using the ABSS rule instead of the SRSS in Eq. 3.24. A lower bound was estimated by taking only the larger of the two terms in Eq. 3.24. These upper and lower bounds are also plotted in the same figures.

It can be seen that a reasonable agreement exists between the measured and calculated amplification. The agreement is approximately the same for elastic ($\mu=1.0$) and inelastic supporting structures, and for the small and large appendage mass. In most cases the measured amplifications lie between the calculated lower and upper bounds.

Some exceptions, where the measured amplifications of the appendages are smaller than the lower bound, can be seen in the figures. These cases can be divided in two groups. One group includes cases where the combined

system is close to the boundary between slight detuning and detuning (Eq. 3.65). Such cases are appendage AS3 on structure S4 (Figure 5.46) and appendage AS3 on structure S5 (Figure 5.47) that are close to the boundary at low ductility and become detuned for larger ductilities. Recalculation of these cases as slightly detuned gave a better agreement with the measurements. Other examples are appendage AS2 on structure S4 (Figure 5.46) and appendage AS2 on structure S5 (Figure 5.47) that are detuned at low ductilities and approach the boundary for larger ductilities. Recalculation of these cases as slightly detuned provided results which were lower than the measurements.

The second group includes cases of large ductilities of structure S2 (Figures 5.45). These systems are not close to the boundary of slight detuning. An inspection of Eq. 3.24 leads to the suggestion that the reason for the differences should be found by examining the response spectra, $SA(\Omega, \zeta)$, of the (equivalent linear) supporting structure. For detuned systems the terms containing the frequency ratios should not be sensitive to relatively small changes in the frequency, Ω , and the response spectrum, $SA(\omega_0, \zeta_0)$, of the (elastic) appendage does not change.

The response spectra amplifications of the equivalent linear supporting structures are given in Table 5.14. The measured amplifications of these structures are also given in the table. It is noted that for large ductilities the response spectra of the equivalent linear system overestimate the response which is limited by the resistance of the structure. Also given in Table 5.14 are the Newmark and Hall (33) modified response spectra amplifications calculated using Eq. 5.5. It is

noted that generally the modified spectra underestimate the response but give better estimates for large ductilities.

Amplification factors for the appendages were recalculated using the yield resistances instead of response spectra of the equivalent linear systems. In most cases the results were slightly lower than those obtained using the equivalent linear system. In some cases of large ductility the results were substantially lower. The lower bounds for these cases are also plotted in Figures 5.45 and 5.47. It can be seen that in the cases of Figure 5.45 a better agreement between the measured and calculated response is achieved when the response spectra of the equivalent linear systems are replaced by the resistances of the structures. However, in the case of Figure 5.47 this procedure may underestimate the appendage response.

It can be concluded that the response of a detuned appendage mounted on a SDOF structure that behaves inelastically can be estimated from Eq. 3.24 by replacing the actual structure with an equivalent linear system. The procedure can be used for appendage weight of up to at least 10 percent of the weight of the structure. In cases of large ductilities, this procedure may overestimate the appendage response. If the response spectrum of the (equivalent linear) structure, $SA(\Omega, \zeta)$, used in Eq. 3.24, is limited to the resistance of the structure, a better estimate of the appendage response can be obtained in cases of large ductilities. However, in some cases the appendage response will be underestimated. When the combined (elastic or inelastic) system is close to the boundary of slight detuning, Eq. 3.24 will overestimate the appendage response.

5.2.2.3 Tuned and Slightly Detuned Systems

The measured amplification factors of the tuned and slightly detuned appendages, normalized to the calculated \ddot{x}_ζ are plotted as a function of $\sqrt{\gamma}/2\zeta$ in Figure 5.49a. It should be noted that these experiments include the large and small appendage masses, two earthquakes (El Centro and Melendy) and different levels of inelastic behavior. Four curves from Figure 3.1 are also plotted in Figure 5.49a. These curves are the line of the upper bound suggested in this study (Eq. 3.37), the curve based on the maximum of the beat envelope (Eq. 3.43) and the two curves of the lower bound suggested in this study (Eq. 3.51).

It can be seen that a good agreement is obtained and that most of the measured results are located between the calculated lower and upper bounds and follow the curve of the maximum of the beat envelope, Eq. 3.43.

At this stage the difference between Eq. 3.40 in which the FAS is used and Eq. 3.42 in which the response spectra is used will be discussed briefly. The responses of the tuned and slightly detuned appendages were calculated also using Eq. 3.40. The results were similar to those obtained from Eq. 3.42 but the scatter was large. This scatter is attributed to the erratic behavior of the FAS. In the following Eq. 3.40 will be used.

A few exceptions (5 tests) can be seen in Figure 5.49a, where the measured appendage amplifications are underestimated even by the suggested upper bound. An inspection of the three tuned cases shows that these systems, which are tuned when the supporting structure responds elastically, approach the boundary of detuning for large ductilities (and large equivalent damping). Recalculation of these cases as detuned gave

results that were in better agreement with the measurements (slightly overestimated). The two slightly detuned cases are elastic systems with a large appendage mass and light damping, also close to the boundary of detuning. Recalculation of these cases as detuned gave results that overestimated the measurements by approximately 60 percent and 70 percent.

Figure 5.49b depicts the same results grouped according to the two earthquakes used in these tests. It can be seen that although generally the agreement is similar for both earthquakes, the calculations tend to underestimate the measurements in the case of El Centro earthquake and to overestimate the measurements in the case of Melendy earthquake. This tendency is not a coincidence since the systems of the three cases, which approach detuning at large ductilities when subjected to El Centro, were also subjected to Melendy ground motion and reached the same levels of ductility; however, the results were not underestimated by the calculations. Actually these test results are located close to the curves of the lower bound near the origin of Figure 5.49b.

Figure 5.49c presents the results according to the size of the mass. Typically either a small mass (approx. 1 percent of floor weight) or a large mass (approx. 10 percent of floor weight) is used in the comparison. No specific relationship between amplification and mass size can be seen in this figure.

Figure 5.50 depicts the results according to the level of inelastic response of the supporting structure: elastic, inelastic with moderate ductility of up to 2.0, and inelastic with large ductility of 2.0 or larger. It seems that the scatter in the results of the elastic tests is slightly larger. This is attributed to the erratic behavior of the

response spectra at low damping. It can also be seen that several tests, where large ductilities were reached, are located close or even below the estimated lower bound (overestimated). Similarly to the case of the detuned systems the reason for the differences between the measured and calculated results should be located in the response spectra of the (equivalent linear) supporting structure, which is limited to the resistance of the structure. However, in the case of a tuned (or slightly detuned) system the response spectrum of the combined system is used instead of the response spectra of the decoupled structure and appendage. At this stage it should be reminded that when the tuned case was interpreted as an absolute sum in Section 3.2.2 it was assumed that the response spectra of the structure and the appendage were approximately the same (Eq. 3.29). This is not the case when the response of the structure is limited by its resistance. Therefore it will be assumed that in cases of large ductilities the response spectrum of the combined system can be approximated as the average of the resistance of the structure and the response spectrum determined for the combined (equivalent linear) system. This approximation can be interpreted as an absolute sum with two different response spectra. The results were corrected by using this average response spectra in the calculations. This correction was applied only to the cases where the ductility was equal or larger than 2.0. The results are replotted in Figure 5.51 and it can be seen that generally the agreement with the calculated values is improved. However, some of the measurements are underestimated by the correction.

It was noted earlier that the scatter in the results was approximately the same in both elastic and inelastic cases. However, only

a limited number of elastic tests were performed. Therefore, additional "numerical tests" of elastic tuned and slightly detuned systems were carried out. The systems were chosen so that their elastic stiffnesses and damping ratios were equal to those of the elastic and equivalent linear systems used in the experiments, and were subjected to the same ground motions. The results are plotted in Figure 5.52 and it can be seen that only a small improvement of the scatter is obtained.

It was observed earlier that the size of the appendage mass did not have a significant influence on the agreement between the measured and calculated appendage amplifications. To see the influence of the size of the mass on the response, the values of the transfer function were calculated for all the tests given in Figure 5.49a, using Eq. 3.61. These values are shown in Figure 5.53 as a function of the frequency ratio. Since some mass was added on the appendage to obtain tuning, the effective mass, $\gamma + 4\zeta_0\zeta$, of the small tuned appendages varied between 1.0 percent and 2.5 percent of the floor mass. Therefore, the results for the small mass are given in three groups according to the size of the mass. Some curves from Figures 3.2 and 3.3 also are plotted in Figure 5.53. These curves are those for the detuned case (SRSS and ABSS) and those for the slightly detuned case with mass ratios of 1.0 and 10.0 percent. Curves for the slightly detuned case with mass ratios of 1.5, 2.0 and 2.5 percent were added in Figure 5.53. It should be remembered that the curves of the slightly detuned case are based on Eq. 3.37 and therefore represent the upper bounds. Although some scatter can be seen, the agreement between the measurements and the calculations is remarkable. Only a few measurements lie above the relevant curves. These exceptions are the same

cases treated earlier in relation with Figure 5.49a. It is interesting to note that the detuned ABSS gives a good estimate of these cases. Also, it is interesting to note that even in these cases the response does not exceed the calculated response of the tuned case with the same appendage effective mass. This is in agreement with considerations of energy transfer between the structure and appendage (38).

Selected measured results are presented in Figure 5.54 through 5.69. These experiments were chosen so that certain trends in the behavior of the combined systems could be observed. Ground acceleration, structure deformation and acceleration, as well as appendage acceleration are plotted as a function of time. Also given in these figures are calculated maximum appendage responses and the equation used to calculate them.

Results for structure S8 supporting appendage AT2 and subjected to different levels of El-Centro are given in Figures 5.54 to 5.57. The beat phenomenon is apparent in cases of low ductility. In these cases, Eq. 3.43 based on the maximum of the beat envelope gives a good estimate of the maximum appendage response, which is located in the nearly free beats after the first main ground shock (Figures 5.54 and 5.55). As the ductility increases the beat is still apparent in the appendage response. Eq. 3.43 underestimates the maximum response which occurs later during the earthquake (Figure 5.56). However, the maximum response is less than the upper bound calculated using Eq. 3.37 and also given in Figure 5.56. For larger ductility this particular combined system becomes detuned and the maximum appendage response is slightly underestimated even when Eq. 3.37 is used (Figure 5.57). This is one of the cases discussed earlier in relation to Figure 5.49.

Results for structure S8 supporting appendage AT3 and subjected to different levels of Melendy are given in Figures 5.58 to 5.61. In cases of low ductility Eq. 3.43 gives a good estimate of the maximum appendage response (figures 5.58 and 5.59). As the ductility increases, Eq. 3.43 overestimates the maximum response (Figure 5.60). However, the maximum response is larger than the lower bound estimated from Eq. 3.51 and also given in Figure 5.60. For larger ductility the maximum appendage response is overestimated even when Eq. 3.51 is used (Figure 5.61). A slightly better agreement is obtained when Eq. 3.43 is used with the yield resistance of the structure.

Results for structure S4 supporting appendage AT6, subjected to El-Centro and Melendy, are given in Figures 5.62 to 5.65. Only one case of low ductility and one case of high ductility is shown for each earthquake. In this combined system both structure and appendage have elastic damping ratios that are higher than those of the systems discussed previously. The general behavior and the predictions of the maximum appendage response are similar to the systems with low elastic damping.

Results for structure S9 supporting appendage AT7 subjected to El-Centro and Melendy are given in Figures 5.66 to 5.69. Again only one case of low ductility and one case of high ductility is shown for each earthquake. In this combined system elastic damping ratios are low but the appendage mass is large. Although the beat phenomenon can hardly be seen even in the cases of low ductility, Eq. 3.43 still provides good estimates of the appendage maximum response. Generally the trends are similar to the cases described earlier.

It can be concluded that the response of a tuned or slightly detuned appendage mounted on a SDOF structure that behaves inelastically can be estimated from Eq. 3.43 by replacing the actual structure with an equivalent linear system. An upper bound of the response can be estimated from Eq. 3.37. The use of the average of the resistance of the structure and the response spectrum of the (equivalent linear) combined system is not recommended since it may lead to underestimates of the appendage maximum response, particularly in cases of long earthquakes.

5.3 Appendages on Two-Story Structures

5.3.1 Free Vibrations

The natural frequencies and eigenvectors of the combined two-story structures with appendages were calculated from the 3-DOF eigenvalue problem and are given in Table 5.15a for structure M1 and in Table 5.15b for structure M2. These values will be called the "exact undamped" frequencies and eigenvectors in the following. The natural frequencies of the decoupled structures and appendages, and the approximate eigenvectors calculated from Eqs. 3.3 and 3.14 are also given in Tables 5.15a and 5.15b for comparison. These values will be called the "approximate undamped" frequencies and eigenvectors in the following. The agreement is good.

Typical measured free vibrations acceleration records of the combined two-story structures with appendages mounted on either story, are given in Figures 5.70 to 5.75. It is possible to perform a modal decomposition of these accelerations by using Eq. 5.4 (but for three degrees of freedom) and the approximate eigenvectors.

The modal accelerations are plotted in Figures 5.76 to 5.81 for the same systems given in Figures 5.70 to 5.75. It can be seen that uncoupling of the two structural modes is very good. Some coupling remains in the mode of the appendage. This is not surprising since the frequency of the appendage is close (although not in the range of slight detuning) to one frequency of the structure and damping is nonproportional. It should be remembered that some coupling also was observed in the free vibrations of the appendages on SOF structures.

The modal free vibrations of the combined systems can now be compared with the free vibrations of the decoupled systems. For example, the modes of the structure from Figures 5.76, 5.77 and 5.78 are compared with the modes in Figure 5.6. Similarly, the modes of the structure from Figures 5.79, 5.80 and 5.81 are compared with the modes in Figure 5.7. Also, the appendage modes from Figures 5.76 and 5.79 are compared with Figure 5.8. The agreement is good in the case of the modes of the structures. Although coupling exists in the case of the modes of the appendage, the general behavior of the frequency and even the damping is similar. There is a good agreement with the assumption made in Section 3.2.1, that the mode shape of the combined detuned system is composed of the unchanged mode shape of either the decoupled structure or appendage and the deformed shape of the other decoupled system. These observations were also confirmed in Section 5.2.1.1, where the free vibrations of the combined single-story structures with appendages were treated.

The method described in Section 5.1.2.1 was used to determine the natural frequencies from the modal acceleration records. These values which will be called the "measured" natural frequencies in the following

are also given in Tables 5.15a and 5.15b. There is a good agreement with the exact and approximate undamped frequencies and it can be concluded that the use of approximate natural frequencies and eigenvectors is justified in the case of detuned appendages on MDOF structures. The approximate eigenvectors will be used to determine the modal responses of the supporting structure from floor responses, when the combined systems will be subjected to earthquakes.

5.3.2 Earthquakes

The measured appendage amplification factors determined using Eq. 5.8, are plotted as a function of the maximum ground acceleration in Figures 5.82 to 5.84. Results are given for structure M1 subjected to El Centro in Figure 5.82, for structure M2 subjected to El Centro in Figure 5.83, and for structure M1 subjected to Melendy in Figure 5.84.

The combined systems with the two-story structures were designed to be detuned in the elastic range. Therefore, Eq. 3.21 was used to calculate the maximum response of the appendage. An upper bound was also calculated using the ABSS rule instead of the SRSS rule. Modal ductilities and equivalent linear modes were determined from story ductilities and were used in the calculations. The calculated appendage amplification factors also are given in Figures 5.82 to 5.84. It can be seen that a good agreement is obtained between the calculated and the measured amplifications in all the cases of supporting structure M1 and the measured amplifications are always less than the calculated upper bound. In the case of supporting structure M2, reasonable agreement is obtained when appendage AS2 is mounted on either story. However, in the

case of appendage AS3 on structure M2, Eq. 3.21 overestimates the measured appendage response. The differences between the measured and calculated responses are particularly large when appendage AS3 is mounted on the first floor of structure M2. Actually, in this case most of the calculated values lie outside the boundary of the relevant plot in Figure 5.83.

The natural frequency of appendage AS3 (5.89 Hz) is close to the natural frequency of mode 2 (7.23 Hz) of the structure. As the inelastic response of the structure increases, its natural frequencies decrease. In the case where the appendage is mounted on the first floor, the system approaches and then enters the range of slight detuning. In the case where the appendage is mounted on the second floor, the appendage approaches slight detuning for large ductility. The response was recalculated for these cases, assuming slight detuning of the appendage with mode 2 of the structure and the results are also plotted in Figure 5.83. The SRSS rule was used to combine the amplification of the slightly detuned mode (Eq. 3.43) with those of the detuned mode. The upper bound was determined by calculating the upper bound of the slightly detuned case (Eq. 3.37) and using the ABSS rule to combine this result with the terms of the detuned mode. It can be seen that the agreement is improved.

Selected measured results are presented in Figures 5.85 through 5.92. These experiments were chosen so that certain trends in the behavior of the appendages could be observed. Ground acceleration, accelerations of the two floors, deformation of the yielding story, as well as appendage acceleration are plotted as a function of time. Also given in these

figures are calculated maximum appendage responses and the equation used to calculate them.

Results for appendage AS3 mounted on the second floor of structure M1 and subjected to El Centro are given in Figure 5.85 and Figure 5.86 for cases of low and high ductility, respectively. It can be seen that the appendage responds in its own frequency as well as the frequencies of the structure (mainly first mode). For such a behavior, the SRSS gives a good estimate of the appendage maximum response for low as well as high ductility. This behavior is representative for both appendages AS3 and AS2 mounted on either story of structure M1.

Results for appendage AS3 mounted on the second floor of structure M1 and subjected to Melendy are given in Figure 5.87 and Figure 5.88 for cases of low and high ductility, respectively. It can be seen that the appendage responds mainly in its own frequency with some contribution from the frequencies of the structure. For such a behavior, the SRSS slightly underestimates, while the ABSS slightly overestimates, the appendage maximum response for low as well as high ductility. This behavior is representative for both appendages AS3 and AS2 mounted on either story of structure M1.

Results for appendage AS2 mounted on the first floor of structure M2 and subjected to El Centro are given in Figure 5.89 and Figure 5.90 for cases of low and high ductility, respectively. It can be seen that the appendage responds essentially in its own frequency with a slowly changing amplitude. For such a behavior, the ABSS gives a good estimate of the appendage maximum response for low as well as high ductility.

Results for appendage AS2 mounted on the second floor of structure M2 and subjected to El Centro, are similar to those of appendages AS2 and AS3 mounted on structure M1.

Results for appendage AS3 mounted on the first floor of structure M2 and subjected to El Centro are given in Figure 5.91 and Figure 5.92 for cases of low and high ductility, respectively. This is the combined system that is close to the boundary of slight detuning in the elastic range (mode 2 of the structure). For larger ductility the system enters the range of slight detuning. A beat that leads to the appendage maximum response can be seen in Figure 5.92. Calculation of this system as detuned delivered results that overestimated the measurements by 100 percent for low ductility and by up to 300 percent for high ductility. Recalculation of the system as tuned, using Eq. 3.37 for the upper bound and SRSS, leads to substantial improvement of the agreement with the measurements (also see Figure 5.83). For low ductility Eq. 3.43 and SRSS gives a slightly better agreement (Figures 5.92 and 5.83).

The two story structures represent MDOF supporting structures in general. It is anticipated that the maximum response of a SDOF appendage with a single support, and mounted in a MDOF structure that behaves inelastically, can be estimated by replacing the actual structure with an equivalent linear MDOF system. The properties of this linear system can be estimated by using the concept of modal ductilities. The maximum response can be estimated for a detuned appendage, as well as an appendage that is tuned (or slightly detuned) to one mode of the structure.

CHAPTER 6. DESIGN APPROACH FOR APPENDAGES ON INELASTIC STRUCTURES

6.1 General

In this chapter a design approach for appendages on elastic and inelastic structures which is based on the results of this study is suggested. This approach is valid for a SDOF appendage supported on a SDOF structure or supported at one point in a MDOF structure. The appendage can be detuned or tuned to one frequency of the supporting structure. This approach can be easily expanded to a MDOF appendage with one tuned frequency. Also, it is expected that the method could be used in cases where more than one tuned frequency exists if these tuned frequencies are not close to each other.

6.2 SDOF Supporting StructureA. Equivalent Linear System

Given the force-deformation relation of the structure and the design (or evaluated) ductility, determine the properties of the equivalent linear system:

- a) Determine the ellipse of viscous damping for harmonic ground motion (eq. 3.76).
- b) Rotate the ellipse to obtain the best fit with the actual hysteresis loop. The rotated abscissa gives the equivalent linear stiffness (and frequency) for harmonic ground motion.
- c) Determine the equivalent viscous damping from Eq. 3.81.

Note: In many cases the secant stiffness gives a good approximation of the equivalent linear stiffness. In such

cases, the equivalent viscous damping can be determined from Eq. 3.82.

- d) Determine the equivalent linear frequency and damping for earthquakes from Eq. 3.86 and Eq. 3.85b, respectively. This equivalent linear system replaces the actual structure in the following.

B. Check for Tuning

- a) Calculate the effective mass ratio from Eq. 3.45b.
 b) Calculate the frequency ratio, ω_0/Ω .
 c) Check if the system is detuned or slightly detuned (or tuned) using Eq. 3.66, and the results of (a) and (b).

C. Maximum Response of a Detuned Appendage

- a) Use Eq. 3.24 to evaluate the maximum response of the appendage.
 b) Use Eq. 3.24 but with ABSS instead of SRSS to obtain an estimate of the upper bound of the maximum response of the appendage.

D. Maximum Response of a Tuned Appendage

Proportional Damping ($\zeta_0 = \zeta$)

- a) Calculate the coefficient κ from Eq. 3.41.
 b) Calculate the maximum response of the appendage from Eq. 3.42.
 c) Use Eq. 3.37 to obtain an estimate of the upper bound of the maximum response of the appendage.

Nonproportional Damping ($\zeta_0 \neq \zeta$)

- a) Calculate the effective mass ratio from Eq. 3.45a.
 b) Calculate the average damping of the combined system.
 c) Calculate the coefficient κ using Eq. 3.41 and (a) and (b).
 d) Determine the denominator of Eq. 3.42 from Eq. 3.45b.

- e) Determine the acceleration response spectrum at the tuning frequency and average damping.
- f) Calculate the maximum response of the appendage from Eq. 3.42 and (c), (d), and (e).
- g) Use Eq. 3.37 to obtain an estimate of the upper bound of the maximum response of the appendage.

E. Maximum Response of a Slightly Detuned Appendage

Proportional Damping

- a) Calculate the effective mass ratio by substitution of Eq. 3.54 into Eq. 3.56.
- b) Calculate the effective tuning frequency as the average frequency of the combined system.
- c) Repeat steps (a), (b) and (c) for a tuned appendage using the effective mass ratio and tuning frequency calculated in this section.

Nonproportional Damping

- a) Calculate the effective mass ratio by substitution of Eqs. 3.45a and 3.54 into Eq. 3.56.
- b) Calculate the effective tuning frequency as the average frequency of the combined system.
- c) Repeat steps (b) through (g) for a tuned appendage using the effective mass ratio and tuning frequency calculated in this section.

6.3 MDOF Supporting Structure

A. Equivalent Linear System

- a) Evaluate member (or story) ductilities using a conventional procedure for nonlinear analysis.
- b) Estimate modal ductilities from member ductilities. Eq. 3.95 should be used for chain structures. In the case of more complex structures, the matrix (Eq. 3.96) should be determined case by case. In such cases Eq. 3.93 can be used as an alternative.
- c) Calculate the equivalent linear modal stiffnesses for harmonic ground motion as the secant stiffness using the modal ductilities.
- d) Calculate the equivalent linear modal damping ratios for harmonic ground motion using Eq. 3.82.
- e) Determine the equivalent linear frequencies and damping ratios for earthquake from Eq. 3.86 and Eq. 3.85b, respectively.

In the following each mode is treated as a SDOF equivalent linear system which replaces the actual structure. The elastic mode shapes are used in the calculations.

B. Check for Tuning

- a) Calculate the effective mass ratio assuming that the modal mass of the structure is concentrated at the point of the support of the appendage (Eq. 3.71) and from Eq. 3.45b.
- b) Repeat steps (a) and (b) from Section 6.2 - D - Proportional Tuning, for each mode.

- C. Maximum Response of a Detuned Appendage
- a) Use Eq. 3.21 to evaluate the maximum response of the appendage.
 - b) Use Eq. 3.21 but with ABSS instead of SRSS to obtain an estimate of the upper bound of the maximum response of the appendage.
- D. Maximum Response of an Appendage with a Tuned or Slightly Detuned Mode
- a) The response of the detuned modes is obtained using the procedure outlined in paragraph 3 of this section.
 - b) The response of the tuned mode is evaluated employing the procedure outlined in paragraph 4 (or 5) of Section 6.2 and using Eq. 3.72 instead of 3.43.
 - c) An upper bound of the maximum response of the tuned mode can be obtained by setting the exponent in the numerator of Eq. 3.72 equal to 1.0 (analogy with Eq. 3.37).
 - d) The responses obtained in (a) and (b) (or (c)) should be combined using the SRSS rule.
 - e) An upper bound of the total response can be estimated by using ABSS instead of SRSS.

CHAPTER 7. CONCLUSIONS

7.1 Summary and Conclusions

In this study a procedure is suggested for estimating the maximum response of an appendage mounted on an inelastic structure using the concepts of equivalent linear system and modal ductility. An extensive experimental program was undertaken to evaluate the suggested procedure.

A simple interpretation of an elastic detuned appendage is derived. It is shown that the tuned appendage can be considered as a limiting case of the detuned appendage and that the transition can be approximated using the slightly detuned appendage.

In the case of a SDOF inelastic supporting structure, the actual structure is replaced by an equivalent linear system. In the case of a MDOF inelastic supporting structure, the concept of modal ductility is used to obtain equivalent linear modes.

A series of experiments of SDOF appendages mounted on one- and two-story structures was performed. The combined systems were subjected to earthquake motions. A good agreement was obtained between the measurements and the maximum appendages responses evaluated using the suggested procedure. In fact, even certain trends of behavior, such as tuning or detuning as a result of inelastic behavior, were apparent in both the experimental and calculated results.

The main conclusion of this study is that the concepts of equivalent linear system and modal ductility provide a good tool for estimating the maximum response of an appendage mounted on an inelastic supporting structure. The expected accuracy is about the same for elastic and

inelastic supporting structures. It seems that inaccuracy resulting from the approximations in the evaluation of the maximum responses of the different tuned, detuned and particularly slightly detuned modes, as well as that resulting from the rules for the summation of these responses is larger than the inaccuracy introduced by using the equivalent linear system and modal ductility.

7.2 Suggestions for Future Research

The concept of the equivalent linear system has been in use for a long time, while the concept of modal ductility was introduced only recently. A refinement of these procedures is recommended for the use in the analysis of both inelastic primary structures and supported equipment.

The most crucial problems in evaluating the maximum response of an appendage are:

to decide when to use upper (or lower) bounds to estimate the response of the tuned and slightly detuned modes; and to decide how to combine the responses of different modes.

It is recommended that some work will be devoted to these subjects. A random vibrations approach will probably be needed to do this.

TABLES

Table 3.1 Normalized Expressions for the Maximum Response of a Tuned Appendage

Study	Reference	Equation	$\ddot{x}_{\max}/\ddot{x}_\zeta$
Ruzicka Sackman	37 38	3.43	$e^{-\kappa}$
Villaverde	53	3.46	$\frac{1}{\sqrt{2}}$
Nakhata	29	3.48	$\frac{1}{[1 + \delta]^{1/2}}$
This Study	-----	3.37	1
Undamped	-----	3.32	$\left[1 + \left(\frac{2\zeta}{\sqrt{\gamma}}\right)^2\right]^{1/2}$

Table 4.1 List of the Single-Story Structures

Structure	Floor weight* (lb)	Design Natural frequency (Hz)	Design Yield strength (lb)
S1	264.0	3.16	183
S2	264.0	2.90	100
S3	264.0	3.01	46
S4	264.0	5.75	195
S5	264.0	5.99	88
S7	267.5	7.22**	390
S8	258.0	5.81**	208
S9	270.0	5.68**	207
S4	264.0	5.75***	195

* Floor weights include all fixtures and measurement devices.

** Tuning systems with all columns restrained.

*** Tuning systems with hinged structure.

Table 4.2 List of the Two-Story Structures

Structure	Floor	Floor Type	Floor Weight* (lb)	Floor Natural Frequency (Hz)	Floor Yield Strength (lb)
M1	1	S1	264.0	3.16	183
	2	S1	253.0	3.23	183
M2	1	S6**	264.0	7.27	372
	2	S2	253.0	2.96	100

* Floor weights include all fixtures and measurement devices.

** Not used as a single-story structure.

Table 4.3 List of the Appendages

Appendage	Weight* (lb)	Design Natural Frequency (Hz)	Remarks
AS1	3.30	1.5	
AS2	3.30	3.0	
AS3	3.30	6.0	
AS4	3.30	9.0	
AL1	26.09	1.5	
AL1a	26.46	1.5	damper
AL1b	26.46	1.5	damper
AL1c	26.46	1.5	damper
AL1d	26.46	1.5	damper
AL2	26.09	3.0	
AL3	26.09	6.0	
AL4	26.09	9.0	
AT1	3.23	6**	
AT2	3.73	6**	
AT3	4.49	6**	
AT4	3.66	6**	damper
AT5	4.25	6**	
AT6	4.23	6**	damper
AT7	26.09	6**	

* Appendage weights include all fixtures and measurement devices.
 ** Tuning systems.

Table 4.4 List of the Combined Systems Composed of Single-Story Structures and Appendages and the Earthquake Ground Motions Used in the Tests

Appendage	Structure							
	S1	S2	S3	S4	S5	S7	S8	S9
AS1	E	E						
AS2	E	E M T		E	E			
AS3	E	E M		E	E			
AS4	E	E		E	E			
AL1	E	E	E					
AL1a			E					
AL1b			E					
AL1c			E					
AL1d			E					
AL2	E	E						
AL3	E	E						
AL4	E	E						
AT1						E M		
AT2							E M	
AT3							M	
AT4							E M	
AT5				E M				
AT6				E M				
AT7								E M

Remark: E = El Centro earthquake
M = Melendy earthquake
T = Taft earthquake

Table 4.5 List of the Combined Systems Composed of Two-Story Structures and Appendages and the Earthquake Ground Motions Used in the Tests

Appendage	Structure			
	M1		M2	
	Story		Story	
	1	2	1	2
AS2	E M	E M	E	E
AS3	E M	E M	E	E

Remark: E - El Centro earthquake
M - Melendy earthquake

Table 5.1 Measured Natural Frequencies, Masses, Stiffnesses and Equivalent Viscous Damping Ratios of the Single-Story Structures

Structure	Mass (lb*sec ² /in)	Natural Frequency (Hz)	Elastic Stiffness (lb/in)	Average Viscous Damping (%)	Viscous Damping for Large Excitations (%)
S1	0.683	2.90	226.66	3.69	3.00
S1a	0.751	2.74	223.07	4.66	4.00
S2	0.683	2.59	181.08	4.72	4.00
S3	0.683	2.43	159.55	7.03	4.50
S4	0.683	5.26	747.58	6.85	6.00
S5	0.683	4.62	575.63	7.97	6.50
S6*	0.683	6.67	1200.60	2.95	2.50
S7**	0.692	6.732	1238.76	0.20	0.20
S8**	0.668	5.479	791.40	0.33	0.33
S9**	0.699	5.345	788.12	0.49	0.49

* First story of structure M2

** Tuning systems with all columns restrained

Table 5.2 Comparison of Magnifications, Measured and Calculated Using Average Viscous Damping. Elastic Single-Story Structure S1, Natural Frequency 2.89 Hz, Damping 3%, Subjected to Harmonic Excitation

Forcing Frequency (Hz)	Calculated Magnification	Average Measured Magnifications		Number of Tests*	Standard Deviations	
		Displacements	Accelerations		Displ.	Accel.
10.0	0.093	0.123	0.109	1		
7.0	0.208	0.211	0.204	1		
5.0	0.504	0.563	0.543	1		
4.0	1.091	1.139	1.118	3	0.054	0.052
3.5	2.123	2.196	2.186	1		
2.0	1.915	1.930	1.946	6	0.024	0.024
1.0	1.136	1.105	1.090	7	0.011	0.056

* Tests performed at different levels of excitation at the same frequency

Table 5.3 Comparison of Acceleration Amplifications Measured and Calculated Using Average and Scaled Viscous Damping, Elastic Single-Story Structures Subjected to Earthquake Excitation

Structure and Natural Frequency (Hz)	Ground Motion	Maximum Accelerations (in/sec ²)		Measured Amplification	Calculated Amplifications				
		Ground	Floor		Average Viscous Damping (%)		Scaled Viscous Damping (%)		
S1	2.89	EL CENTRO	11.42	13.80	1.21	3.69	1.86	24.27	1.08
	2.89		22.90	36.57	1.60	3.69	1.86	9.54	1.42
	2.89		34.77	53.48	1.54	3.69	1.86	6.71	1.58
	2.89		46.17	79.48	1.72	3.69	1.86	4.71	1.75
	2.89		58.13	108.74	1.87	3.69	1.86	3.61	1.87
S2	2.59		23.26	42.82	1.84	4.72	1.91	5.22	1.83
S3	2.43		11.61	14.92	1.28	7.03	1.46	13.91	1.27
S4	5.26		46.27	92.14	1.99	6.85	1.74	4.49	1.86
S5	4.62		23.50	39.26	1.67	7.97	1.70	6.69	1.77
S2	2.59	MELENDY	50.79	34.81	0.71	4.72	0.72	5.18	0.69
S2	2.59	TAFT	10.94	15.68	1.43	4.72	1.93	10.56	1.51
	2.59		21.66	39.58	1.83	4.72	1.93	4.65	1.94

Table 5.4 Comparison of Displacement Amplifications Measured and Calculated Using Average and Scaled Viscous Damping, Elastic Single-Story Structures Subjected to Earthquake Excitation

Structure and Natural Frequency (Hz)		Ground Motion	Maximum Displacements (in)		Measured Amplification	Calculated Amplifications			
			Ground	Floor*		Average Viscous Damping (%)	Scaled Viscous Damping (%)		
S1	2.89	EL CENTRO	0.135	0.029	0.215	3.69	0.474	24.27	0.276
	2.89		0.272	0.099	0.364	3.69	0.474	9.54	0.357
	2.89		0.413	0.154	0.373	3.69	0.474	6.71	0.399
	2.89		not available			3.69	0.474	4.71	0.446
	2.89		0.691	0.328	0.475	3.69	0.474	3.61	0.476
S2	2.59		0.277	0.172	0.623	4.72	0.604	5.22	0.578
S3	2.43		0.138	0.069	0.500	7.03	0.522	13.91	0.442
S4	5.26		0.550	0.084	0.153	6.85	0.132	4.49	0.142
S5	4.62		0.279	0.039	0.142	7.97	0.169	6.69	0.177
S2	2.59	MELENDY	0.147	0.120	0.820	4.72	0.932	5.18	0.899
S2	2.59	TAFT	0.150	0.052	0.346	4.72	0.529	10.56	0.415
	2.59		0.298	0.140	0.470	4.72	0.529	4.65	0.531

* Displacements of the floor are relative (deformations)

Table 5.5a Calculated Natural Frequencies, Mode Shapes, Modal Masses, Modal Stiffnesses and Modal Viscous Damping Ratios of the Two-Story Structures

Structure and Mode		Natural Frequency (Hz)	Mode Shape		Modal Mass (lb*sec ² /in)	Modal Stiffness (lb/in)	Modal Viscous Damping	
			Story 1	Story 2			Average (%)	Lower*
M1	1	1.83	0.731	1.175	1.2687	176.04	2.31	1.88
	2	4.74	0.269	-0.175	0.0693	61.38	6.00	4.88
M2	1	2.44	0.167	1.129	0.8536	201.04	3.96	3.35
	2	7.23	0.833	-0.129	0.4844	999.56	4.91	4.16

* Lower value of damping for large excitations.

Table 5.5b Comparison of Measured and Calculated Natural Frequencies and Modal Damping Ratios of the Two-Story Structures

Structure and Mode		Measured			Calculated*			
		Natural Frequency (Hz)	Modal Viscous Damping		Natural Frequency (Hz)	Modal Viscous Damping		
			Average (%)	Lower** (%)		Average (%)	Lower** (%)	Lower** (%)
M1	1	1.78	3.93	3.00	1.83	2.31	1.88	
	2	4.77	4.58	4.00	4.74	6.00	4.88	
M2	1	2.45	3.19	1.50	2.44	3.96 (2.96)	3.35 (2.50)	
	2	7.23	4.99	4.50	7.23	4.91 (3.66)	4.16 (3.11)	

* Damping values in parentheses are corrected (Eq. (e5.3)).

** Lower value of damping for large excitations.

Table 5.6 Comparison of Measured and Calculated Responses of the Two-Story Structures Subjected to Earthquake Excitation

Structure	Ground Motion	Mode	Frequency (Hz)	Damping (%)	Amplification	
					Measured	Calculated
M1	El Centro	1	1.78	3.0	2.46	2.40
		2	4.77	4.0	1.78	1.69
M1	Melendy	1	1.78	3.0	0.21	0.22
		2	4.77	4.0	2.74	2.87
M2	El Centro	1	2.45	1.5	1.83	1.82
		2	7.23	4.5	1.52	1.60

Remark: Results for El-Centro ground motion are averages of two tests performed at different levels of excitation.
Maximum Standard Deviation 0.185.

Table 5.7 Masses, Measured Natural Frequencies, Stiffnesses and Damping Ratios of the Appendages

Appendage	Mass (lb*sec ² /in)	Natural Frequency (Hz)	Stiffness (lb/in)	Damping Ratio (%)	Standard Deviations	
					Frequency	Damping
AS1	0.00853	1.565	0.825	0.18		
AS2	0.00853	3.268	3.597	0.25	0.037	0.10
AS3	0.00853	5.898	11.712	0.17	0.042	0.06
AS4	0.00853	8.879	26.545	0.40		
AL1	0.06752	1.722	7.901	0.22		
AL1a	0.06848	1.732	8.107	1.57		
AL1b	0.06848	1.765	8.424	4.44		
AL1c	0.06848	1.780	8.563	8.40		
AL1d	0.06848	1.823	8.989	12.54		
AL2	0.06752	3.197	27.249	0.03		
AL3	0.06752	5.877	92.078	0.14		
AL4	0.06752	8.286	183.039	0.17		
AT1	0.00835	6.699	14.788	0.11		
AT2	0.00966	5.557	11.777	0.15		
AT3	0.01163	5.119	12.036	0.14		
AT4	0.00947	5.464	11.162	1.48		
AT5	0.01100	5.270	12.066	0.12		
AT6	0.01094	5.279	12.040	1.94		
AT7	0.06752	5.393	77.518	0.05		

Table 5.8a Comparison of Measured and Calculated Amplifications of the Decoupled Appendages Subjected to Earthquakes

Appendage and Ground Motion	Measured Amplification	Calculated Amplification Using Average Frequency and Damping	Range of Amplifications Calculated Using Frequency and Damping Range of Average \pm Standard Deviation*			
			Minimum		Maximum	
AS2 EL CENTRO	4.734	4.223	3.516	(3.667)	5.733	(5.080)
MELENDY	1.521	1.927	1.699	(1.731)	2.034	(2.006)
AS3 EL CENTRO	2.655	3.803	2.540	(2.548)	4.535	(4.055)
MELENDY	7.312	7.787	7.272	(7.403)	8.124	(7.976)

* Values in parentheses were calculated using average damping ratios

Table 5.8b Comparison of Amplifications Measured and Calculated Using Corrected Natural Frequencies of the Decoupled Appendages Subjected to Earthquakes

Appendage	Ground Motion	Measured Amplification	Natural Frequency (Hz)	Corrected Natural Frequency* (Hz)	Calculated Amplification
AS2	EL CENTRO	4.734	3.268	3.25	4.46
	MELENDY	1.521	3.268	3.22	1.77
AS3	EL CENTRO	2.655	5.898	5.78	2.61
	MELENDY	7.312	5.898	5.91	7.71

* Measured near maximum response

Table 5.9a Measured Magnification Factors, Ductilities and Dissipated Energies. Inelastic Single-Story Structure S1, Elastic Natural Frequency 2.89 Hz, Elastic Damping 3%, Subjected to Harmonic Excitation

Forcing Frequency (Hz)	Max. Displacements		Magnification	Deformation (in)	Ductility	Energy Dissipated in One Cycle	
	Ground (in)	Structure (in)				(lb*in)	η^*
2.0	0.938	2.166	2.31	1.57	1.64	456.99	3.42
	1.097	2.265	2.06	1.92	1.95	725.15	3.44
2.5	0.156	0.685	4.39	0.53	1.03**	8.83	5.79
2.8	0.154	0.892	5.79	0.97	1.15	86.38	3.45
	0.311	0.955	3.07	1.16	1.33	172.46	3.05
	0.466	1.012	2.17	1.33	1.46	275.33	3.17
	0.624	1.053	1.69	1.50	1.61	386.60	3.21
	0.786	1.099	1.40	1.65	1.75	498.26	3.29
	0.938	1.433	1.53	1.77	1.92	625.21	3.49
3.0	0.157	0.733	4.67	0.86	1.11	49.27	3.22
4.0	0.472	0.447	0.95	0.88	1.11	61.49	3.81
	0.630	0.577	0.92	1.07	1.24	136.87	3.31

* For elastoplastic systems $\eta = 4.0$.

** Very small value of ductility and dissipated energy ($\eta > 4.0$).

Table 5.9b Measured Secant Stiffness, Calculated Equivalent Stiffness and Damping Ratio, and Comparison of the Calculated and Measured Magnifications. Inelastic Single-Story Structure S1, Elastic Natural Frequency 2.89 Hz, Elastic Damping 3%, Subjected to Harmonic Excitation

Forcing Frequency (Hz)	Secant Stiffness (lb/in)	Equivalent Linear Stiffness (lb/in)	Equivalent Damping Ratio (%)	Calculated Magnification	Measured Magnification
2.0	132.78	139.18	24.15	2.26	2.31
	113.54	118.64	27.59	2.12	2.07
2.5	222.55	223.60	2.60	4.06	4.39
2.8	195.46	198.50	7.08	6.22	5.78
	172.22	177.97	10.06	3.49	3.07
	155.32	161.99	13.39	2.39	2.17
	140.67	146.02	15.65	1.81	1.69
	127.04	132.33	17.47	1.46	1.40
	118.67	127.77	19.26	1.35	1.53
3.0	202.76	205.34	4.75	4.69	4.67
4.0	198.13	212.19	4.15	0.96	0.95
	165.60	189.37	6.64	0.78	0.92

Table 5.10a Comparison of Measured and Calculated Story and Modal Ductilities. Two Story Structure M1, With or Without Appendage, Subjected to El Centro Earthquake

Maximum Ground Accele- ration (g)	Measured Ductilities				Modal Ductilities Calculated from Story Ductilities						Story Ductilities Calculated from Modal Ductilities	
					Eq. 3.93		Eq. 3.94		Eq. 3.95		Ref. 25	
	Story		Mode		Mode		Mode		Mode		Story	
	1	2	1	2	1	2	1	2	1	2	1	2
1) 0.122 0.244 0.305 0.434 0.495	1.73	1.00	1.06	1.54	1.45	1.13	1.73	1.73	1.36	2.10	1.61	1.59
	2.91	1.00	1.70	3.22	1.92	1.21	2.91	2.91	1.89	3.74	2.73	2.61
	3.40	1.00	2.25	3.75	2.07	1.23	3.40	3.40	2.13	4.38	3.55	3.29
	2.84	1.00	1.50	2.91	1.90	1.21	2.84	2.84	1.75	3.30	2.74	2.13
	4.24	1.06	2.13	4.94	2.34	1.32	3.94	2.88	2.32	4.79	4.00	3.23
2) 0.123 0.247 0.368	1.19	1.00	1.00	1.09	1.13	1.04	1.19	1.19	1.10	1.29	1.41	1.54
	1.46	1.00	1.00	1.57	1.30	1.09	1.46	1.46	1.21	1.73	1.54	1.51
	3.11	1.09	1.45	4.40	2.07	1.32	2.89	2.15	1.97	4.02	2.47	2.53
3) 0.246 0.365 0.434	1.31	1.08	1.00	1.77	1.24	1.14	1.28	1.19	1.16	1.37	1.54	1.52
	4.12	1.06	2.29	5.23	2.33	1.33	3.81	2.72	2.43	5.57	3.81	3.60
	5.12	1.08	2.59	7.60	2.56	1.37	4.56	2.92	2.84	6.90	4.51	4.33
4) 0.122 0.238 0.362	1.11	1.00	1.00	1.14	1.08	1.03	1.11	1.11	1.06	1.18	1.44	1.56
	1.62	1.00	1.00	1.93	1.39	1.11	1.62	1.62	1.30	1.95	1.53	1.58
	4.11	1.00	2.31	5.02	2.24	1.26	4.11	4.11	2.36	5.34	3.99	3.49
5) 0.121 0.243 0.364	1.17	1.00	1.00	1.32	1.12	1.04	1.17	1.17	1.09	1.29	1.47	1.54
	1.48	1.00	1.00	1.68	1.31	1.10	1.48	1.48	1.23	1.74	1.54	1.54
	3.53	1.00	2.16	4.56	2.10	1.24	3.53	3.53	2.11	4.49	3.71	3.24

- 1) No Appendage
- 2) Appendage AS3 on floor 1
- 3) Appendage AS3 on floor 2
- 4) Appendage AS2 on floor 1
- 5) Appendage AS2 on floor 2

Table 5.10b Comparison of Measured and Calculated Story and Modal Ductilities. Two Story Structure M2, With or Without Appendage, Subjected to El Centro Earthquake

Maximum Ground Acceleration (g)	Measured Ductilities				Modal Ductilities Calculated from Story Ductilities						Story Ductilities Calculated from Modal Ductilities	
					Eq. 3.93		Eq. 3.94		Eq. 3.95		Ref. 25	
	Story		Mode		Mode		Mode		Mode		Story	
	1	2	1	2	1	2	1	2	1	2	1	2
1) 0.361 0.487 0.576	1.00	1.69	1.43	1.17	1.51	1.07	1.69	1.69	1.50	1.48	1.40	1.66
	1.00	2.71	1.92	2.17	2.11	1.12	2.71	1.71	2.16	1.93	2.49	3.63
	1.00	3.54	2.56	2.28	2.56	1.22	3.39	2.03	2.76	2.16	2.32	3.21
2) 0.243 0.365 0.490 0.580	1.00	1.55	1.28	1.00	1.42	1.06	1.55	1.55	1.38	1.42	1.30	1.55
	1.00	2.12	1.59	1.32	1.79	1.10	2.12	2.12	1.76	1.83	1.65	1.97
	1.00	2.88	2.06	1.64	2.19	1.12	2.88	2.88	2.27	2.20	1.99	2.57
	1.01	5.87	4.03	3.31	3.25	1.17	5.81	4.62	4.30	3.90	3.80	5.05
3) 0.243 0.366 0.489 0.578	1.00	1.46	1.19	1.05	1.36	1.06	1.46	1.46	1.33	1.36	1.26	1.42
	1.00	1.84	1.41	1.02	1.61	1.08	1.84	1.84	1.58	1.65	1.41	1.68
	1.00	2.96	2.13	1.62	2.23	1.12	2.96	2.96	2.30	1.71	2.01	2.62
	1.05	6.33	4.45	3.62	3.44	1.22	5.99	3.01	4.73	2.01	4.04	5.42
4) 0.243 0.365 0.488 0.550	1.00	1.20	1.03	1.00	1.16	1.03	1.20	1.20	1.14	1.16	1.15	1.21
	1.00	2.04	1.57	1.23	1.74	1.09	2.04	2.04	1.71	1.75	1.58	1.94
	1.00	2.78	2.02	1.54	2.14	1.12	2.78	1.87	2.21	2.09	1.86	2.50
	1.00	4.13	2.96	2.05	2.71	1.14	4.13	4.13	3.16	2.68	2.42	3.63
5) 0.243 0.366 0.489 0.580	1.00	1.61	1.33	1.49	1.48	1.07	1.61	1.61	1.42	1.47	1.59	1.63
	1.00	1.86	1.43	1.04	1.62	1.08	1.86	1.86	1.59	1.63	1.41	1.73
	1.00	2.85	2.08	1.68	2.18	1.12	2.85	2.85	1.92	2.10	1.92	2.55
	1.08	4.29	3.07	1.99	2.86	1.23	4.06	2.19	3.27	2.63	2.36	3.77

- 1) No Appendage
- 2) Appendage AS3 on floor 1
- 3) Appendage AS3 on floor 2
- 4) Appendage AS2 on floor 1
- 5) Appendage AS2 on floor 2

Table 5.10c Comparison of Measured and Calculated Story and Modal Ductilities. Two Story Structure M1, With or Without Appendage, Subjected to Melendy Earthquake

Maximum Ground Accele- ration (g)	Measured Ductilities				Modal Ductilities Calculated from Story Ductilities						Story Ductilities Calculated from Modal Ductilities	
					Eq. 3.93		Eq. 3.94		Eq. 3.95		Ref. 25	
	Story		Mode		Mode		Mode		Mode		Story	
	1	2	1	2	1	2	1	2	1	2	1	2
1) 1.078	1.13	1.08	1.00	1.86	1.12	1.09	1.12	1.10	1.08	1.04	1.88	1.14
1.634	1.19	1.39	1.00	1.85	1.24	1.33	1.26	1.35	1.22	1.42	1.69	1.33
2.191	1.40	1.40	1.00	2.18	1.40	1.40	1.40	1.40	1.33	1.25	1.68	1.41
2.580	1.80	1.38	1.36	2.53	1.67	1.48	1.70	1.51	1.51	1.08	2.25	1.80
2) 1.087	1.38	1.06	1.00	2.31	1.28	1.13	1.35	1.25	1.18	1.22	1.84	1.23
2.207	1.69	1.48	1.44	2.49	1.63	1.53	1.64	1.54	1.50	1.16	2.35	1.73
2.458	1.76	1.40	1.84	2.40	1.64	1.48	1.67	1.51	1.46	1.01	3.14	1.98
3) 1.070	1.17	1.04	1.00	2.13	1.14	1.07	1.16	1.12	1.09	1.07	1.86	1.20
2.158	1.53	1.33	1.44	2.43	1.47	1.37	1.48	1.39	1.37	1.07	2.36	1.76
2.564	2.16	1.37	1.82	2.59	1.87	1.52	1.98	1.62	1.67	1.34	2.96	2.03
4) 1.073	1.09	1.09	1.00	1.92	1.09	1.09	1.09	1.09	1.07	1.09	1.93	1.21
1.609	1.16	1.34	1.00	2.30	1.20	1.28	1.23	1.30	1.19	1.34	1.75	1.49
2.173	1.36	1.38	1.00	2.47	1.37	1.38	1.37	1.38	1.31	1.25	1.75	1.58
2.559	1.90	1.40	1.58	2.51	1.74	1.51	1.79	1.56	1.57	1.14	2.53	1.80
5) 1.077	1.04	1.00	1.00	2.09	1.03	1.01	1.04	1.04	1.02	1.03	1.93	1.22
1.615	1.19	1.20	1.00	2.23	1.19	1.20	1.19	1.20	1.16	1.13	1.66	1.47
2.174	1.44	1.34	1.32	2.53	1.45	1.38	1.45	1.39	1.35	1.14	2.25	1.64

- 1) No Appendage
- 2) Appendage AS3 on floor 1
- 3) Appendage AS3 on floor 2
- 4) Appendage AS2 on floor 1
- 5) Appendage AS2 on floor 2

Table 5.11 Exact Undamped and Approximate Undamped Natural Frequencies and Eigenvectors and Measured Natural Frequencies of the Detuned Single-Story Structures with Appendage

System and Mode		Exact Undamped			Approximate Undamped			Measured* Natural Frequency (Hz)
		Frequency (Hz)	Eigenvector		Frequency (Hz)	Eigenvector		
			Floor	Appendage		Floor	Appendage	
S1-AS1	1	1.56	1.000	196.184	1.56	1.000	194.838	1.56
	2	2.91	1.000	-0.408	2.90	1.000	-0.411	2.89
S1-AS3	1	2.89	1.000	1.312	2.90	1.000	1.319	2.86
	2	5.95	1.000	-61.061	5.90	1.000	-60.769	5.80
S1-AS4	1	2.88	1.000	1.117	2.90	1.000	1.119	2.88
	2	8.94	1.000	-71.681	8.88	1.000	-71.587	8.53
S1-AL3	1	2.73	1.000	1.276	2.90	1.000	1.321	2.72
	2	6.24	1.000	-7.933	5.88	1.000	-7.657	6.28
S1-AL4	1	2.75	1.000	1.124	2.90	1.000	1.139	2.75
	2	8.73	1.000	-9.041	8.29	1.000	-8.880	8.64
S2-AS2	1	2.55	1.000	2.558	2.59	1.000	2.691	2.50
	2	3.32	1.000	-31.320	3.27	1.000	-29.772	3.25
S2-AS3	1	2.57	1.000	1.235	2.59	1.000	1.239	2.60
	2	5.94	1.000	-64.857	5.90	1.000	-64.662	5.55
S2-AS4	1	2.57	1.000	1.092	2.59	1.000	1.093	2.56
	2	8.94	1.000	-73.372	8.88	1.000	-73.304	8.61
S2-AL3	1	2.45	1.000	1.210	2.59	1.000	1.241	2.42
	2	6.22	1.000	-8.362	5.88	1.000	-8.152	6.11
S2-AL4	1	2.46	1.000	1.097	2.59	1.000	1.108	2.42
	2	8.72	1.000	-9.226	8.29	1.000	-9.129	8.72
S4-AS2	1	3.26	1.000	129.338	3.27	1.000	127.762	3.12
	2	5.29	1.000	-0.619	5.26	1.000	-0.627	5.48
S4-AS4	1	5.22	1.000	1.527	5.26	1.000	1.542	5.17
	2	8.96	1.000	-52.466	8.88	1.000	-51.956	8.58

* The undamped approximate eigenvectors were used to determine the measured natural frequencies. Identical values are obtained if the exact eigenvectors are used.

Table 5.12 Exact Undamped and Tuned Damped Natural Frequencies and Eigenvectors and Measured Natural Frequencies of the Tuned Single-Story Structures with Appendage

System and Mode		Exact Undamped			Tuned Damped			Measured* Natural Frequency (Hz)
		Frequency (Hz)	Eigenvector		Frequency (Hz)	Eigenvector		
			Floor	Appendage		Floor	Appendage	
S7-AT1	1	6.36	1.000	10.068	6.35	1.000	9.593	6.45
	2	7.09	1.000	-8.238	7.08	1.000	-8.593	7.20
S8-AT2	1	5.19	1.000	7.868	5.18	1.000	7.752	5.24
	2	5.86	1.000	-8.782	5.85	1.000	-8.752	5.94
S8-AT3	1	4.93	1.000	13.587	4.90	1.000	7.181	4.89
	2	5.69	1.000	-4.224	5.70	1.000	-6.181	5.68
S8-AT4	1	5.16	1.000	9.125	5.14	1.000	8.837	5.19
	2	5.81	1.000	-7.726	5.80	1.000	-7.837	5.87
S9-AT7	1	4.60	1.000	3.652	4.53	1.000	3.716	4.63
	2	6.27	1.000	-2.834	6.20	1.000	-2.716	6.39
S4-AT5	1	4.89	1.000	7.252	4.88	1.000	8.253	
	2	5.57	1.000	-8.561	5.56	1.000	-7.253	
S4-AT6	1	4.90	1.000	7.174	4.87	1.000	7.785	4.92
	2	5.57	1.000	-8.704	5.58	1.000	-6.785	5.64

* The tuned damped eigenvectors were used to determine the measured natural frequencies. Almost identical values are obtained if the exact eigenvectors are used.

Table 5.13a Exact Undamped and Approximate Undamped Natural Frequencies and Eigenvectors of the Slightly Detuned Single-Story Structures with Appendage

System and $\left(\frac{\omega_0}{\Omega}\right)$	Range of Tuning Eq. 3.65	Mode	Exact Undamped			Approximate Undamped		
			Frequency (Hz)	Eigenvector		Frequency (Hz)	Eigenvector	
				Floor	Appendage		Floor	Appendage
S1-AS2 1.127	1.124	1	2.83	1.000	3.989	2.90	1.000	4.686
		2	3.35	1.000	-20.082	3.27	1.000	-17.099
S1-AL1 0.651	0.654	1	1.82	1.000	15.423	1.89	1.000	13.767
		2	3.00	1.000	-0.656	2.90	1.000	-0.735
S1-AL2 1.103	1.346	1	2.56	1.000	2.806	2.90	1.000	5.620
		2	3.61	1.000	-3.606	3.20	1.000	-1.800
S2-AL1 0.728	0.654	1	1.80	1.000	10.893	1.89	1.000	8.964
		2	2.72	1.000	-0.929	2.59	1.000	-1.129
S2-AL2 1.234	1.346	1	2.35	1.000	2.176	2.59	1.000	2.913
		2	3.52	1.000	-4.649	3.20	1.000	-3.473
S3-AL1 0.709	0.654	1	1.65	1.000	11.924	1.72	1.000	10.075
		2	2.54	1.000	-0.849	2.43	1.000	-1.004
S3-AL1a 0.712	0.647	1	1.66	1.000	11.566	1.73	1.000	9.703
		2	2.58	1.000	-0.863	2.43	1.000	-1.028
S3-AL1c 0.732	0.636	1	1.69	1.000	10.597	1.78	1.000	8.655
		2	2.56	1.000	-0.942	2.43	1.000	-1.153
S3-AL1d 0.750	0.625	1	1.73	1.000	9.792	1.82	1.000	7.773
		2	2.57	1.000	-1.019	2.43	1.000	-1.284
S4-AS3 1.120	1.125	1	5.13	1.000	4.129	5.26	1.000	4.923
		2	6.05	1.000	-19.400	5.90	1.000	-16.276

Table 5.13b Approximate Undamped and Tuned Damped Natural Frequencies and Eigenvectors and Measured Natural Frequencies of the Slightly Detuned Single-Story Structures with Appendage

System and Mode		Approximate Undamped			Tuned Damped			Measured Natural Frequency (Hz)	
		Frequency (Hz)	Eigenvector		Frequency (Hz)	Eigenvector		*	**
			Floor	Appendage		Floor	Appendage		
S1-AS2	1	2.90	1.000	4.686	2.84	1.000	6.754	2.85	2.90
	2	3.27	1.000	-17.099	3.33	1.000	-5.754	3.36	3.44
S1-AL1	1	1.89	1.000	13.767	1.65	1.000	2.108	1.79	1.78
	2	2.90	1.000	-0.753	3.14	1.000	-1.108	2.89	2.94
S1-AL2	1	2.90	1.000	5.620	2.55	1.000	3.549	2.65	2.66
	2	3.20	1.000	-1.800	3.55	1.000	-2.549	3.70	3.71
S2-AL1	1	1.89	1.000	8.964	1.69	1.000	2.549	1.81	1.82
	2	2.59	1.000	-1.129	2.79	1.000	-1.549	2.73	2.76
S2-AL2	1	2.59	1.000	2.913	2.36	1.000	3.224	2.36	2.39
	2	3.20	1.000	-3.473	3.43	1.000	-2.224	3.55	3.56
S3-AL1	1	1.72	1.000	10.075	1.54	1.000	2.427	1.65	1.63
	2	2.43	1.000	-1.004	2.62	1.000	-1.427	2.53	2.28
S3-AL1a	1	1.73	1.000	9.703	1.54	1.000	2.437	1.85	1.62
	2	2.43	1.000	-1.028	2.62	1.000	-1.437	2.70	2.44
S3-AL1c	1	1.78	1.000	8.655	1.59	1.000	2.526	1.78	1.75
	2	2.43	1.000	-1.153	2.63	1.000	-1.526	2.60	2.32
S3-AL1d	1	1.82	1.000	7.773	1.64	1.000	2.674	1.85	1.93
	2	2.43	1.000	-1.284	2.62	1.000	-1.674	2.63	2.51
S4-AS3	1	5.26	1.000	4.923	5.15	1.000	6.900	5.26	5.29
	2	5.90	1.000	-16.276	6.02	1.000	-5.900	6.01	6.03

* Determined using the approximate undamped eigenvectors

** Determined using the tuned damped eigenvectors

Table 5.14 Comparison of Amplifications Determined from Response Spectra of the Equivalent Linear System, from Inelastic Modified Response Spectra and from Measured Floor Response of the Detuned Single-Story Structures with Appendage

System	Ground Motion	Measured Ductility	Response Spectra Amplifications		Measured Floor Amplification
			Equivalent Linear System	Inelastic Modified	
S1-AS1	EL CENTRO	1.000	1.961	1.961	1.660
S1-AS3	EL CENTRO	1.000	1.961	1.961	1.873
		1.202	1.890	1.655	1.774
		1.260	1.878	1.591	1.767
		1.441	1.724	1.430	1.650
		1.664	1.552	1.285	1.456
S1-AS4	EL CENTRO	1.000	1.961	1.961	1.818
		1.240	1.879	1.612	1.710
		1.477	1.708	1.416	1.617
		1.700	1.542	1.266	1.450
S1-AL3	EL CENTRO	1.000	1.961	1.961	1.955
		1.262	1.878	1.589	1.887
		1.722	1.507	1.254	1.456
		2.083	1.345	1.102	1.318
S1-AL4	EL CENTRO	1.000	1.961	1.961	1.857
		1.170	1.889	1.694	2.068
		1.941	1.402	1.155	1.506
		2.175	1.367	1.071	1.370
S2-AS2	EL CENTRO	1.109	1.690	1.861	2.085
		1.227	1.513	1.703	1.906
		1.311	1.457	1.613	1.538
		1.777	1.512	1.285	1.296
		2.628	1.513	0.996	1.136
		3.663	1.477	0.817	1.008
		4.536	1.403	0.723	0.900
S2-AS2	TAFT	1.000	1.998	1.998	2.093
		1.427	2.314	1.467	1.979
		2.679	1.966	0.957	1.455

Table 5.14 (continued)

System	Ground Motion	Measured Ductility	Response Spectra Amplifications		Measured Floor Amplification
			Equivalent Linear System	Inelastic Modified	
S2-AS2	MELENDY	1.000	0.767	0.767	0.749
		1.340	0.512	0.592	0.621
		1.783	0.407	0.479	0.415
		2.337	0.365	0.400	0.298
		2.860	0.355	0.353	0.257
S2-AS3	EL CENTRO	1.000	2.054	2.054	1.991
		1.855	1.511	1.248	1.238
		3.036	1.508	0.912	0.998
		3.677	1.494	0.815	0.878
S2-AS3	MELENDY	1.000	0.767	0.767	0.753
		1.470	0.468	0.551	0.571
		1.782	0.407	0.479	0.401
		2.685	0.357	0.367	0.245
S2-AS4	EL CENTRO	1.000	2.054	2.054	1.914
		2.638	1.509	0.993	1.343
		3.607	1.494	0.824	1.011
		4.324	1.415	0.743	0.896
S2-AL3	EL CENTRO	1.073	1.784	1.919	1.962
		1.409	1.463	1.523	1.735
		1.888	1.511	1.233	1.292
		2.507	1.512	1.025	1.028
		3.687	1.481	0.587	0.977
S2-AL4	EL CENTRO	1.000	2.054	2.054	1.889
		2.539	1.514	1.017	1.229
		4.147	1.452	0.761	0.967
		6.373	1.712	0.599	0.958
S4-AS2	EL CENTRO	1.000	1.781	1.781	1.931
		1.474	1.512	1.276	1.789
		1.846	1.468	1.086	1.720

Table 5.14 (continued)

System	Ground Motion	Measured Ductility	Response Spectra Amplifications		Measured Floor Amplification
			Equivalent Linear System	Inelastic Modified	
S4-AS3	EL CENTRO	1.000	1.781	1.781	2.002
		1.292	1.531	1.416	2.019
		2.194	1.434	0.968	1.435
S4-AS4	EL CENTRO	1.000	1.781	1.781	1.988
		1.373	1.514	1.348	1.935
		2.118	1.443	0.990	1.422
S5-AS2	EL CENTRO	1.000	1.790	1.790	1.708
		1.433	1.731	1.310	1.695
		1.652	1.672	1.179	1.459
S5-AS3	EL CENTRO	1.000	1.790	1.790	1.672
		1.449	1.681	1.299	1.579
		2.261	1.539	0.954	1.185
		2.679	1.500	0.857	0.951
		5.780	1.412	0.551	0.853
S5-AS4	EL CENTRO	1.000	1.790	1.790	1.655
		1.301	1.745	1.414	1.711
		2.108	1.547	0.998	1.266
		2.564	1.507	0.881	0.983
		4.114	1.447	0.666	0.850

Table 5.15a Exact Undamped and Approximate Undamped Natural Frequencies and Eigenvectors and Measured Natural Frequencies of the Two-Story Structure M1 with Appendages AS2 and AS3

System and Mode		Exact Undamped				Approximate Undamped			
		Natural Frequency (Hz)	Eigenvector			Natural Frequency (Hz)	Eigenvector		
			Floor 1	Floor 2	Appen-dage		Floor 1	Floor 2	Appen-dage
AS2 on Floor 1	1	1.82	1.000	1.601	1.450	1.78	1.000	1.606	1.424
	2	3.26	0.003	-0.014	1.000	3.27	0.003	-0.013	1.000
	3	4.76	1.000	-0.641	-0.895	4.77	1.000	-0.650	-0.885
Floor 1	1					1.80	Measured* ** Natural Frequencies		
	2					**			
	3					4.89			
AS2 on Floor 2	1	1.81	0.621	1.000	1.445	1.78	0.623	1.000	1.424
	2	3.28	-0.014	-0.010	1.000	3.27	-0.013	-0.010	1.000
	3	4.75	-1.518	1.000	-0.903	4.77	-1.539	1.000	-0.885
Floor 2	1					1.75	Measured* Natural Frequencies		
	2					3.18			
	3					4.77			
AS3 on Floor 1	1	1.82	1.000	1.602	1.106	1.78	1.000	1.606	1.101
	2	4.68	1.000	-0.676	2.704	4.77	1.000	-0.650	2.893
	3	5.98	-0.028	0.009	1.000	5.90	-0.030	0.010	1.000
Floor 1	1					1.79	Measured* Natural Frequencies		
	2					4.68			
	3					5.96			
AS3 on Floor 2	1	1.82	0.621	1.000	1.105	1.78	0.623	1.000	1.101
	2	4.71	-1.605	1.000	2.768	4.77	-1.539	1.000	2.893
	3	5.96	0.009	-0.020	1.000	5.90	0.010	-0.021	1.000
Floor 2	1					1.76	Measured* Natural Frequencies		
	2					4.67			
	3					5.91			

* The undamped approximate eigenvectors were used to determine the measured natural frequencies. Identical values are obtained if the exact eigenvectors are used.

** Not available as a result of a bad measurement of the appendage acceleration.

Table 5.15b Exact Undamped and Approximate Undamped Natural Frequencies and Eigenvectors and Measured Natural Frequencies of the Two-Story Structure M2 with Appendages AS2 and AS3

System and Mode		Exact Undamped				Approximate Undamped			
		Natural Frequency (Hz)	Eigenvector			Natural Frequency (Hz)	Eigenvector		
			Floor 1	Floor 2	Appendage		Floor 1	Floor 2	Appendage
AS2 on Floor 1	1	2.44	1.000	6.717	2.263	2.44	1.000	6.741	2.265
	2	3.26	0.002	-0.005	1.000	3.27	0.003	-0.005	1.000
	3	7.24	1.000	-0.154	-0.256	7.23	1.000	-0.155	-0.257
	1					2.48	Measured* Natural Frequencies		
	2					3.11			
	3					7.44			
AS2 on Floor 2	1	2.41	0.148	1.000	2.190	2.44	0.148	1.000	2.265
	2	3.31	-0.005	-0.028	1.000	3.27	-0.005	-0.029	1.000
	3	7.23	-6.436	1.000	-0.257	7.23	-6.460	1.000	-0.257
	1					2.44	Measured* Natural Frequencies		
	2					3.23			
	3					7.50			
AS3 on Floor 1	1	2.44	1.000	6.728	1.207	2.44	1.000	6.741	1.207
	2	5.83	0.022	-0.006	1.000	5.90	0.024	-0.006	1.000
	3	7.31	1.000	-0.151	-1.860	7.23	1.000	-0.155	-1.989
	1					2.51	Measured* Natural Frequencies		
	2					5.77			
	3					7.77			
AS3 on Floor 2	1	2.42	0.148	1.000	1.203	2.44	0.148	1.000	1.207
	2	5.94	-0.006	-0.015	1.000	5.90	-0.006	-0.015	1.000
	3	7.23	-6.272	1.000	-1.986	7.23	-6.460	1.000	-1.989
	1					2.52	Measured* Natural Frequencies		
	2					5.78			
	3					7.66			

* The undamped approximate eigenvectors were used to determine the measured natural frequencies. Identical values are obtained if the exact eigenvectors are used.

FIGURES

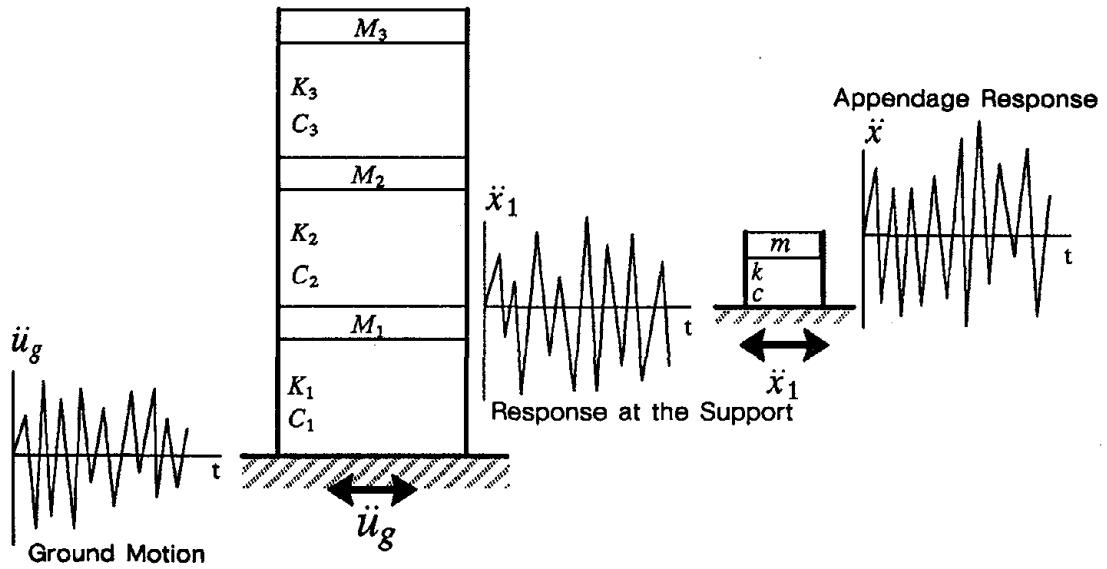


Figure 2.1 Decoupled Systems

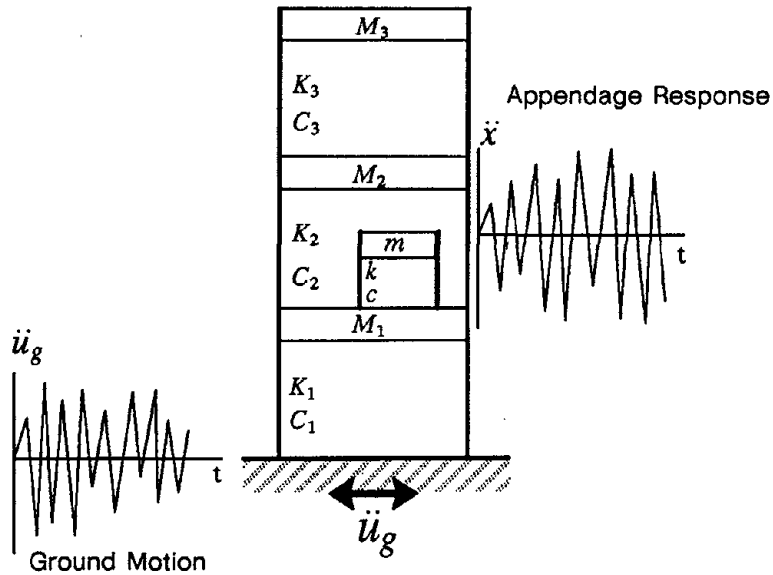


Figure 2.2 Combined System

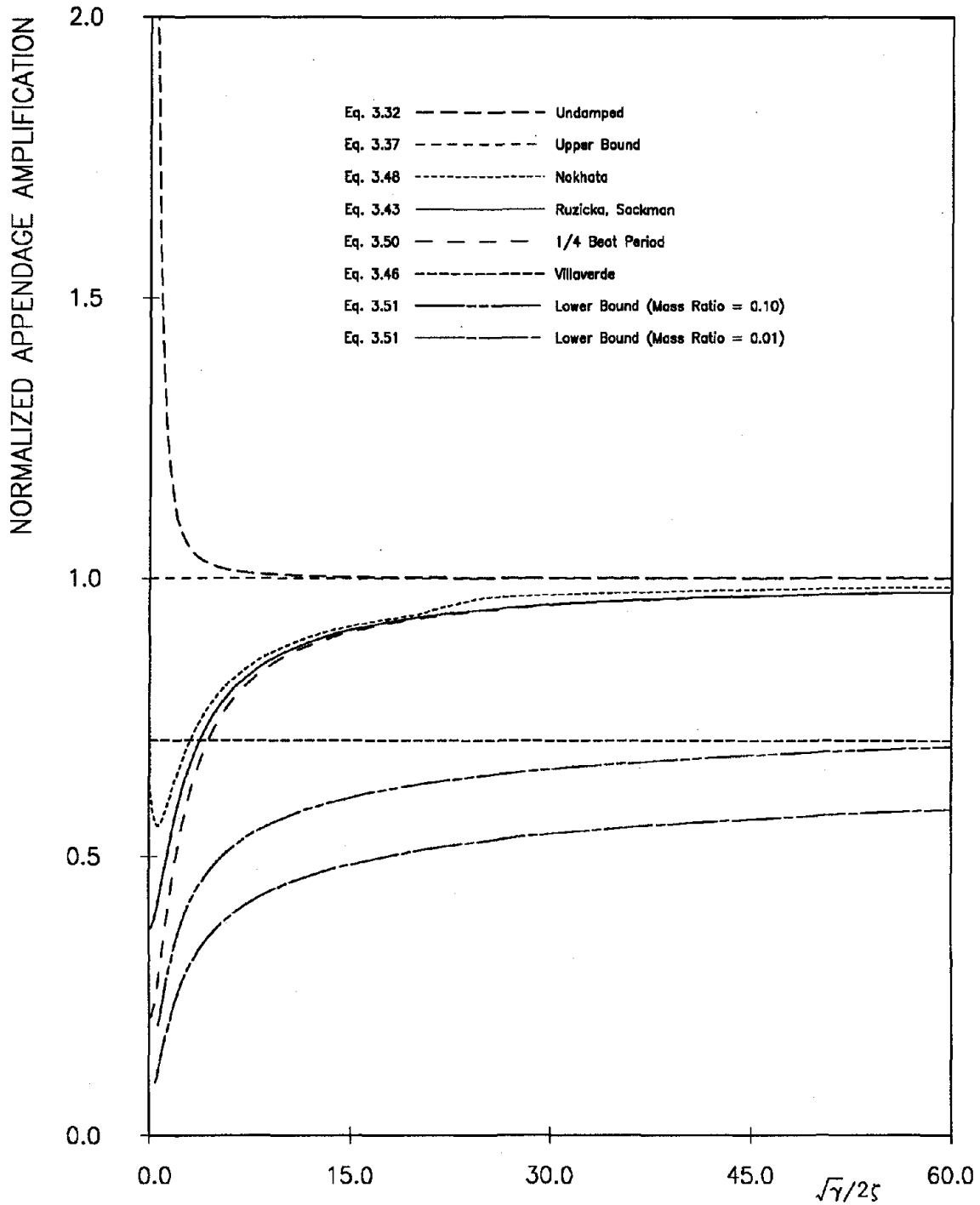


Figure 3.1 Comparison of Calculated Normalized Amplifications of a Tuned Appendage, $\ddot{x}_{max}/\ddot{x}_T$, as a Function of $\sqrt{\gamma}/2\zeta$

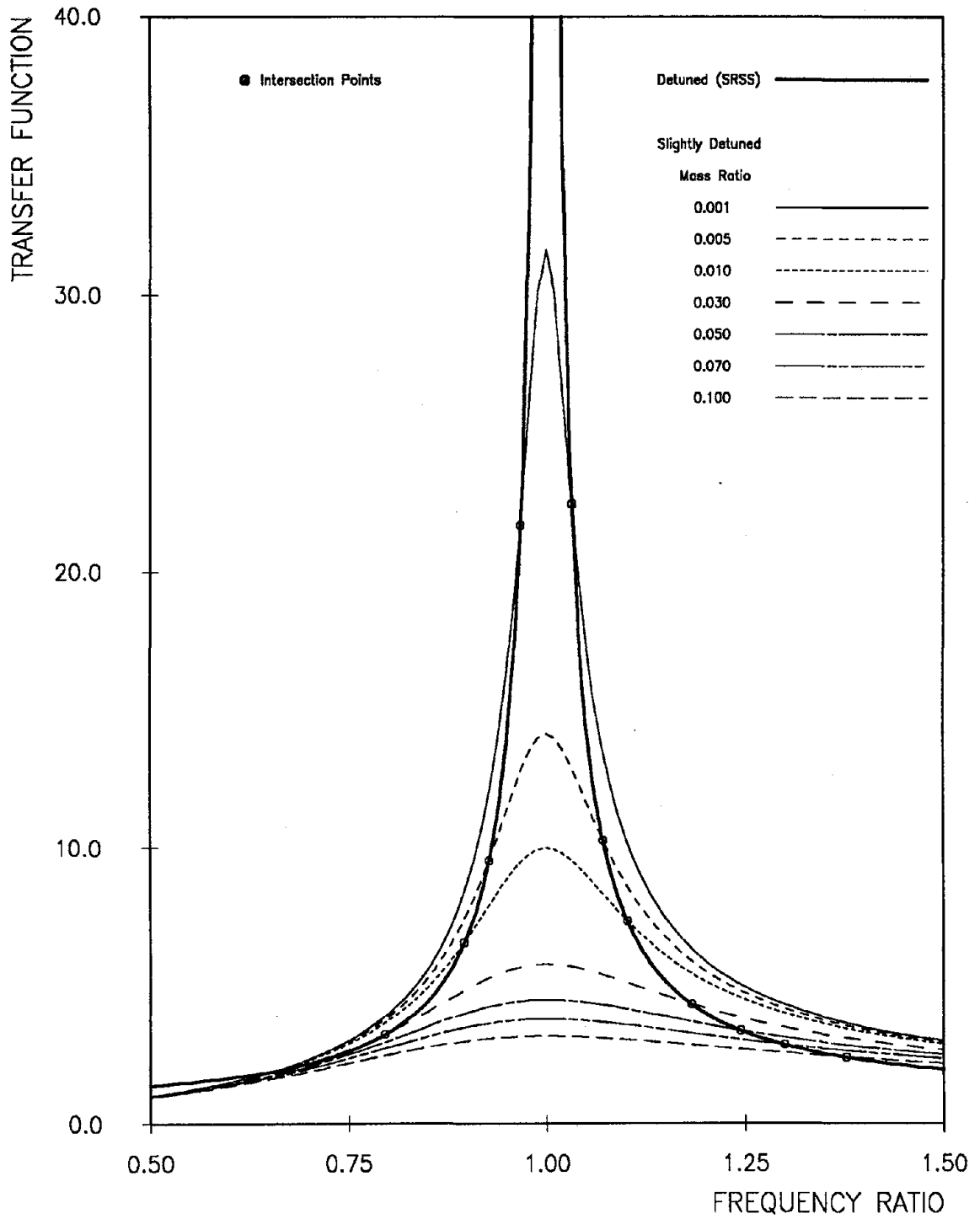


Figure 3.2 Transfer Functions of a Detuned Appendage (SRSS) and a Slightly Detuned Appendage as a Function of the Frequency Ratio, ω_0/Ω

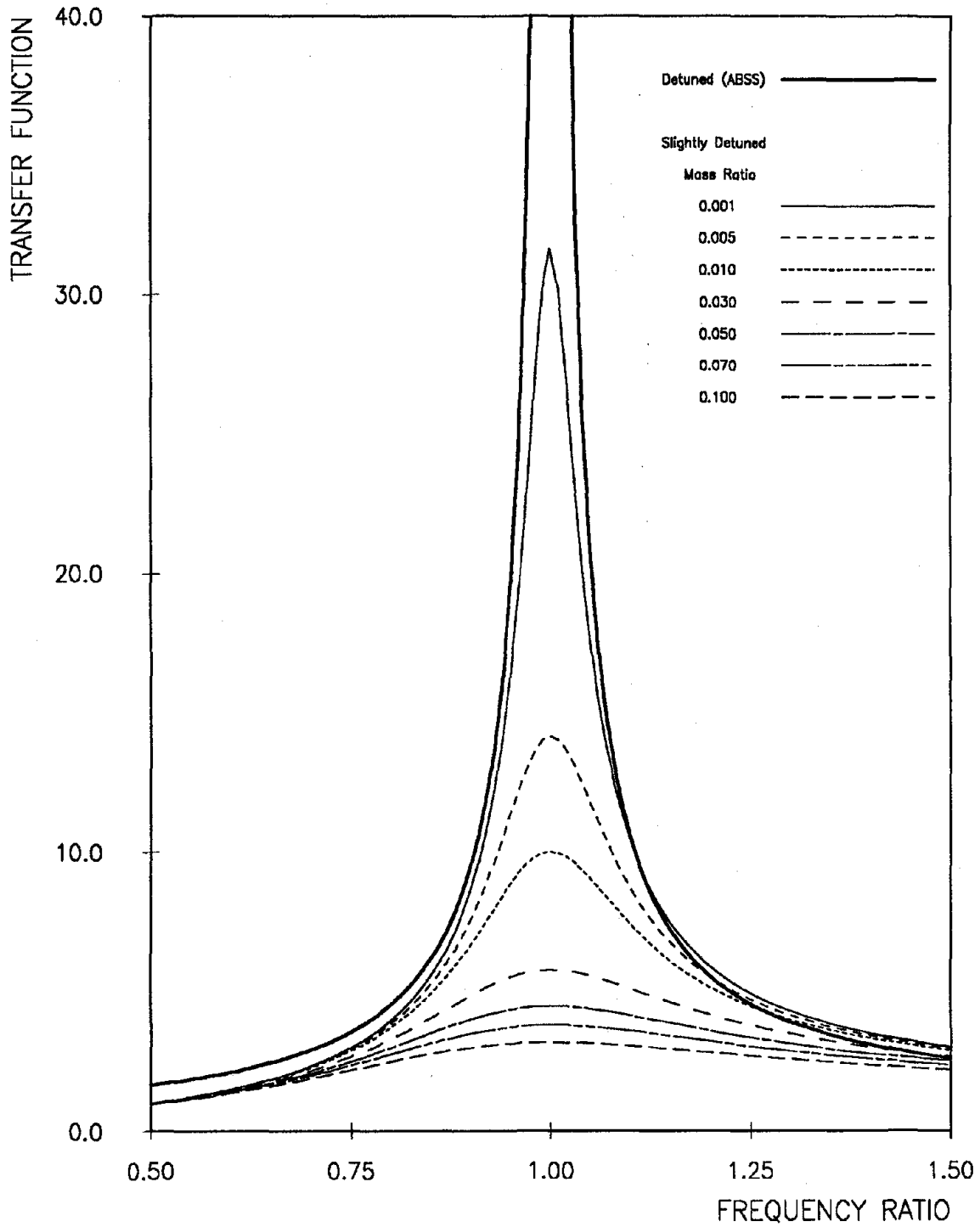


Figure 3.3 Transfer Functions of a Detuned Appendage (ABSS) and a Slightly Detuned Appendage as a Function of the Frequency Ratio, ω_0/Ω

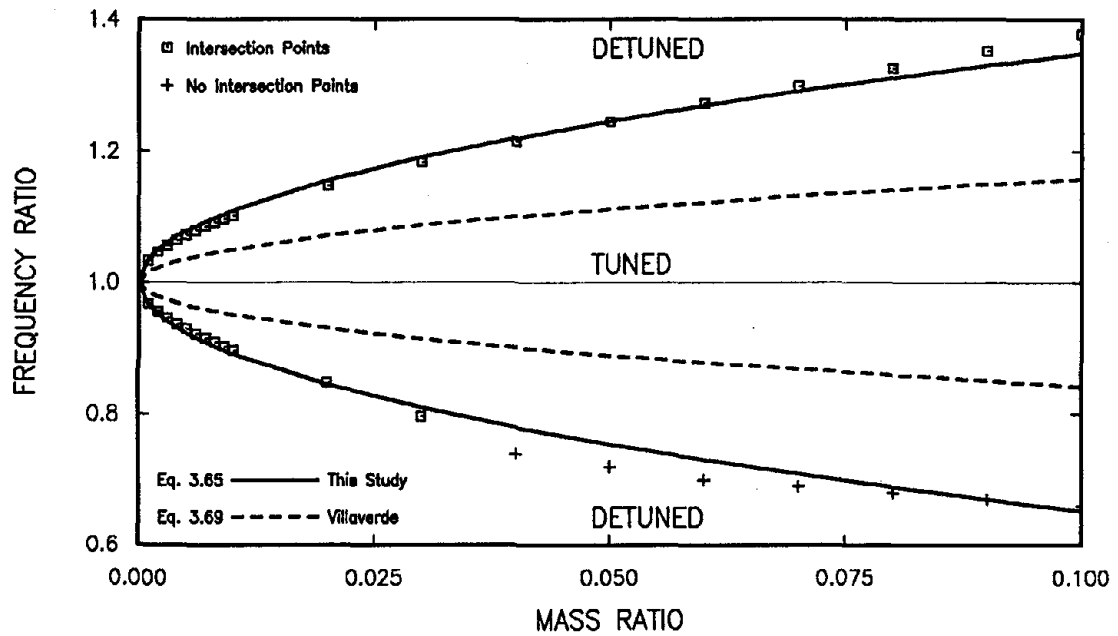


Figure 3.4 Frequency Ratio, ω_0/Ω , at the Boundary Between Tuning and Detuning as a Function of the Mass Ratio, γ

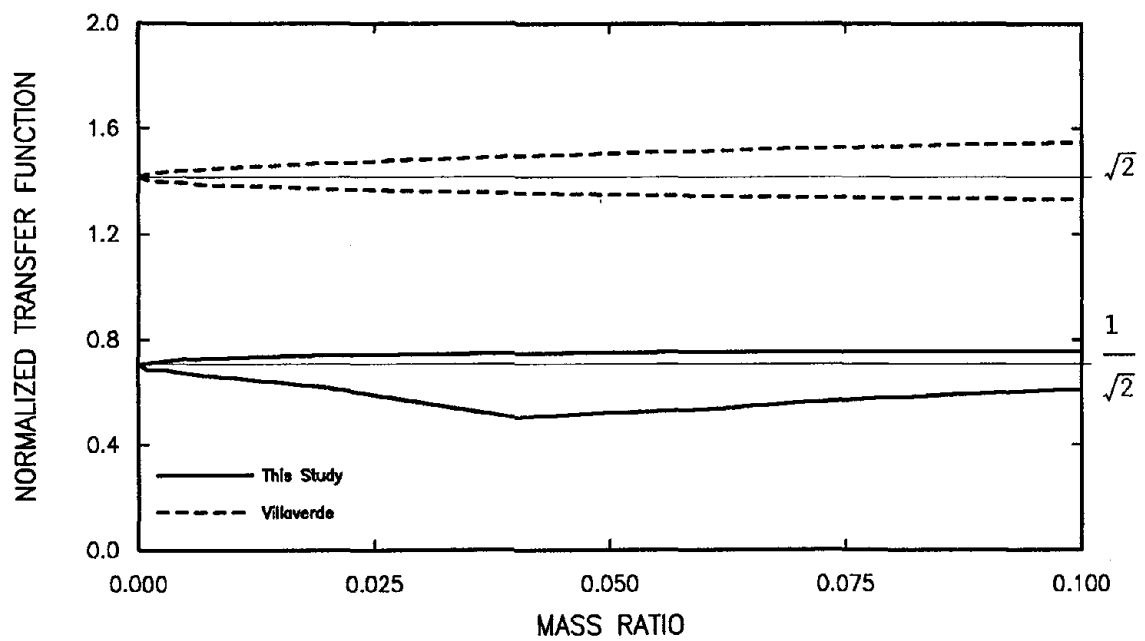


Figure 3.5 Transfer Function Values at the Boundary Between Tuning and Detuning, Normalized to $\sqrt{\gamma}$ as a Function of the Mass Ratio, γ

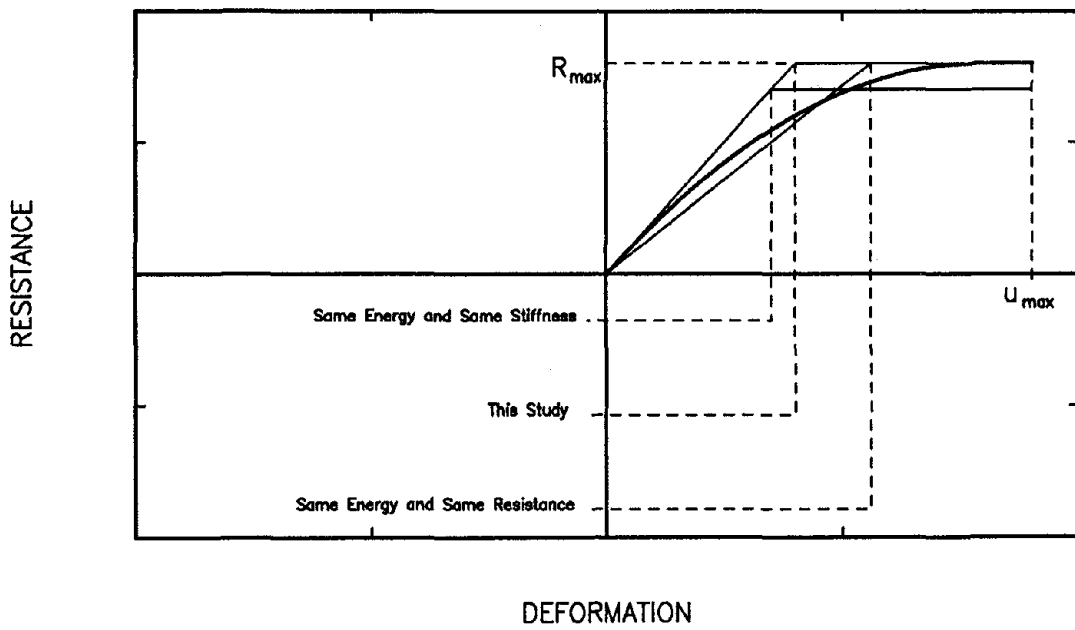
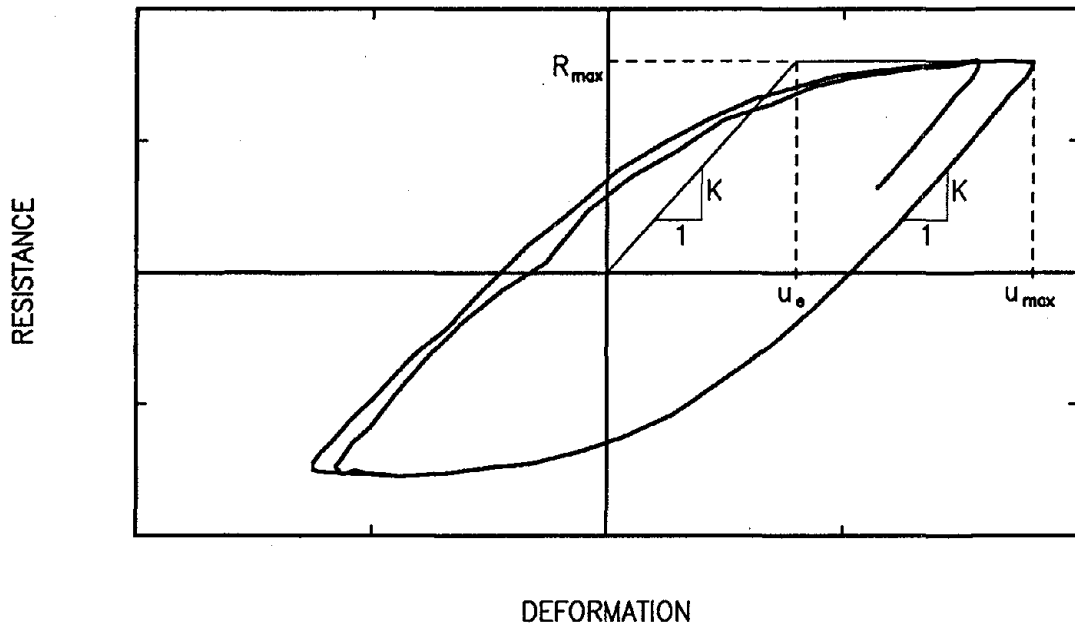
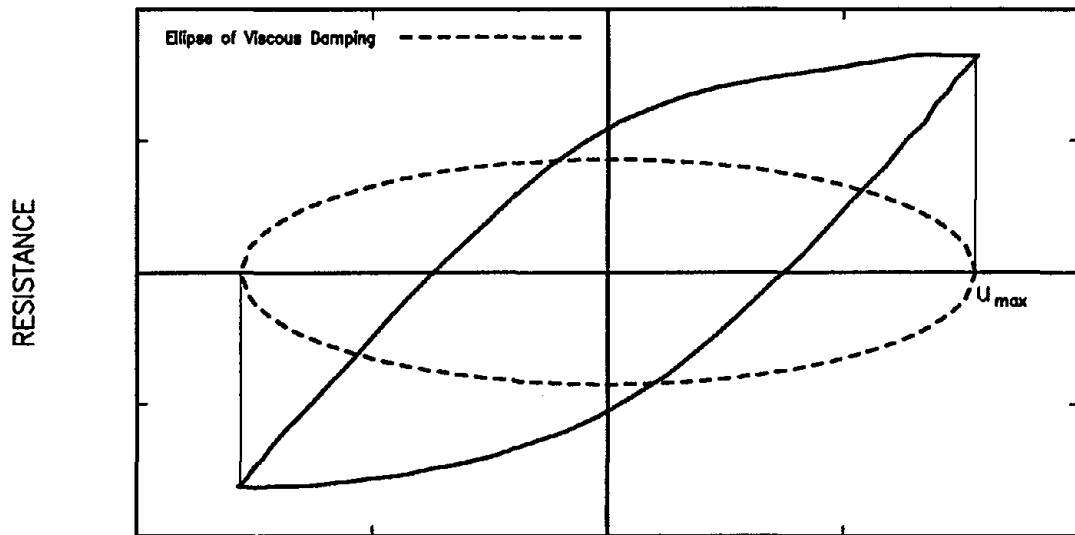
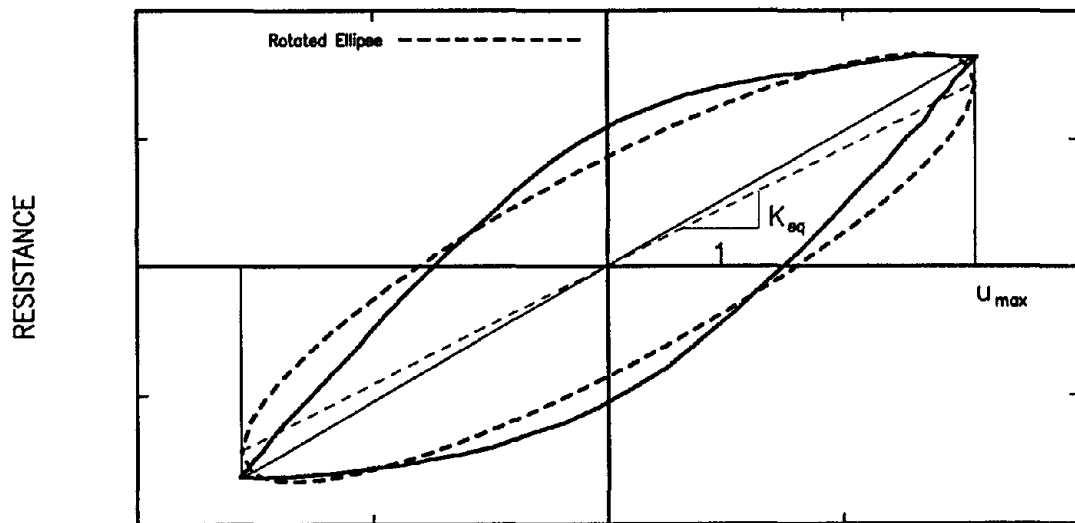


Figure 3.6 Definition of Ductility



DEFORMATION



DEFORMATION

Figure 3.7 Typical Hysteresis Loop and the Ellipse of Equivalent Linear Viscous Damping

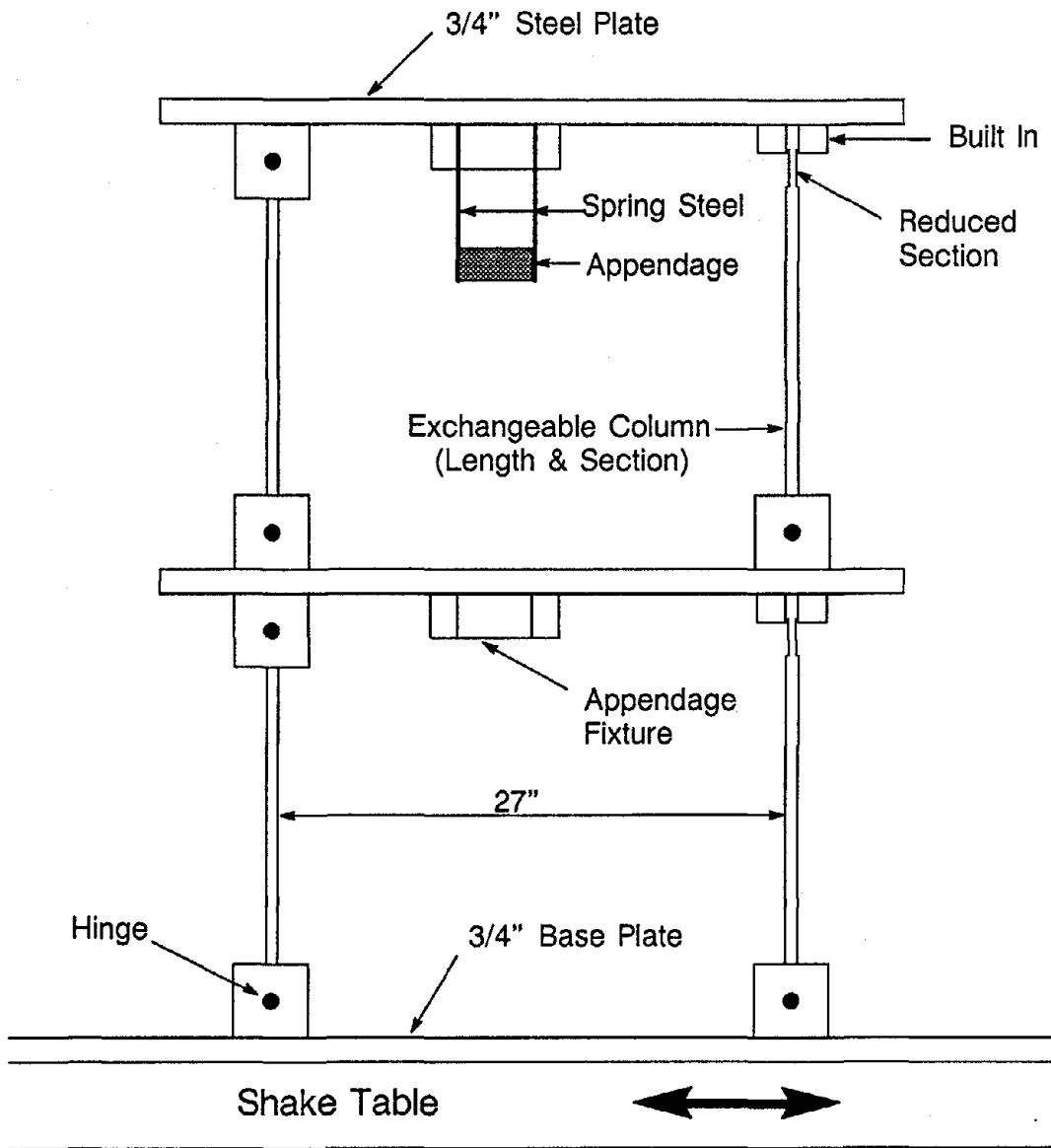


Figure 4.1 Typical Two-Story Structure with an Appendage Mounted on the Second Story

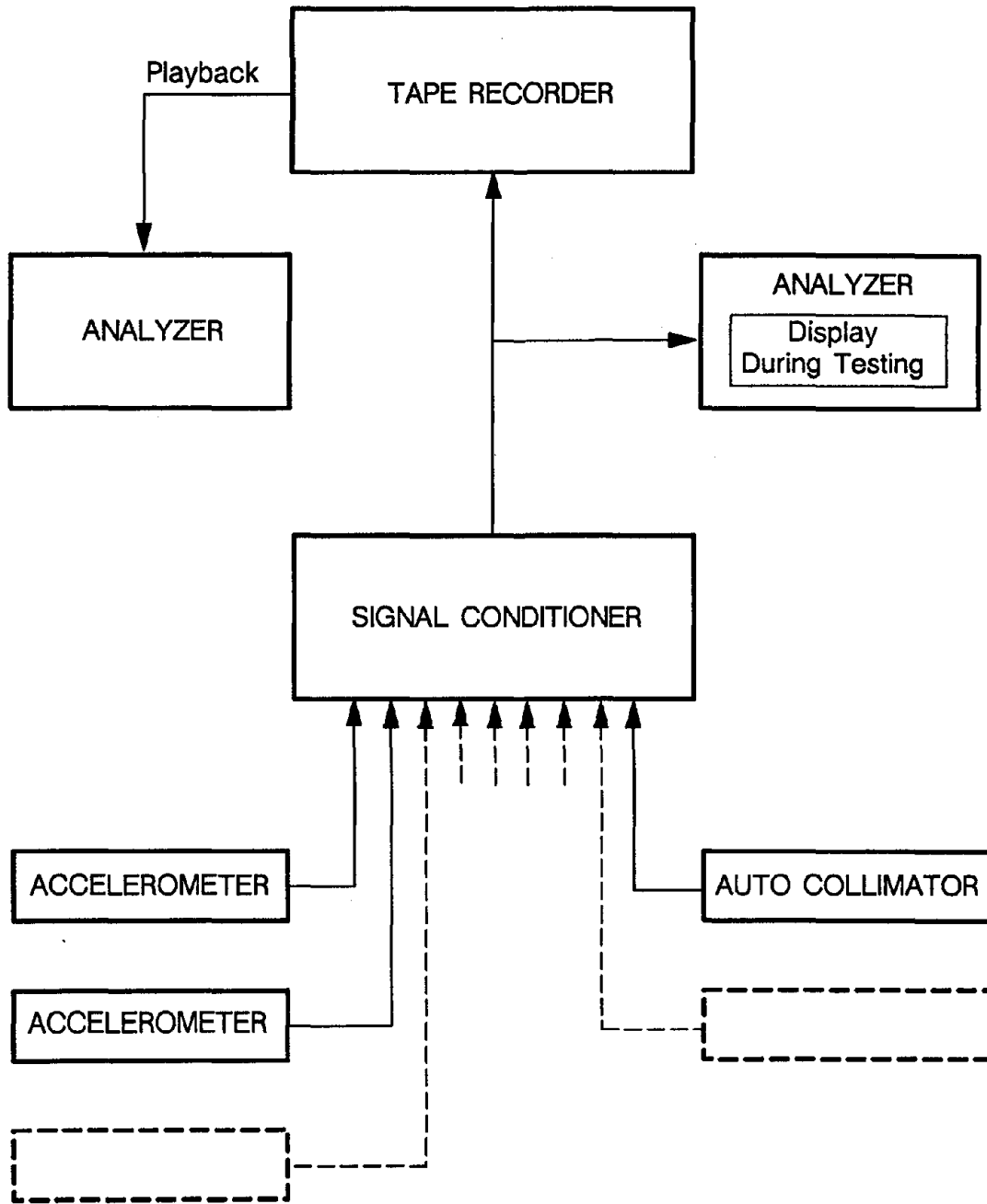


Figure 4.2 Schematic Layout of the Equipment Used for Data Acquisition

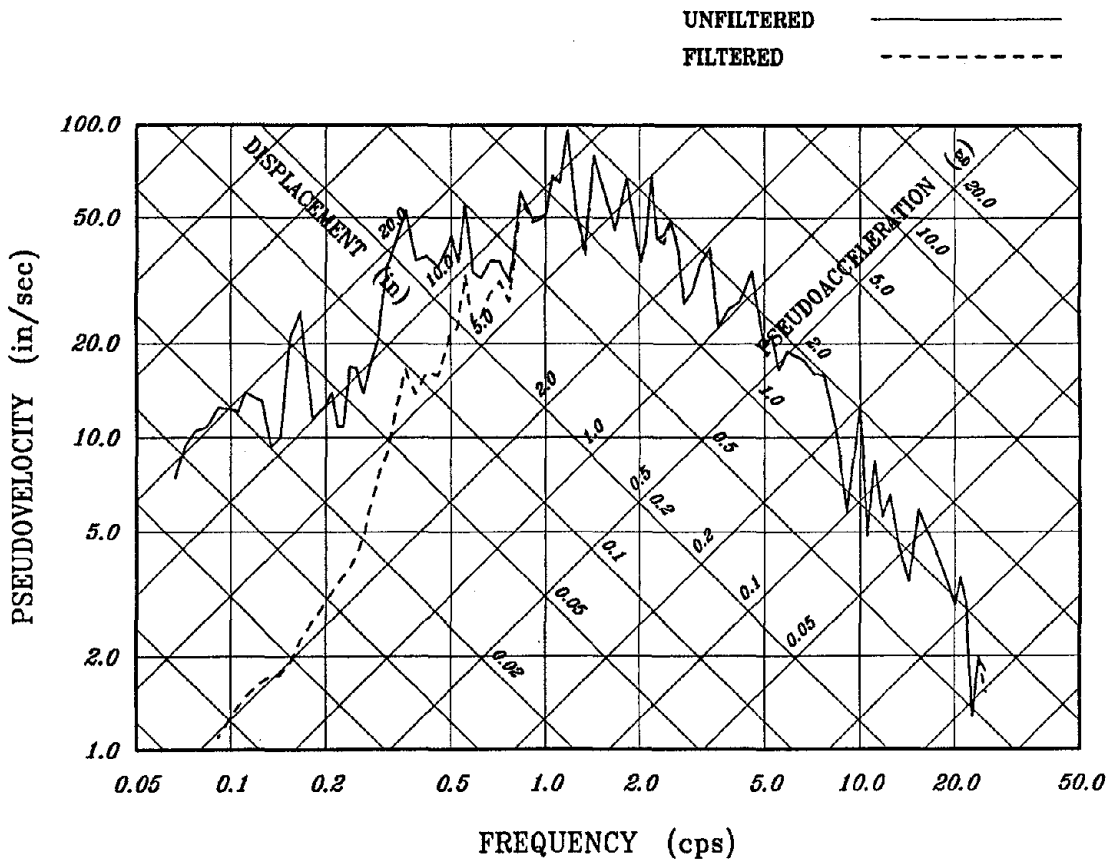
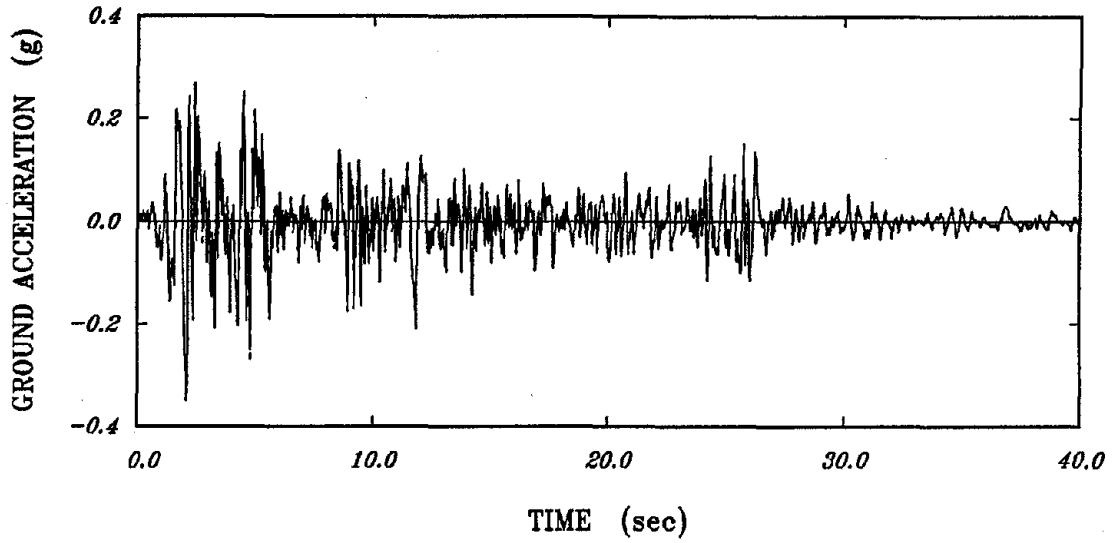


Figure 4.3 Ground Acceleration Records and Undamped Response Spectra of the Unfiltered and Filtered El Centro Earthquake

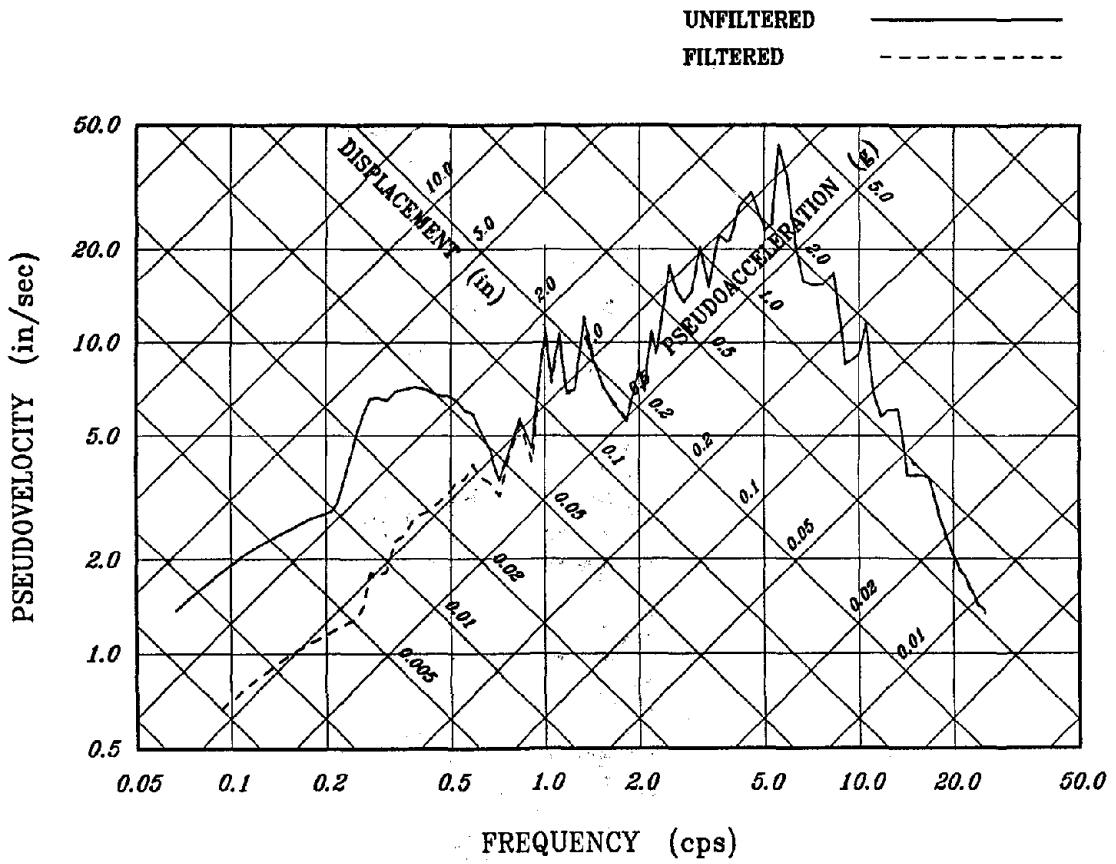
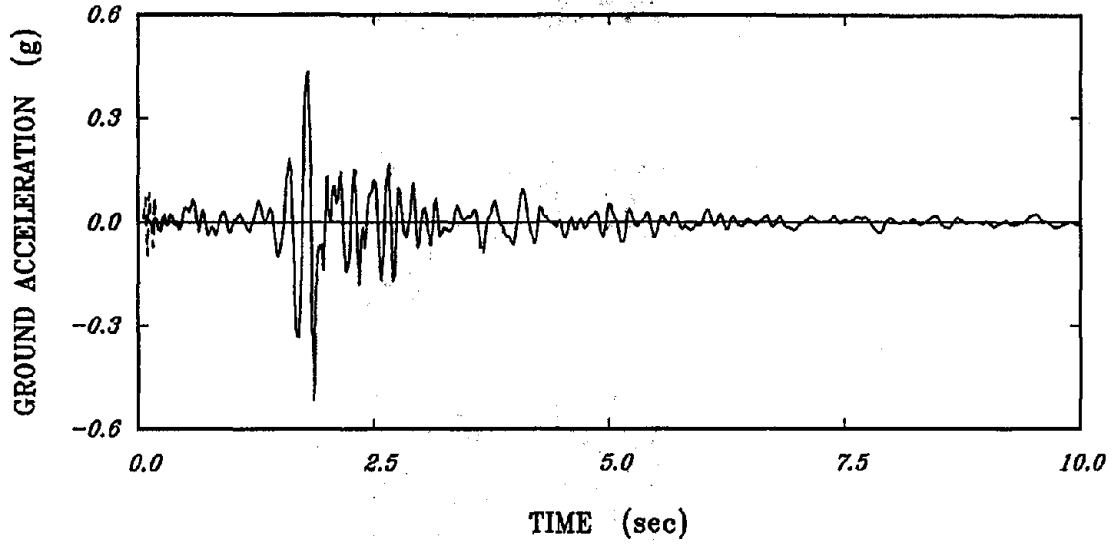


Figure 4.4 Ground Acceleration Records and Undamped Response Spectra of the Unfiltered and Filtered Melendy Earthquake

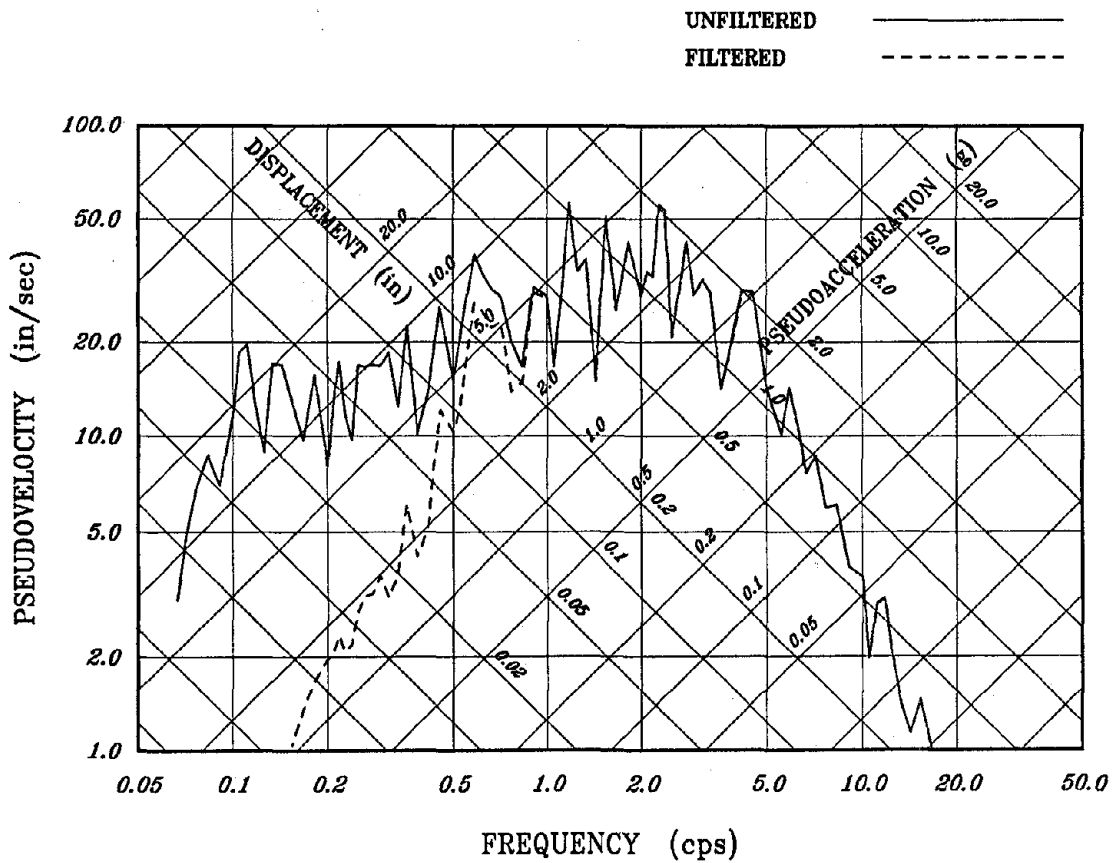
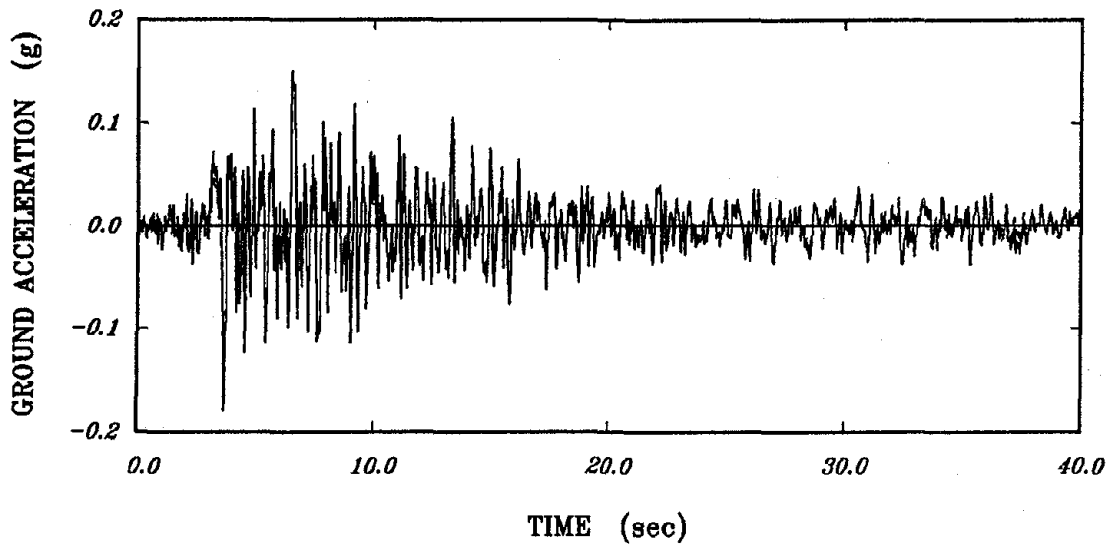


Figure 4.5 Ground Acceleration Records and Undamped Response Spectra of the Unfiltered and Filtered Taft Earthquake

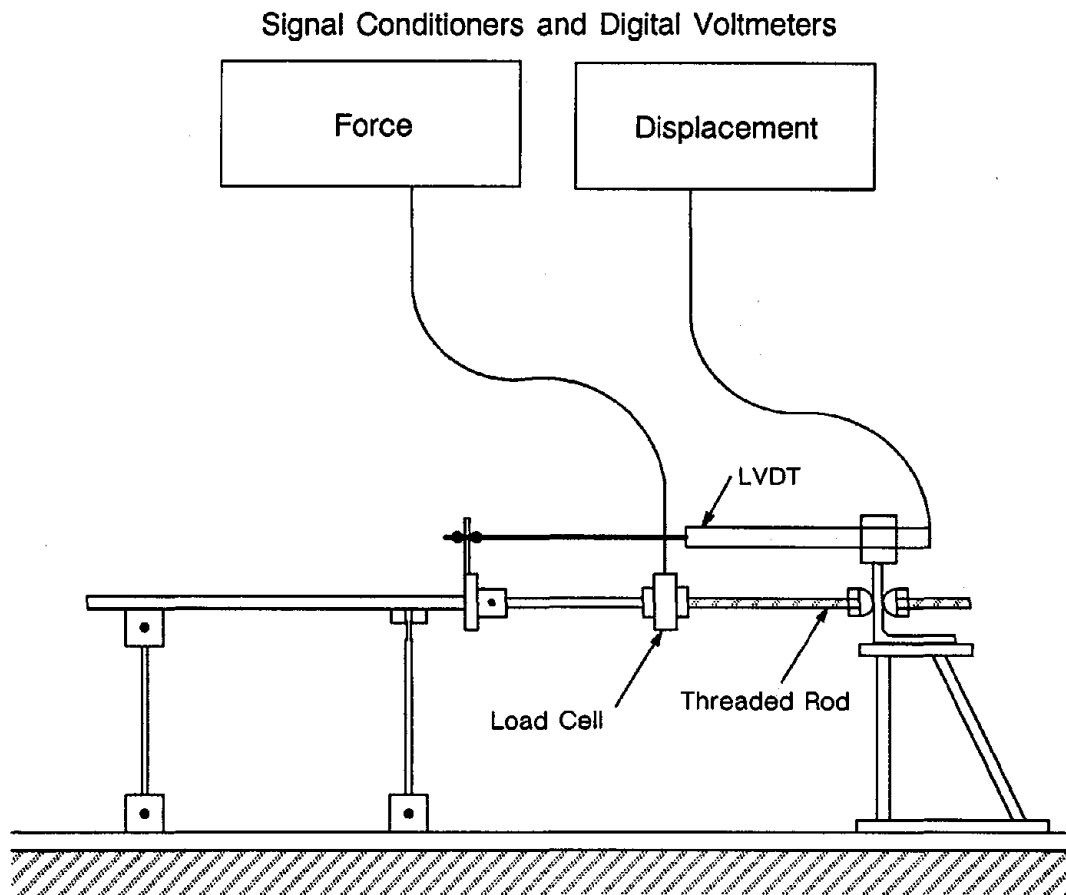


Figure 4.6 Schematic Arrangement of a Static Test

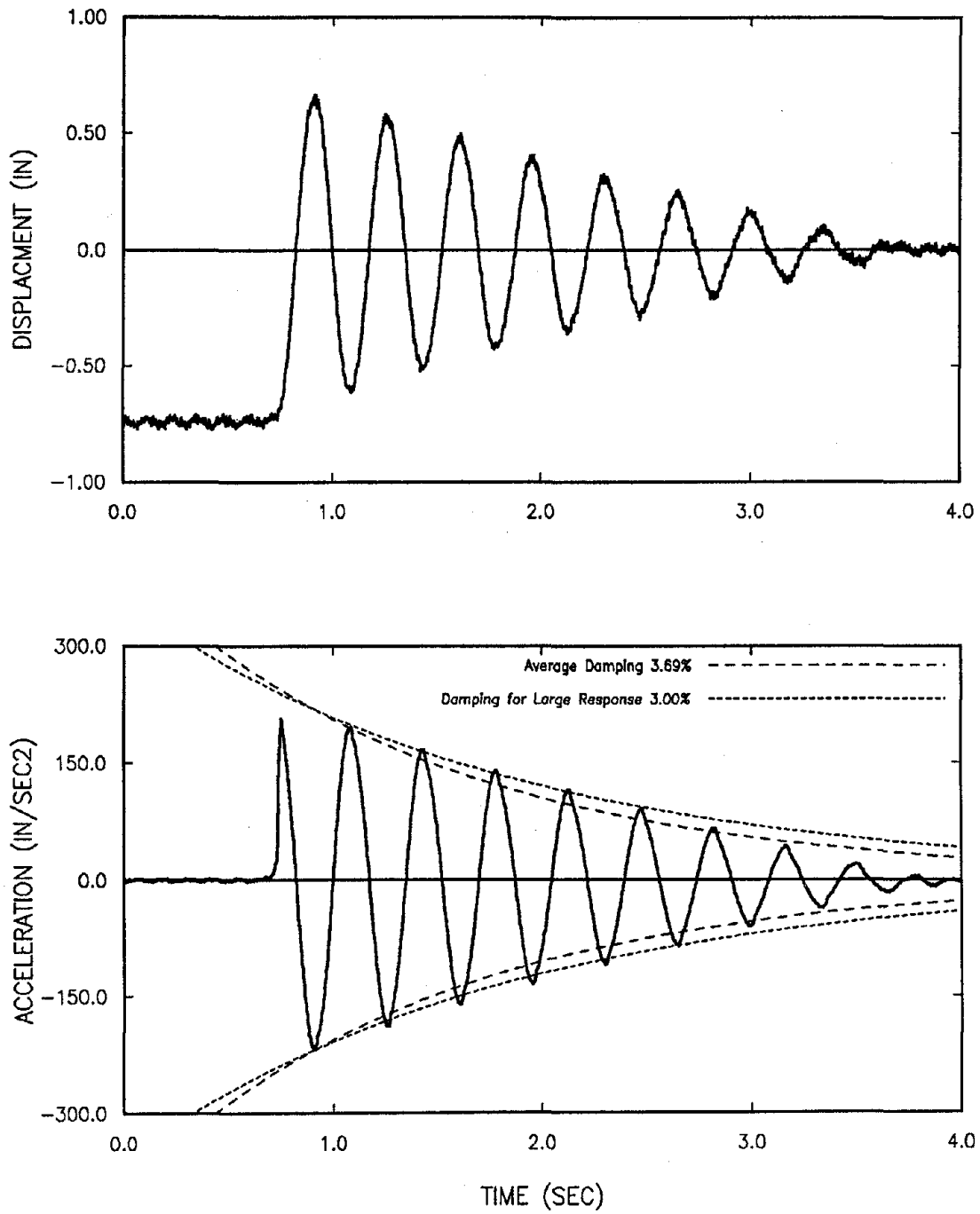


Figure 5.1 Measured Free Vibrations, Acceleration and Displacement, of the Single-Story Structure S1

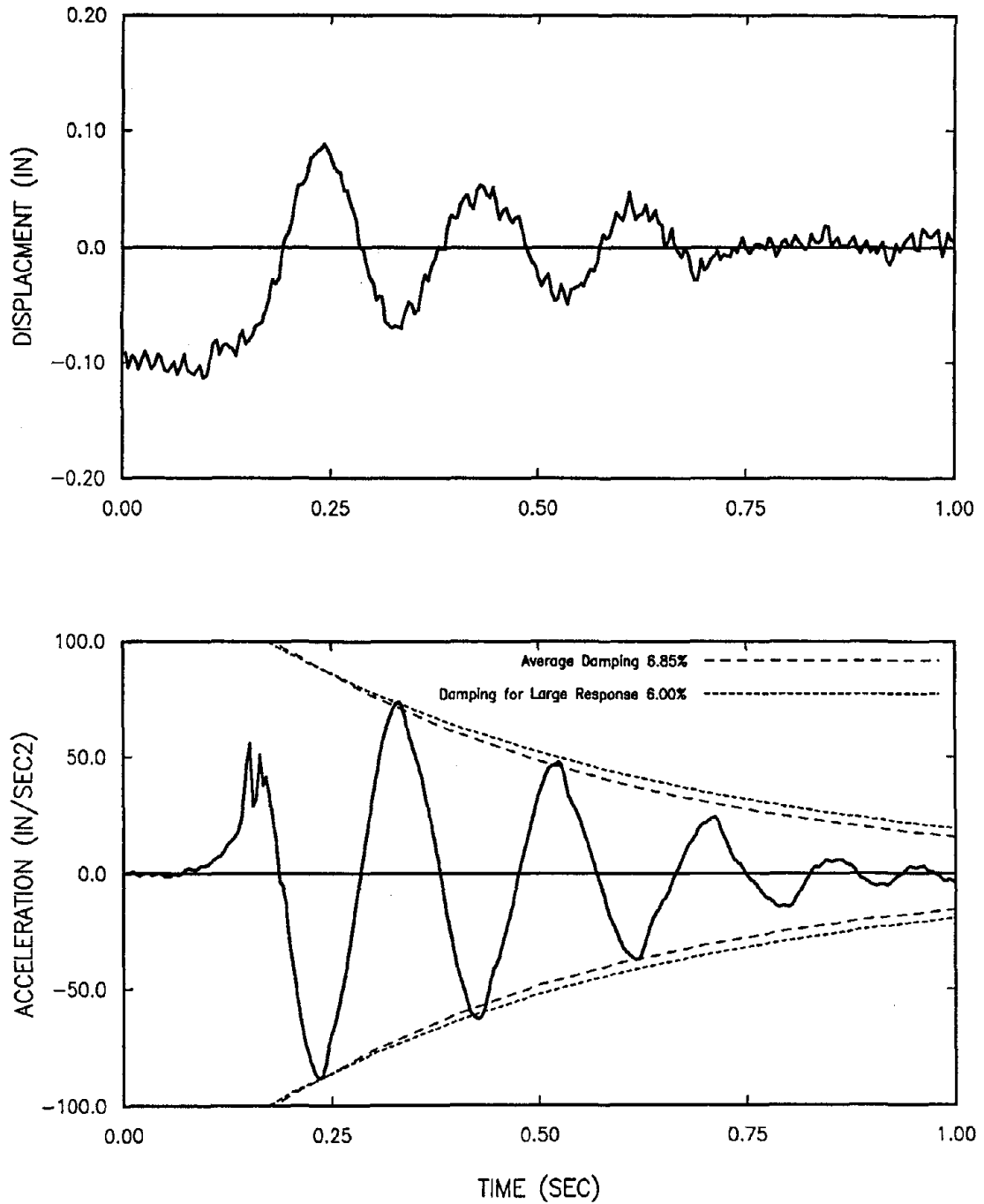


Figure 5.2 Measured Free Vibrations, Acceleration and Displacement, of the Single-Story Structure S4

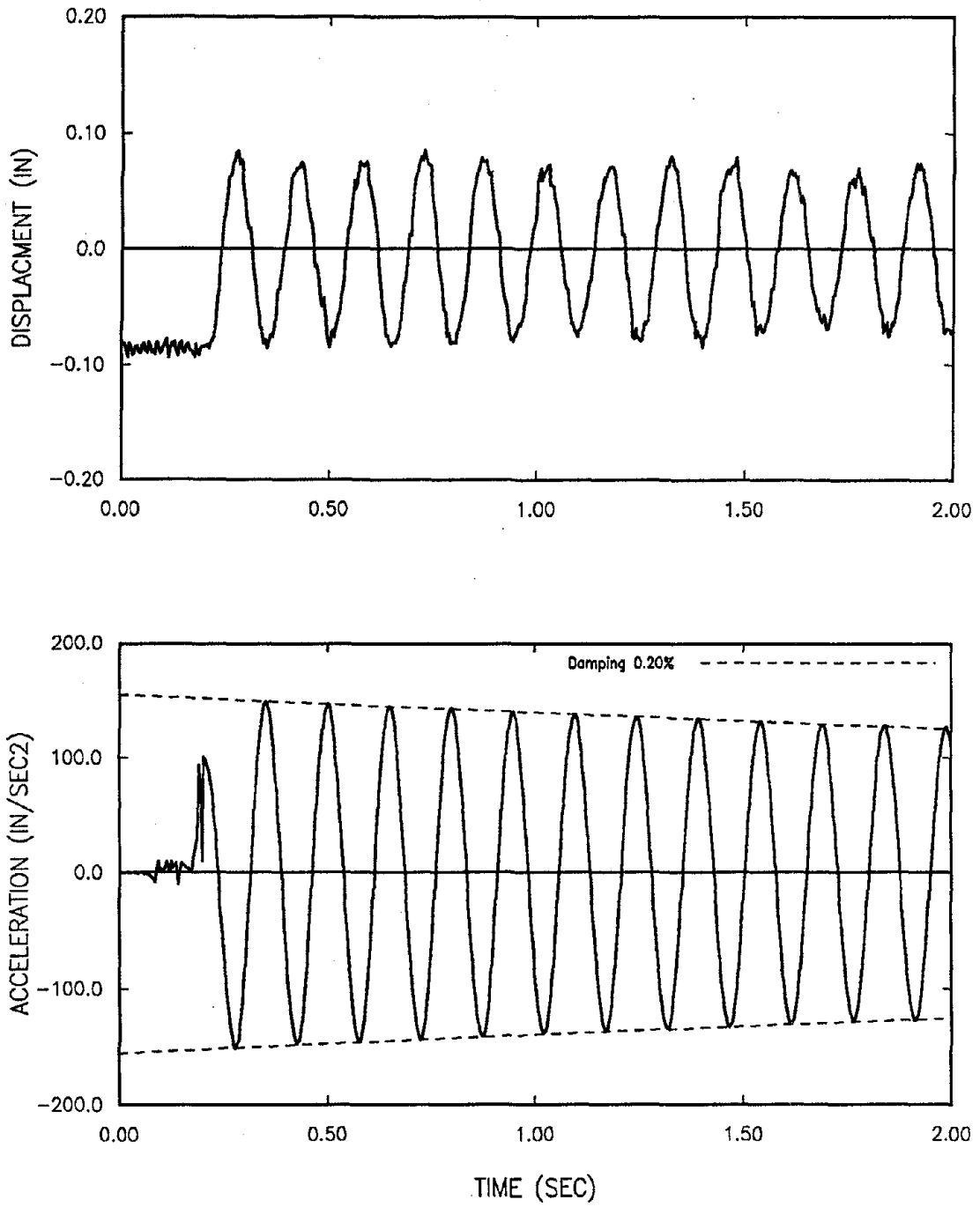


Figure 5.3 Measured Free Vibrations, Acceleration and Displacement, of the Single-Story Structure S7

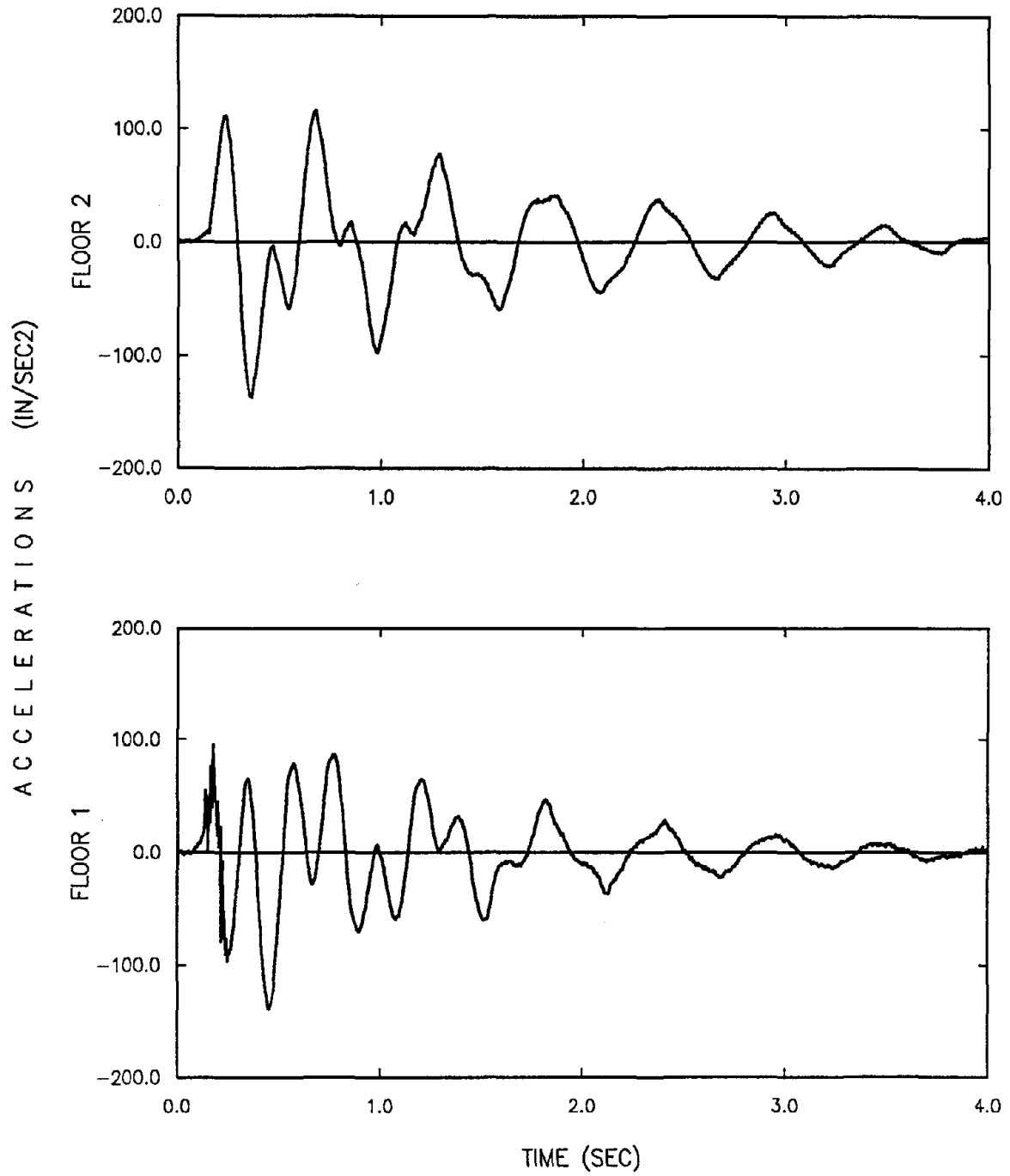


Figure 5.4 Measured Free Vibrations Acceleration of the Two-Story Structure M1

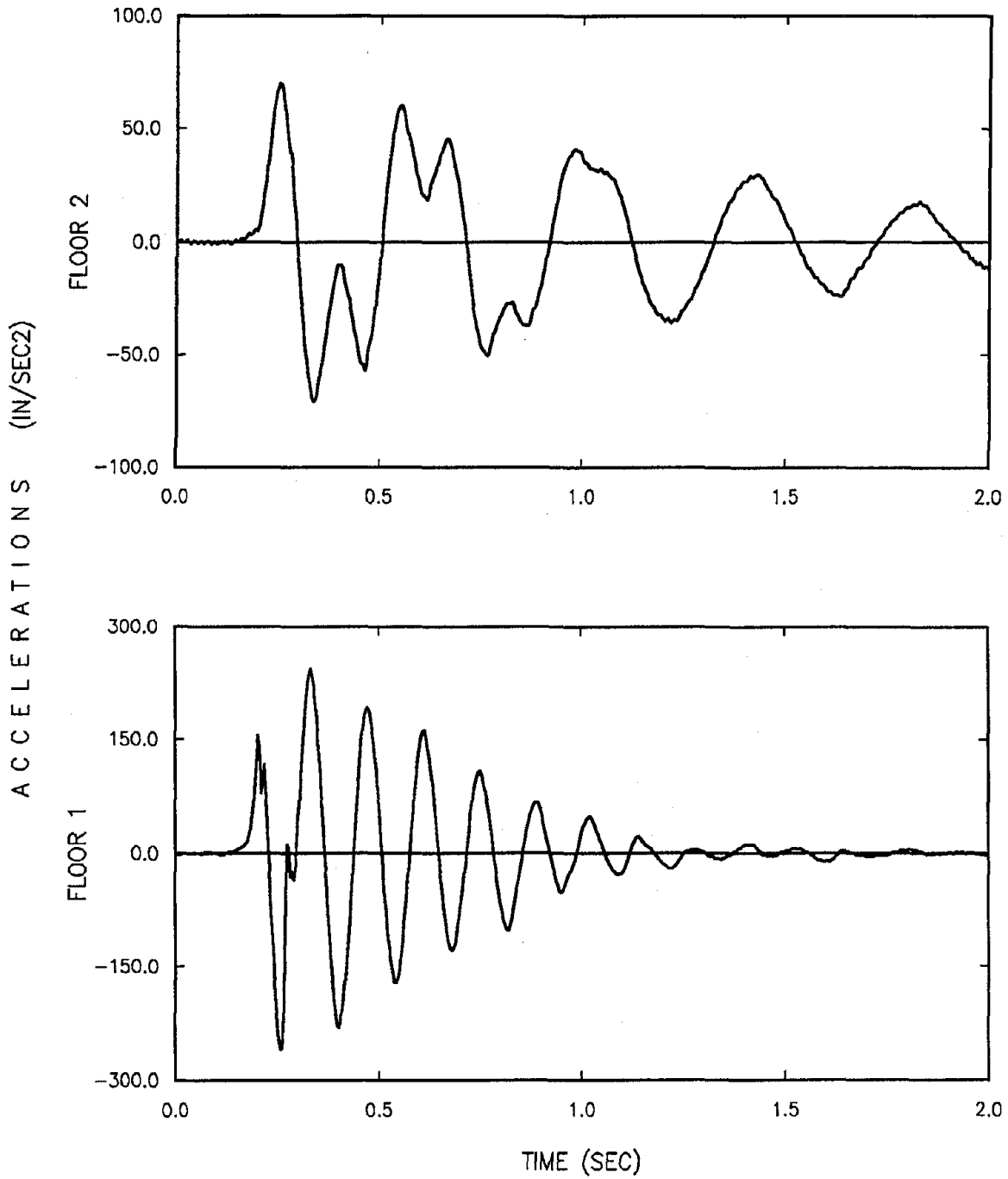


Figure 5.5 Measured Free Vibrations Acceleration of the Two-Story Structure M2

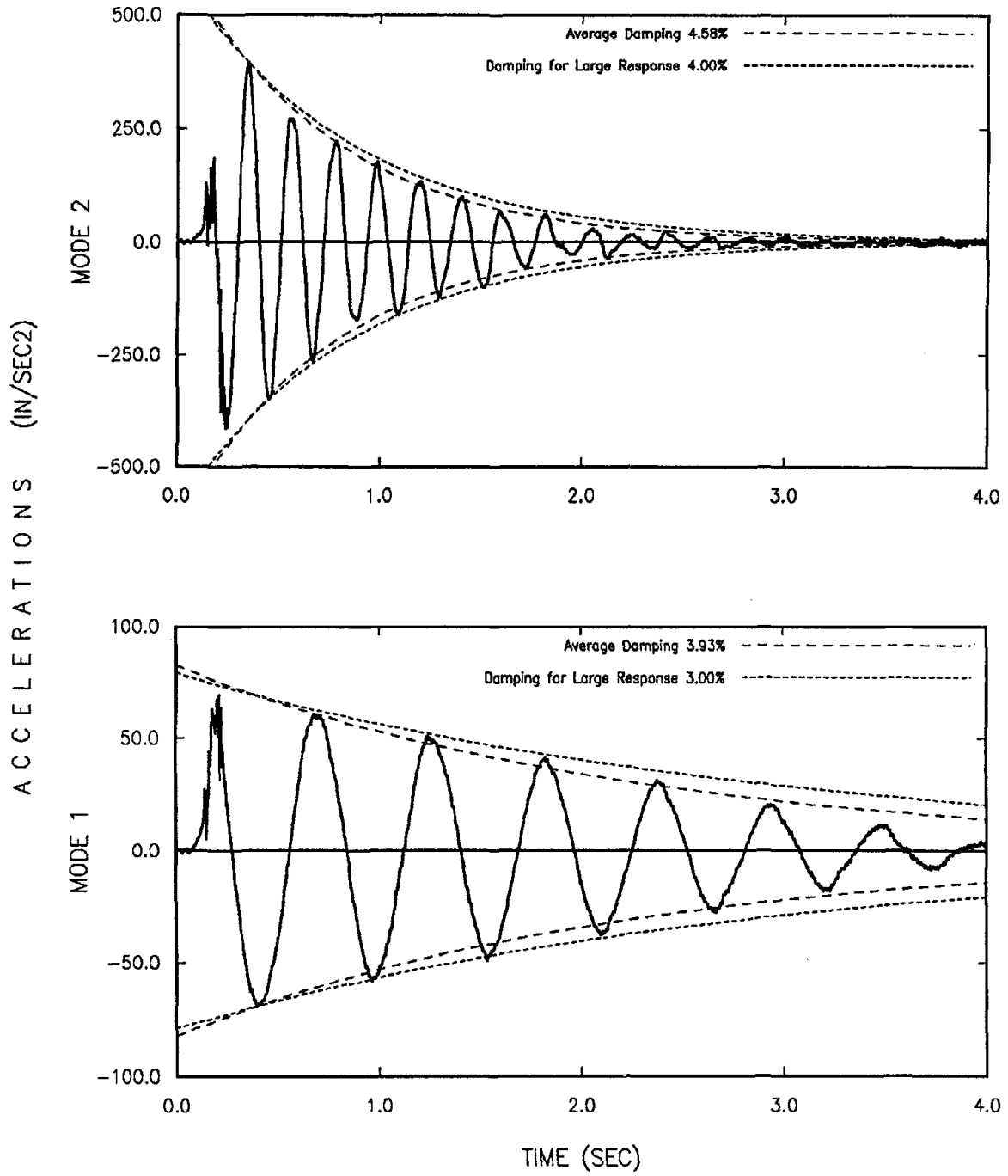


Figure 5.6 Free Vibrations Modal Acceleration of the Two-Story Structure M1

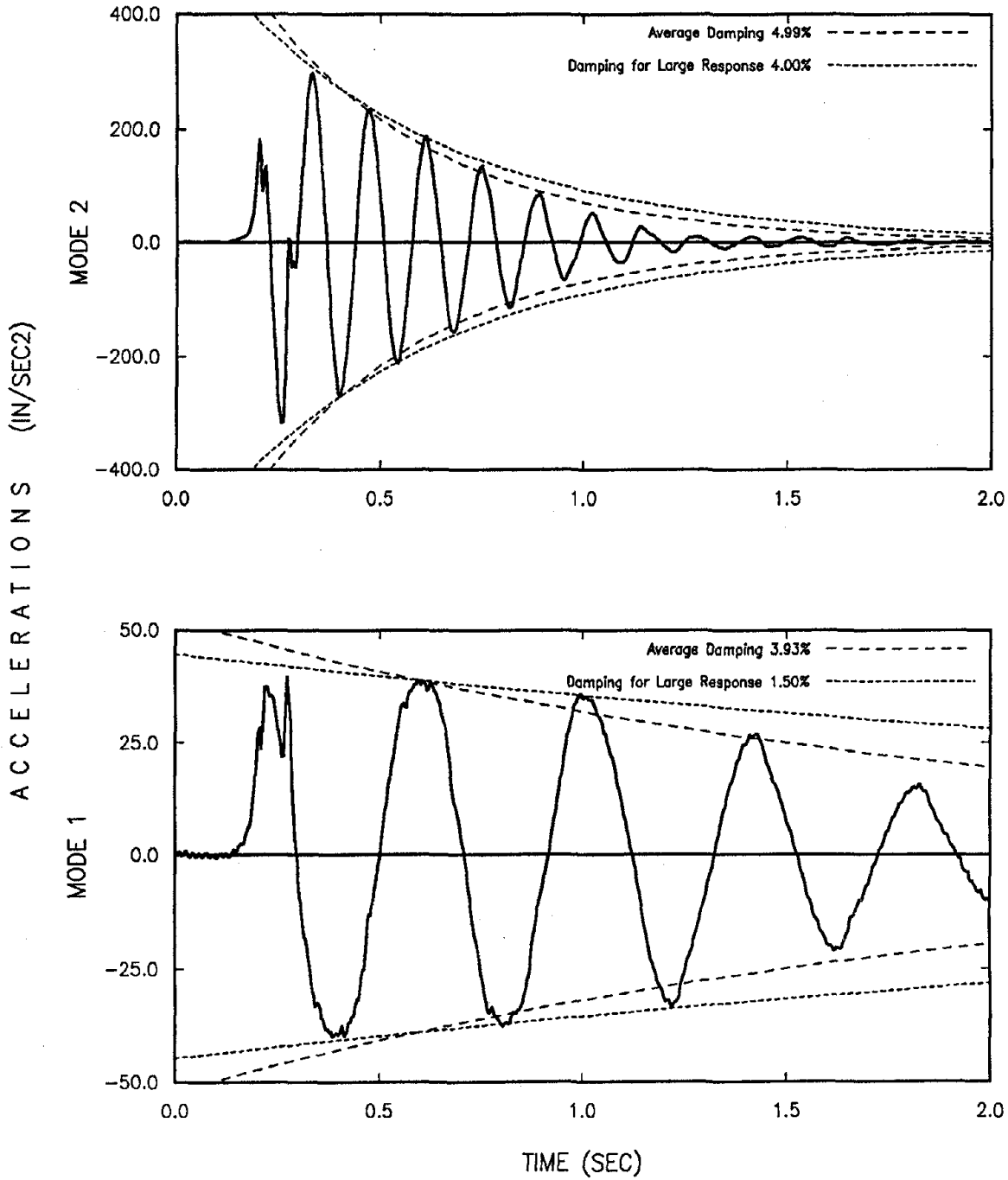


Figure 5.7 Free Vibrations Modal Acceleration of the Two-Story Structure M2

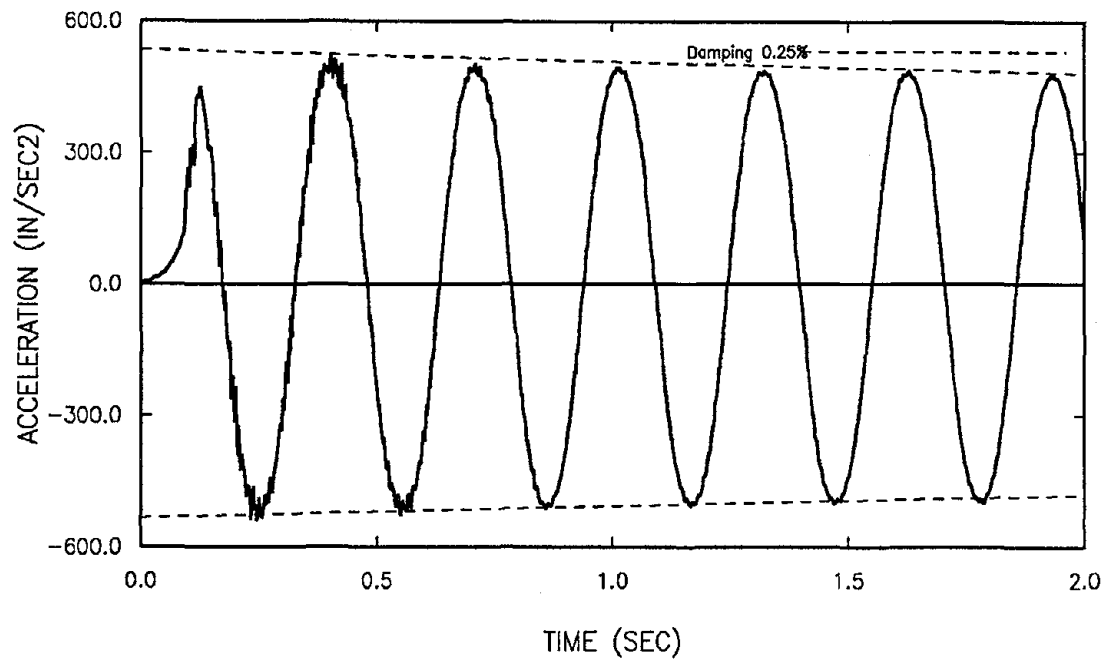


Figure 5.8 Measured Free Vibrations Acceleration of Appendage AS2

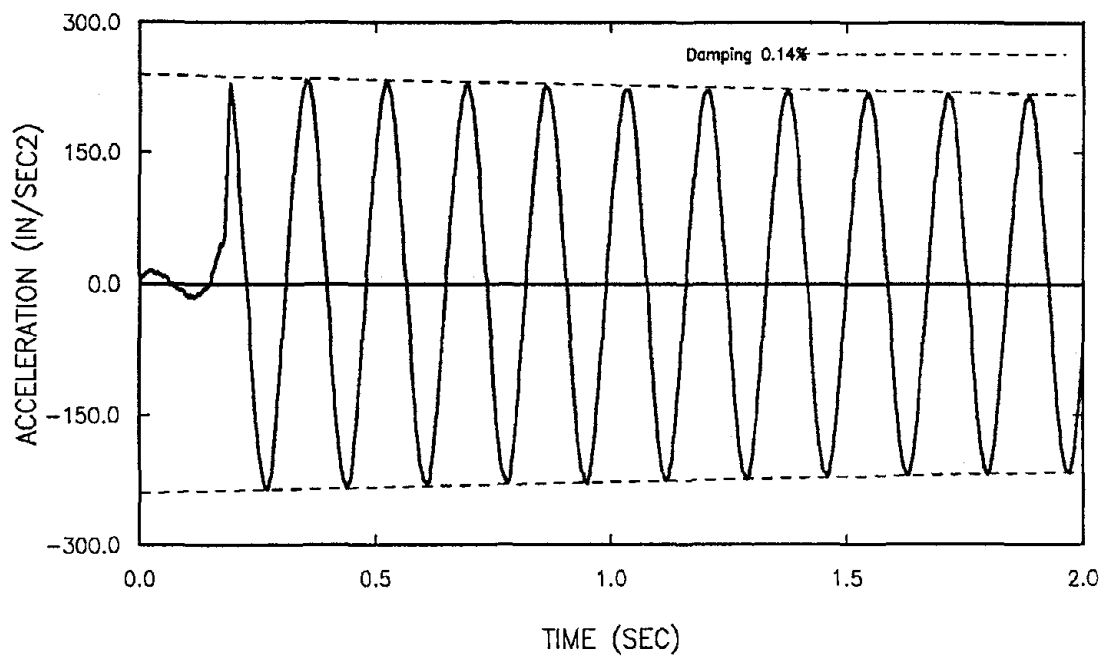


Figure 5.9 Measured Free Vibrations Acceleration of Appendage AL3

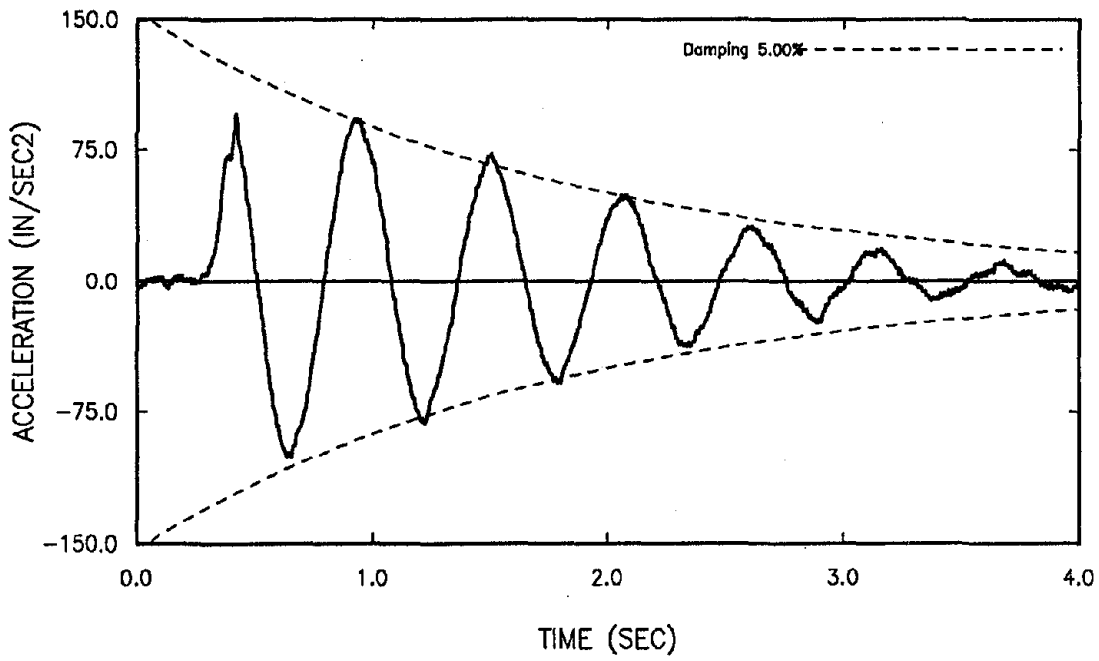


Figure 5.10 Measured Free Vibrations Acceleration of Appendage AS1

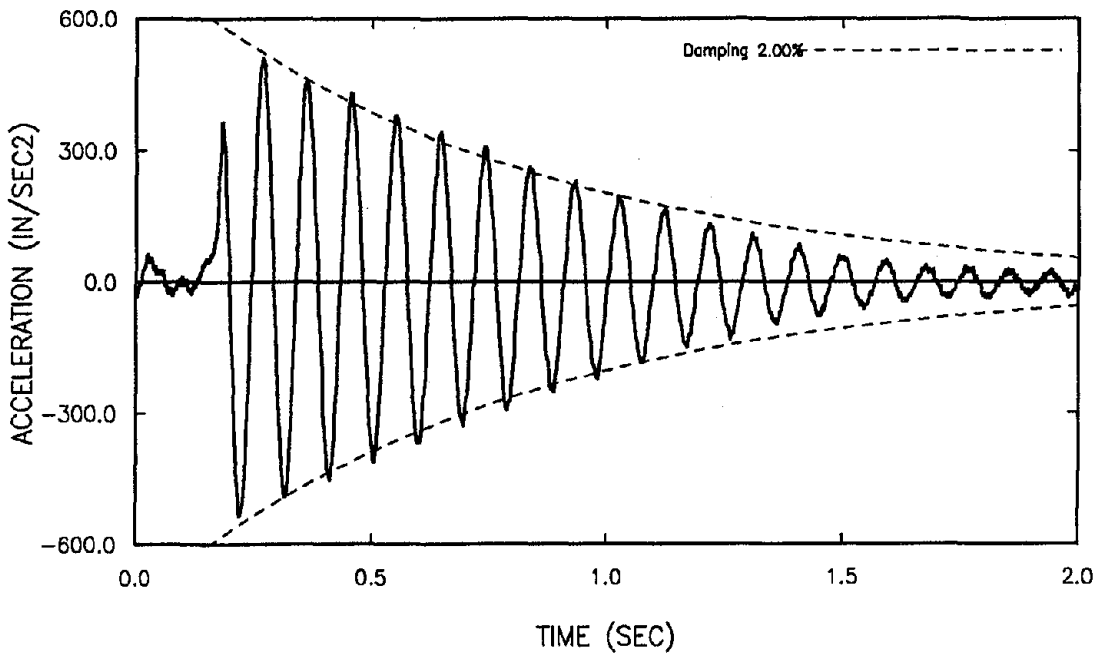


Figure 5.11 Measured Free Vibrations Acceleration of Appendage AT6

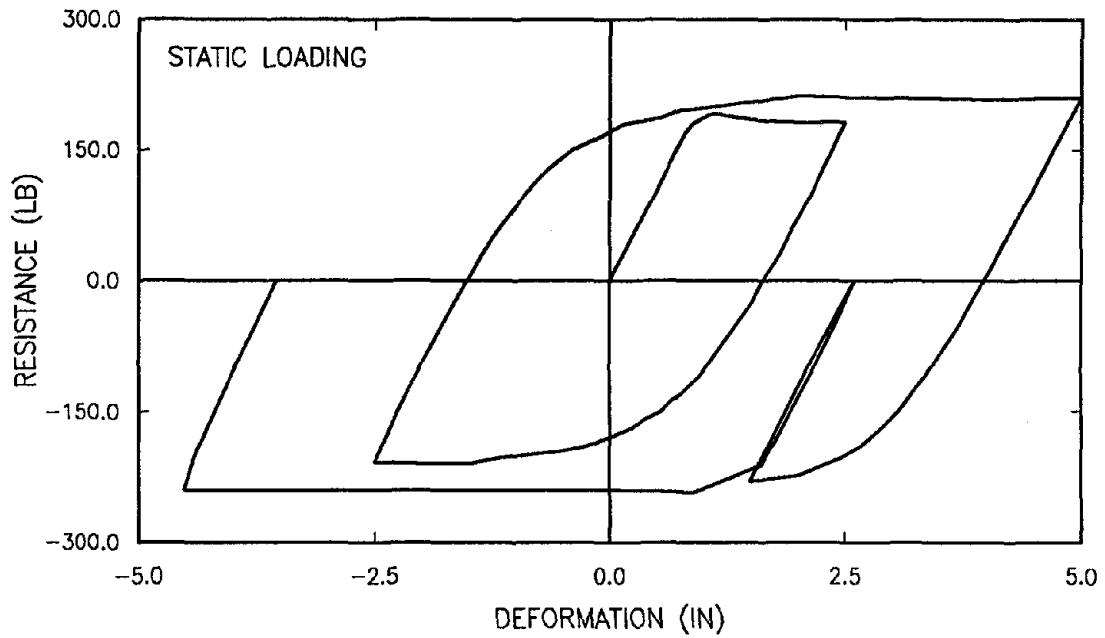


Figure 5.12 Typical Measured Static Force-Displacement Relation of a Single-Story Structure (Structure S1)

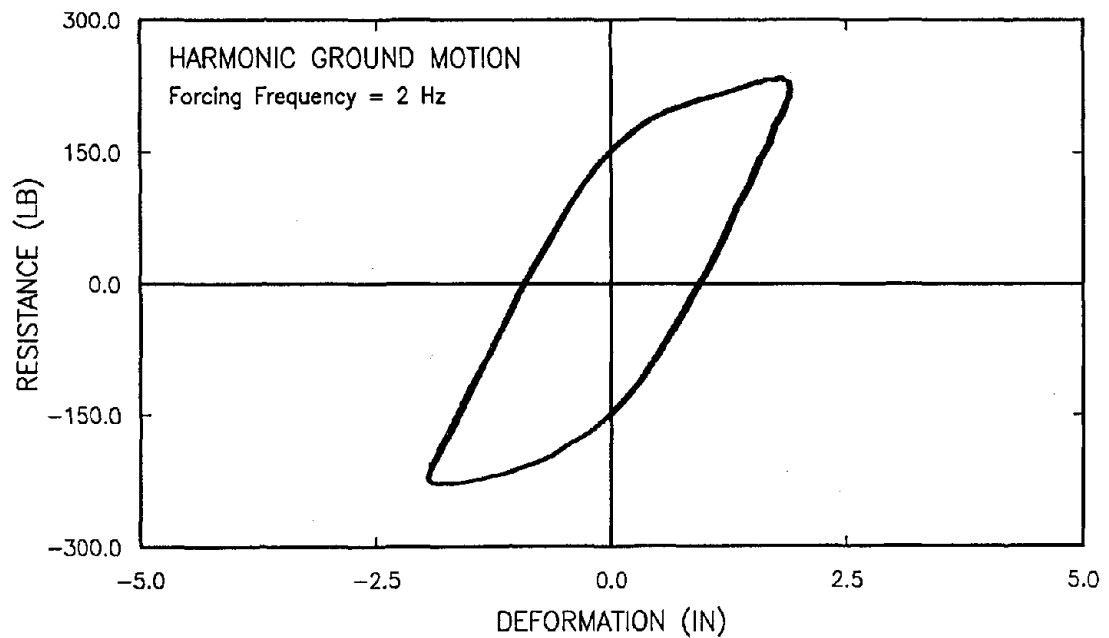


Figure 5.13 Typical Measured Response of a Single-Story Structure (Structure S1) Subjected to Harmonic Ground Motion

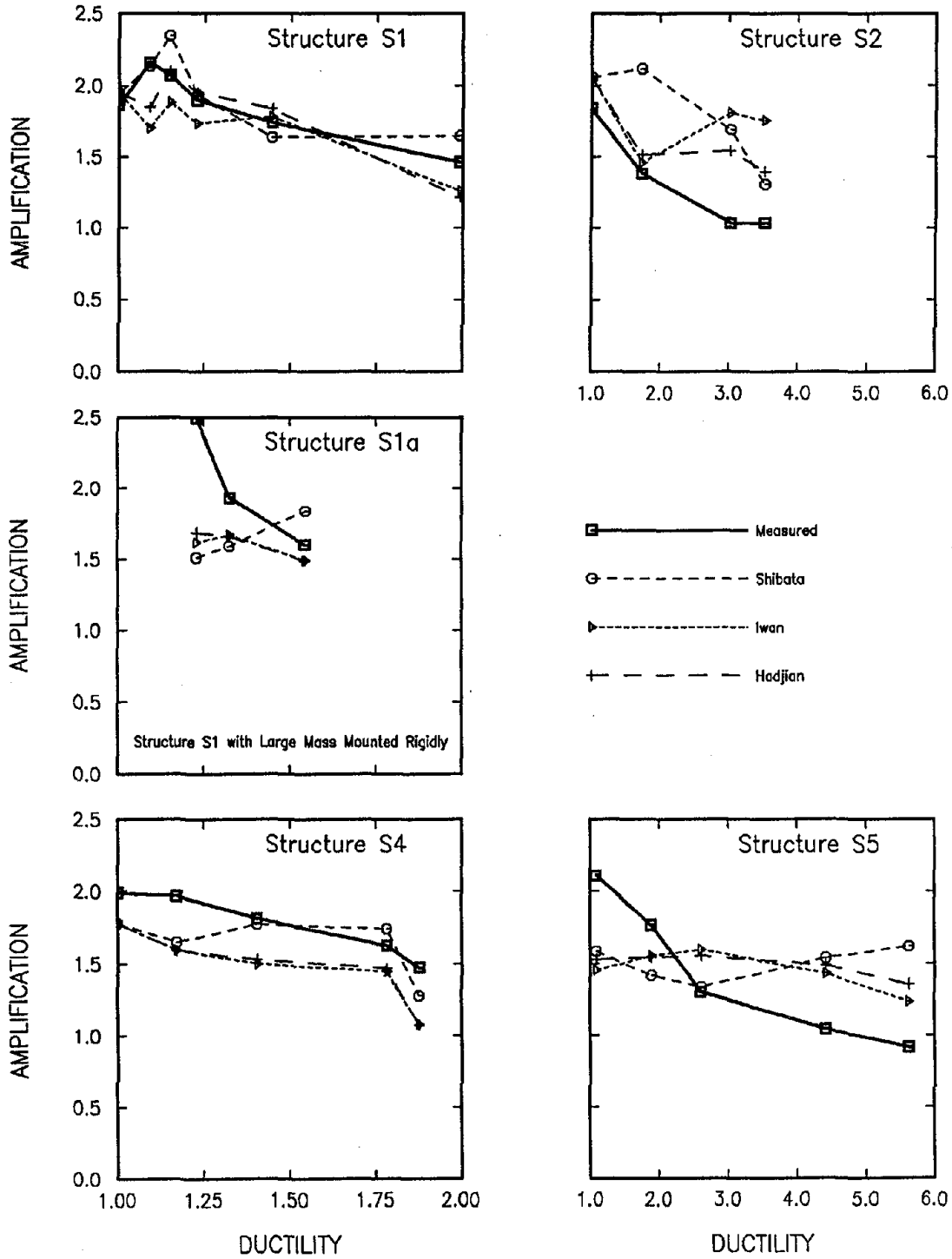


Figure 5.14a Comparison of Measured Amplifications with Amplifications Calculated Using Different Equivalent Linear Systems. Single-Story Structures Subjected to El Centro Earthquake

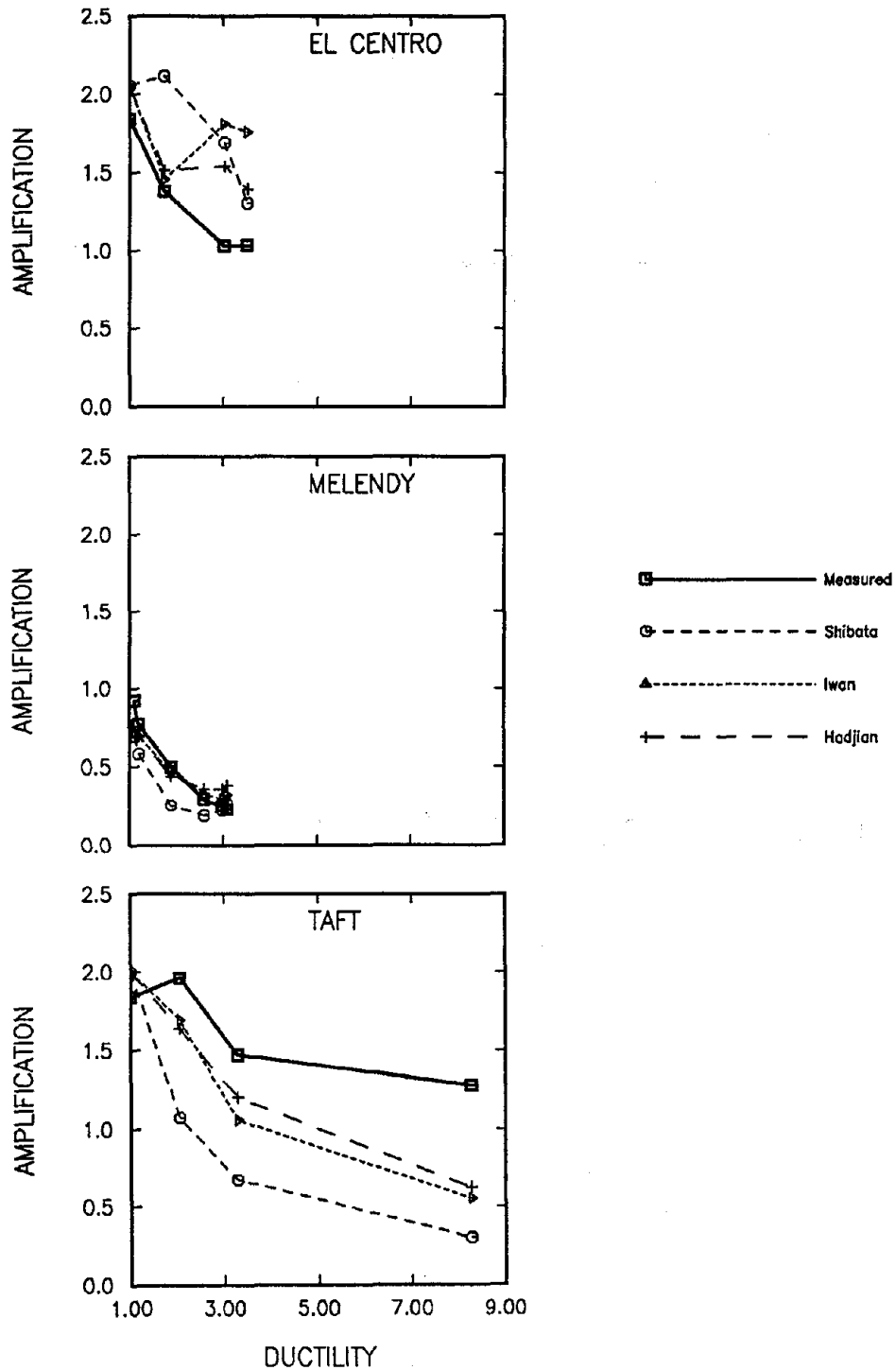


Figure 5.14b Comparison of Measured Amplifications with Amplifications Calculated Using Different Equivalent Linear Systems. Single-Story Structure S2 Subjected to El Centro, Melendy and Taft Earthquakes

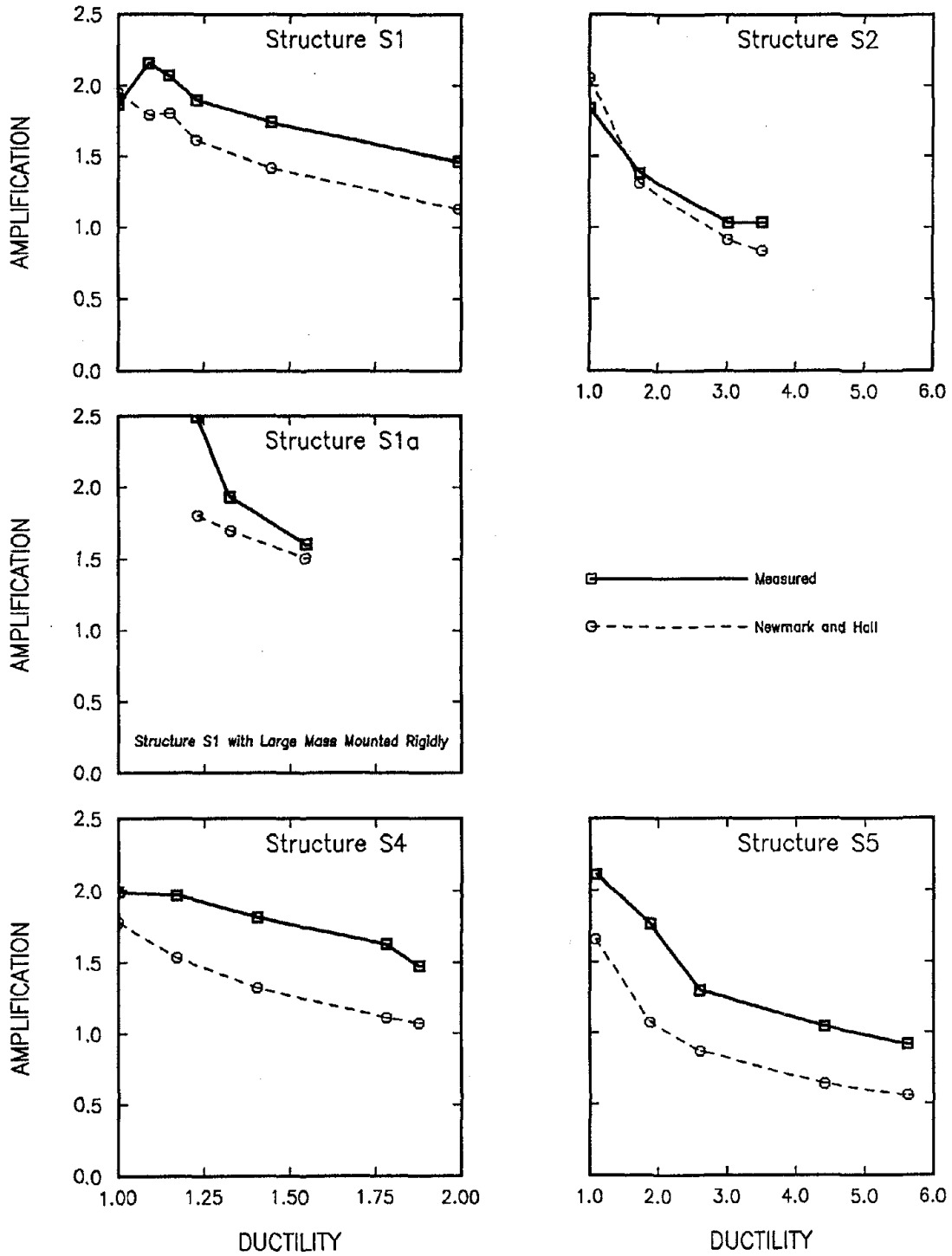


Figure 5.15a Comparison of Measured Amplifications with Amplifications Calculated Using Modified Response Spectra. Single-Story Structure S2 Subjected to El Centro Earthquake

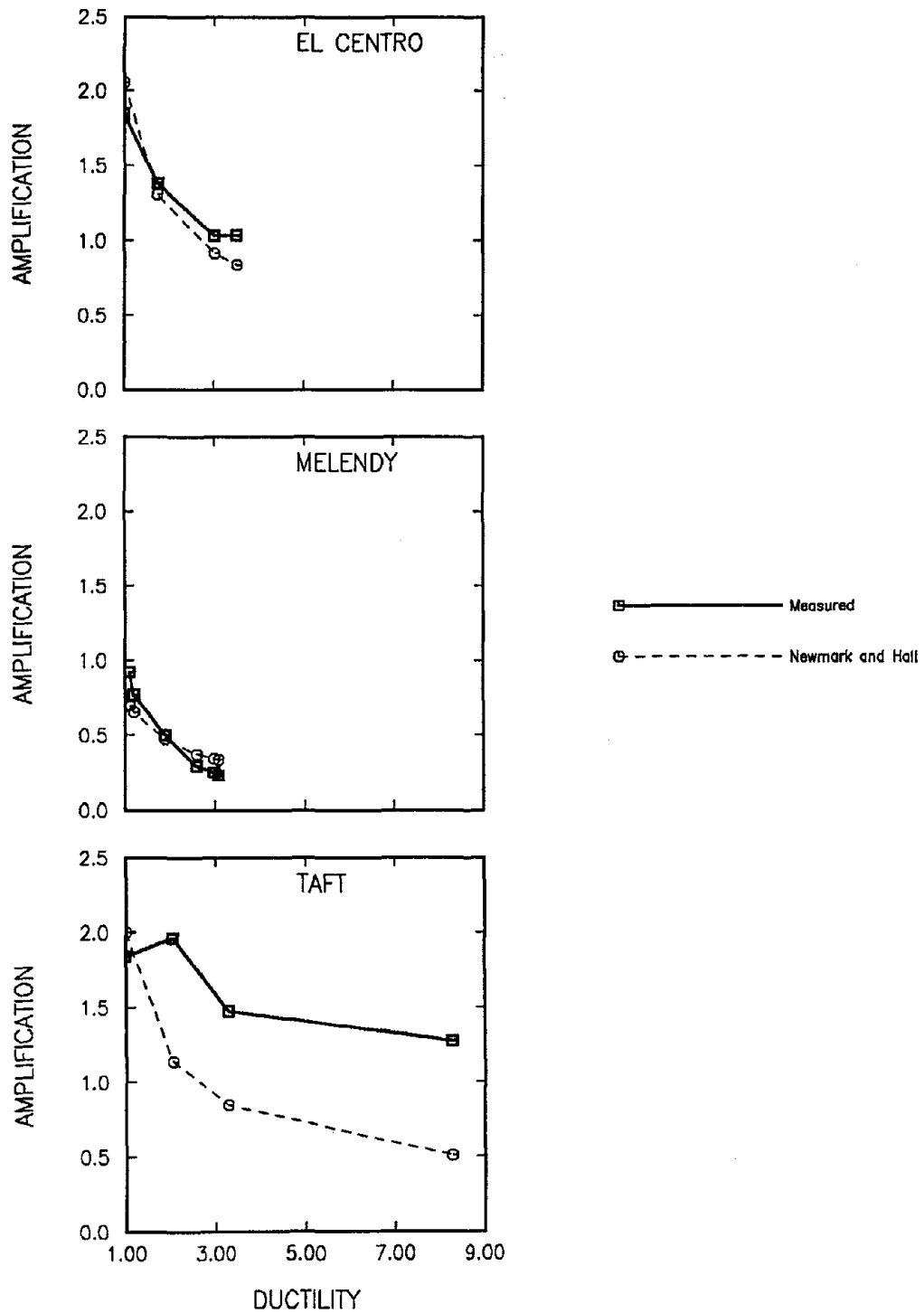


Figure 5.15b Comparison of Measured Amplifications with Amplifications Calculated Using Modified Response Spectra. Single-Story Structure S2 Subjected to El Centro, Melendy and Taft Earthquakes

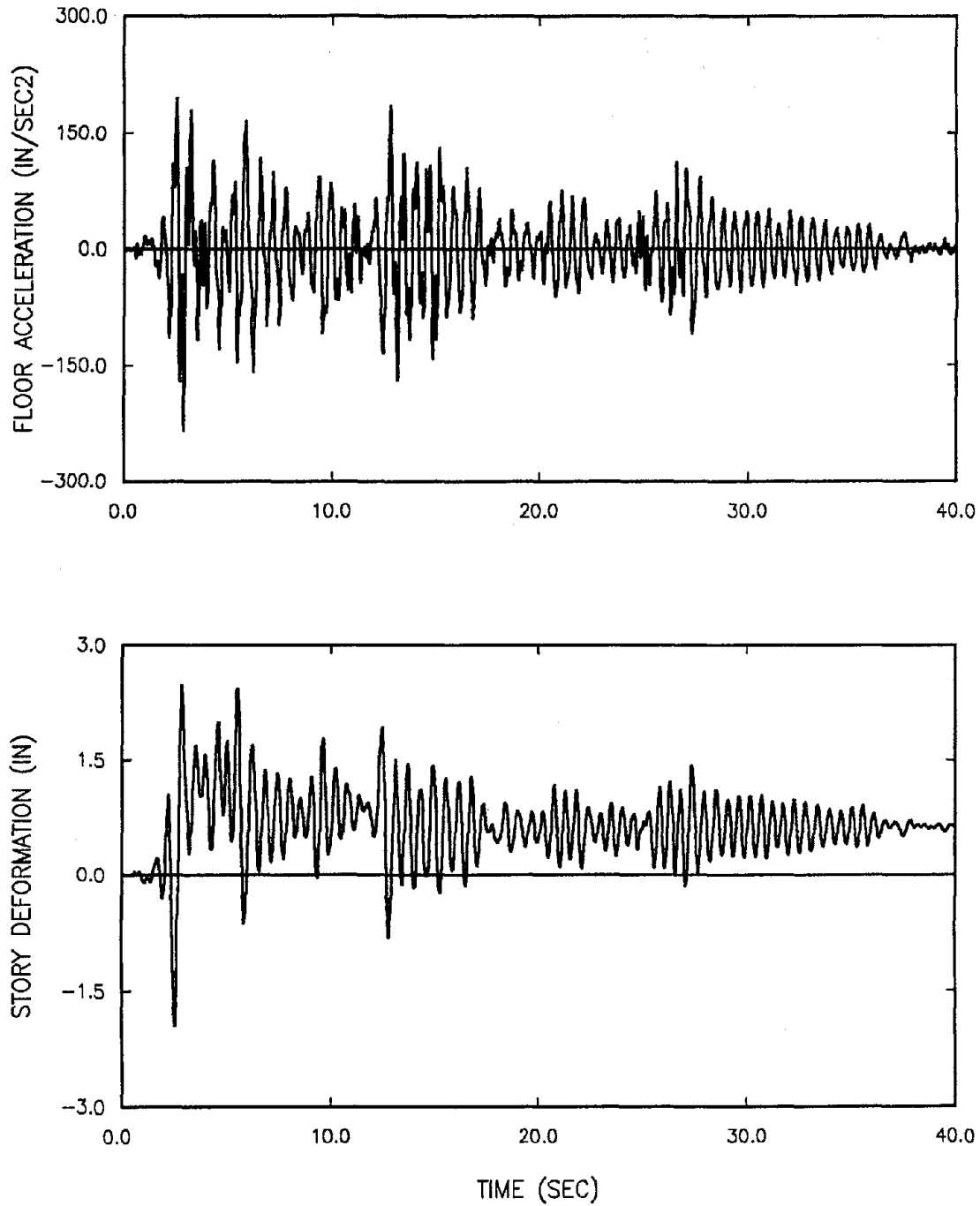


Figure 5.16a Typical Measured Response of the First Story of the Two-Story Structure M1 Subjected to El Centro Earthquake

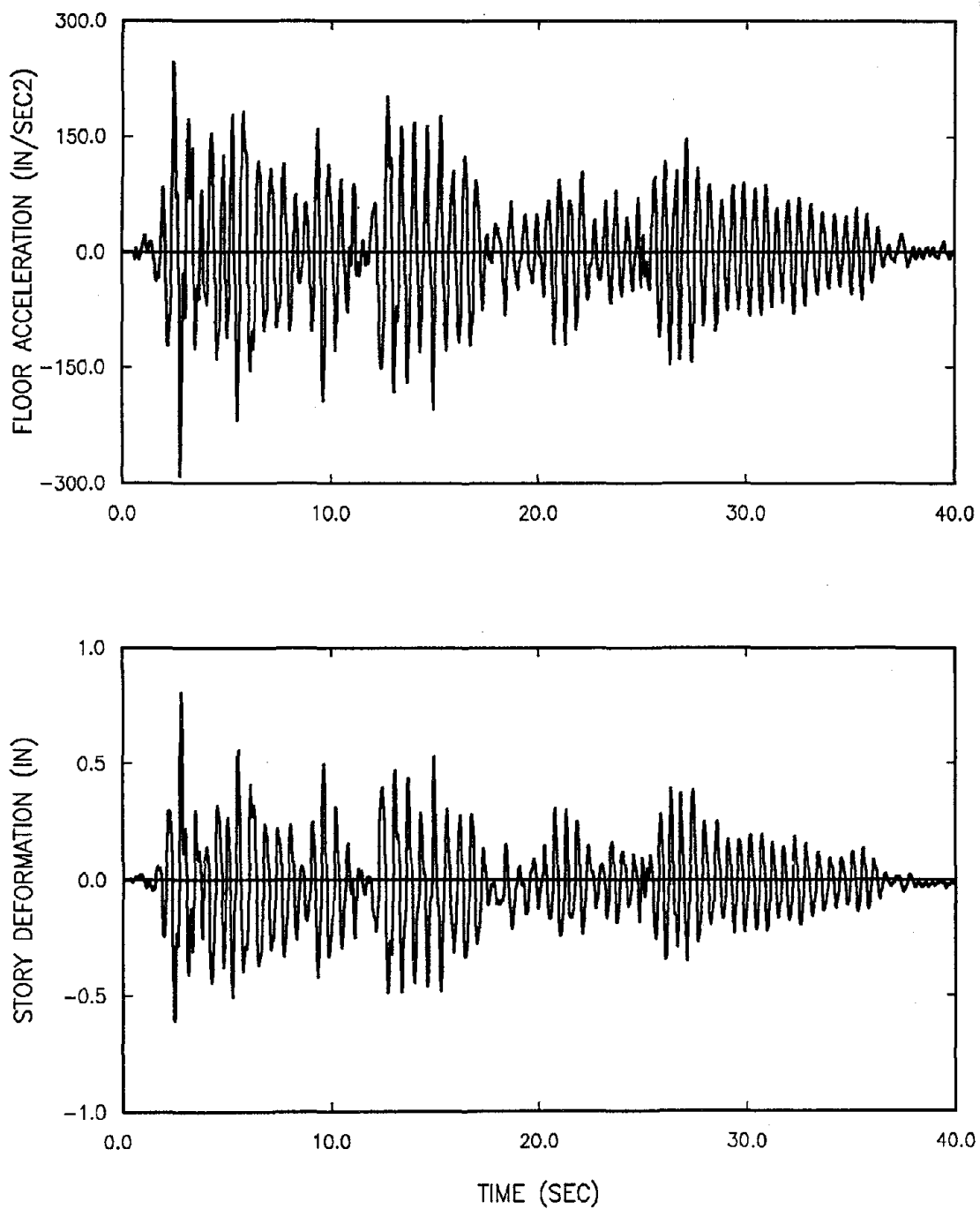


Figure 5.16b Typical Measured Response of the Second Story of the Two-Story Structure M1 Subjected to El Centro Earthquake

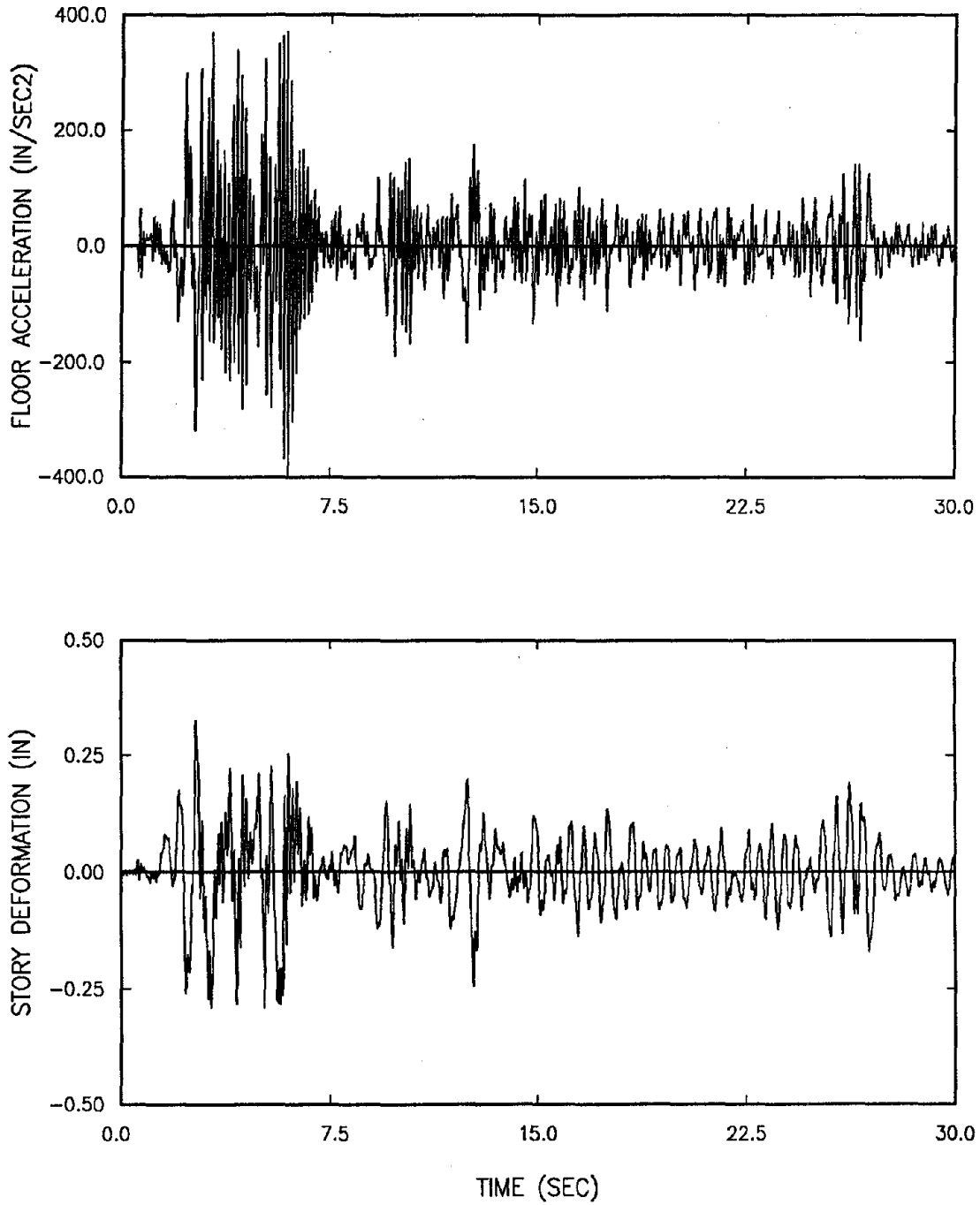


Figure 5.17a Typical Measured Response of the First Story of the Two-Story Structure M2 Subjected to El Centro Earthquake

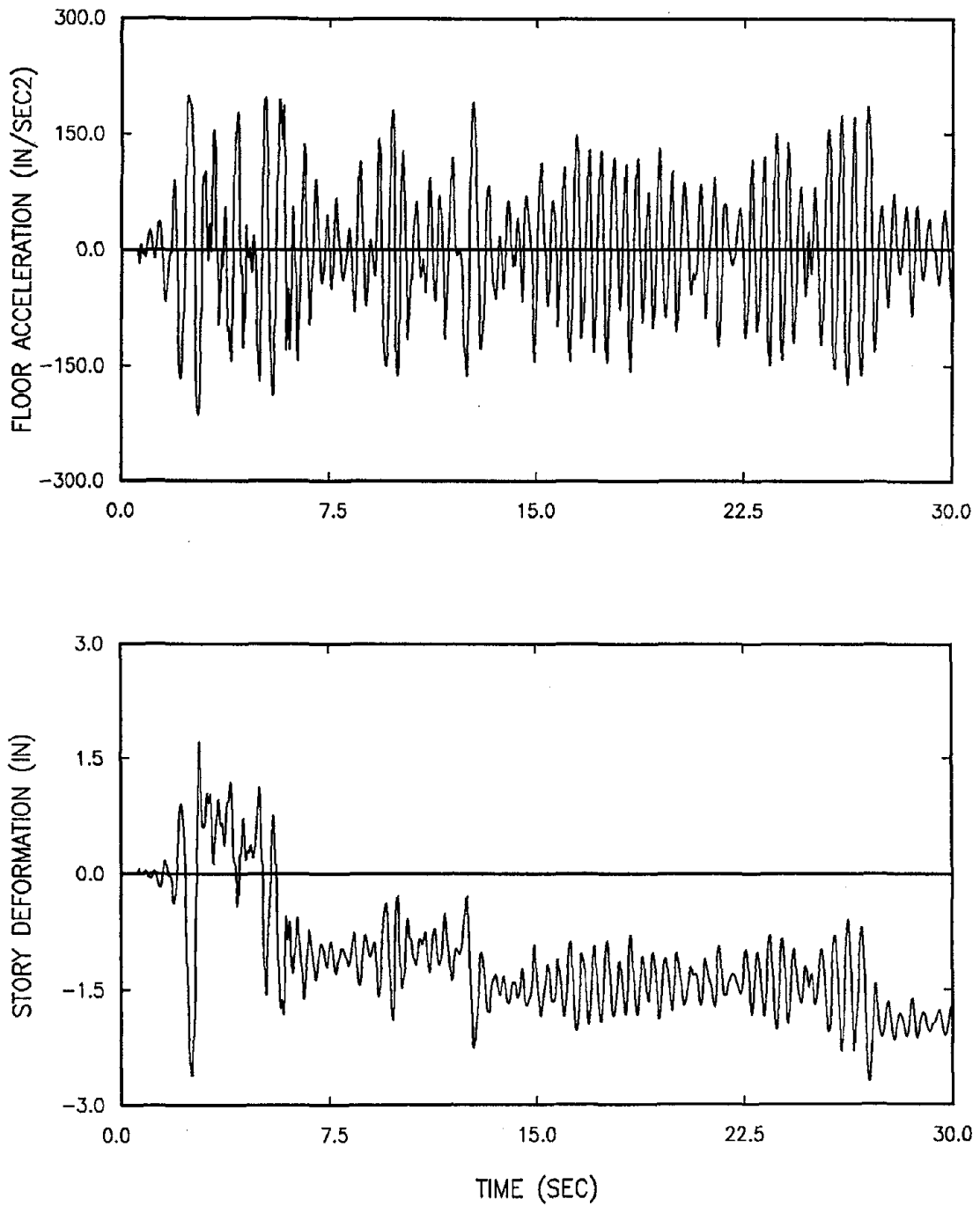


Figure 5.17b Typical Measured Response of the Second Story of the Two-Story Structure M2 Subjected to El Centro Earthquake

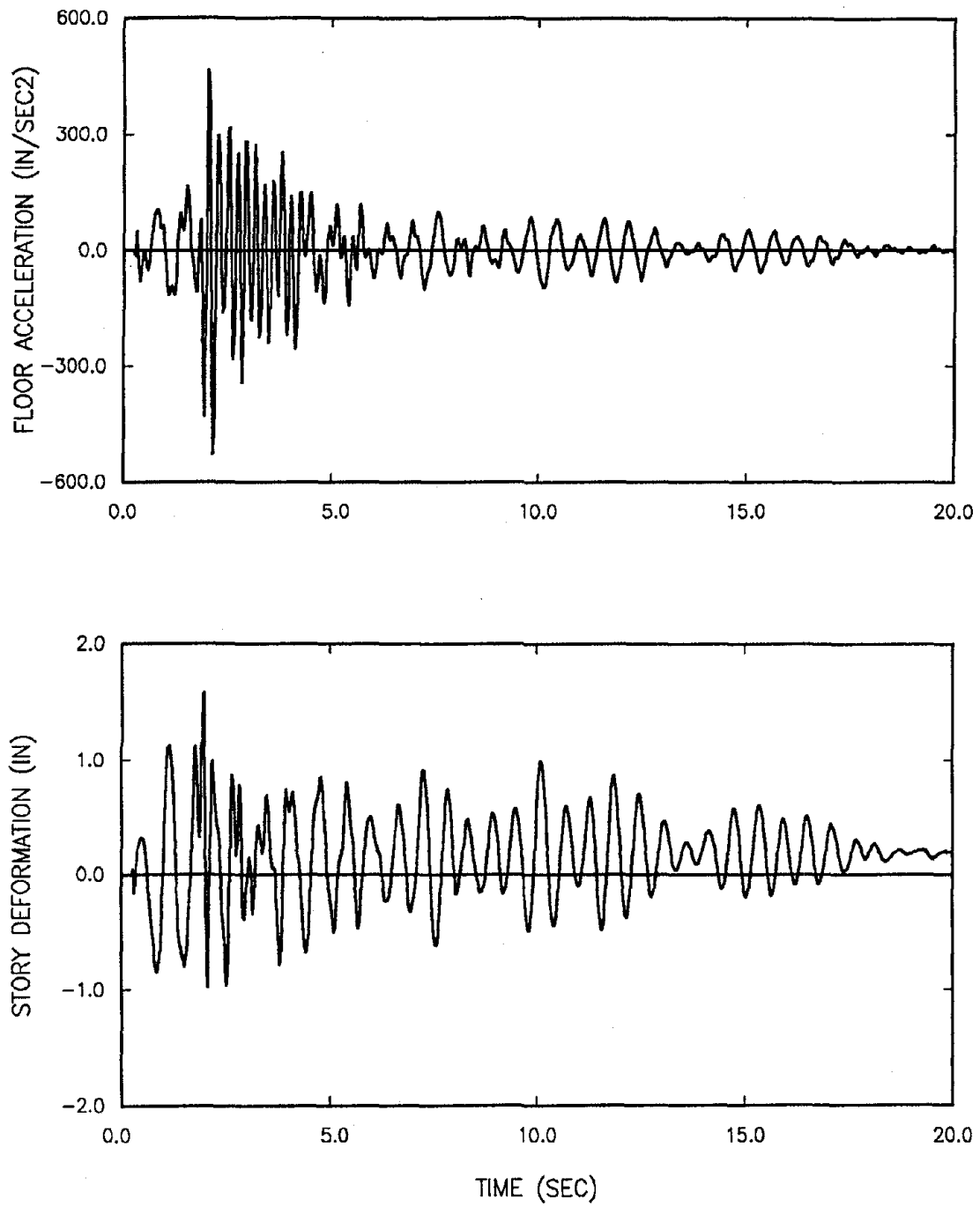


Figure 5.18a Typical Measured Response of the First Story of the Two-Story Structure M1 Subjected to Melendy Earthquake

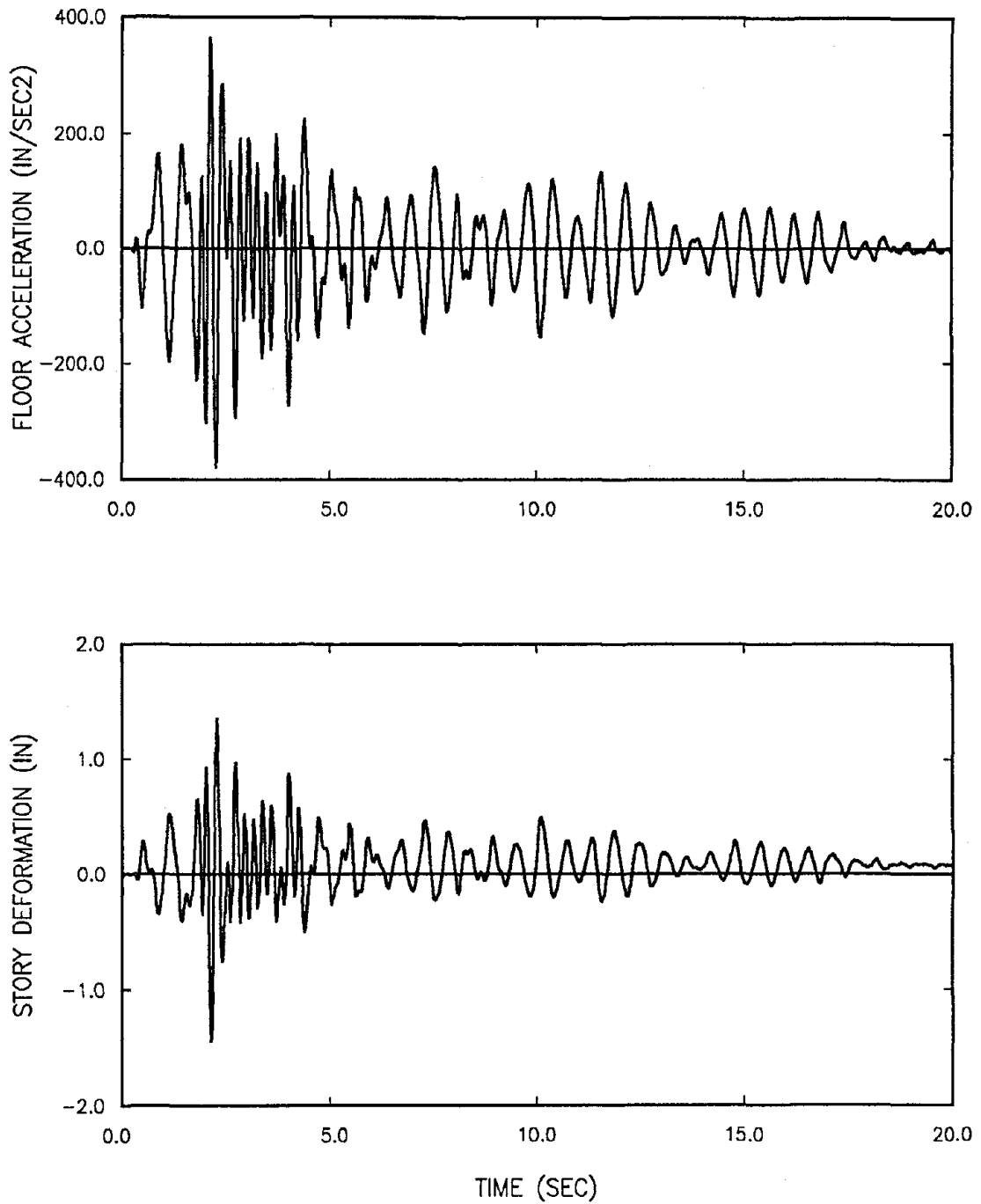


Figure 5.18b Typical Measured Response of the Second Story of the Two-Story Structure M1 Subjected to Melendy Earthquake

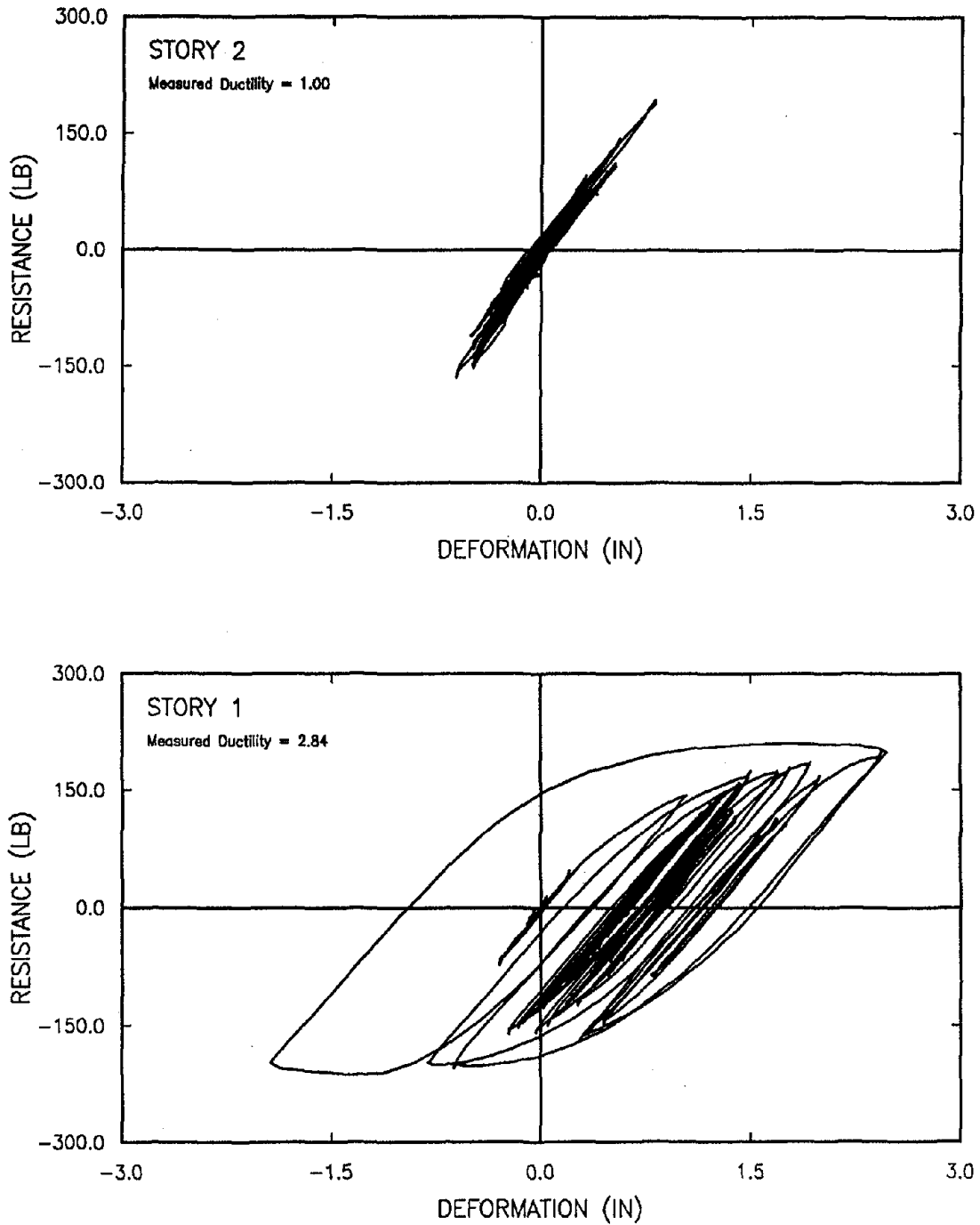


Figure 5.19 Typical Storys Hysteretic Behavior of the Two-Story Structure M1 Subjected to El Centro Earthquake

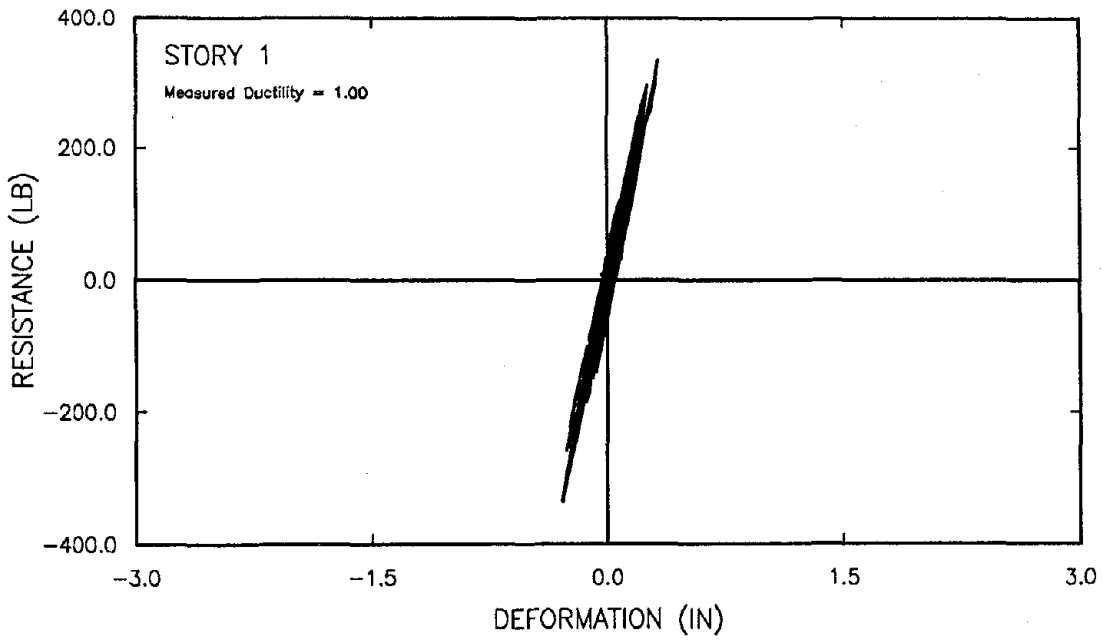
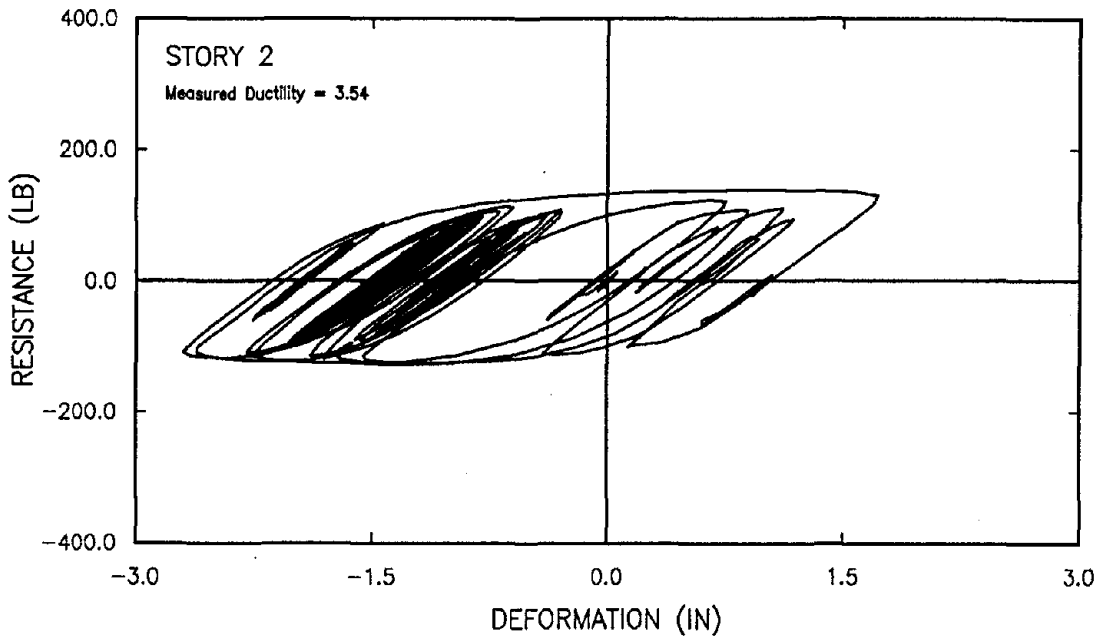


Figure 5.20 Typical Storys Hysteretic Behavior of the Two-Story Structure M2 Subjected to El Centro Earthquake

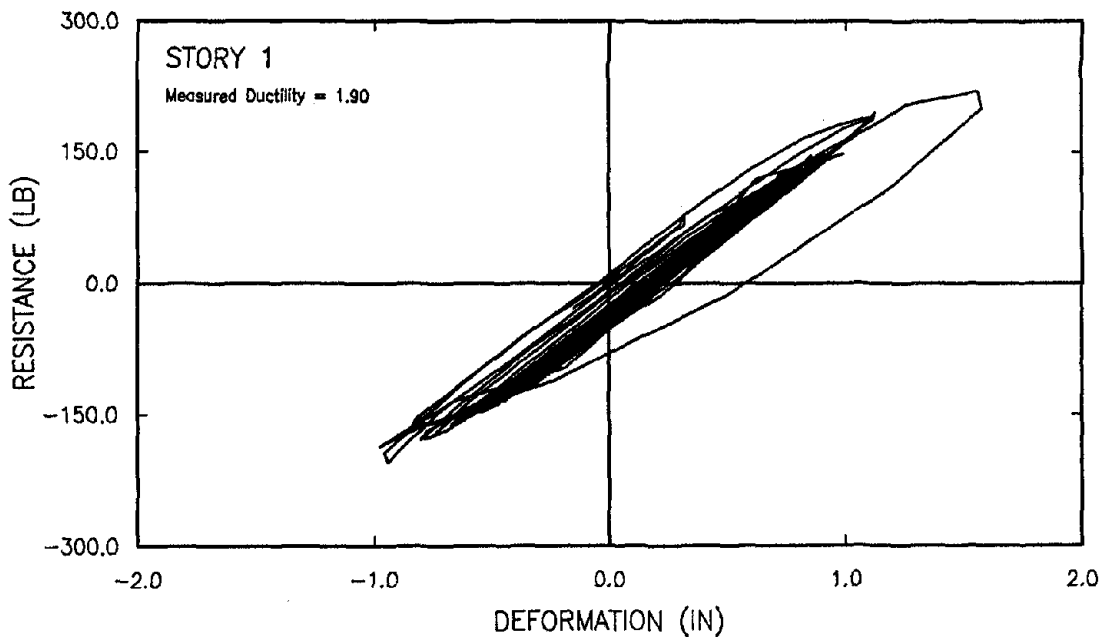
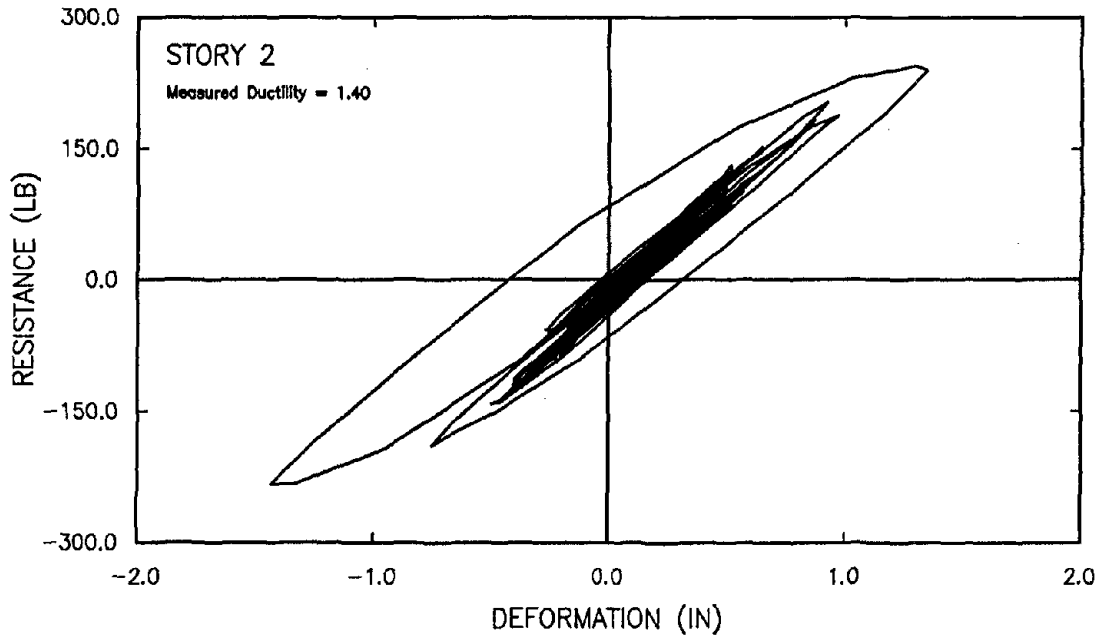


Figure 5.21 Typical Storys Hysteretic Behavior of the Two-Story Structure M1 Subjected to Melendy Earthquake

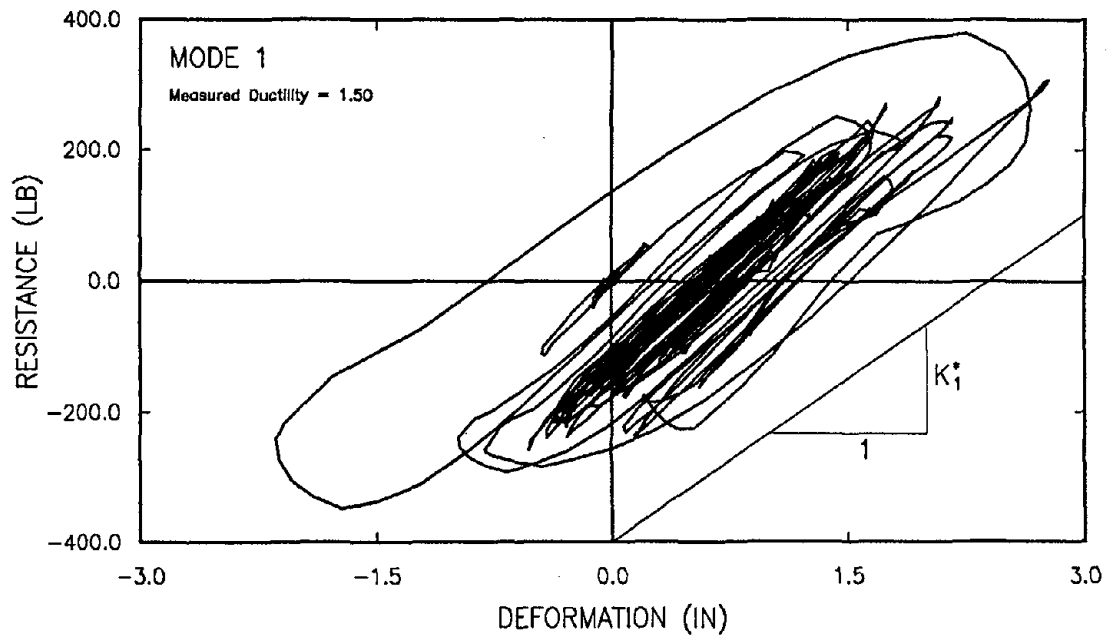
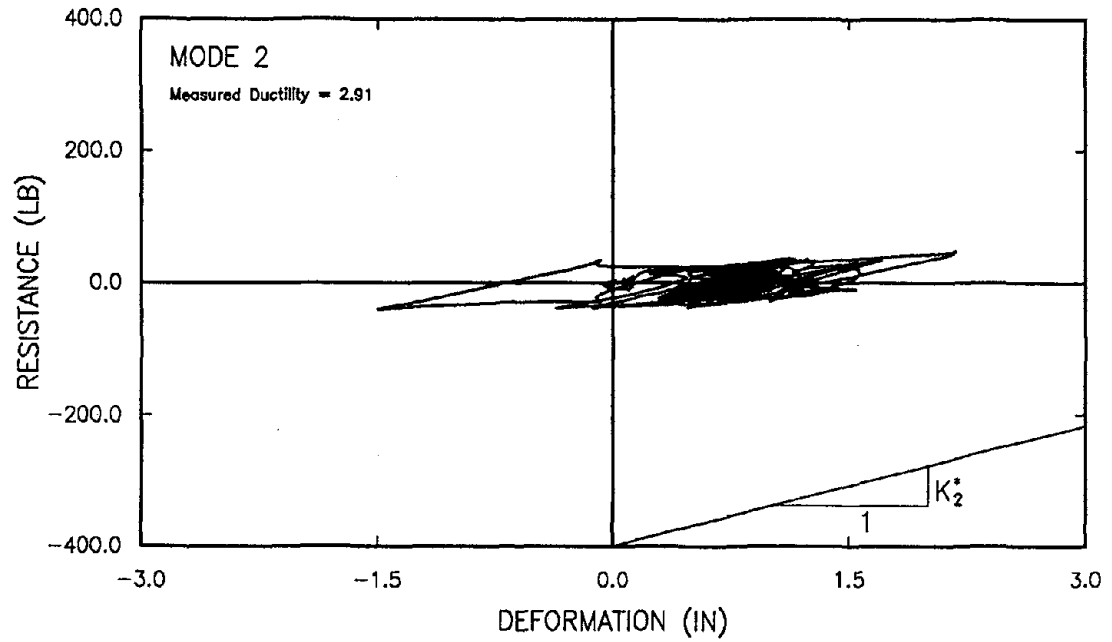


Figure 5.22 Typical Modal Hysteretic Behavior of the Two-Story Structure M1 Subjected to El Centro Earthquake

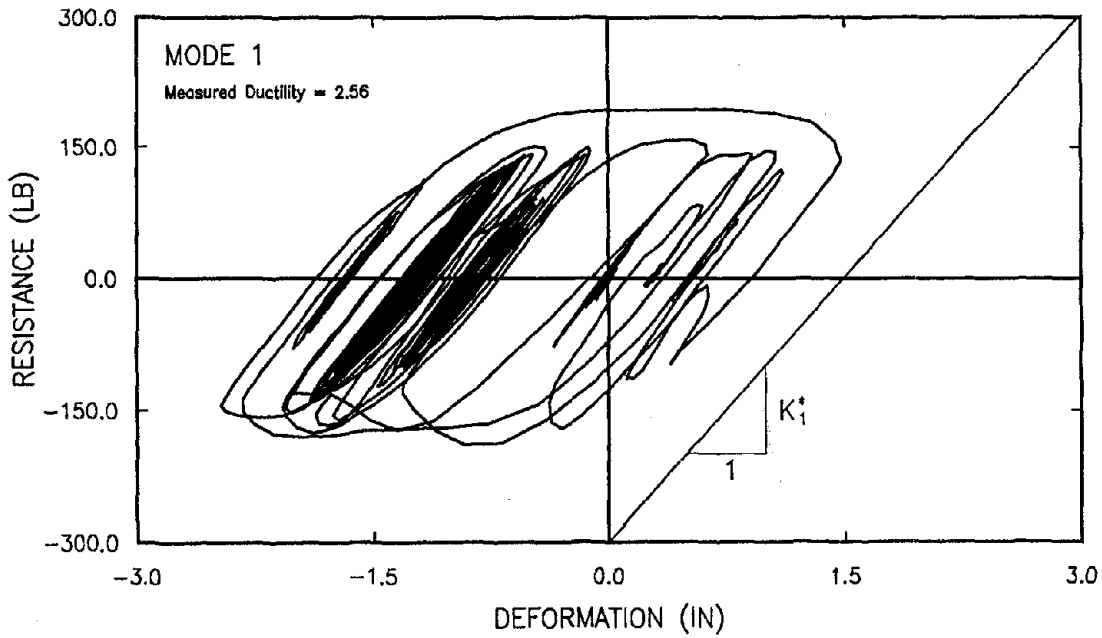
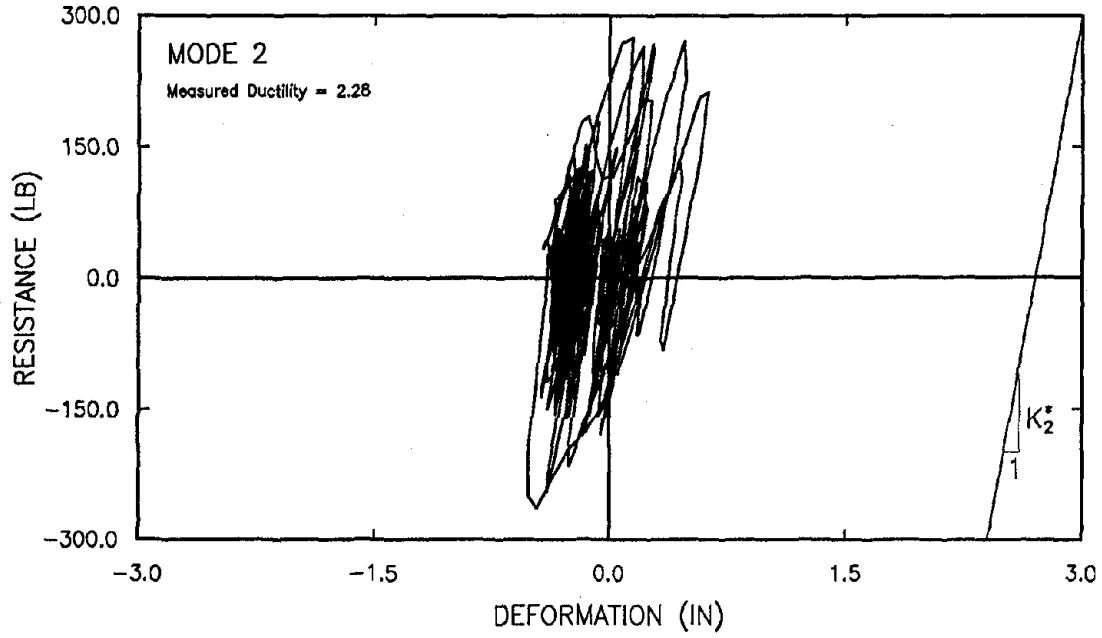


Figure 5.23 Typical Modal Hysteretic Behavior of the Two-Story Structure M2 Subjected to El Centro Earthquake

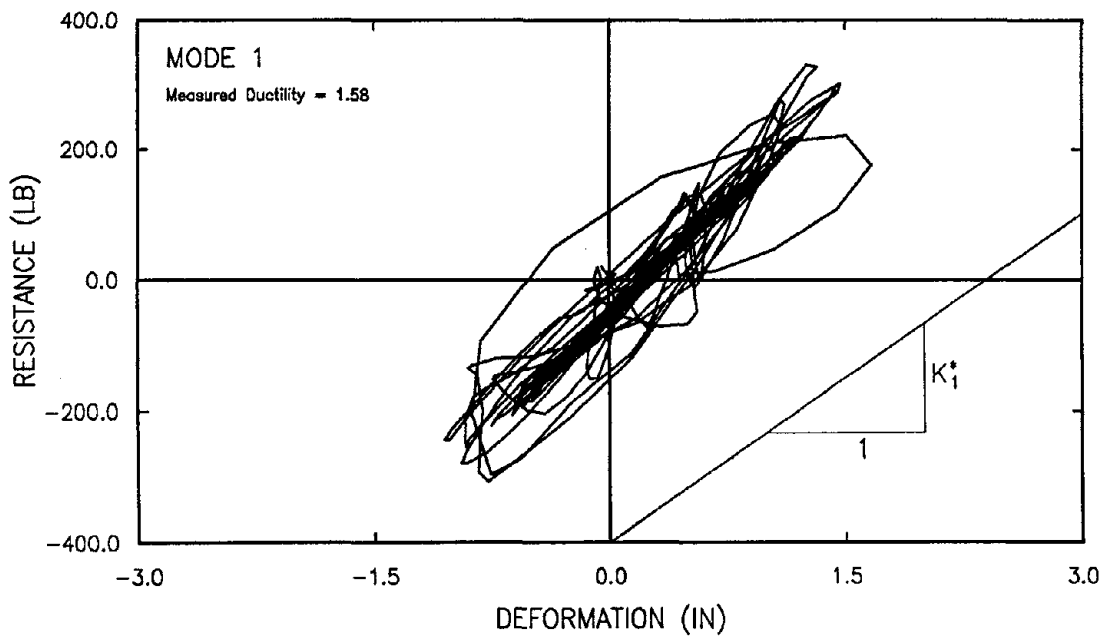
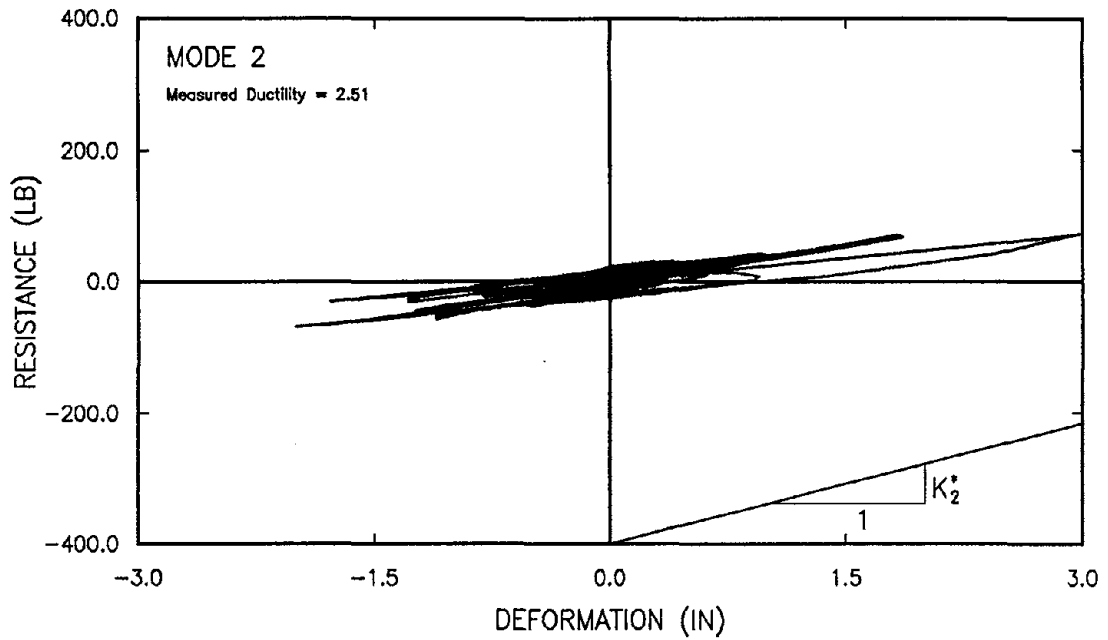


Figure 5.24 Typical Modal Hysteretic Behavior of the Two-Story Structure M1 Subjected to Melendy Earthquake

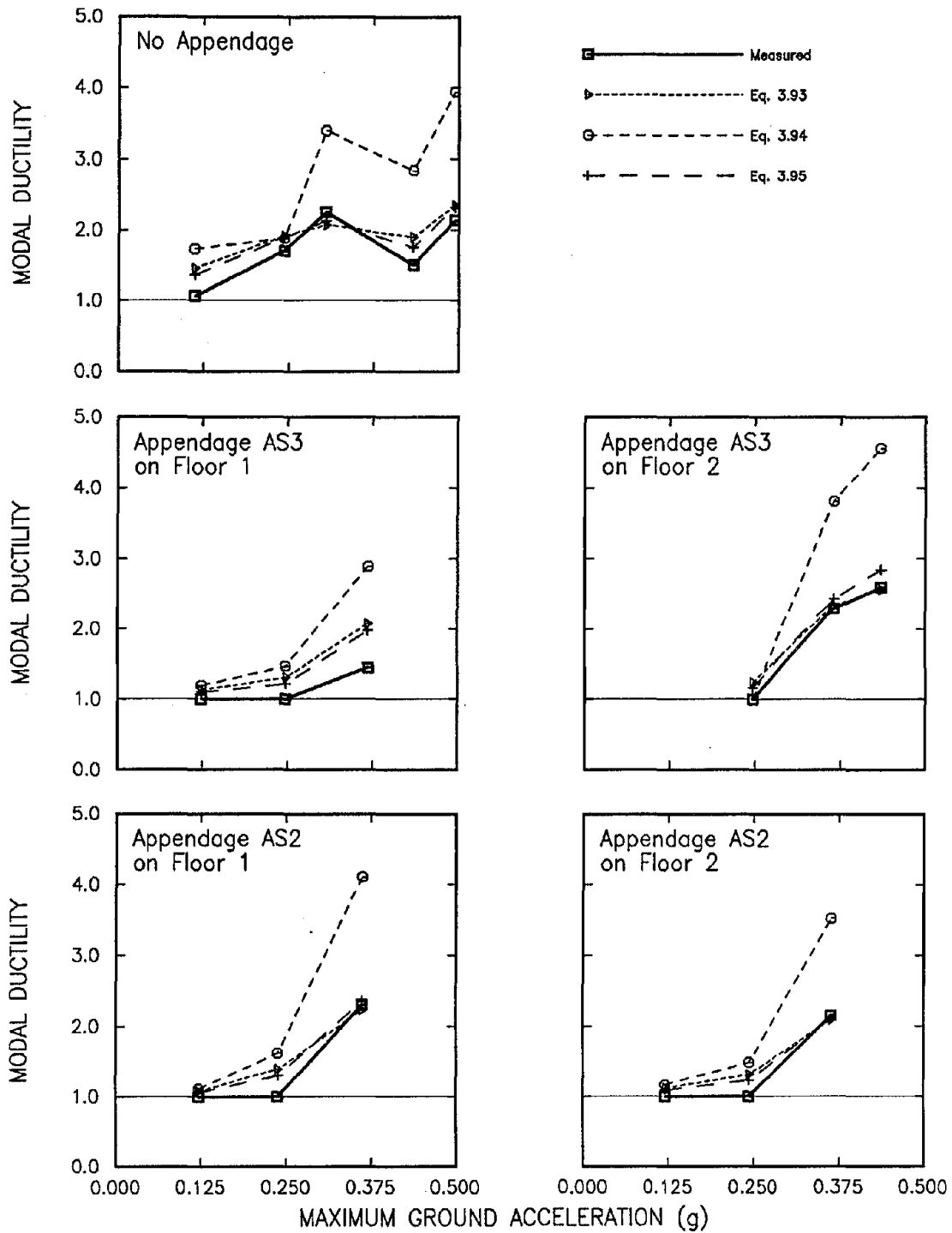


Figure 5.25a Comparison of Measured and Calculated Modal Ductility of Mode 1 of the Structure M1 subjected to El Centro Earthquake

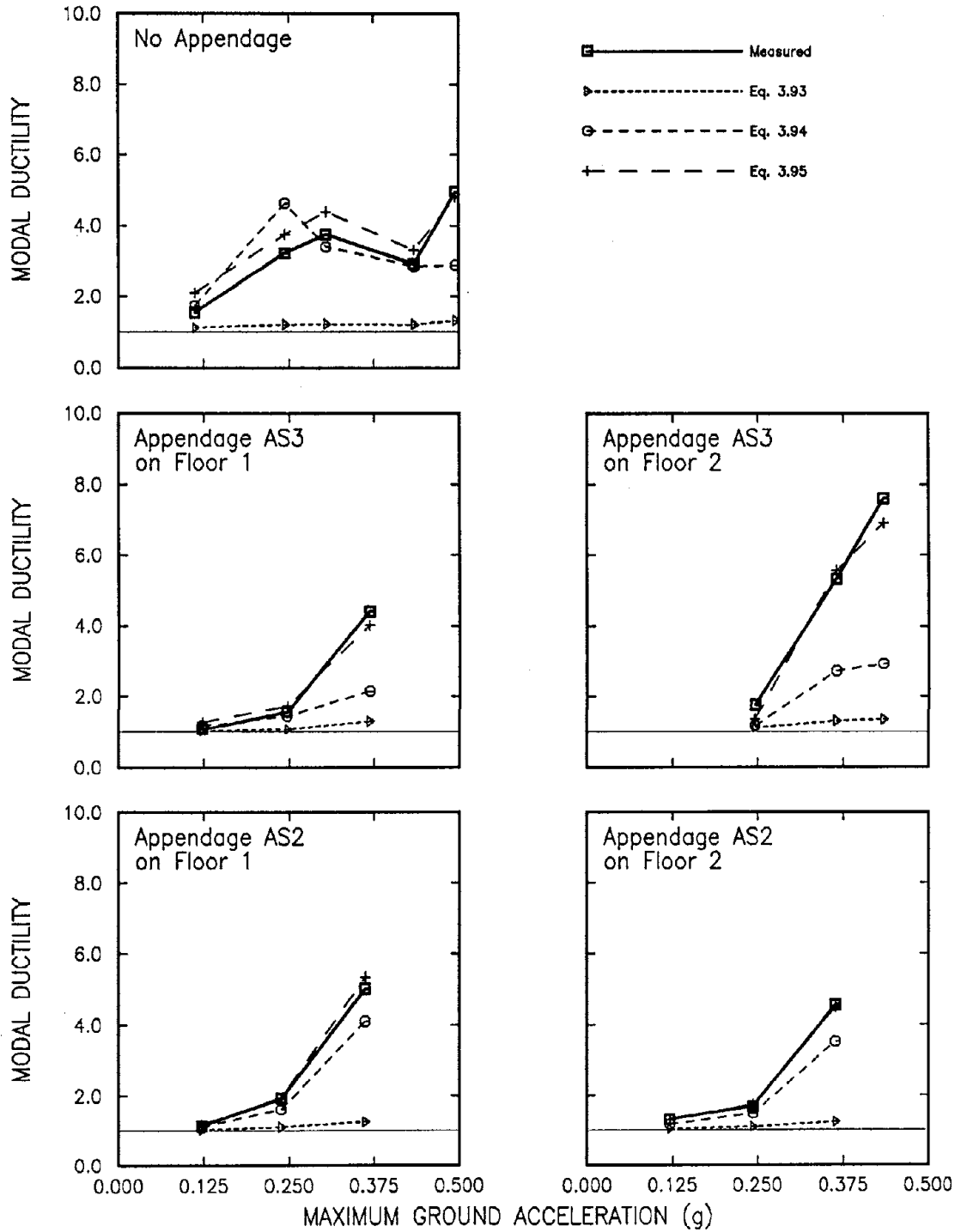


Figure 5.25b Comparison of Measured and Calculated Modal Ductility of Mode 2 of the Structure M1 subjected to El Centro Earthquake

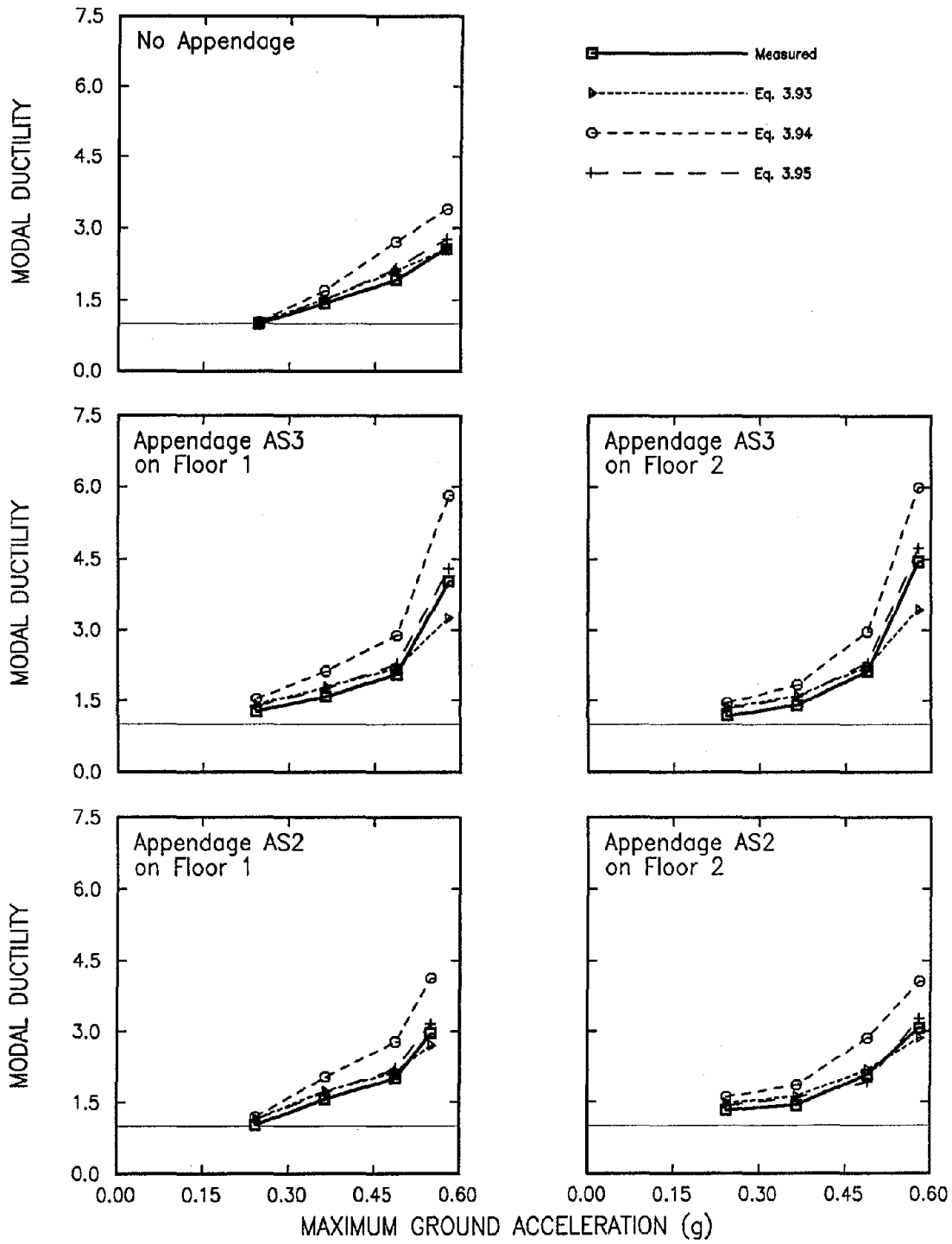


Figure 5.26a Comparison of Measured and Calculated Modal Ductility of Mode 1 of the Structure M2 subjected to El Centro Earthquake

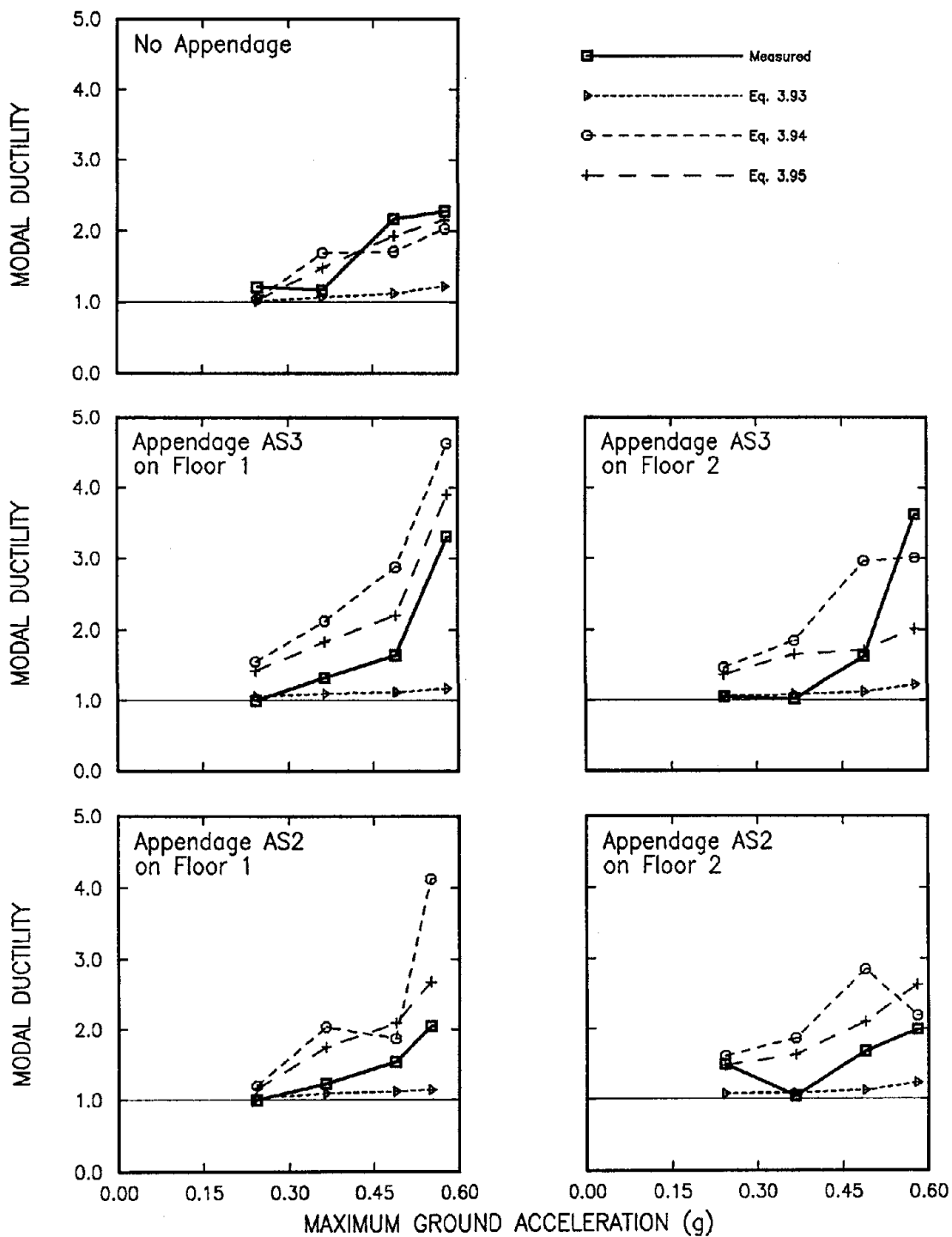


Figure 5.26b Comparison of Measured and Calculated Modal Ductility of Mode 2 of the Structure M2 subjected to El Centro Earthquake

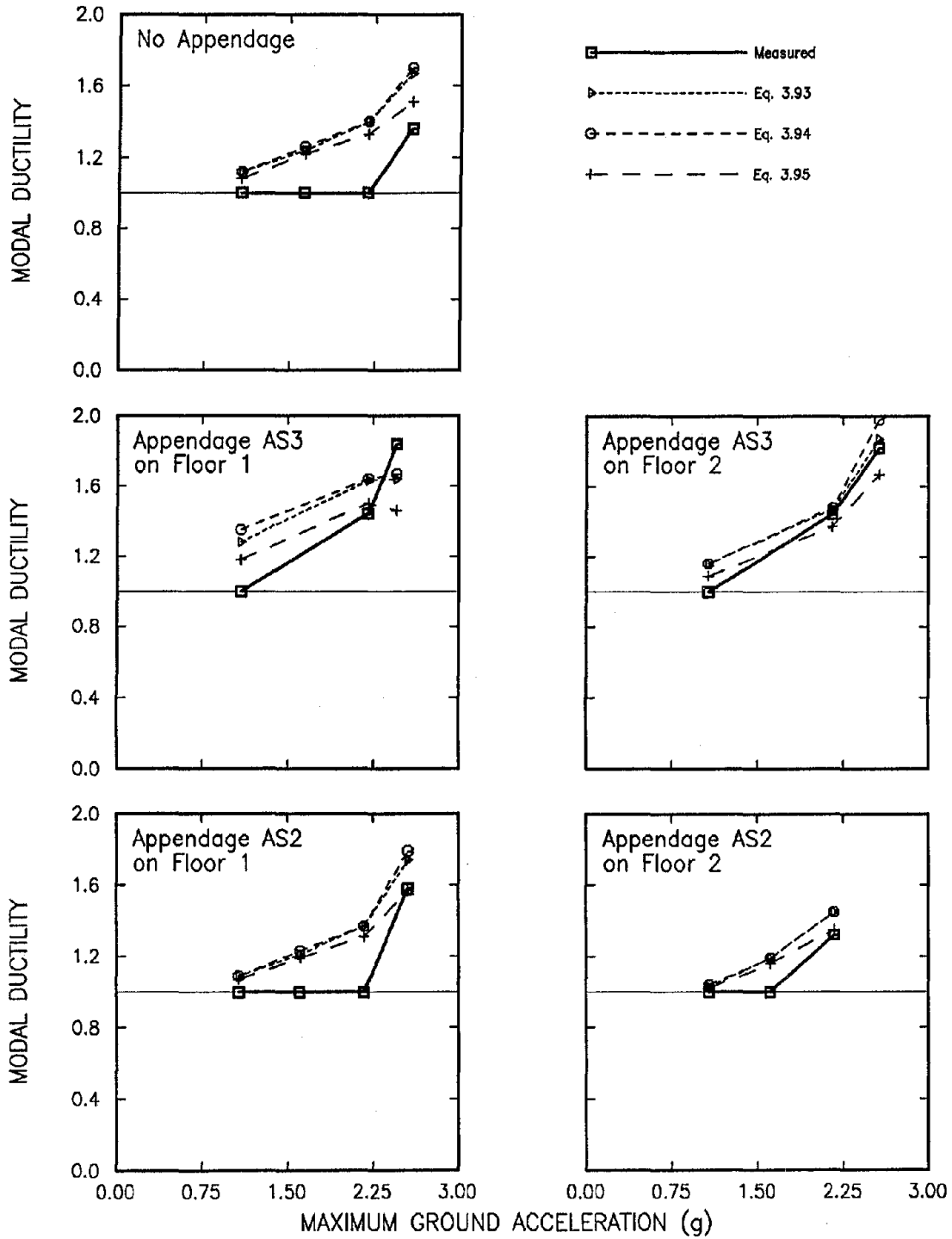


Figure 5.27a Comparison of Measured and Calculated Modal Ductility of Mode 1 of the Structure M1 subjected to Melendy Earthquake

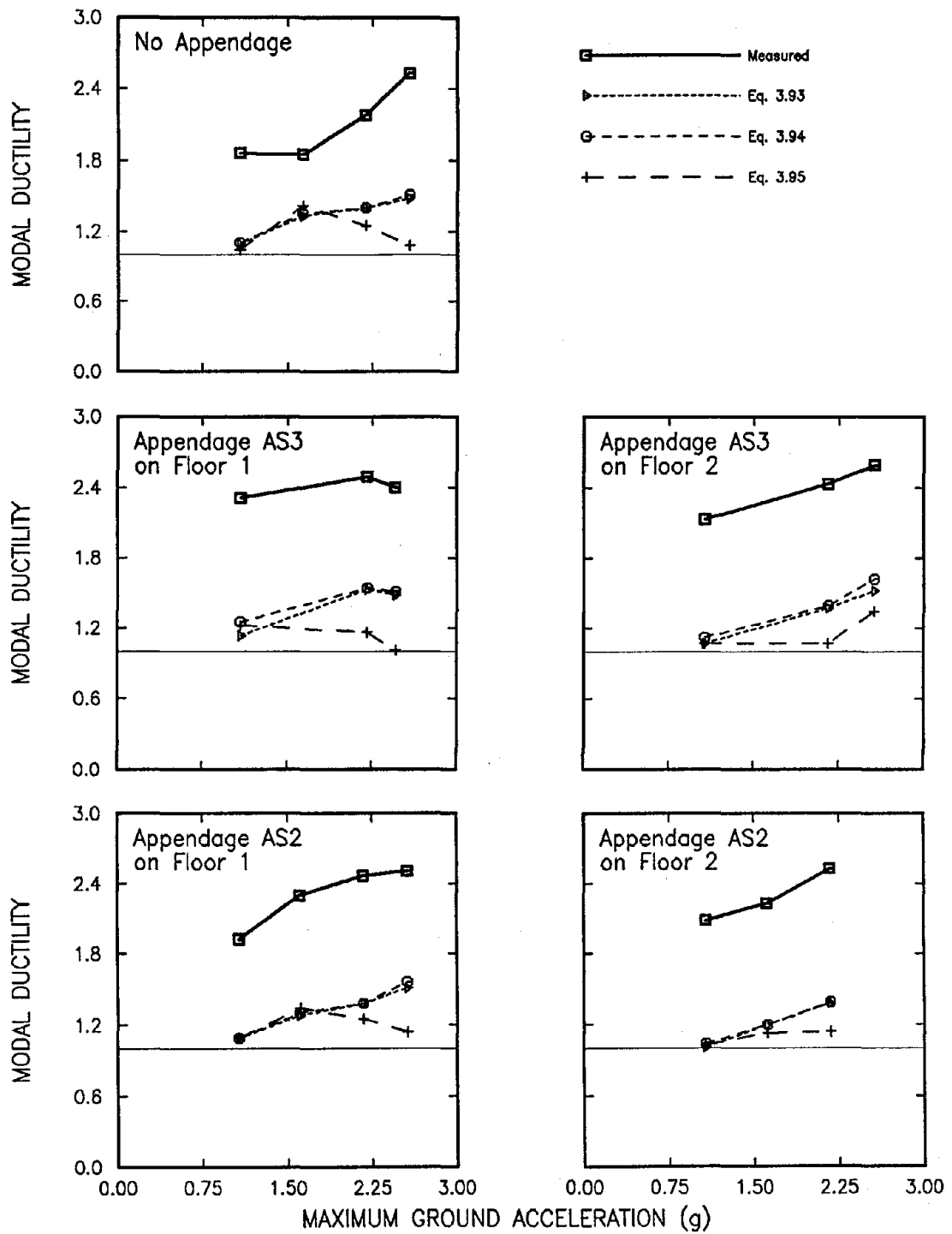


Figure 5.27b Comparison of Measured and Calculated Modal Ductility of Mode 2 of the Structure M1 subjected to Melendy Earthquake

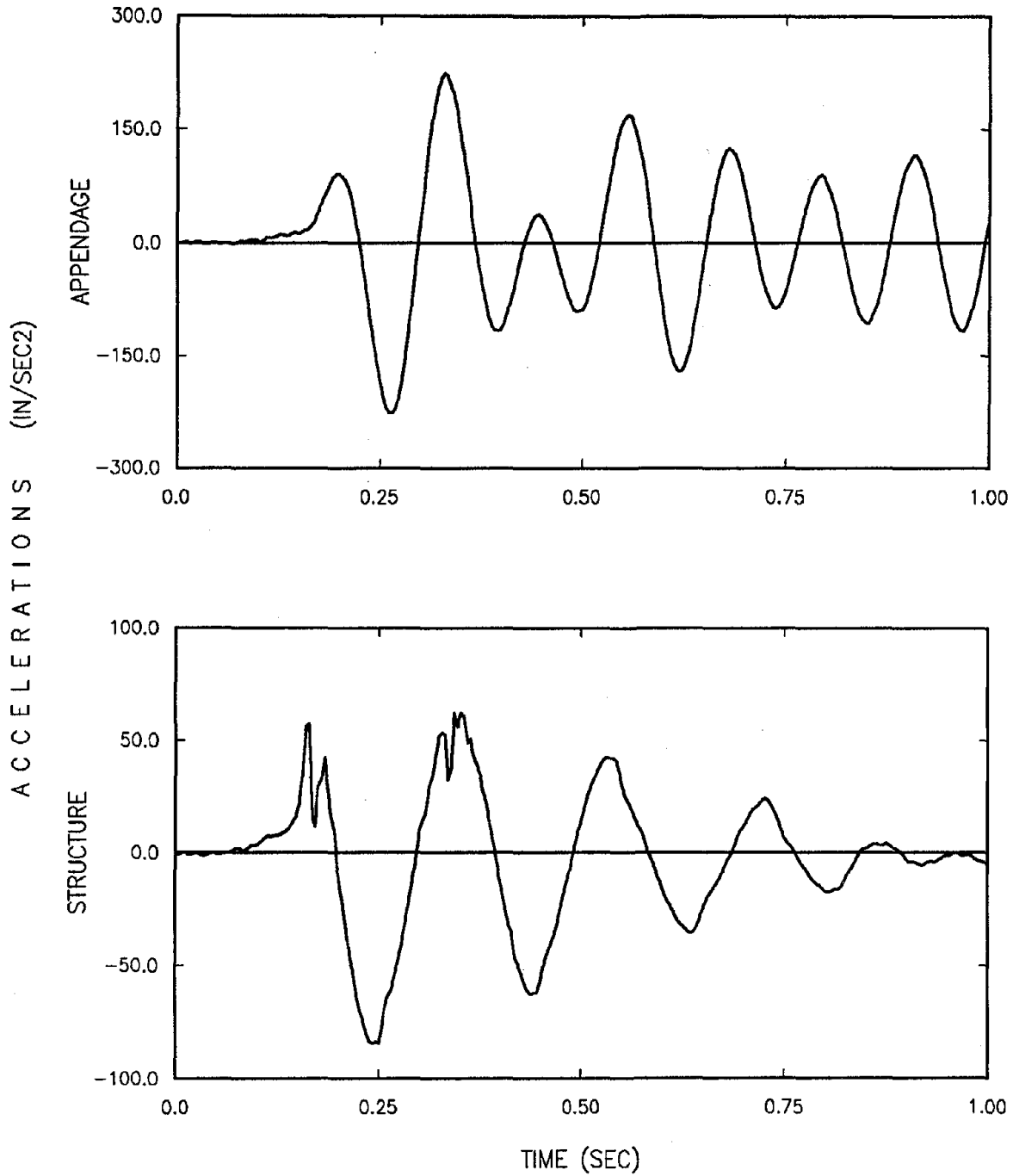


Figure 5.28 Typical Measured Free Vibrations Accelerations of a Combined Detuned System (Single-Story Structure S4 and Small Appendage AS4)

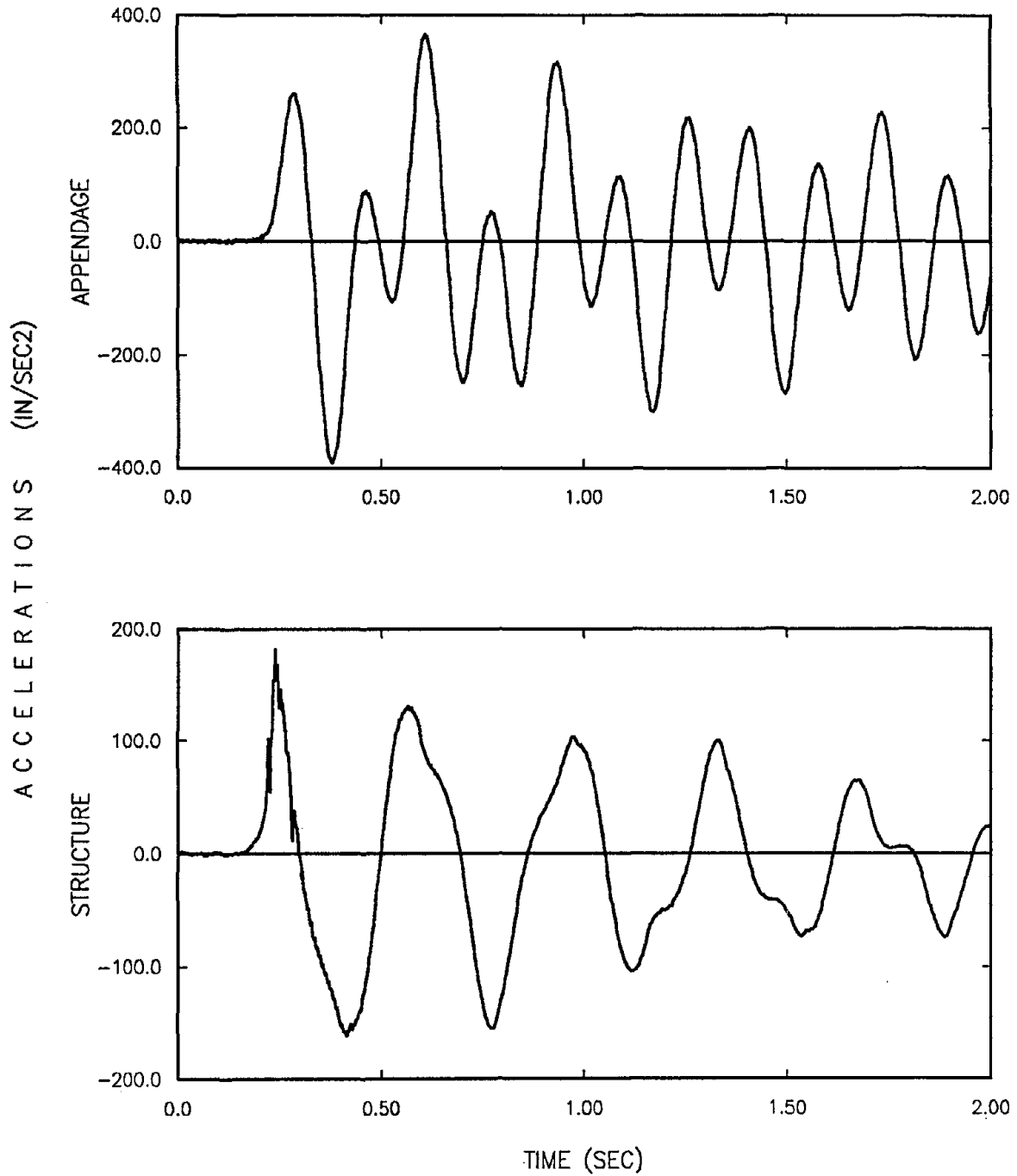


Figure 5.29 Typical Measured Free Vibrations Accelerations of a Combined Detuned System (Single-Story Structure S1 and Large Appendage AL3)

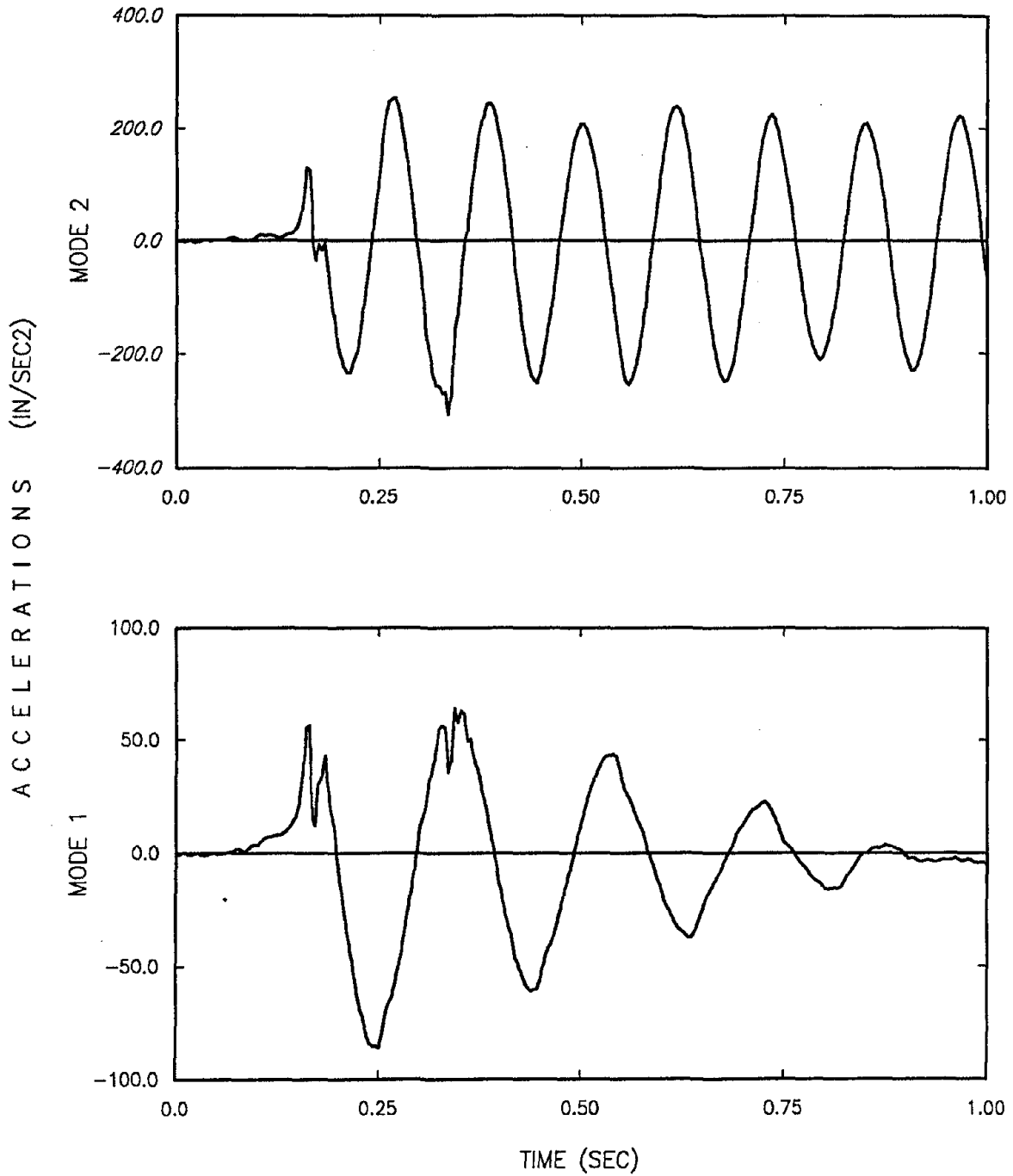


Figure 5.30 Typical Free Vibrations Modal Accelerations of a Combined Detuned System (Single-Story Structure S4 and Small Appendage AS4)

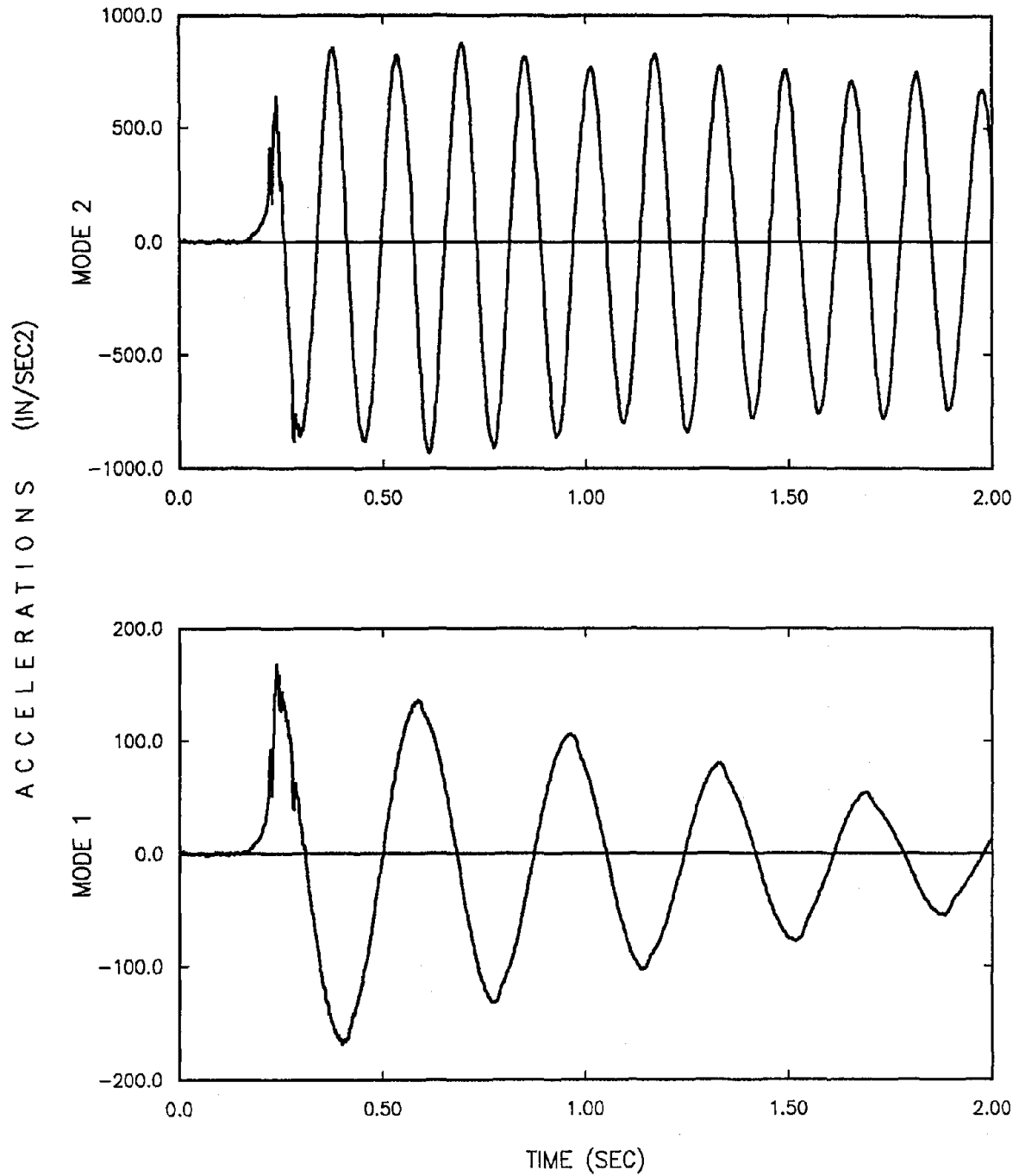


Figure 5.31 Typical Free Vibrations Modal Accelerations of a Combined Detuned System (Single-Story Structure S1 and Large Appendage AL3)

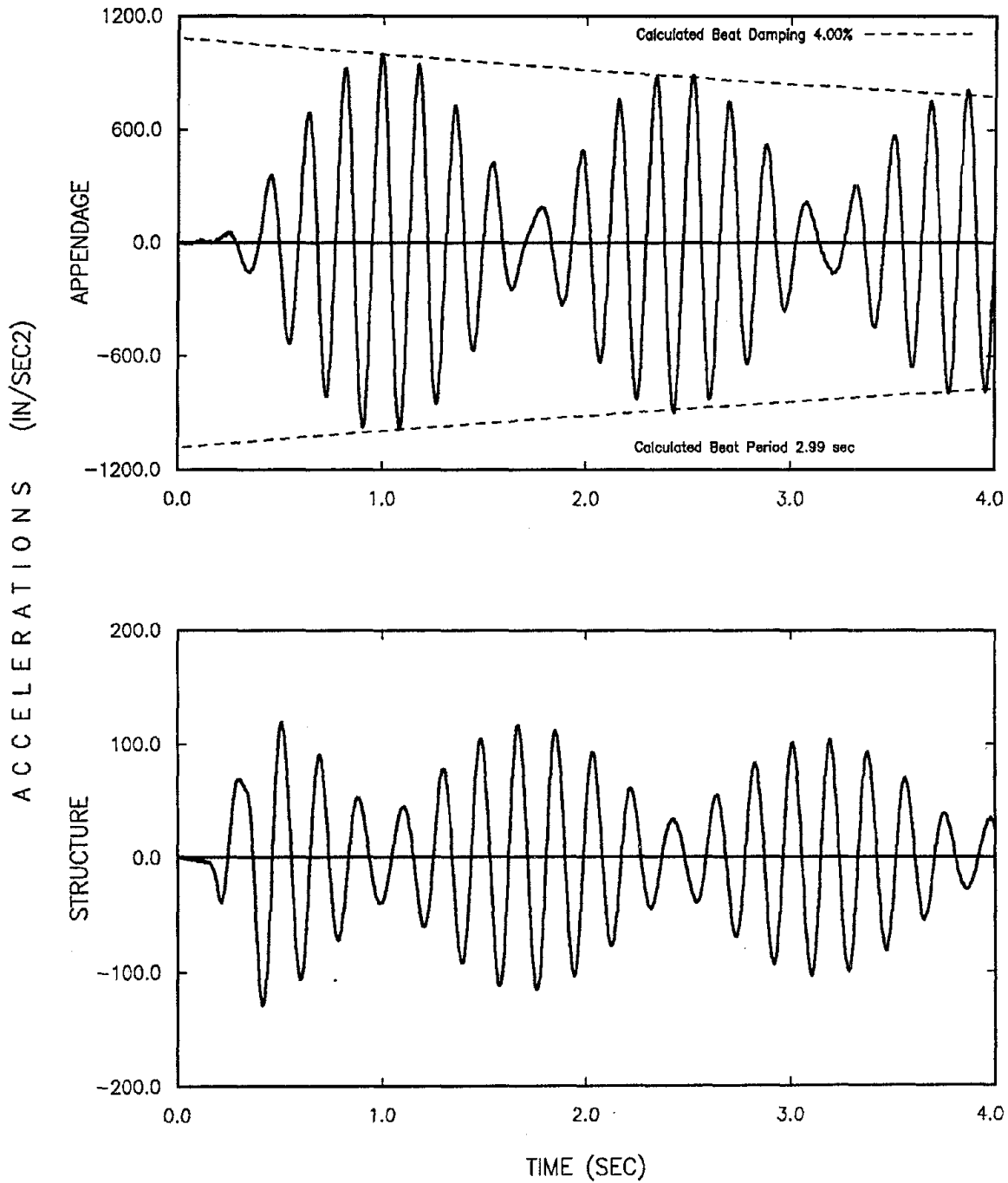


Figure 5.32 Typical Measured Free Vibrations Accelerations of a Combined Tuned System with Low Damping (Single-Story Structure S8 and Small Appendage AT2)

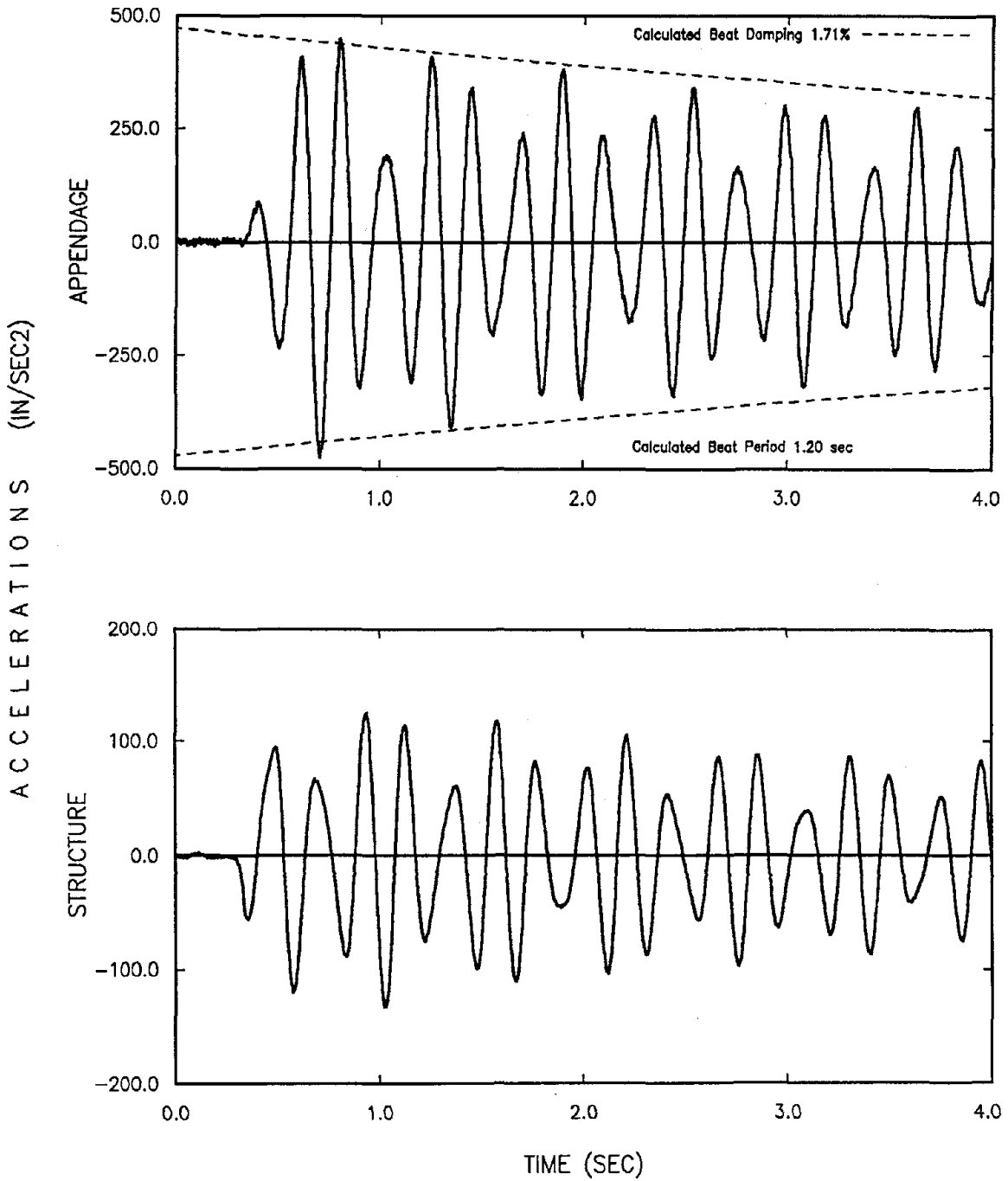


Figure 5.33 Typical Measured Free Vibrations Accelerations of a Combined Tuned System with Low Damping (Single-Story Structure S9 and Large Appendage AT7)

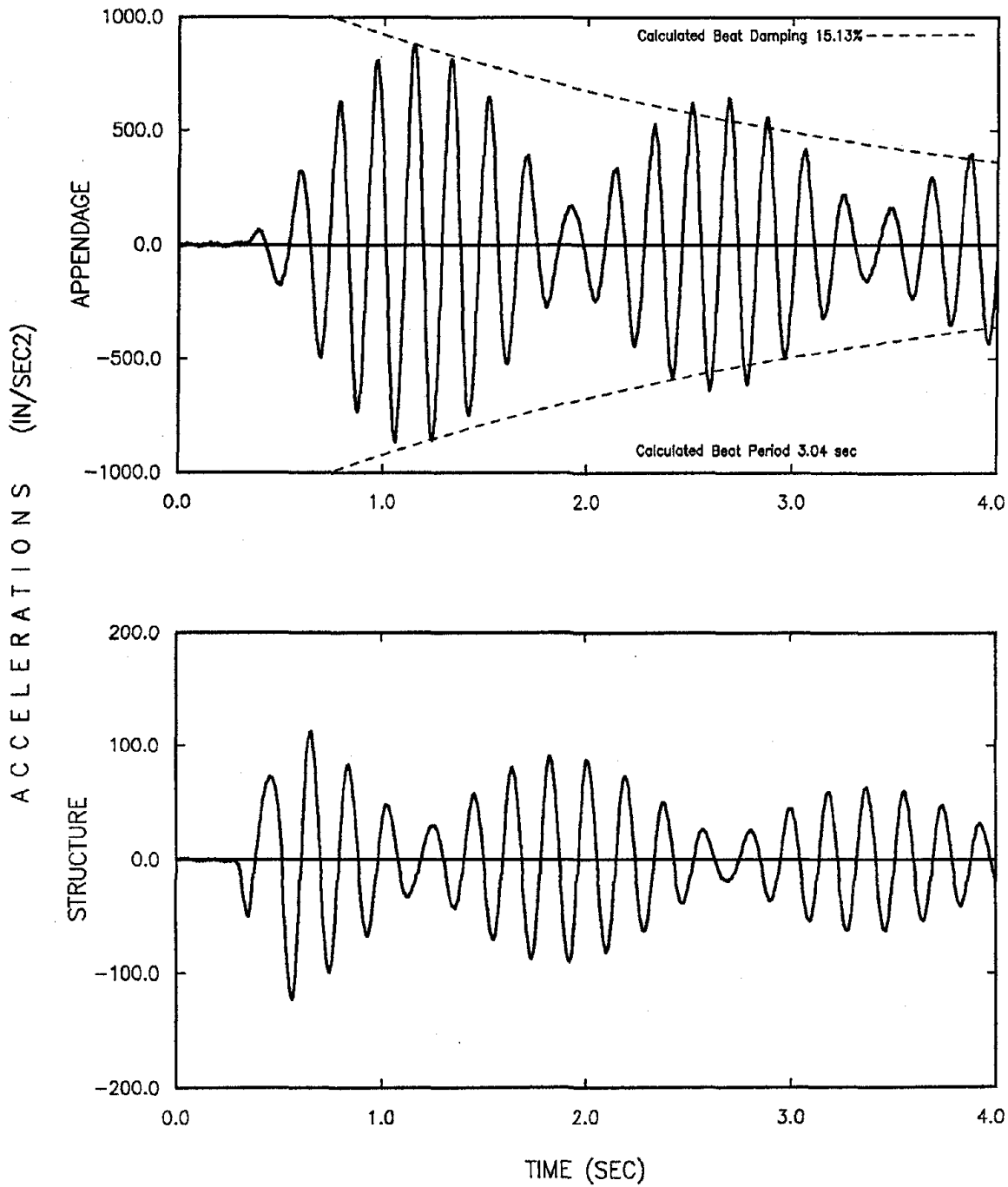


Figure 5.34 Typical Measured Free Vibrations Accelerations of a Combined Tuned System with High Appendage Damping (Single-Story Structure S8 and Small Appendage AT4)

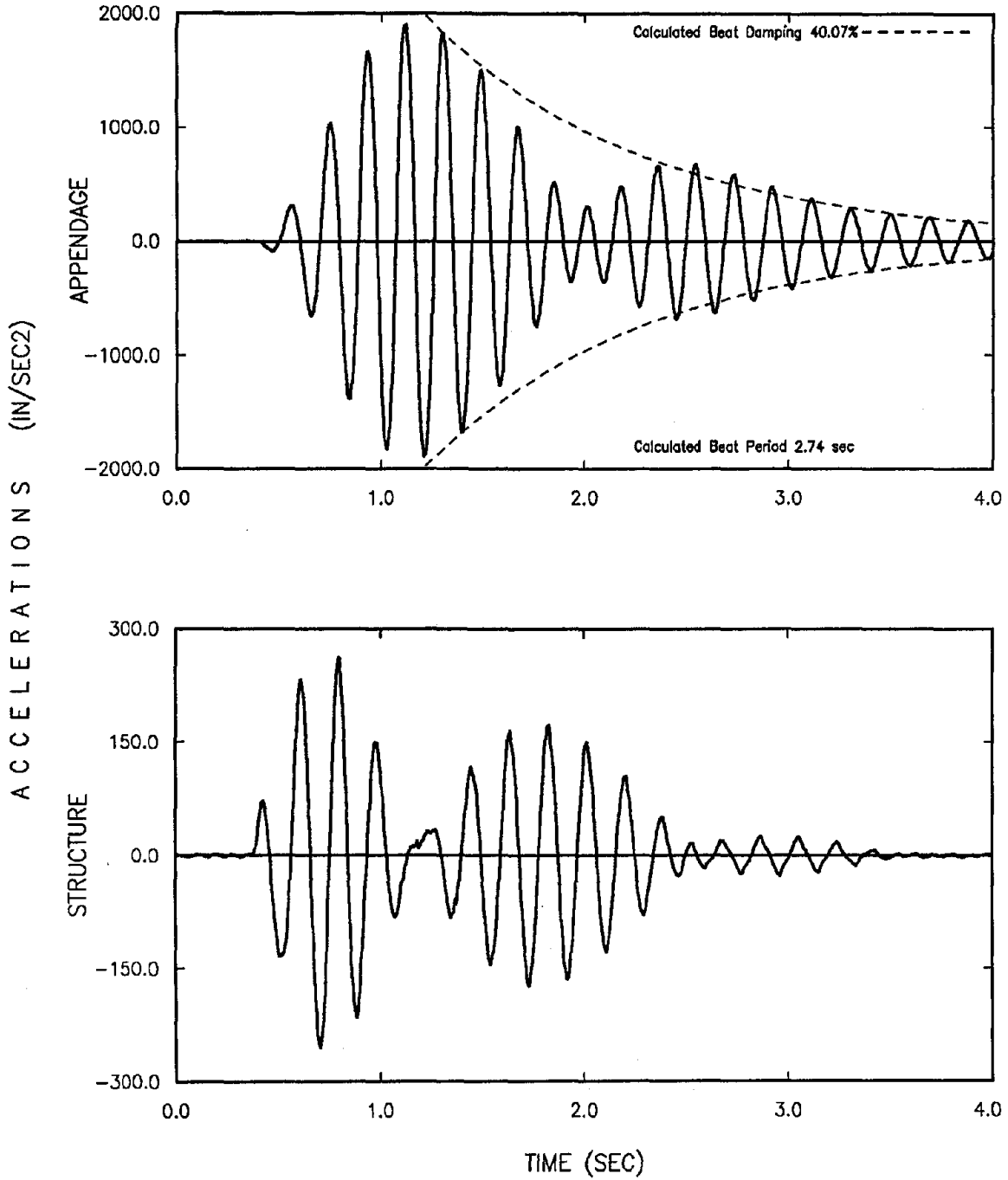


Figure 5.35 Typical Measured Free Vibrations Accelerations of a Combined Tuned System with High Appendage and Structure Damping (Single-Story Structure S4 and Small Appendage AT6)

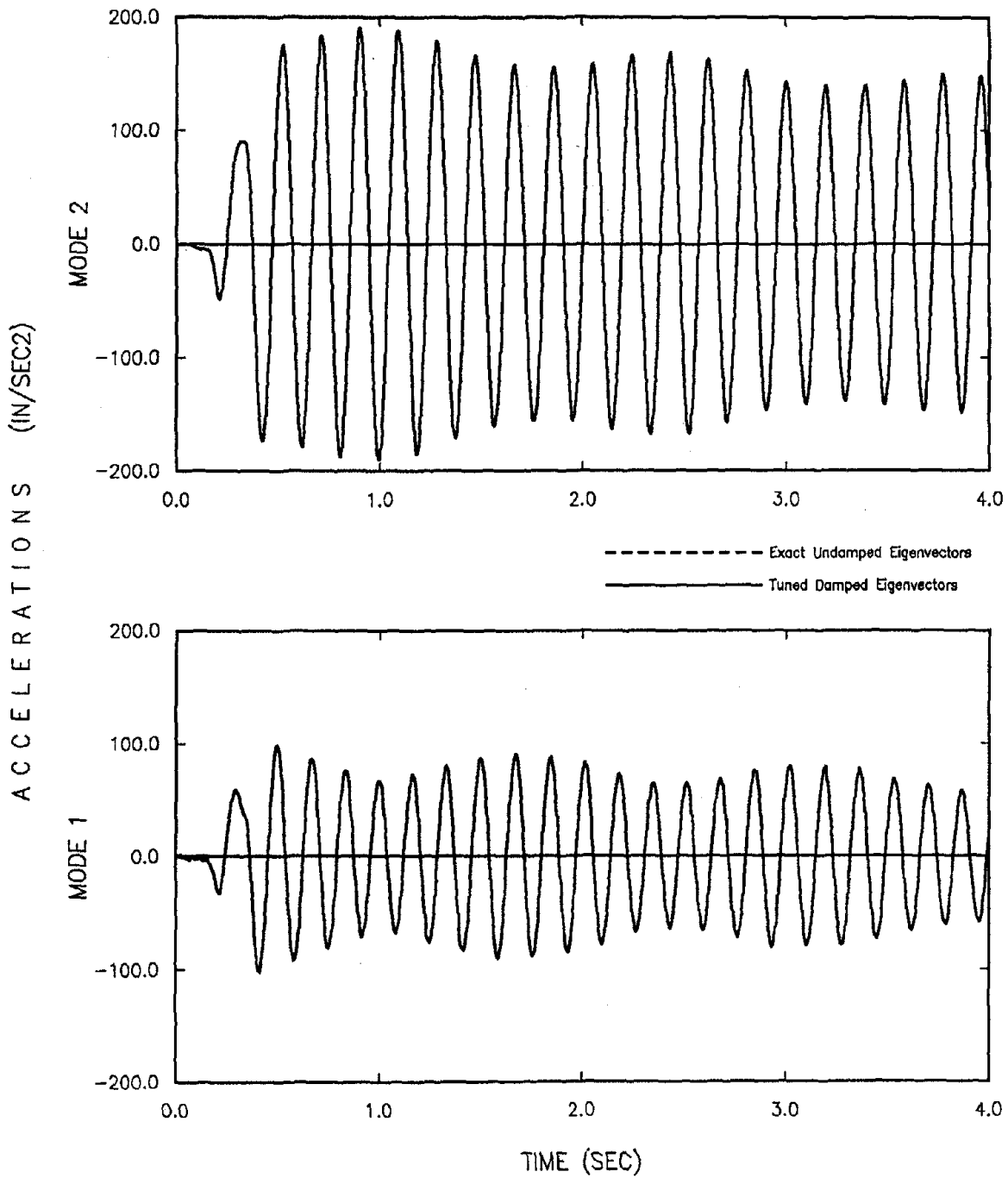


Figure 5.36 Typical Free Vibrations Modal Accelerations of a Combined Tuned System with Low Damping (Single-Story Structure S8 and Small Appendage AT2)

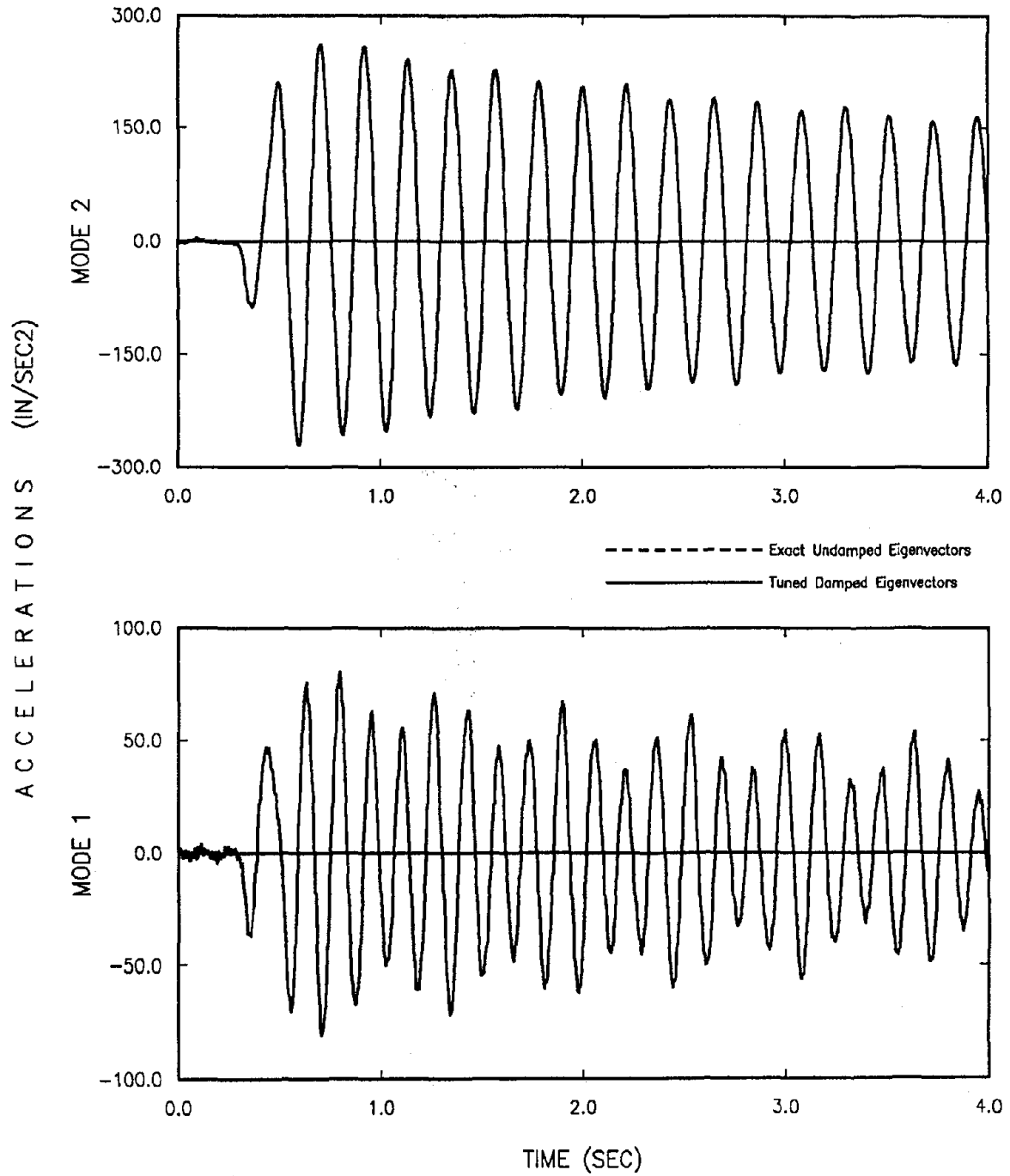


Figure 5.37 Typical Free Vibrations Modal Accelerations of a Combined Tuned System with Low Damping (Single-Story Structure S9 and Large Appendage AT7)

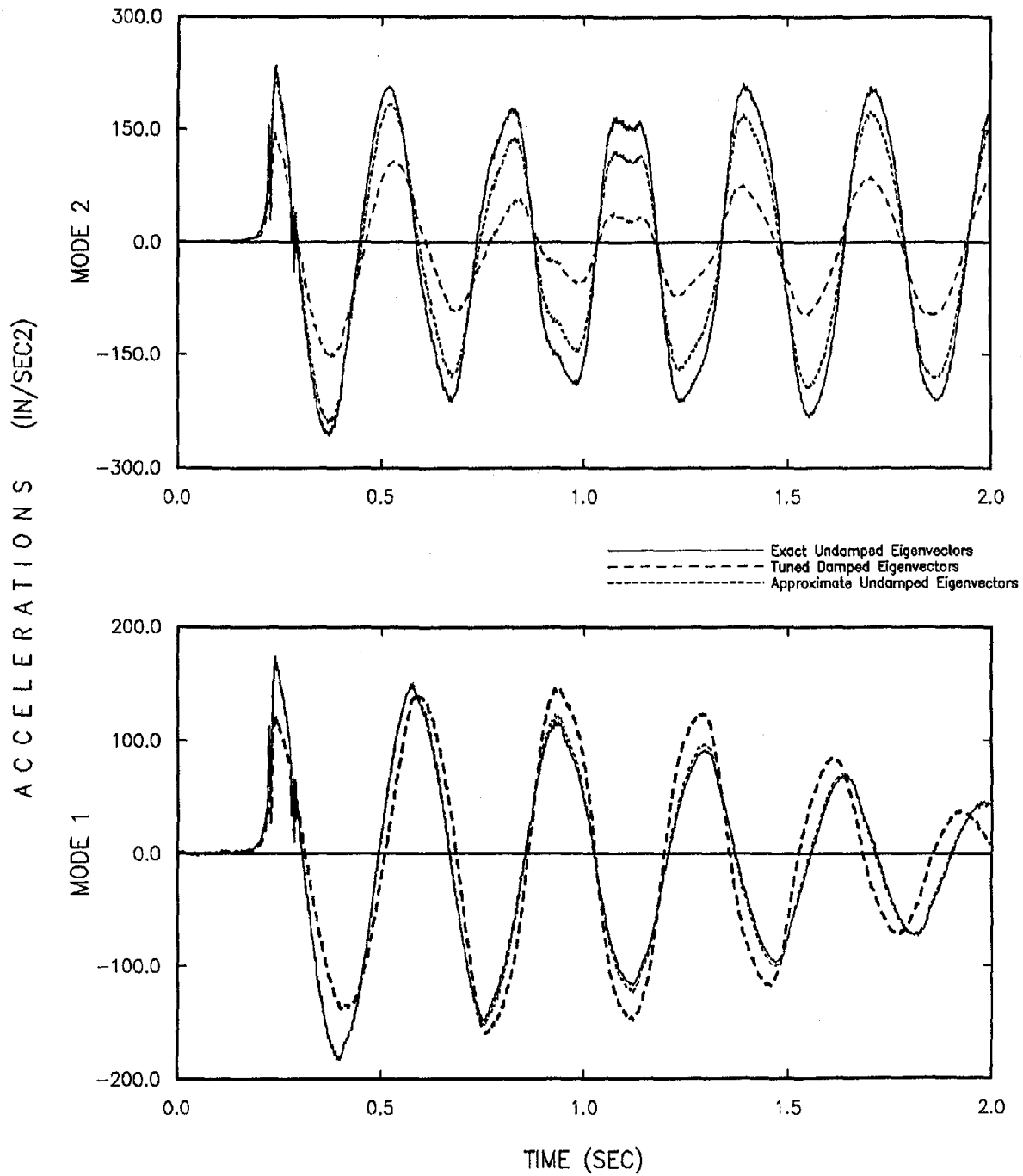


Figure 5.42 Typical Free Vibrations Modal Accelerations of a Combined Slightly Detuned System (Single-Story Structure S1 with Small Appendage AS2)

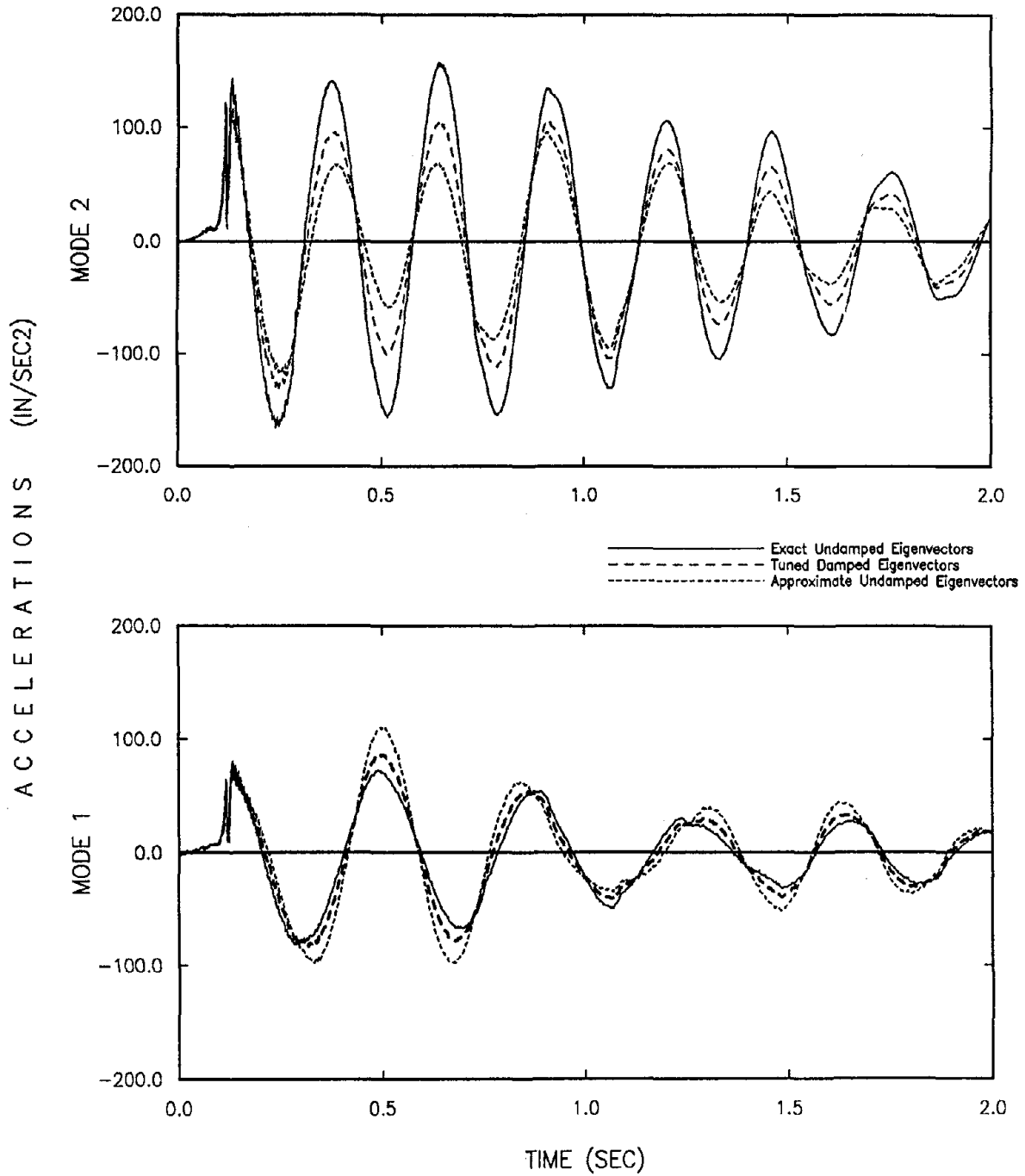


Figure 5.43 Typical Free Vibrations Modal Accelerations of a Combined Slightly Detuned System (Single-Story Structure S1 with Large Appendage AL2)

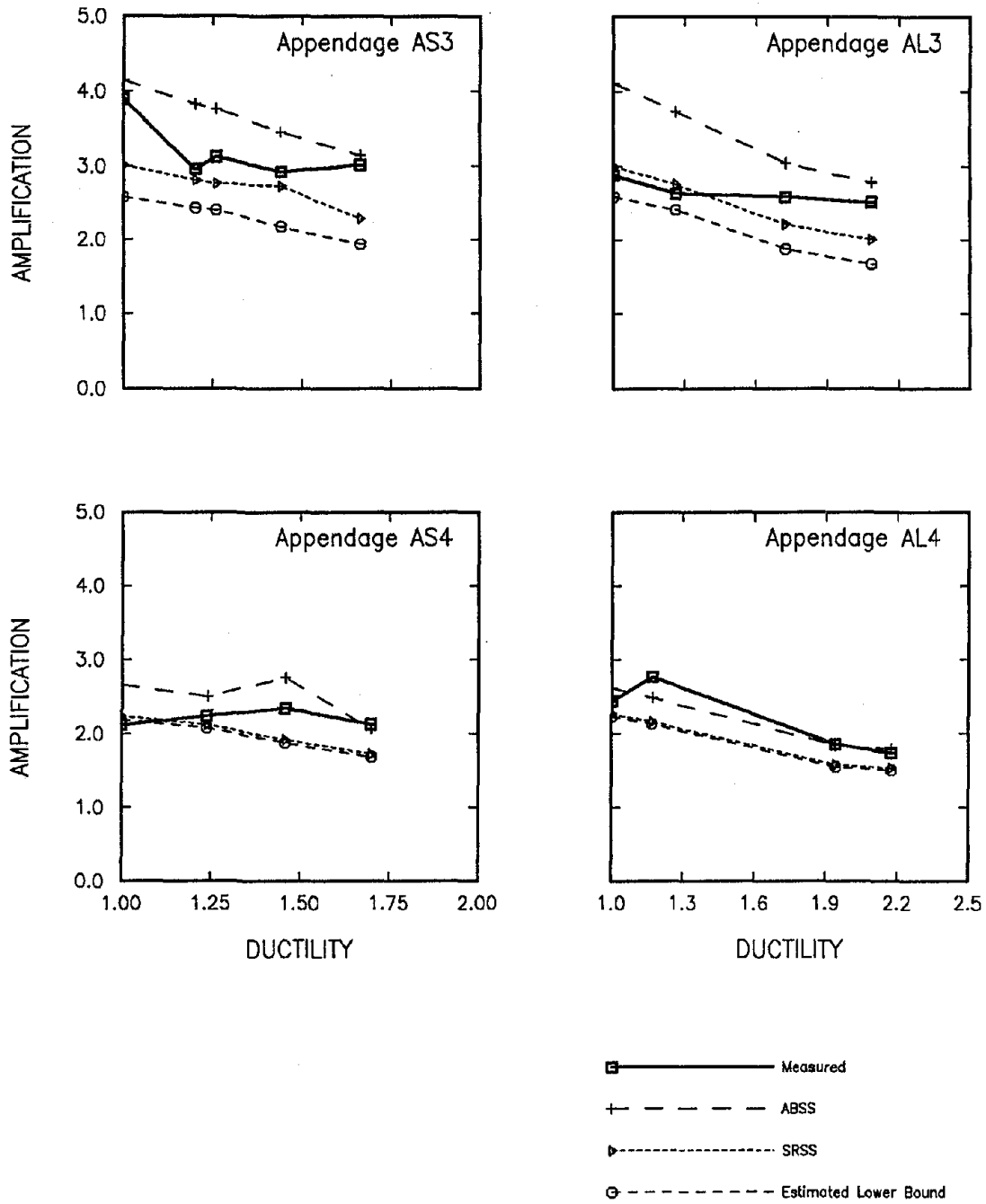


Figure 5.44 Comparison of Measured and Calculated Amplifications of the Detuned Appendages on Structure S1 Subjected to El Centro Earthquake

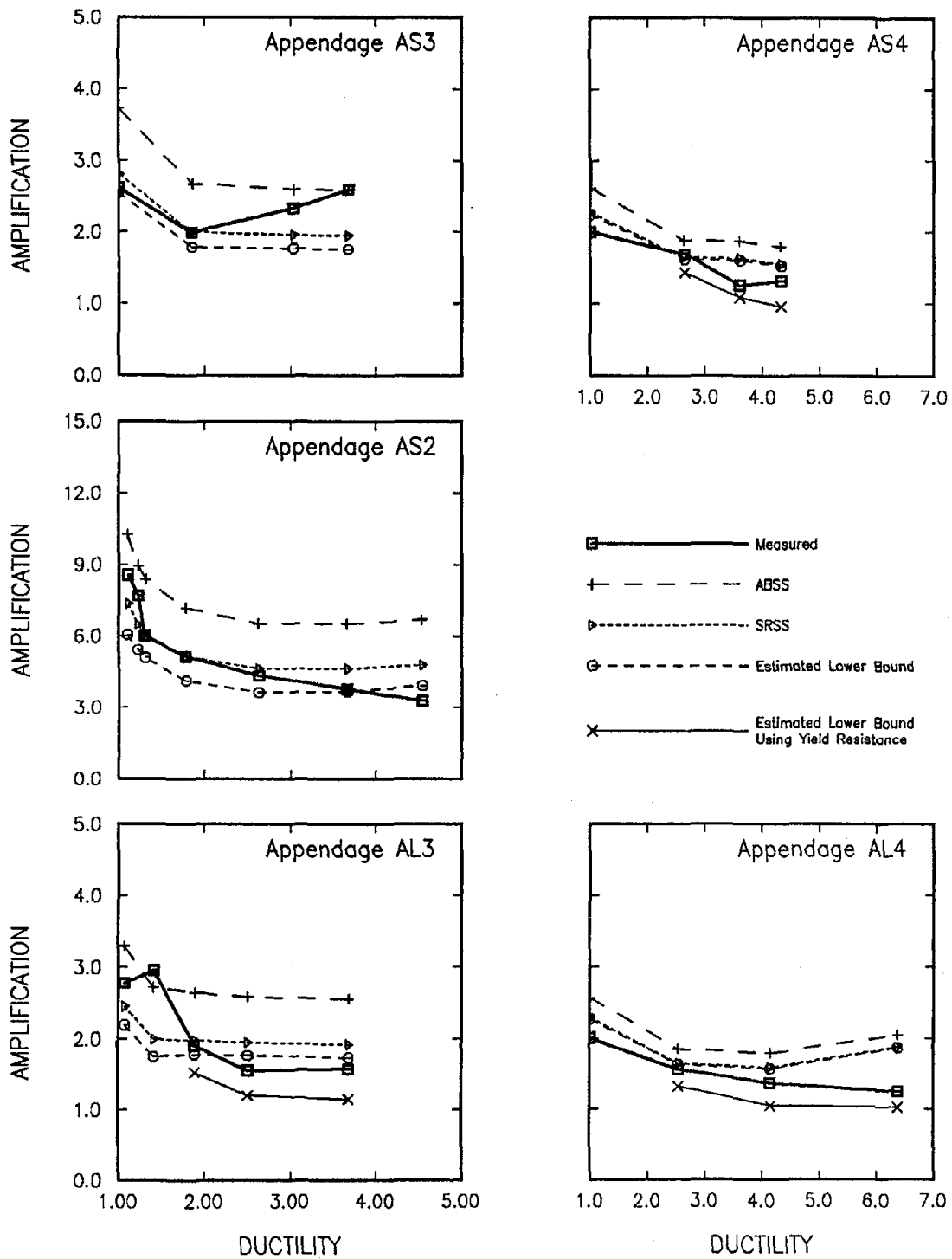


Figure 5.45 Comparison of Measured and Calculated Amplifications of the Detuned Appendages on Structure S2 Subjected to El Centro Earthquake

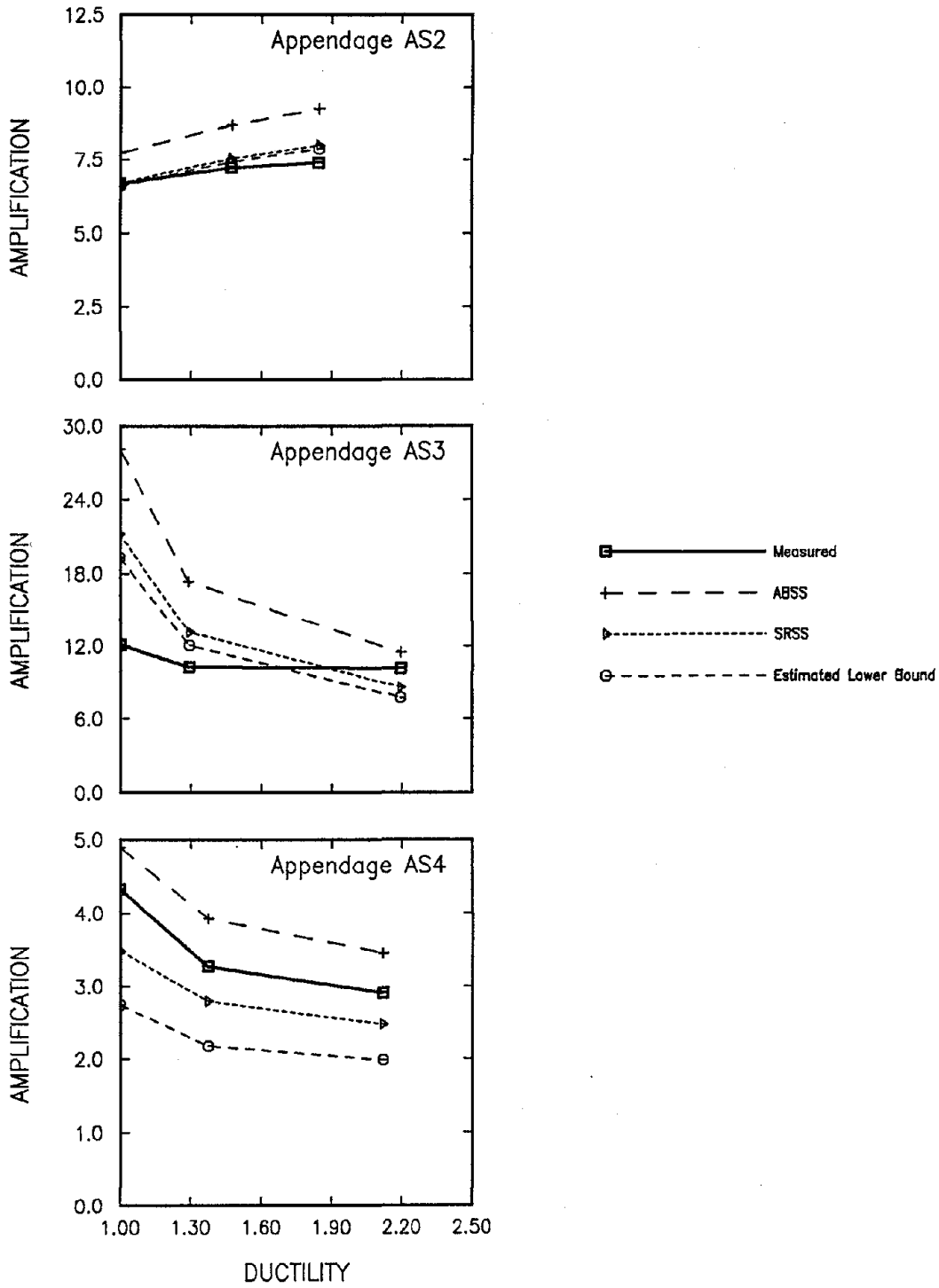


Figure 5.46 Comparison of Measured and Calculated Amplifications of the Detuned Appendages on Structure S4 Subjected to El Centro Earthquake.

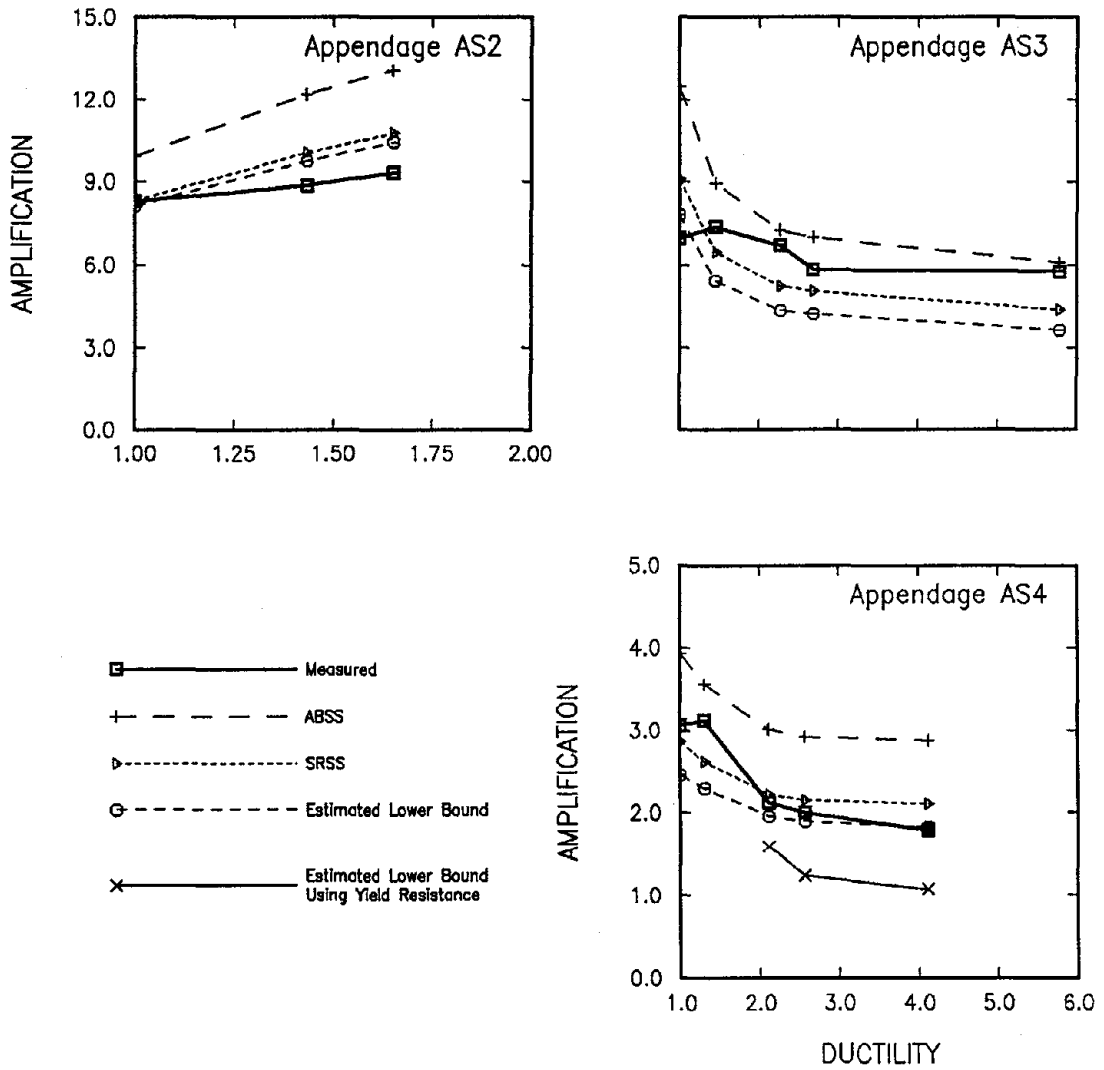


Figure 5.47 Comparison of Measured and Calculated Amplifications of the Detuned Appendages on Structure S5 Subjected to El Centro Earthquake

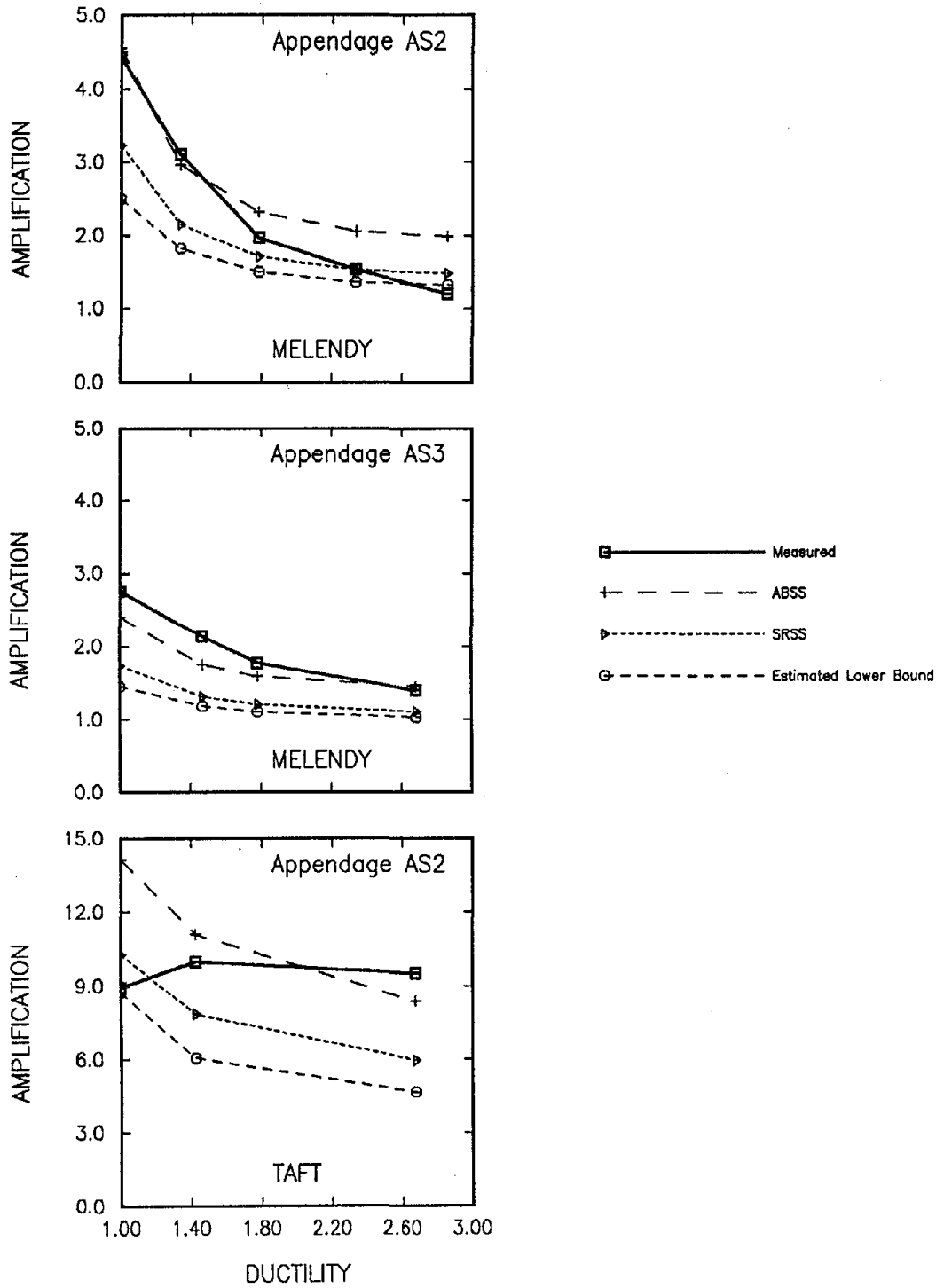


Figure 5.48 Comparison of Measured and Calculated Amplifications of the Detuned Appendages on Structure S2 Subjected to Melendy and Taft Earthquakes

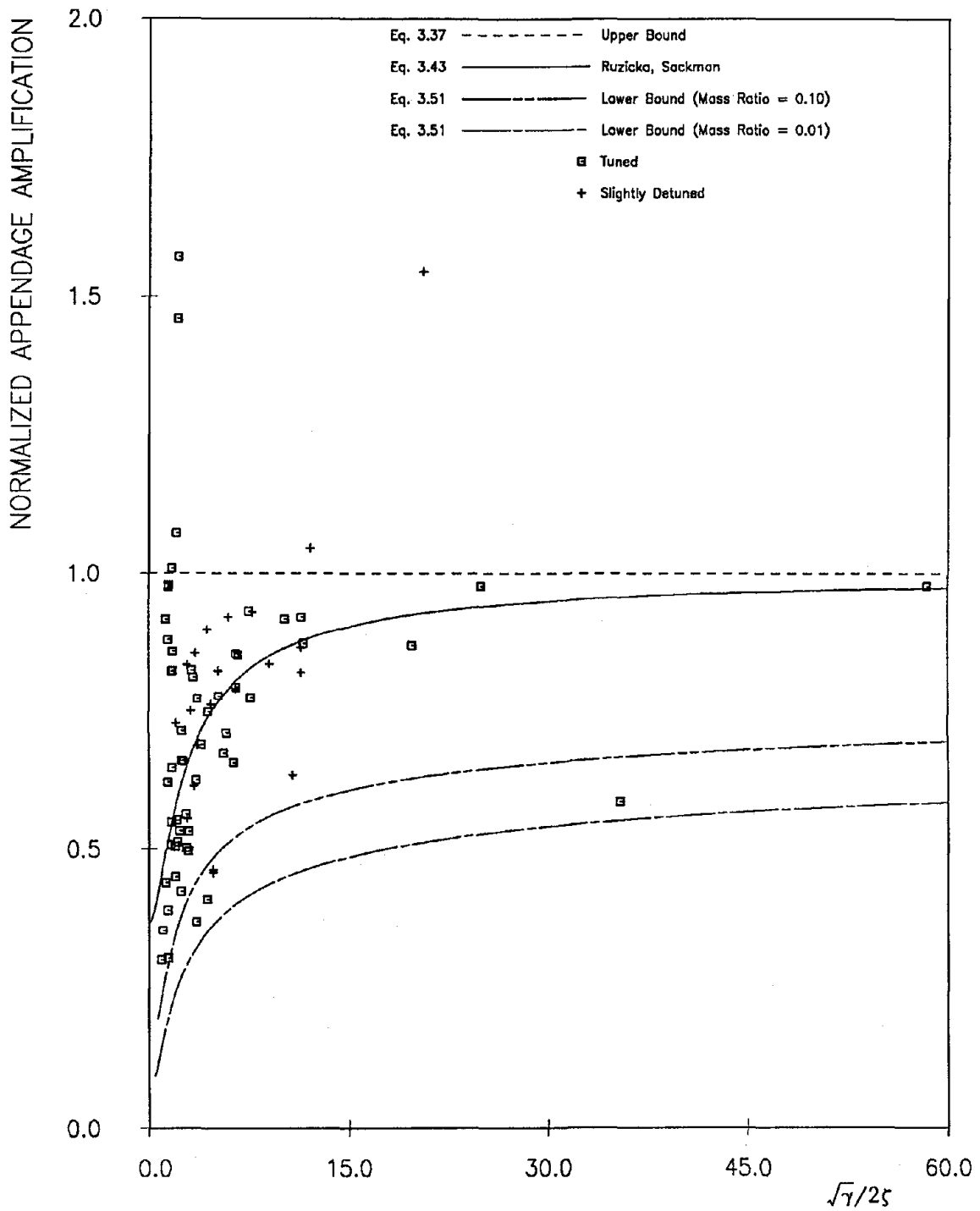


Figure 5.49a Comparison of Measured and Calculated Appendage Normalized Amplifications, $\ddot{x}_{max}/\ddot{x}_g$, for the Single-Story Tuned and Slightly Detuned Systems

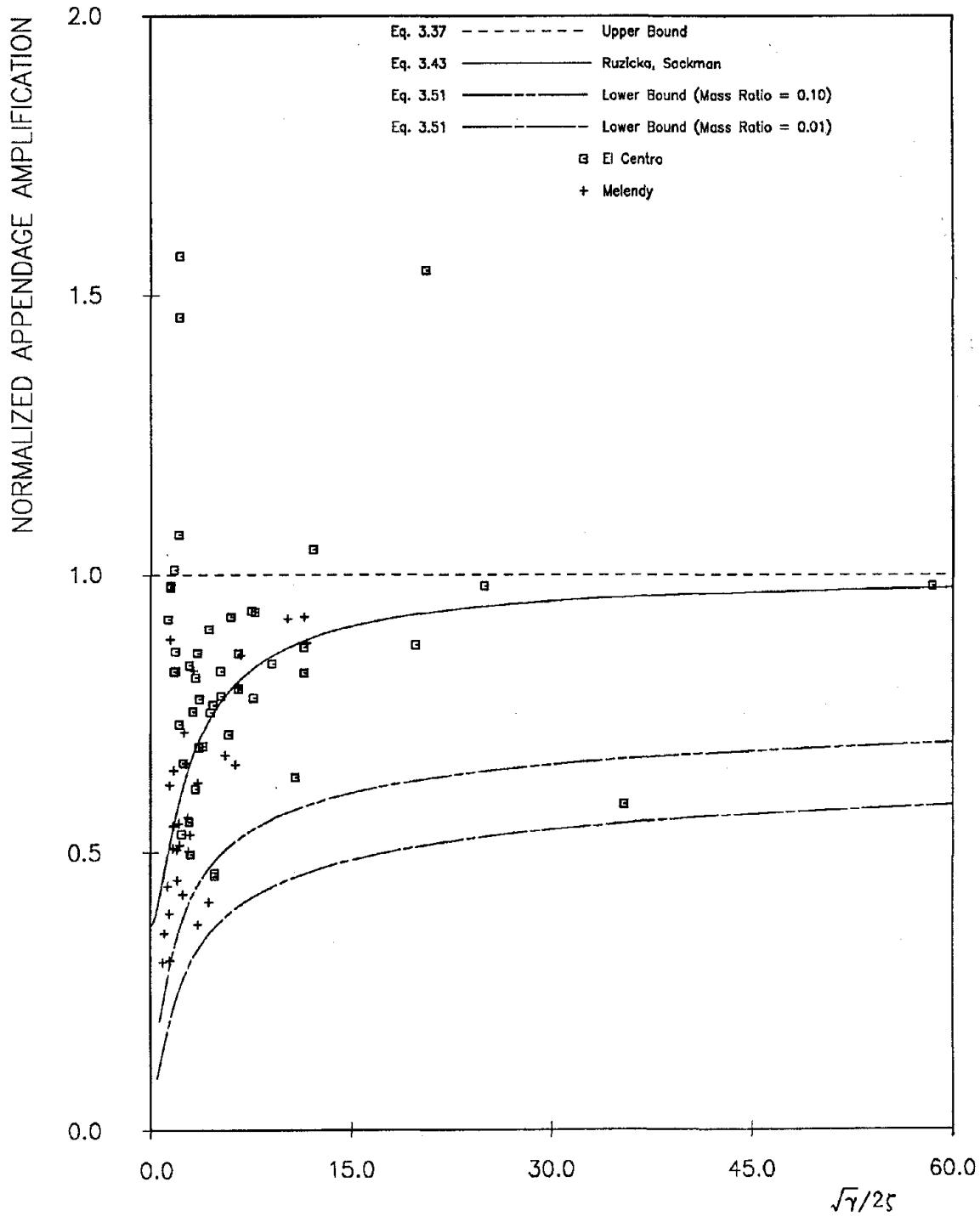


Figure 5.49b Comparison of Measured and Calculated Appendage Normalized Amplifications, $\ddot{x}_{max}/\ddot{x}_g$, of the Single-Story Tuned and Slightly Detuned Systems for Two Earthquakes

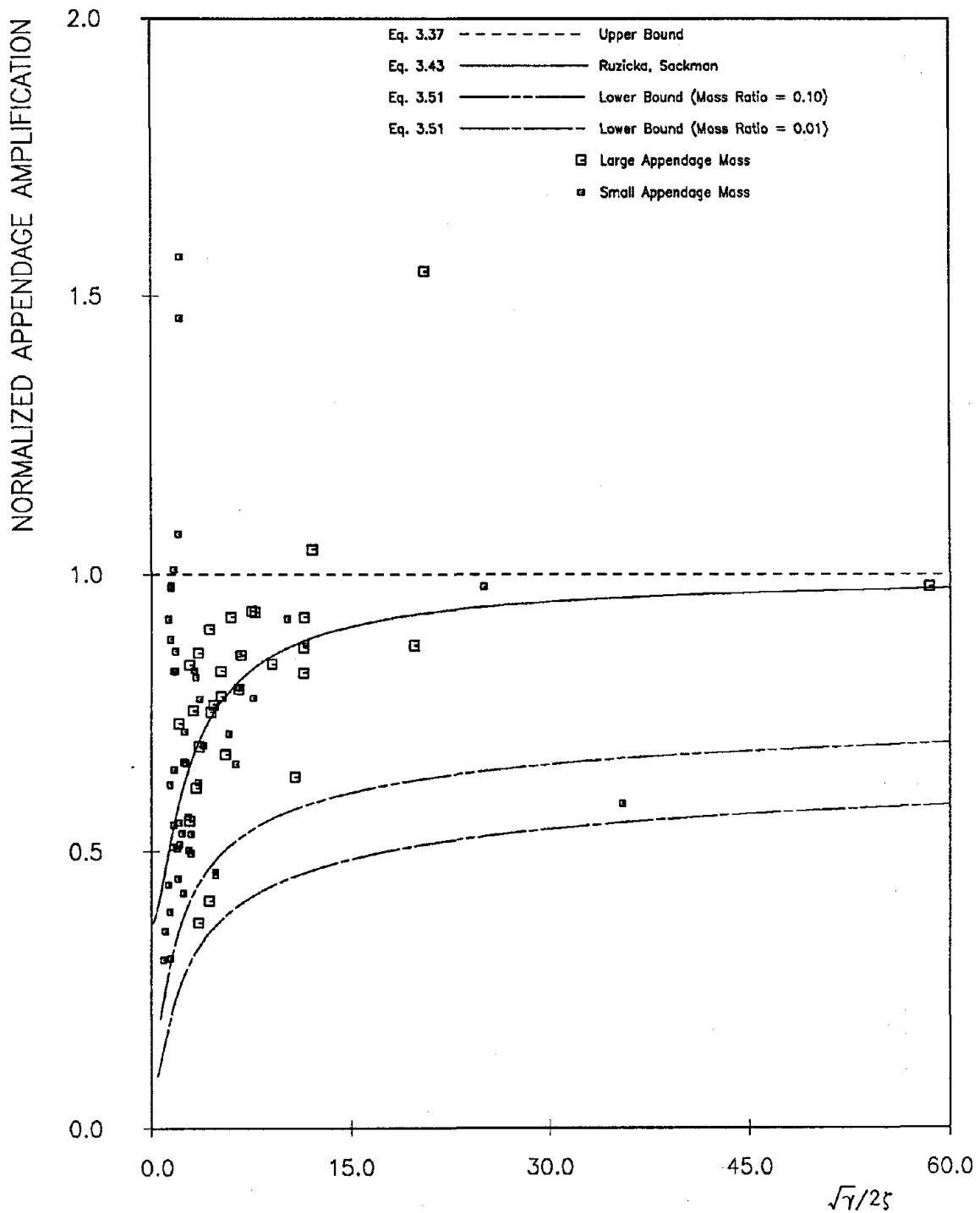


Figure 5.49c Comparison of Measured and Calculated Appendage Normalized Amplifications, $\ddot{x}_{max}/\ddot{x}_\zeta$, of the Single-Story Tuned and Slightly Detuned Systems for Large and Small Appendage Mass

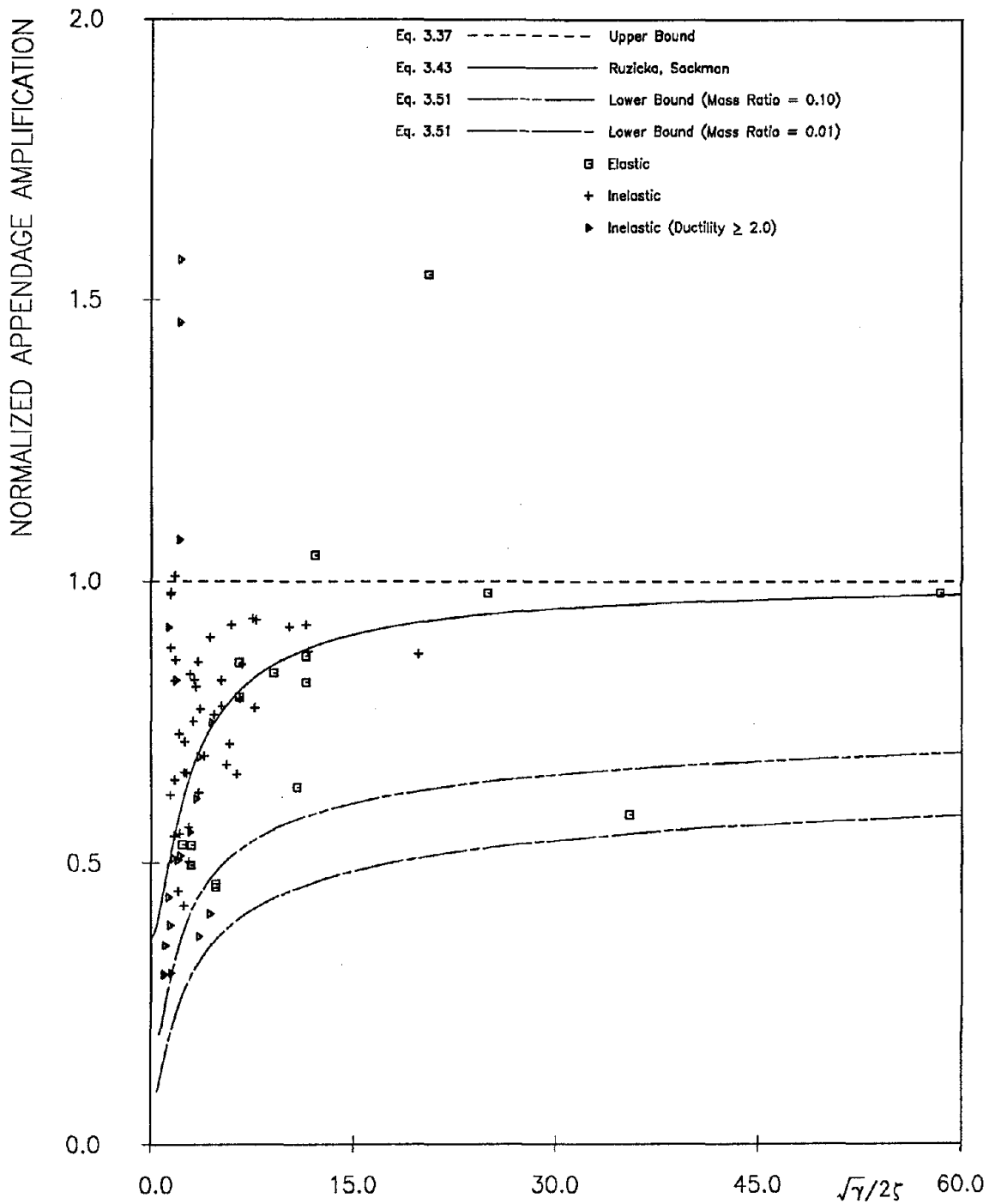


Figure 5.50 Comparison of Measured and Calculated Appendage Normalized Amplifications, $\ddot{x}_{max}/\ddot{x}_{\zeta}$, of the Single-Story Tuned and Slightly Detuned Systems for Elastic and Inelastic Behavior of the Supporting Structure

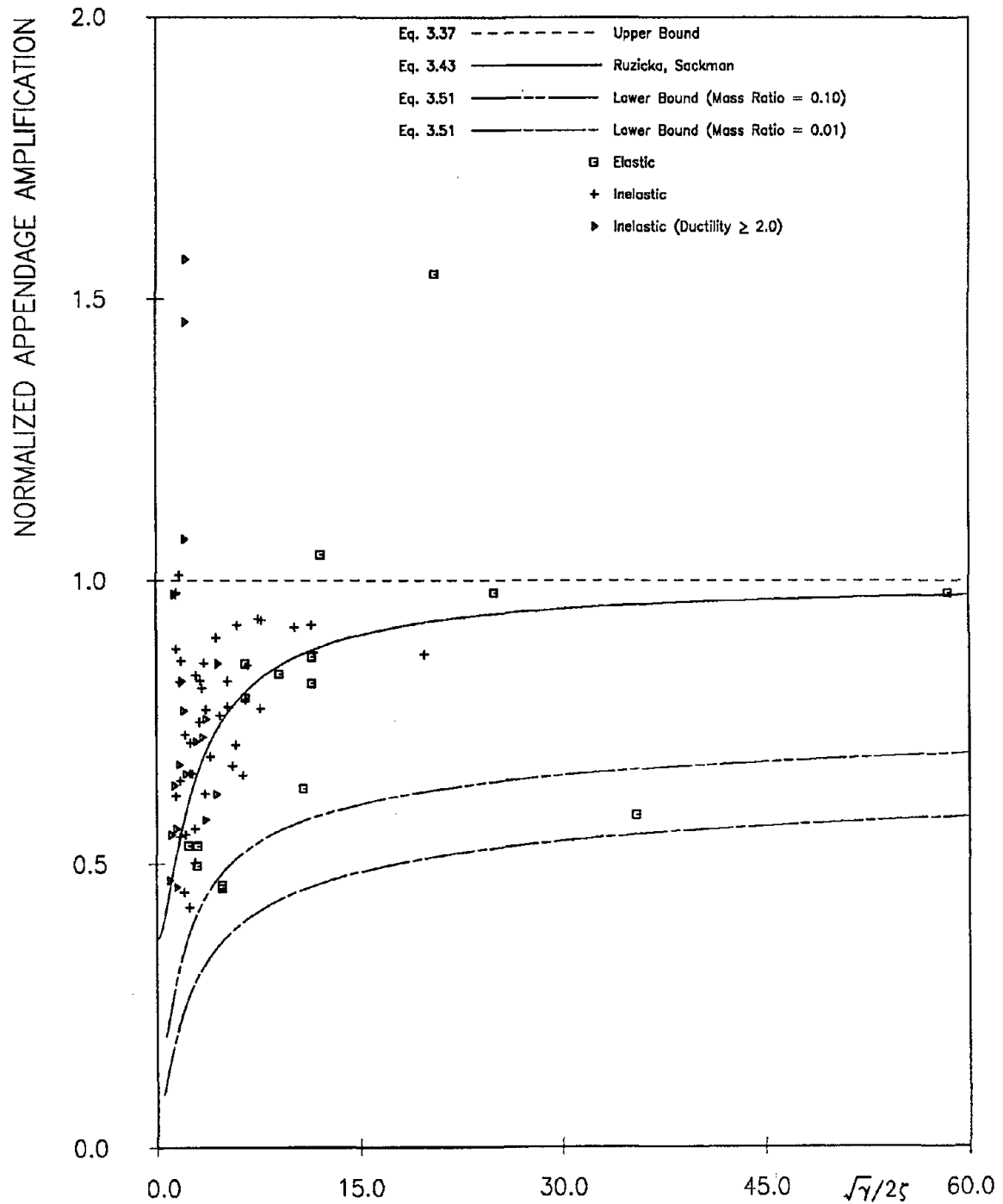


Figure 5.51 Comparison of Measured and Calculated Appendage Normalized Amplifications, $\ddot{x}_{\max}/\ddot{x}_g$, of the Single-Story Tuned and Slightly Detuned Structure After Correction for the Yield Resistance of the Structure

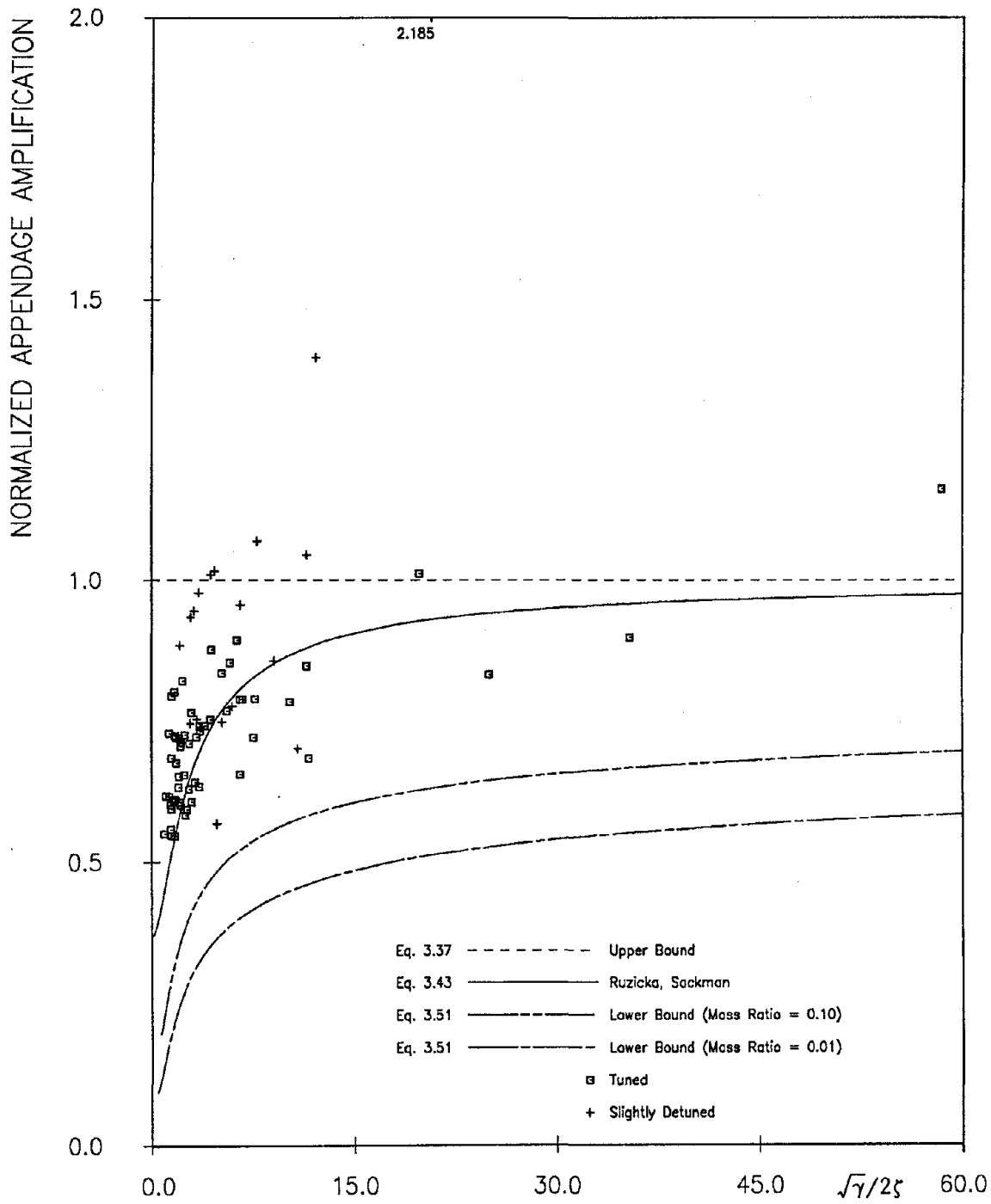


Figure 5.52 Comparison of Appendage Normalized Amplifications, $\ddot{x}_{max}/\ddot{x}_\zeta$, of the Single-Story Tuned and Slightly Detuned Systems Determined Numerically for the Equivalent Linear Systems and Calculated (Eqs. 3.37, 3.43 and 3.51)

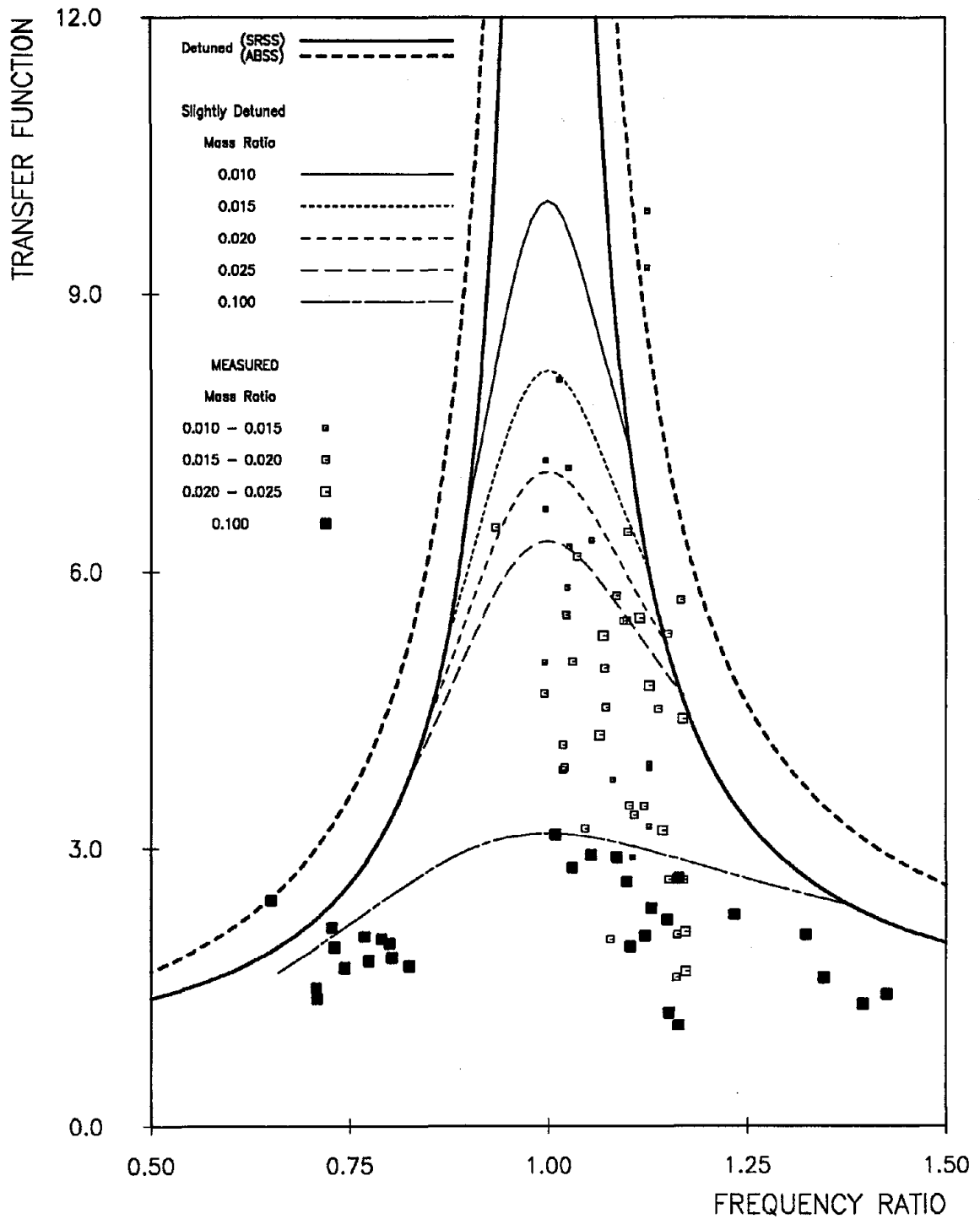


Figure 5.53 Comparison of Measured and Calculated Appendage Transfer Function of the Single-Story Tuned and Slightly Detuned Systems

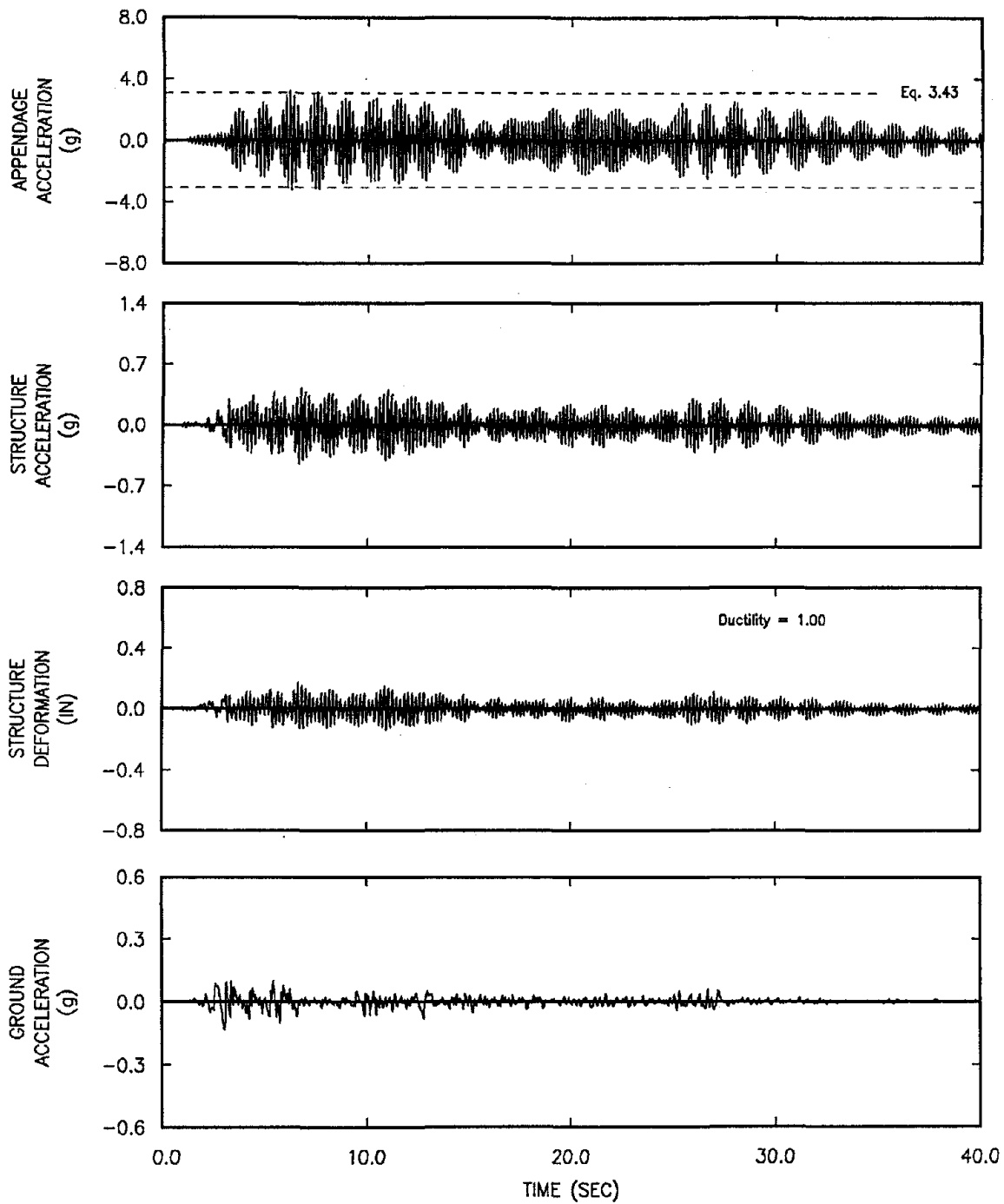


Figure 5.54 Measured Response of a Single-Story Tuned System. Structure S8 and Appendage AT2 Subjected to El Centro Earthquake. Ductility = 1.00

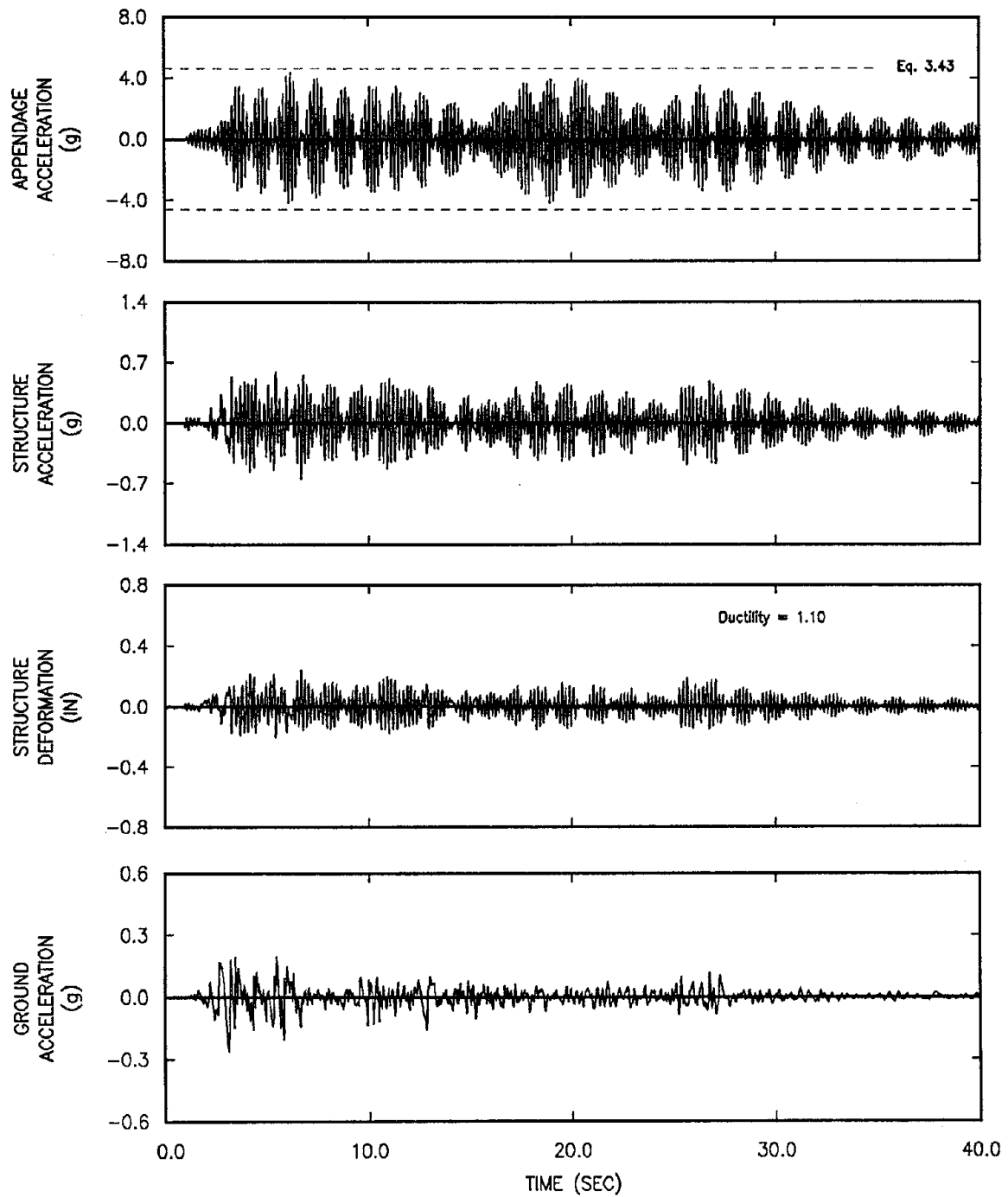


Figure 5.55 Measured Response of a Single-Story Tuned System. Structure S8 and Appendage AT2 Subjected to El Centro Earthquake. Ductility = 1.10

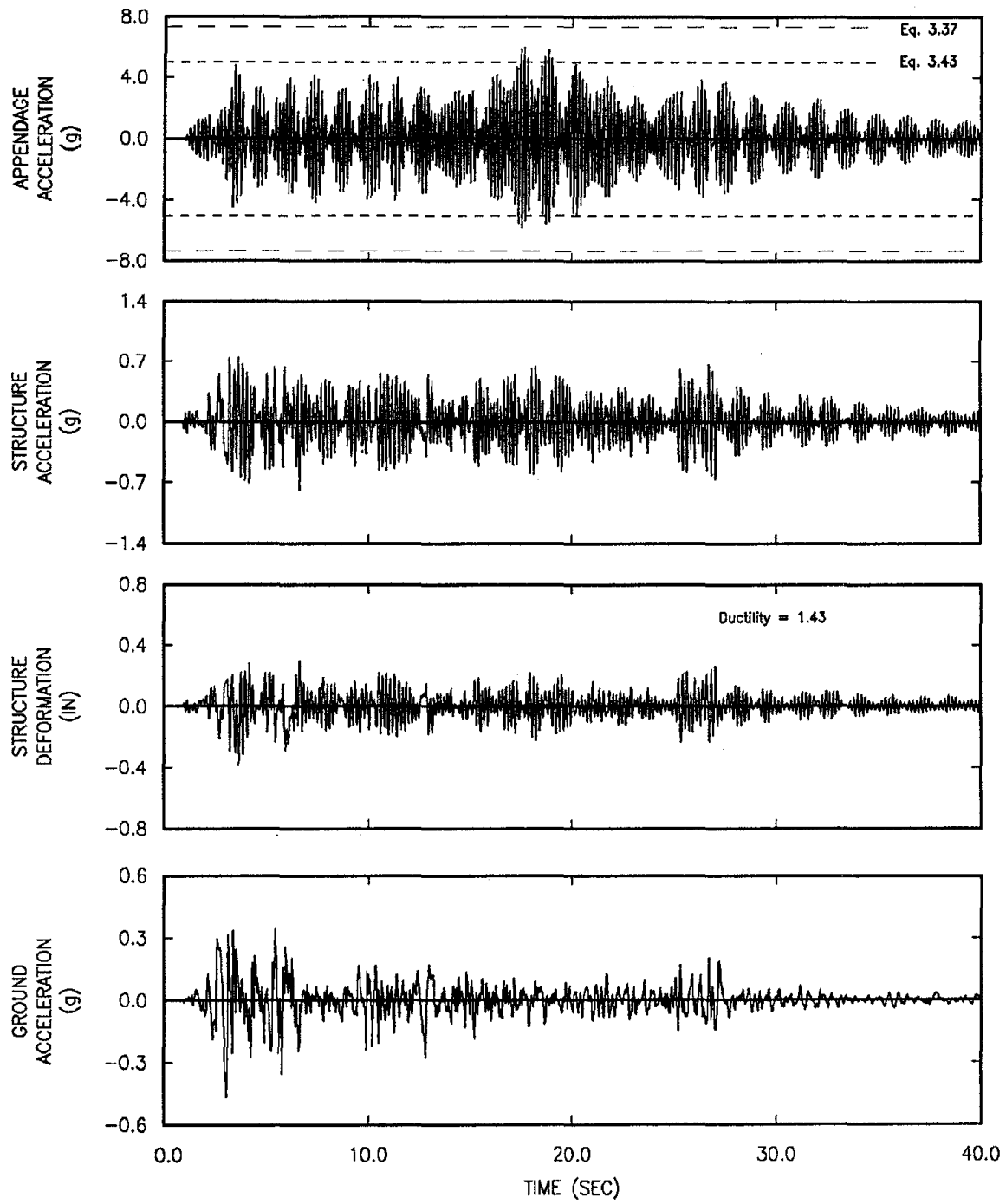


Figure 5.56 Measured Response of a Single-Story Tuned System. Structure S8 and Appendage AT2 Subjected to El Centro Earthquake. Ductility = 1.43

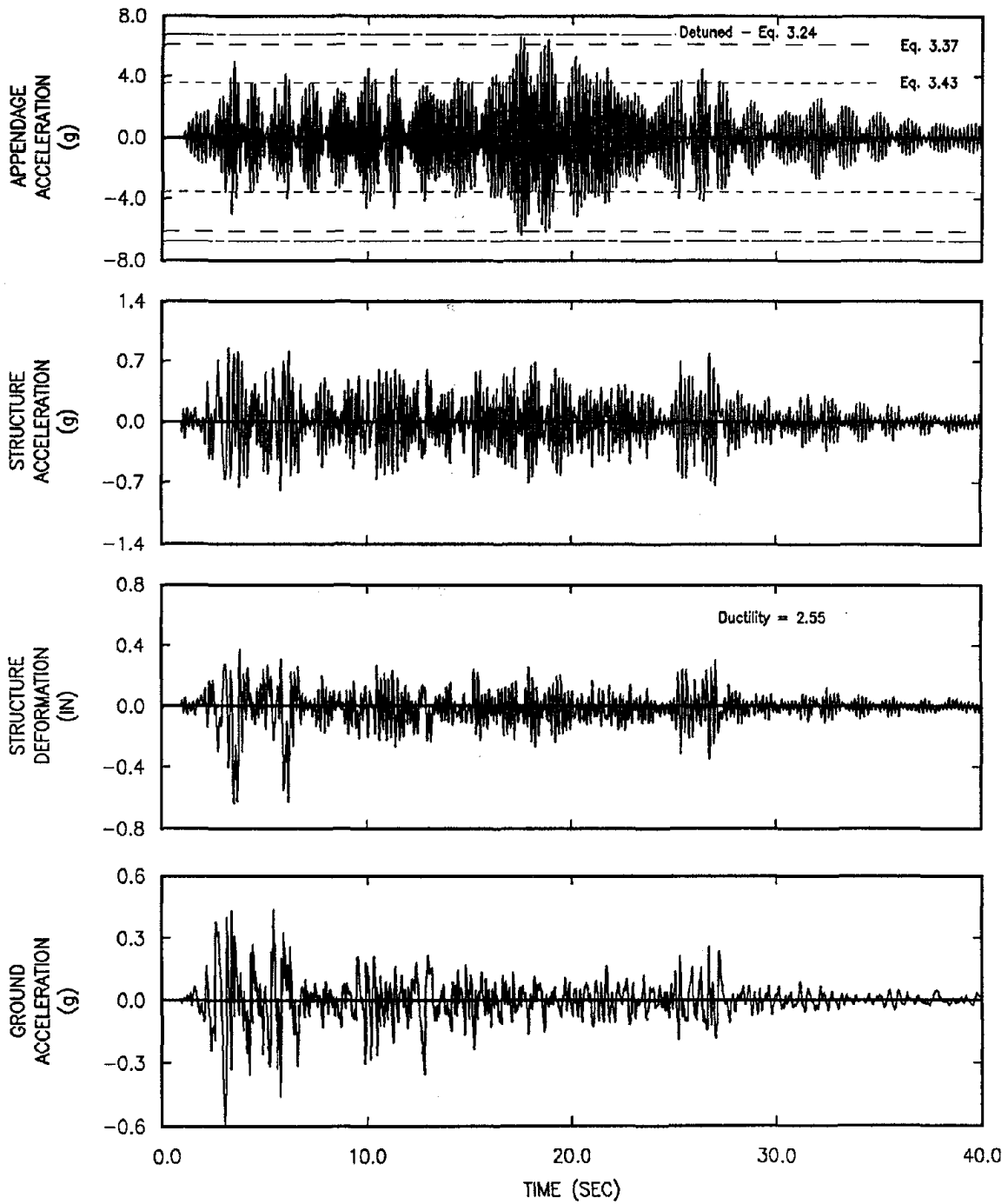


Figure 5.57 Measured Response of a Single-Story Tuned System. Structure S8 and Appendage AT2 Subjected to El Centro Earthquake. Ductility = 2.55

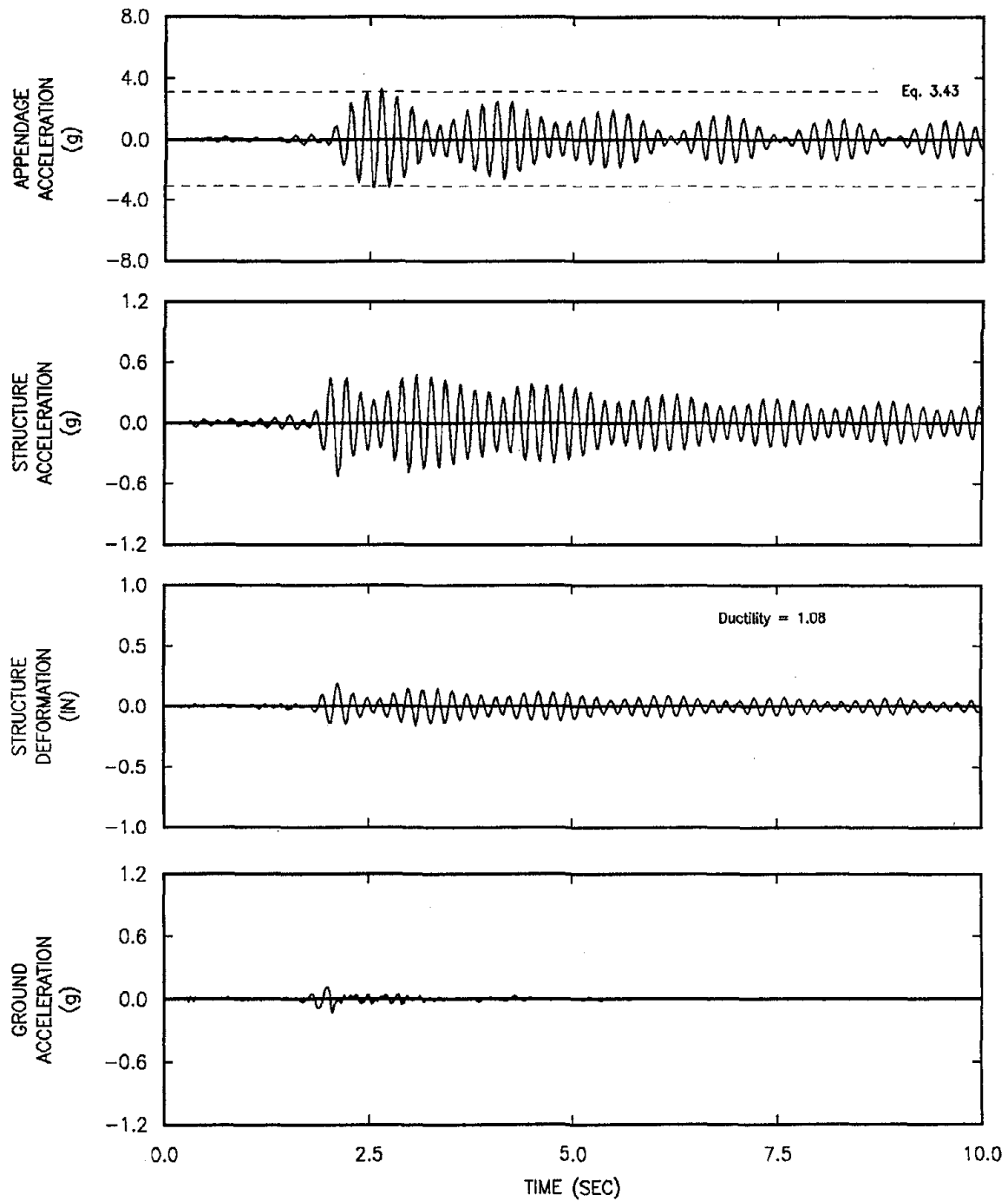


Figure 5.58 Measured Response of a Single-Story Tuned System. Structure S8 and Appendage AT3 Subjected to Melendy Earthquake. Ductility = 1.08

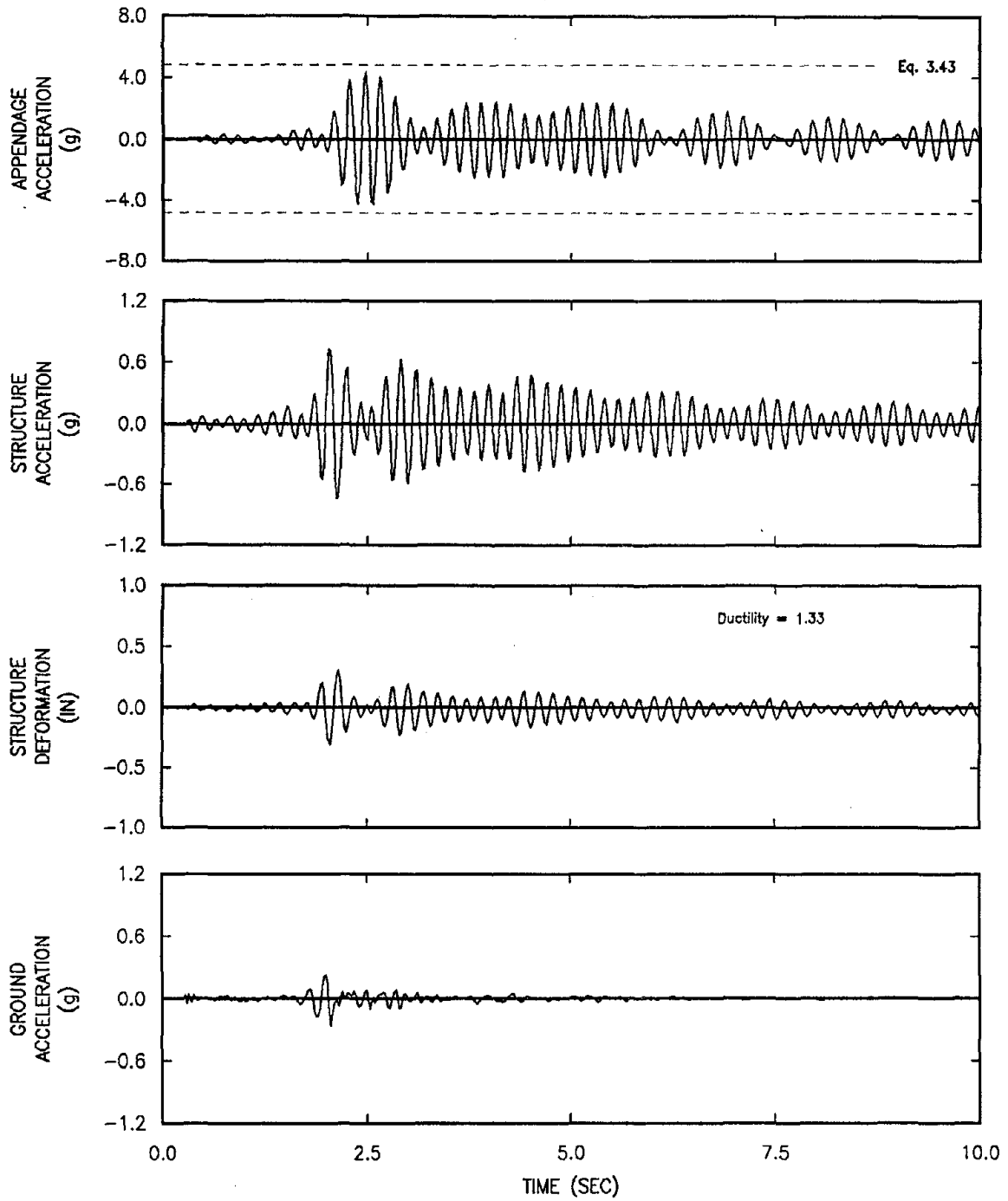


Figure 5.59 Measured Response of a Single-Story Tuned System. Structure S8 and Appendage AT3 Subjected to Melendy Earthquake. Ductility = 1.33

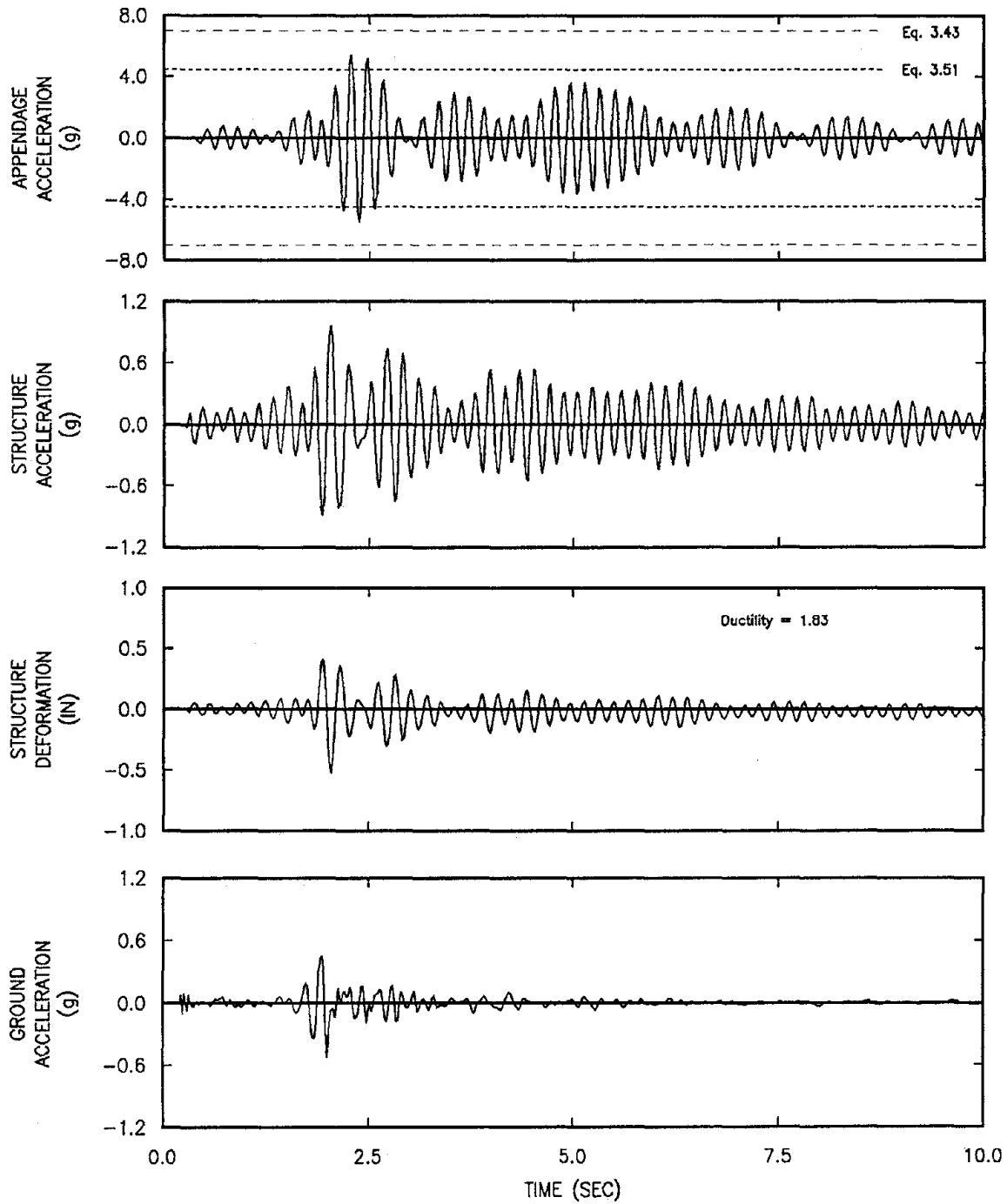


Figure 5.60 Measured Response of a Single-Story Tuned System. Structure S8 and Appendage AT3 Subjected to Melendy Earthquake. Ductility = 1.83

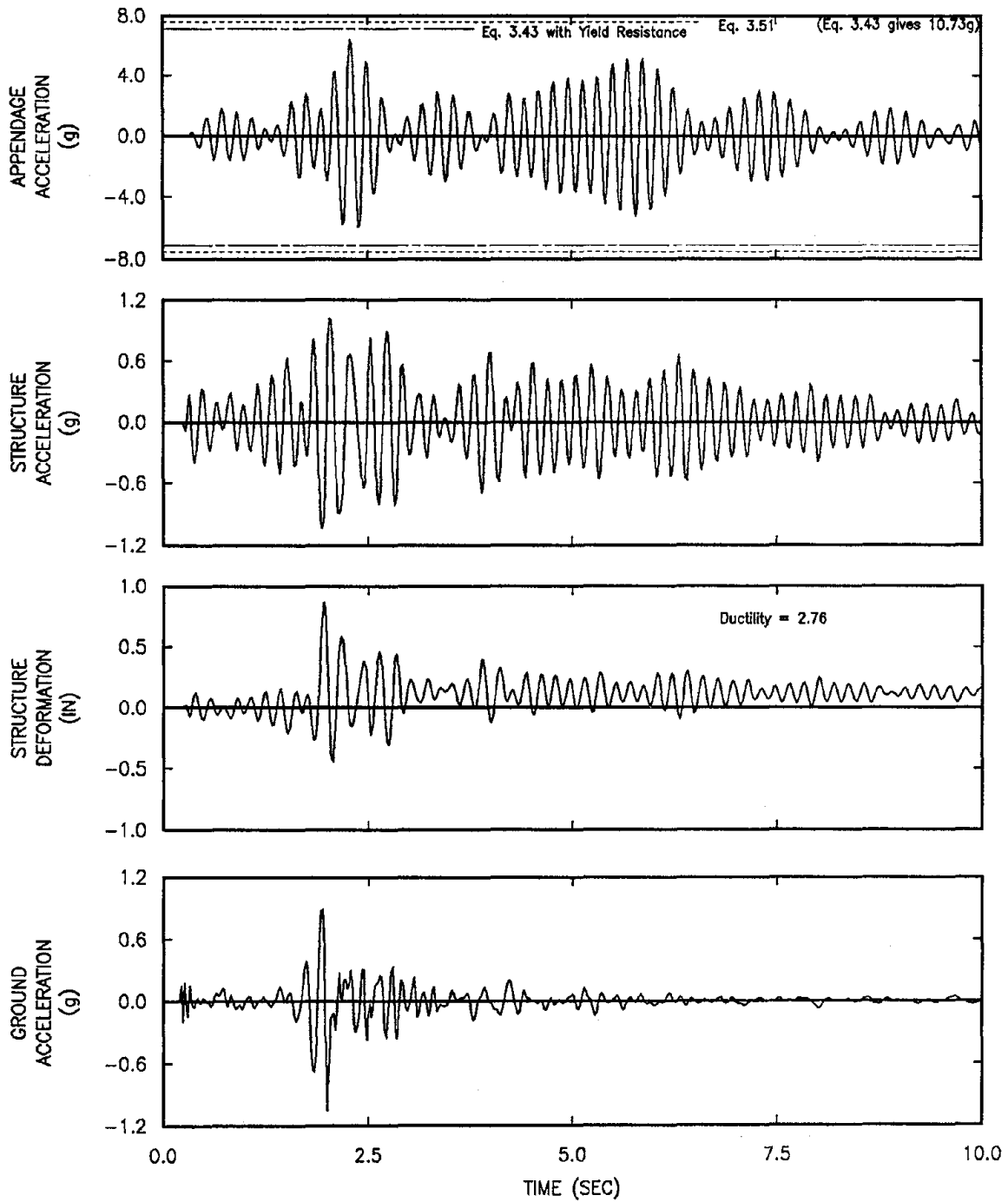


Figure 5.61 Measured Response of a Single-Story Tuned System. Structure S8 and Appendage AT3 Subjected to Melendy Earthquake. Ductility = 2.76

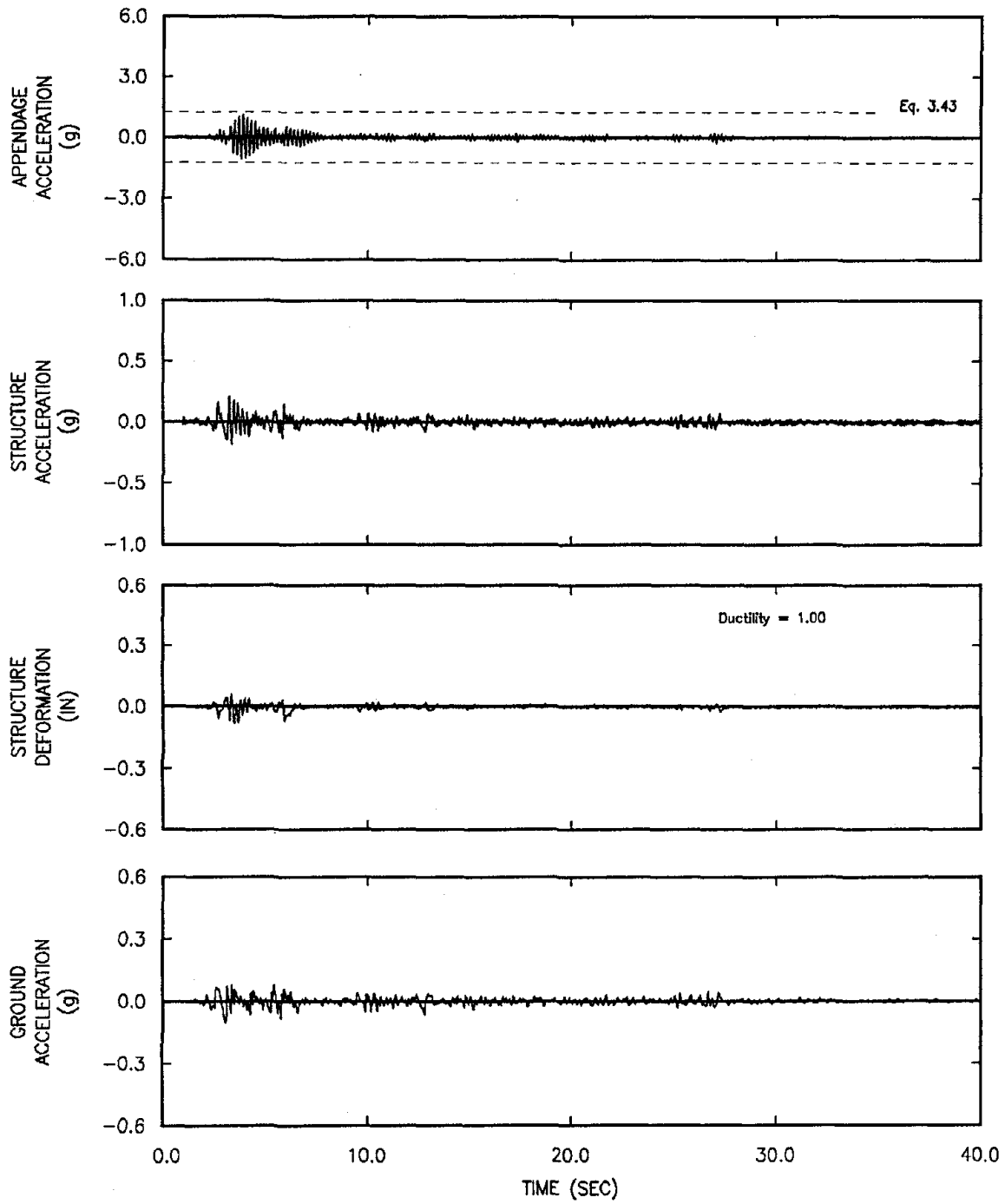


Figure 5.62 Measured Response of a Single-Story Tuned System. Structure S4 and Appendage AT6 Subjected to El Centro Earthquake. Ductility = 1.00

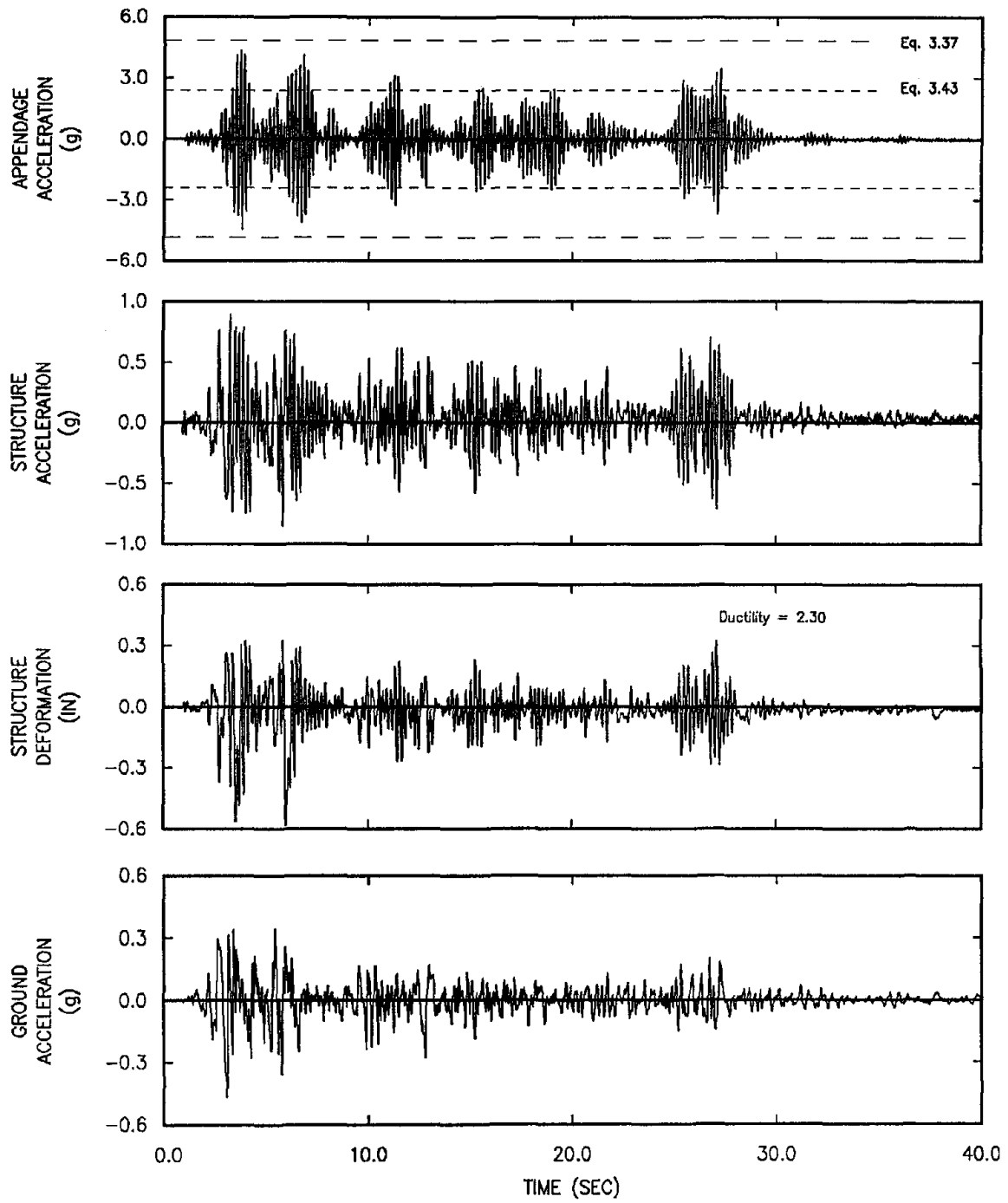


Figure 5.63 Measured Response of a Single-Story Tuned System. Structure S4 and Appendage AT6 Subjected to El Centro Earthquake. Ductility = 2.30

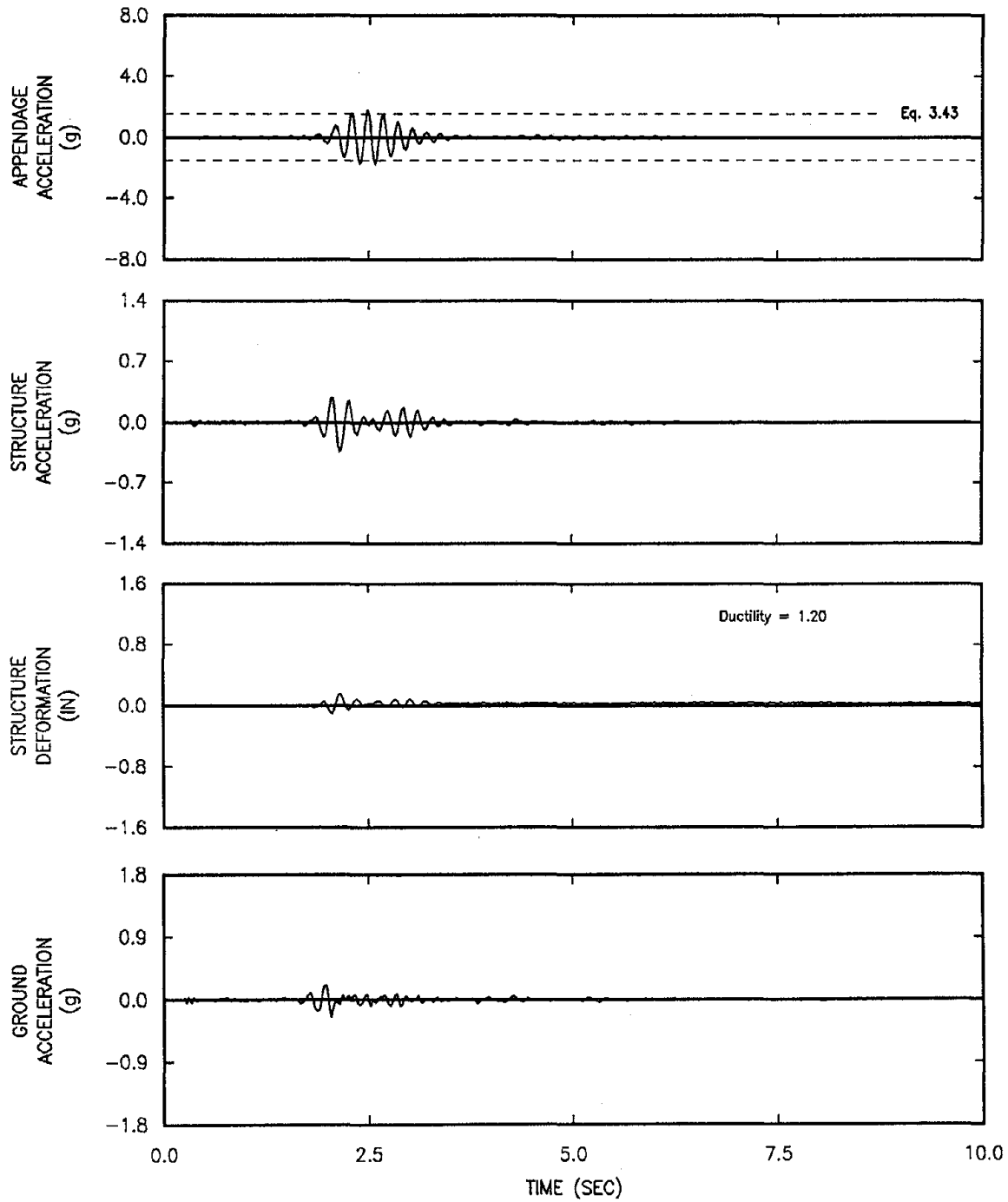


Figure 5.64 Measured Response of a Single-Story Tuned System. Structure S4 and Appendage AT6 Subjected to Melendy Earthquake. Ductility = 1.20

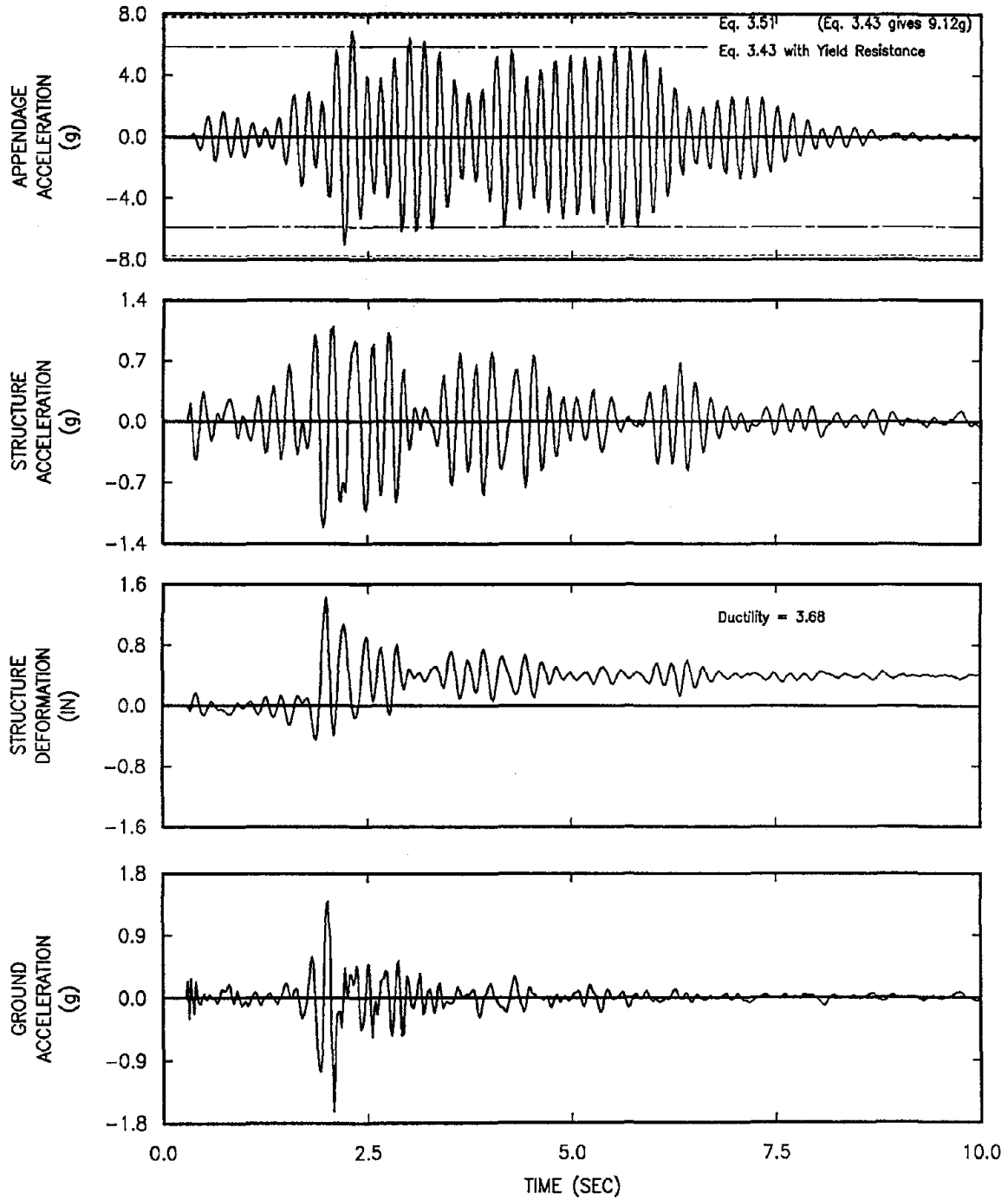


Figure 5.65 Measured Response of a Single-Story Tuned System. Structure S4 and Appendage AT6 Subjected to Melendy Earthquake. Ductility = 3.68

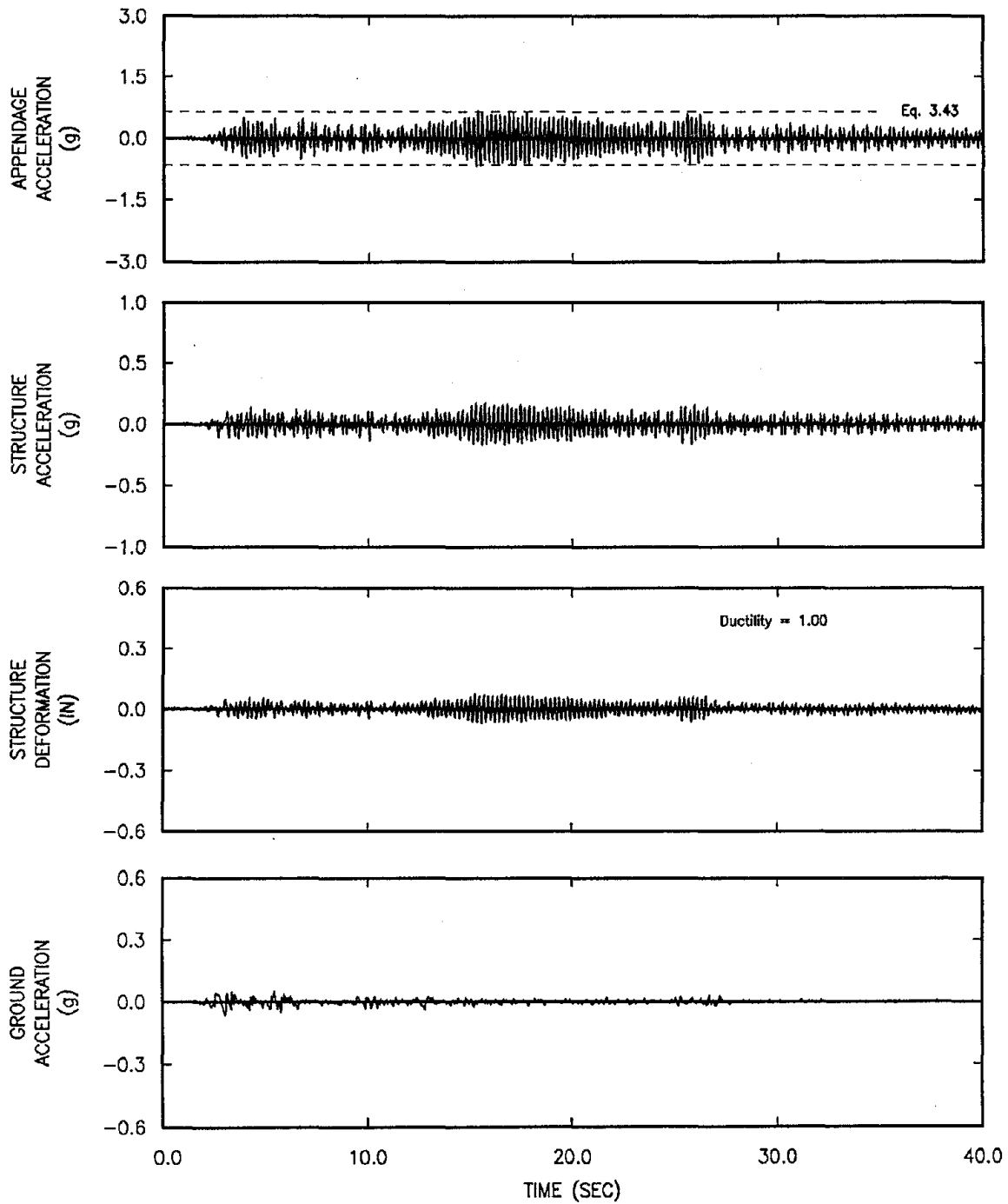


Figure 5.66 Measured Response of a Single-Story Tuned System. Structure S9 and Appendage AT7 Subjected to El Centro Earthquake. Ductility = 1.00

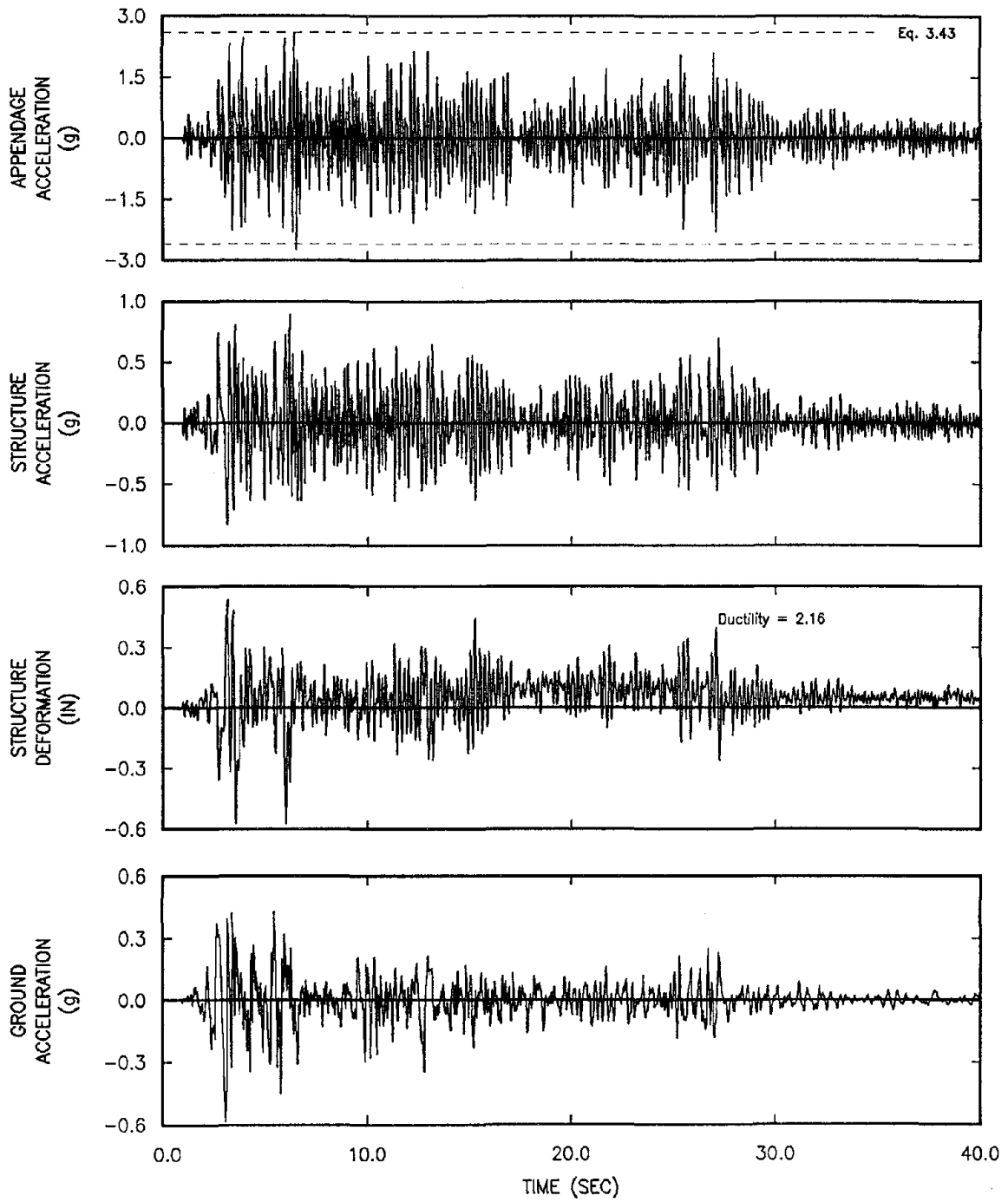


Figure 5.67 Measured Response of a Single-Story Tuned System. Structure S9 and Appendage AT7 Subjected to El Centro Earthquake. Ductility = 2.16

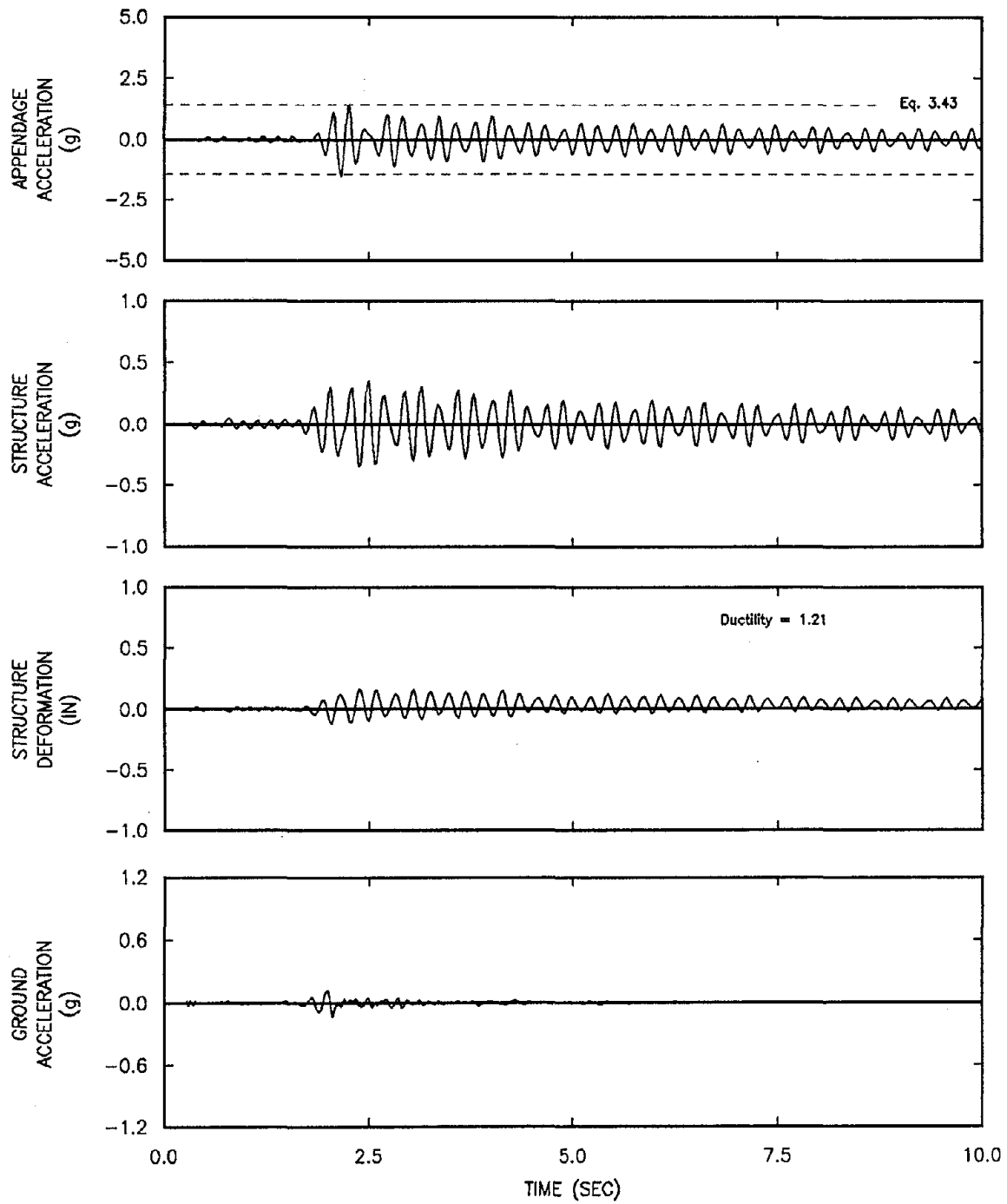


Figure 5.68 Measured Response of a Single-Story Tuned System. Structure S9 and Appendage AT7 Subjected to Melendy Earthquake. Ductility = 1.21

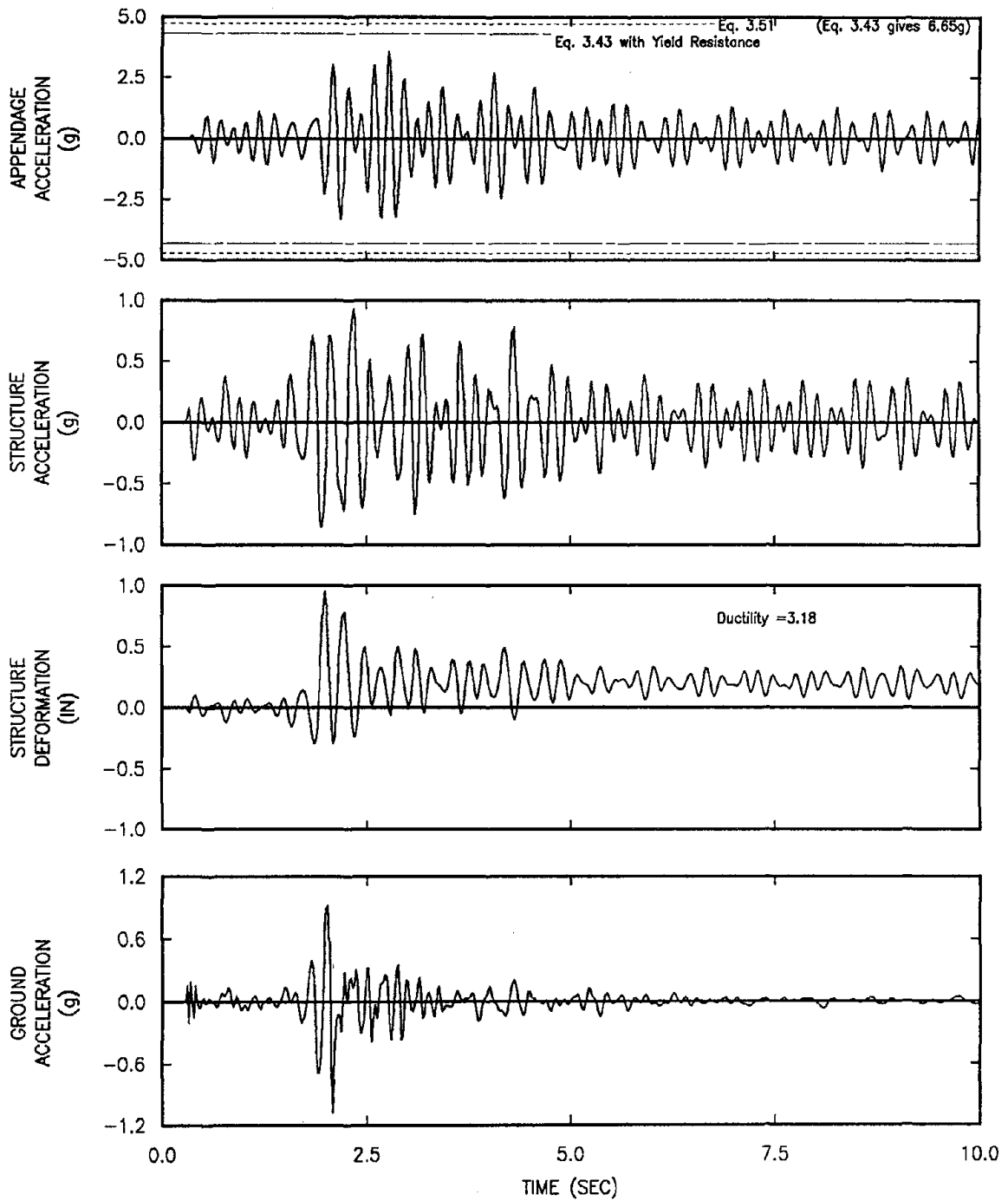


Figure 5.69 Measured Response of a Single-Story Tuned System. Structure S9 and Appendage AT7 Subjected to Melendy Earthquake. Ductility = 3.18

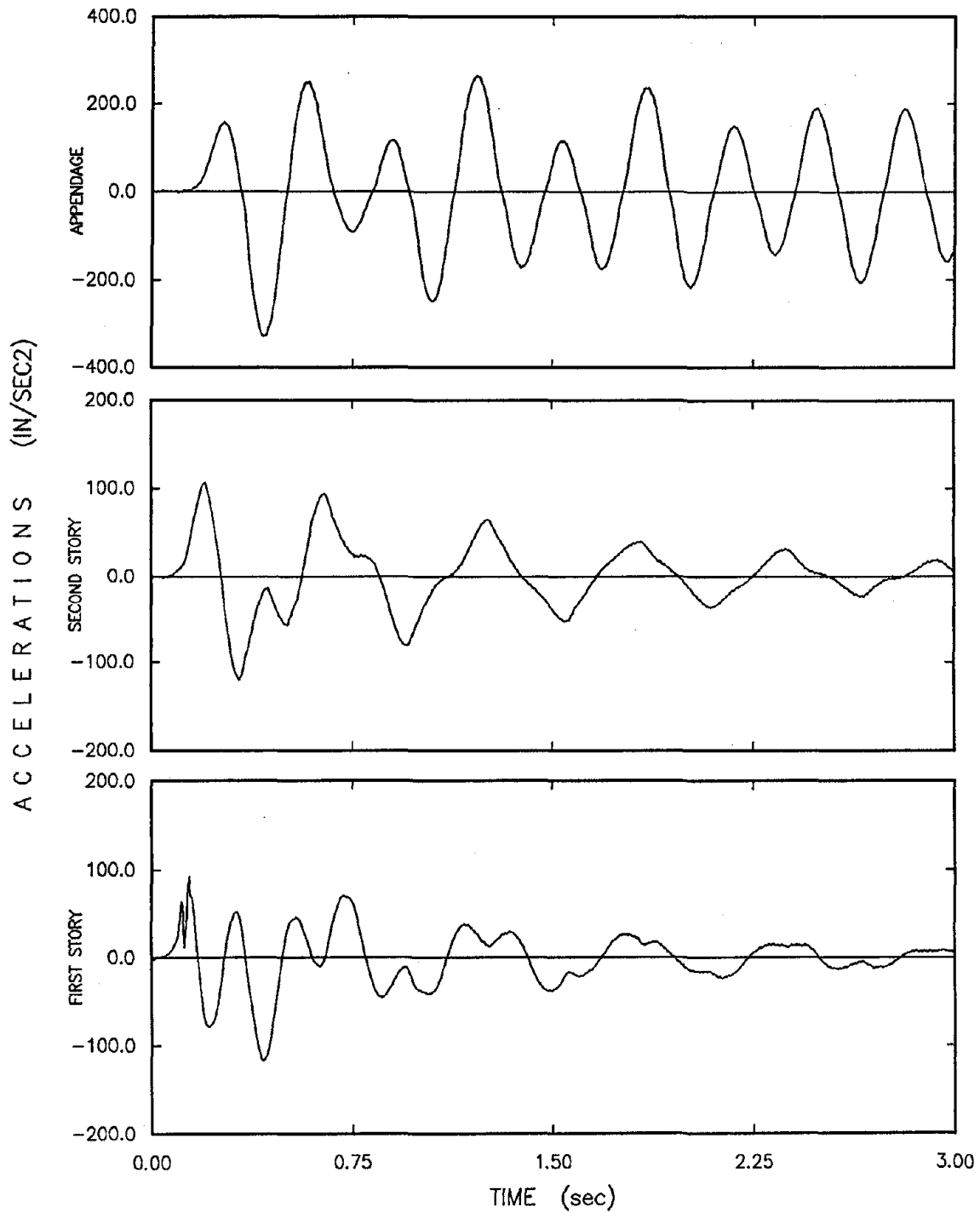


Figure 5.70 Typical Measured Free Vibrations Accelerations of the Combined Two-Story Structure M1 and Appendage AS2 Mounted on the Second Story

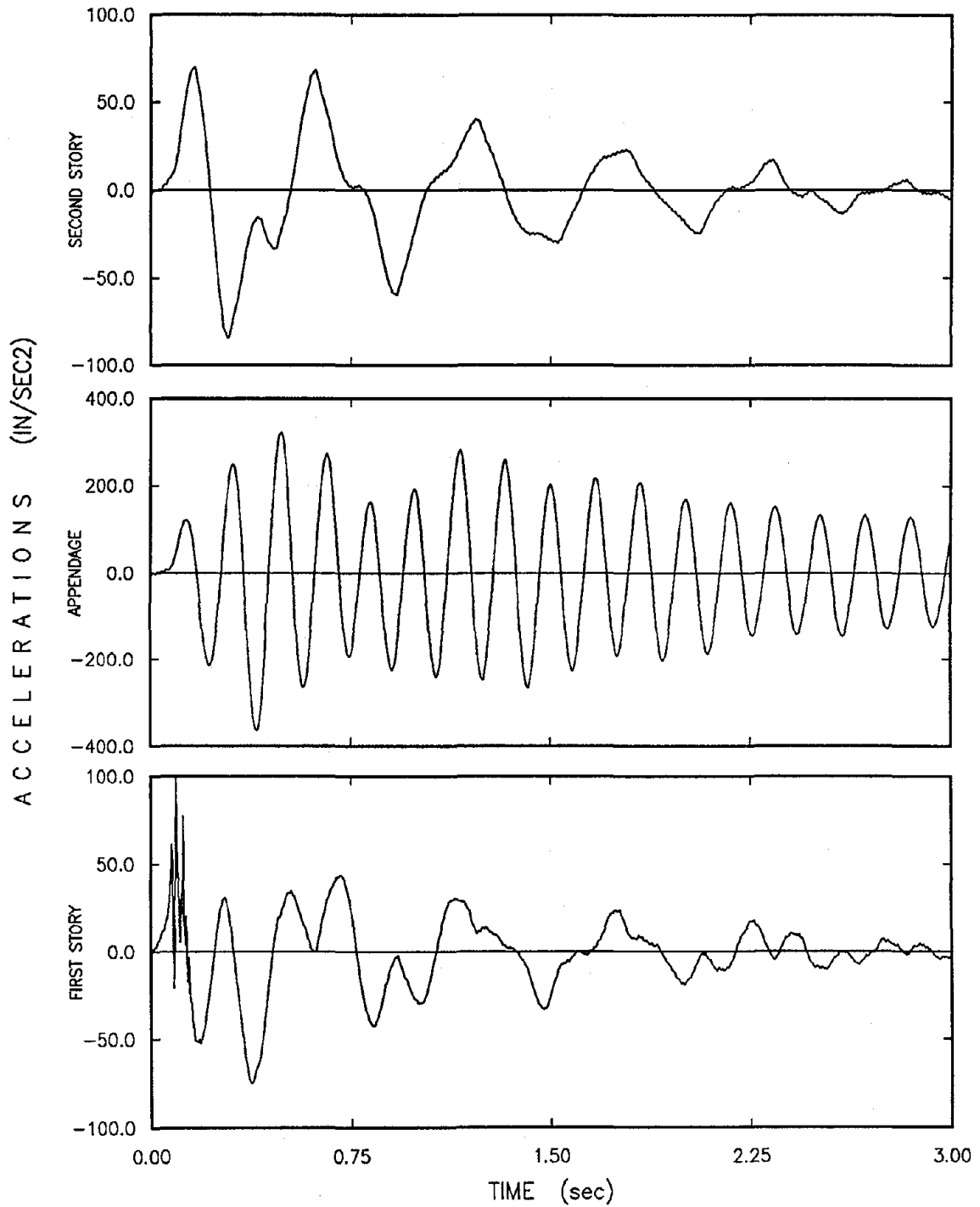


Figure 5.71 Typical Measured Free Vibrations Accelerations of the Combined Two-Story Structure M1 and Appendage AS3 Mounted on the First Story

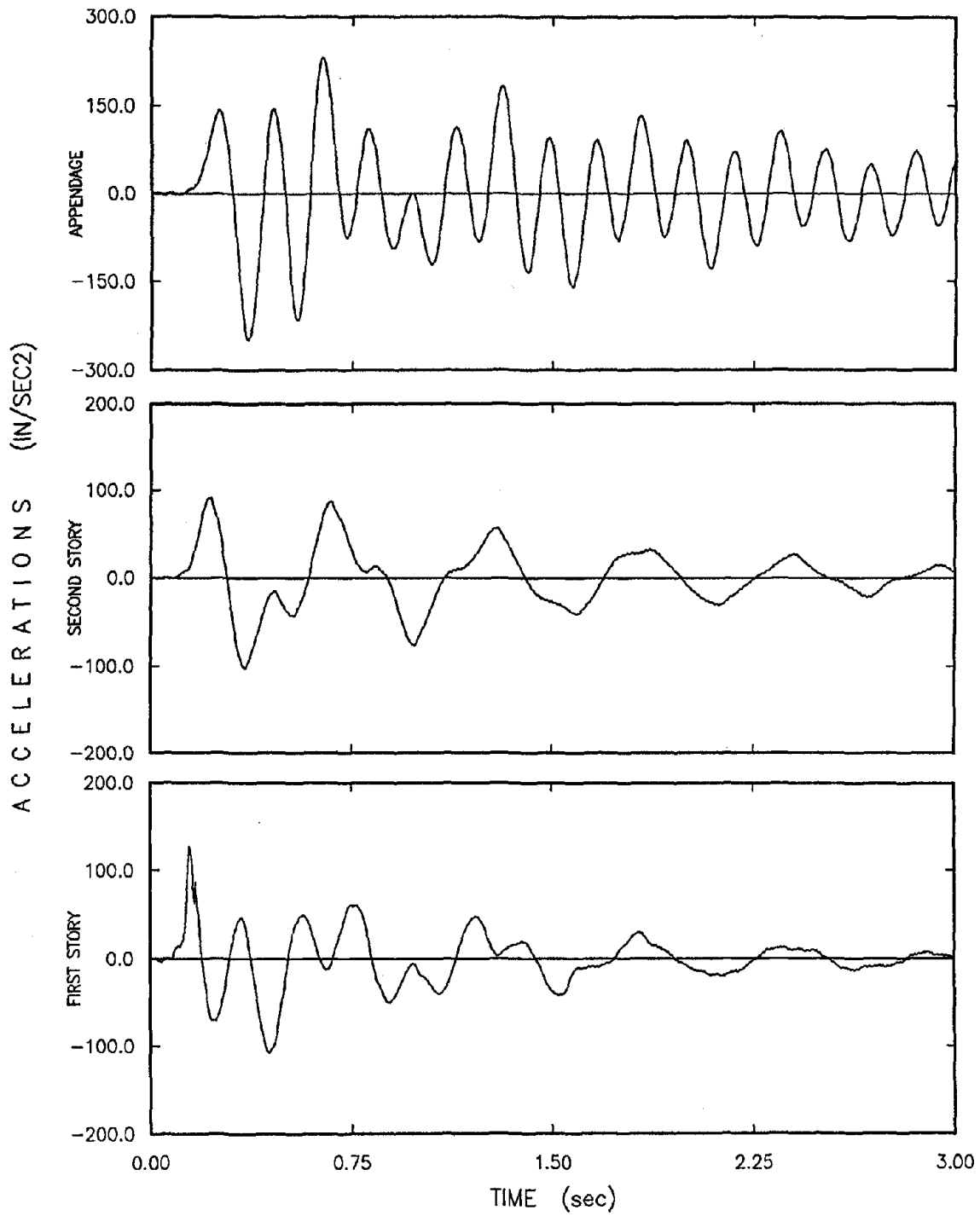


Figure 5.72 Typical Measured Free Vibrations Accelerations of the Combined Two-Story Structure M1 and Appendage AS3 Mounted on the Second Story

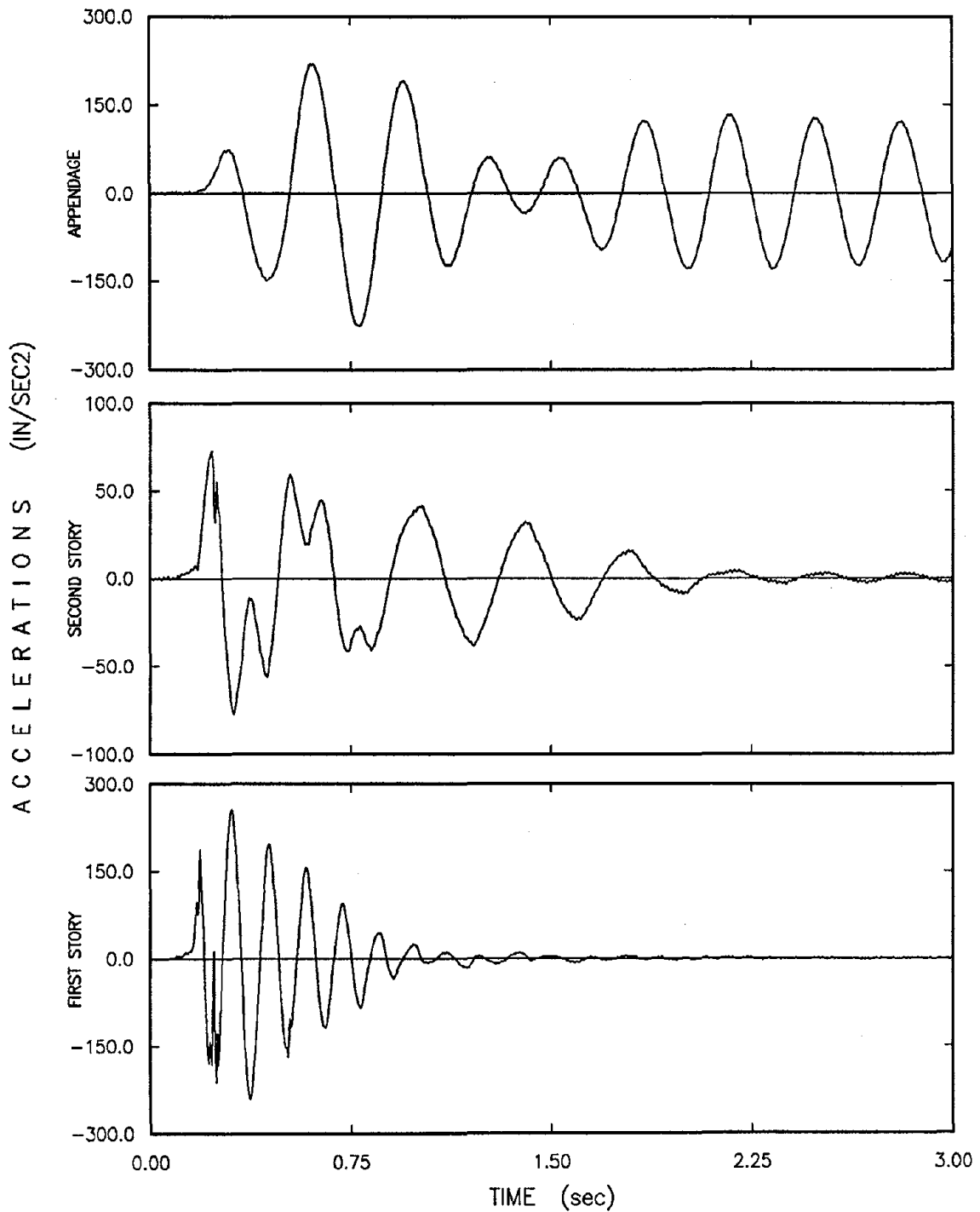


Figure 5.73 Typical Measured Free Vibrations Accelerations of the Combined Two-Story Structure M2 and Appendage AS2 Mounted on the Second Story

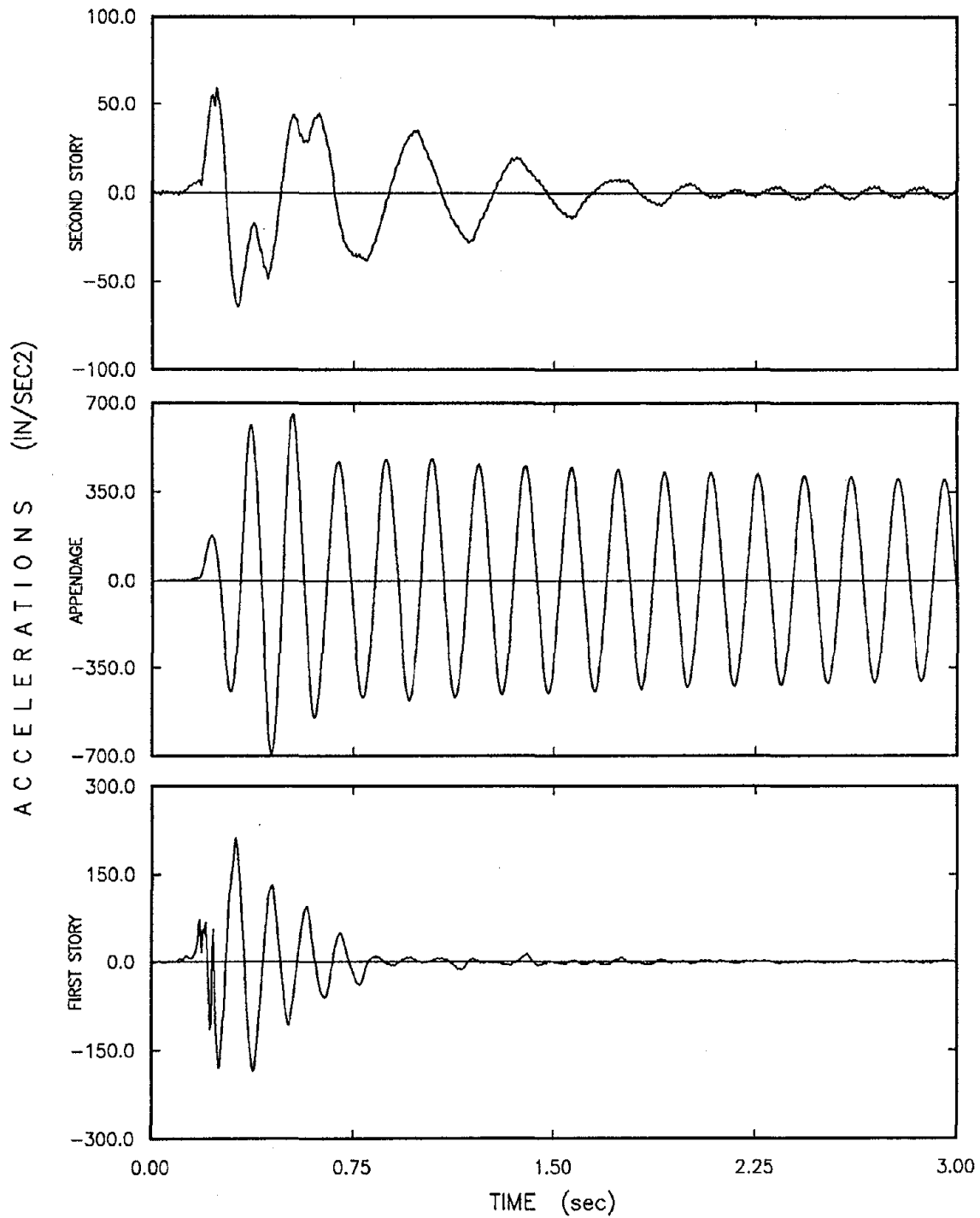


Figure 5.74 Typical Measured Free Vibrations Accelerations of the Combined Two-Story Structure M2 and Appendage AS3 Mounted on the First Story

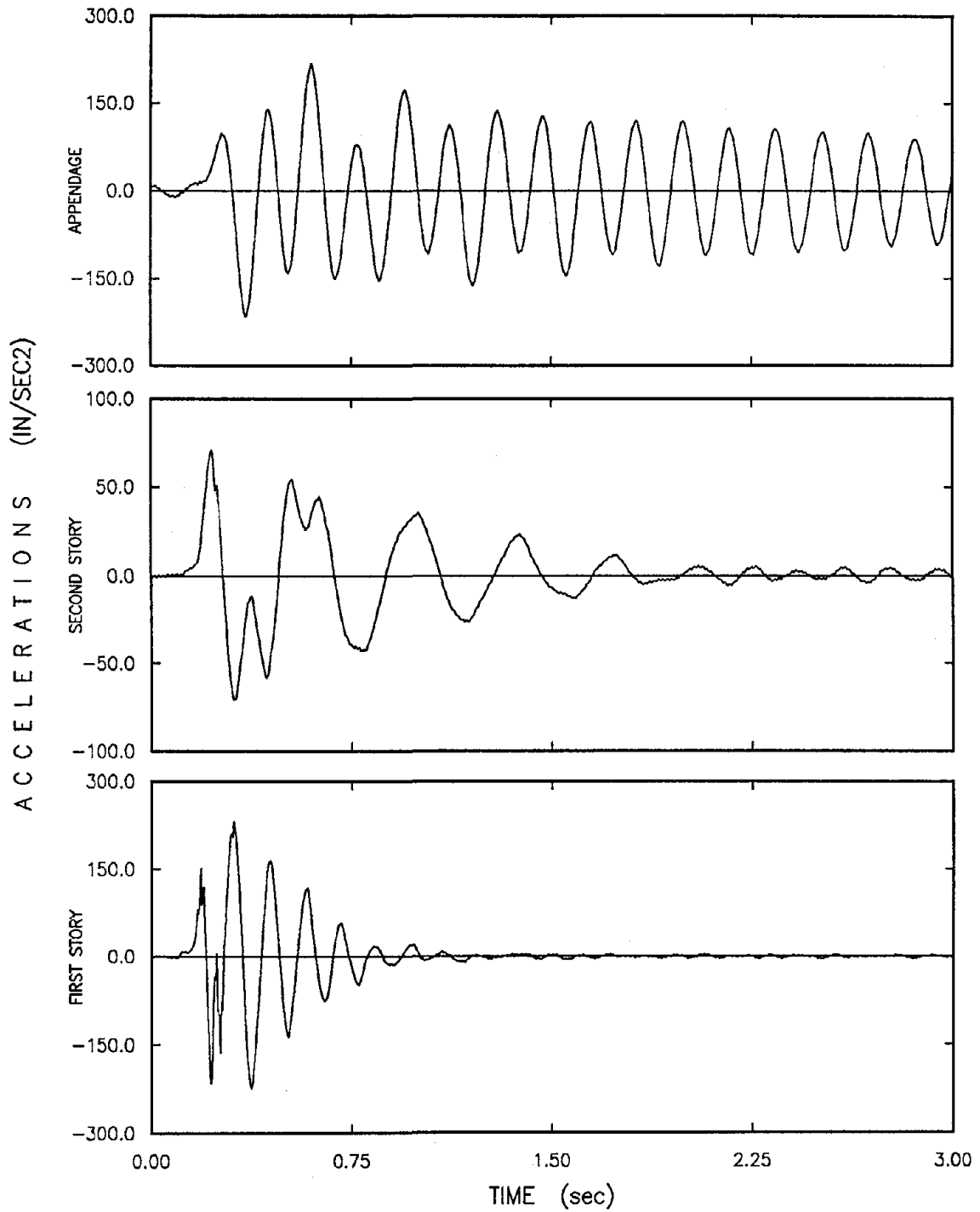


Figure 5.75 Typical Measured Free Vibrations Accelerations of the Combined Two-Story Structure M2 and Appendage AS3 Mounted on the Second Story

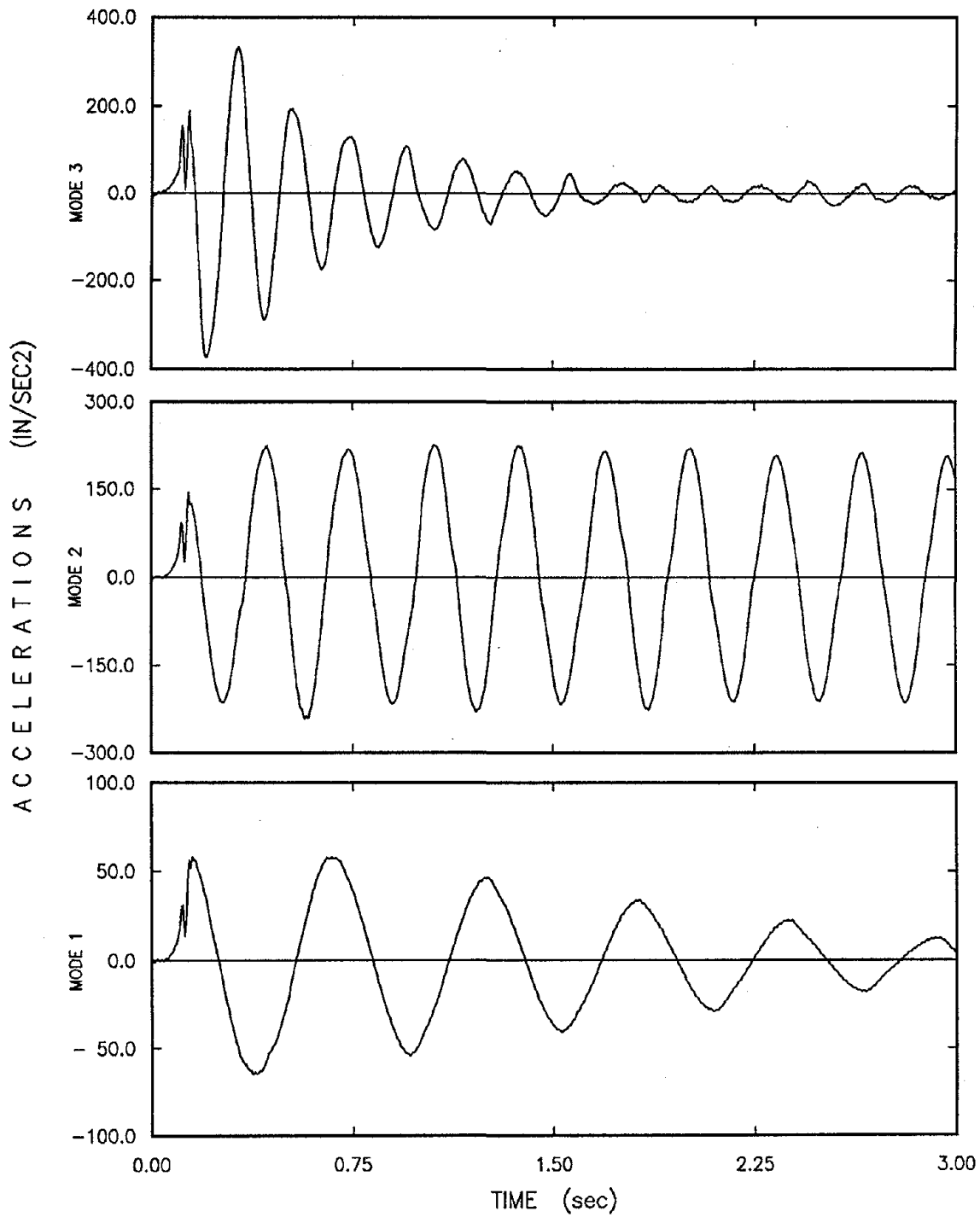


Figure 5.76 Typical Free Vibrations Modal Accelerations of the Combined Two-Story Structure M1 and Appendage AS2 Mounted on the Second Story

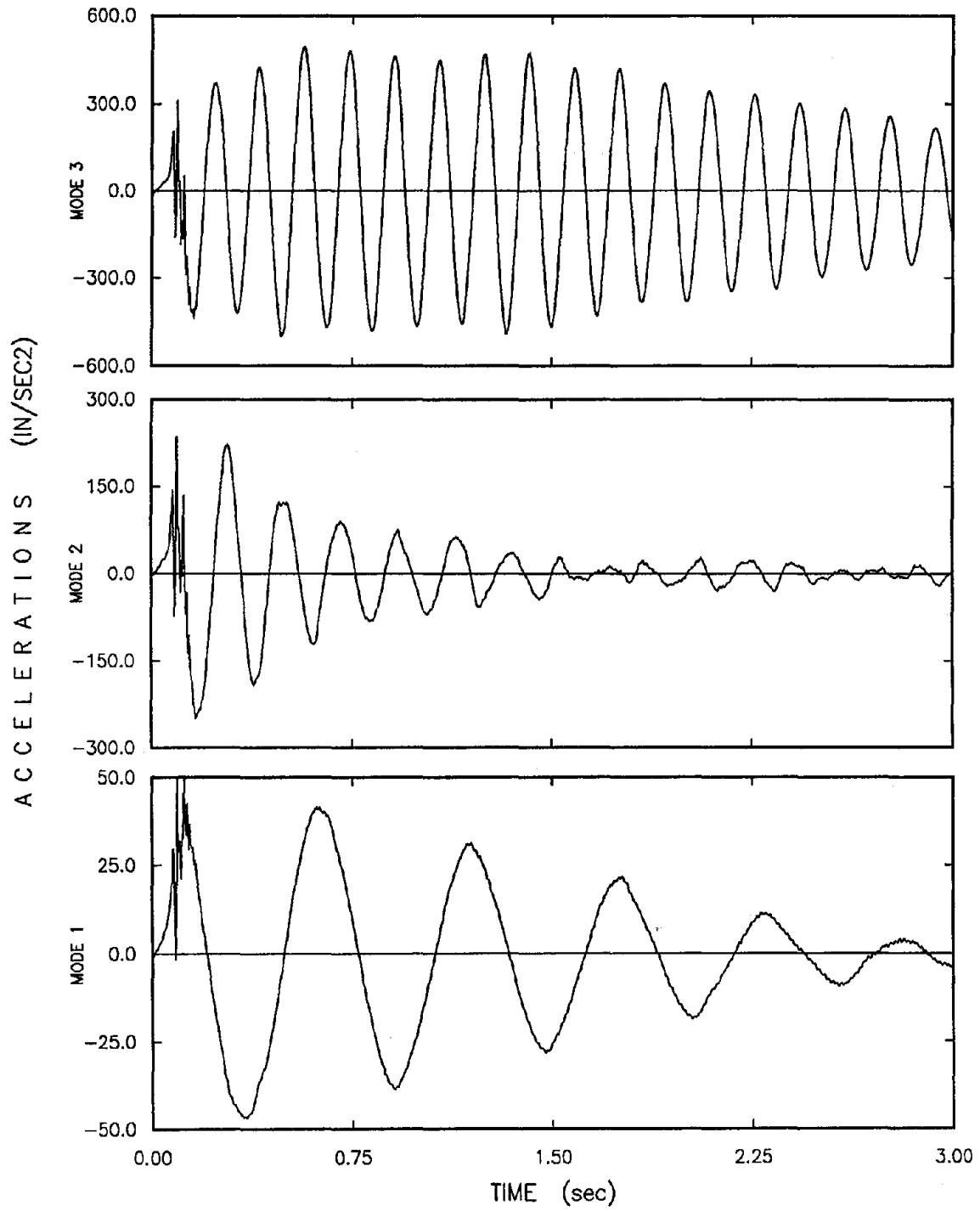


Figure 5.77 Typical Free Vibrations Modal Accelerations of the Combined Two-Story Structure M1 and Appendage AS3 Mounted on the First Story

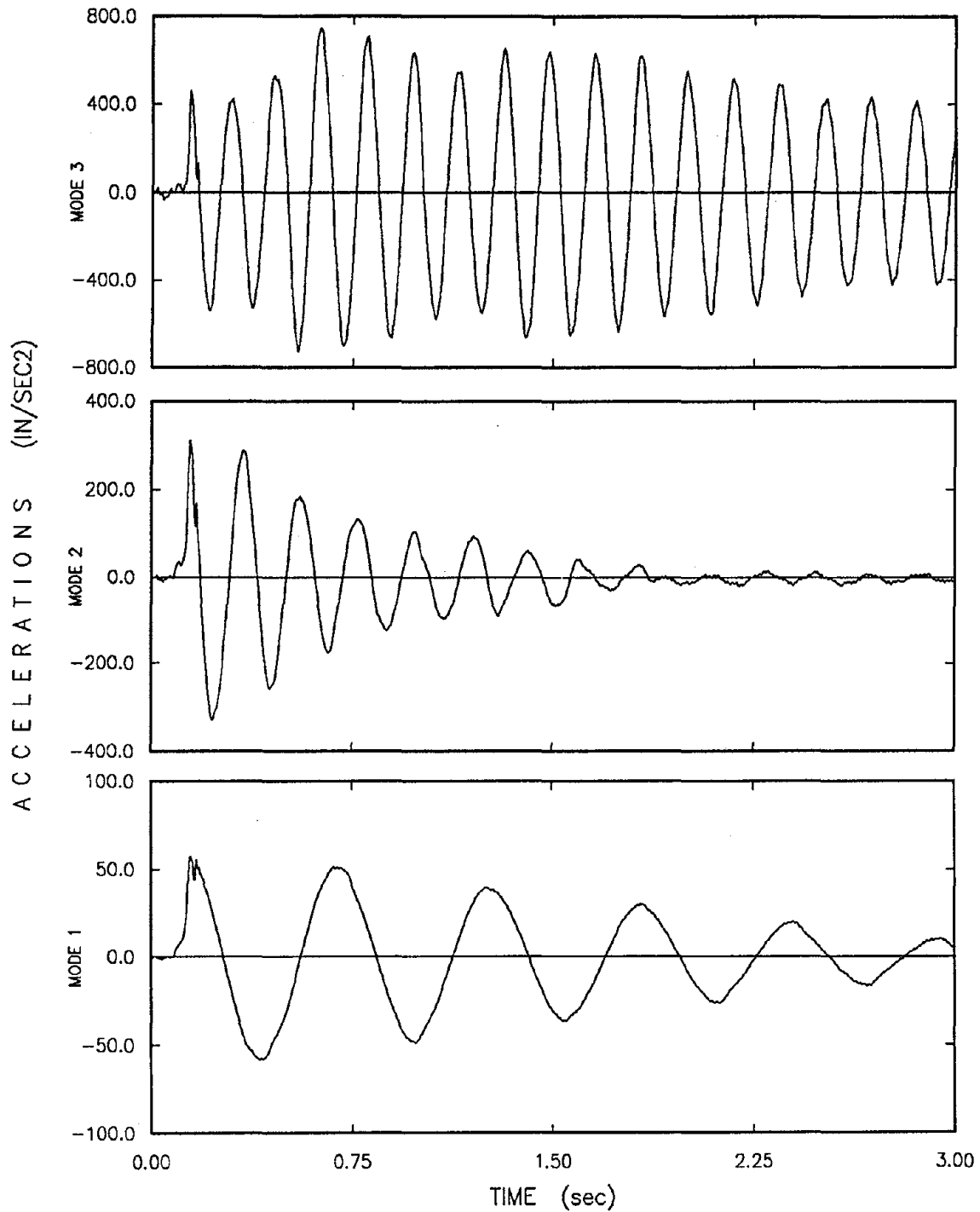


Figure 5.78 Typical Free Vibrations Modal Accelerations of the Combined Two-Story Structure M1 and Appendage AS3 Mounted on the Second Story

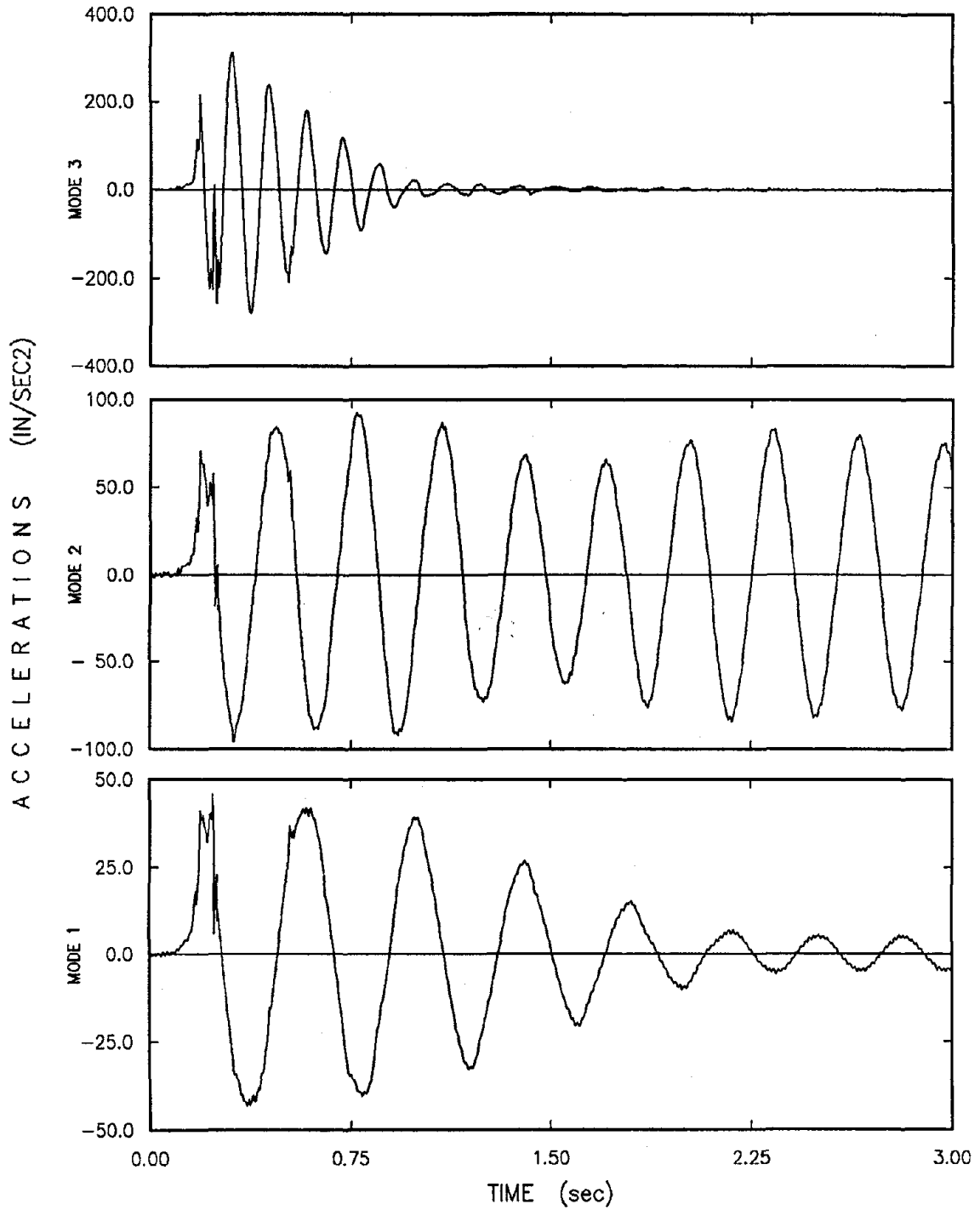


Figure 5.79 Typical Free Vibrations Modal Accelerations of the Combined Two-Story Structure M2 and Appendage AS2 Mounted on the Second Story

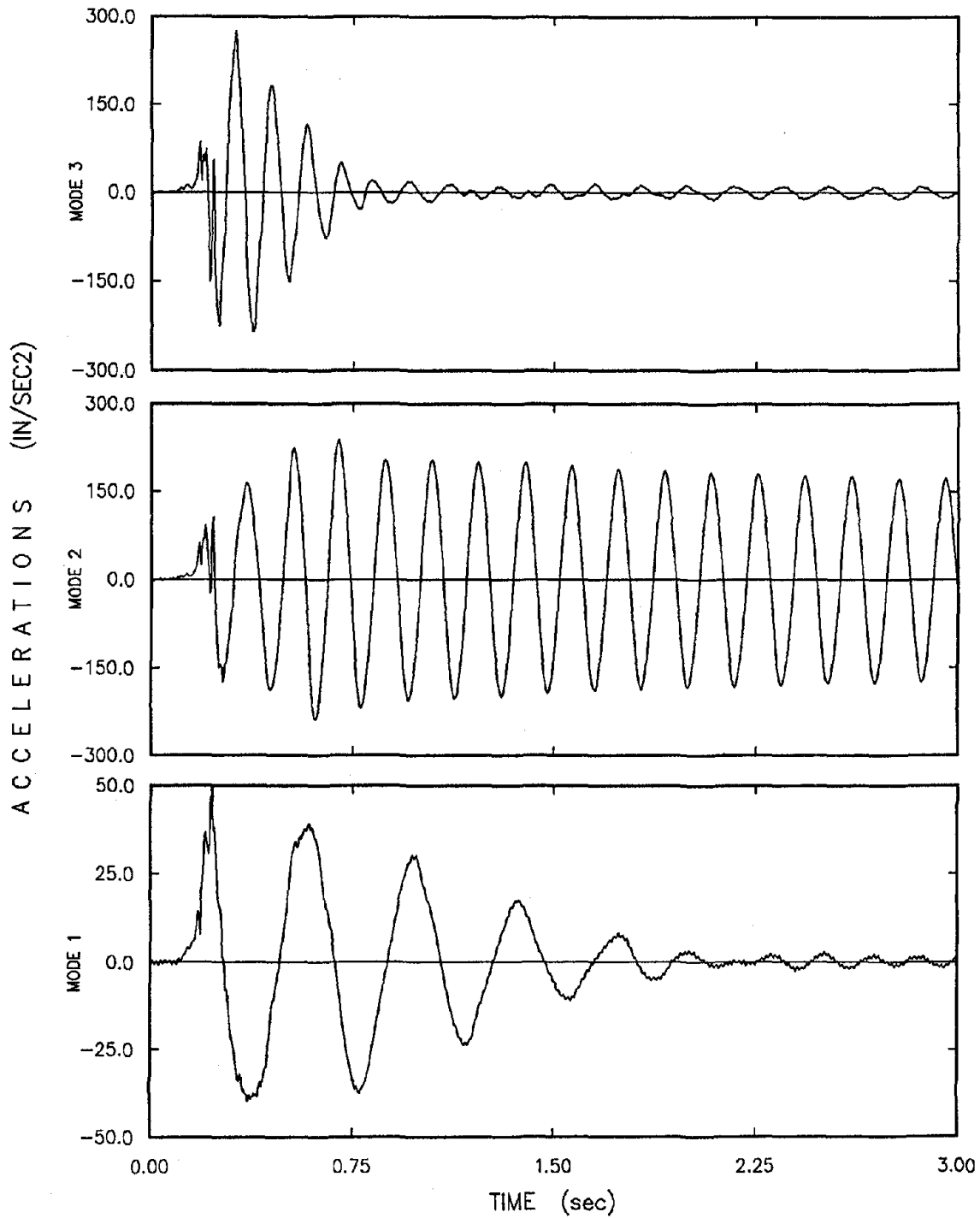


Figure 5.80 Typical Free Vibrations Modal Accelerations of the Combined Two-Story Structure M2 and Appendage AS3 Mounted on the First Story

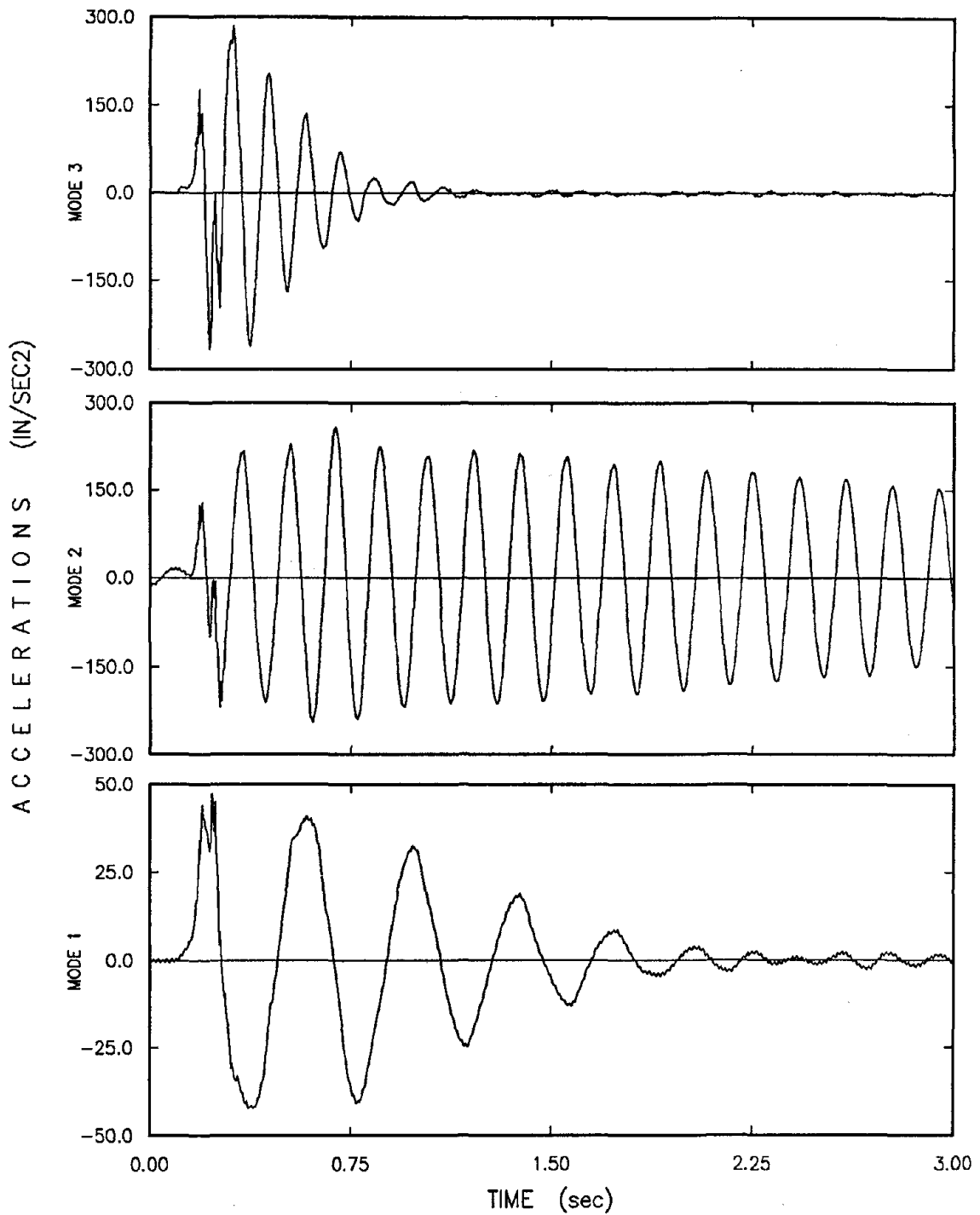


Figure 5.81 Typical Free Vibrations Modal Accelerations of the Combined Two-Story Structure M2 and Appendage AS3 Mounted on the Second Story

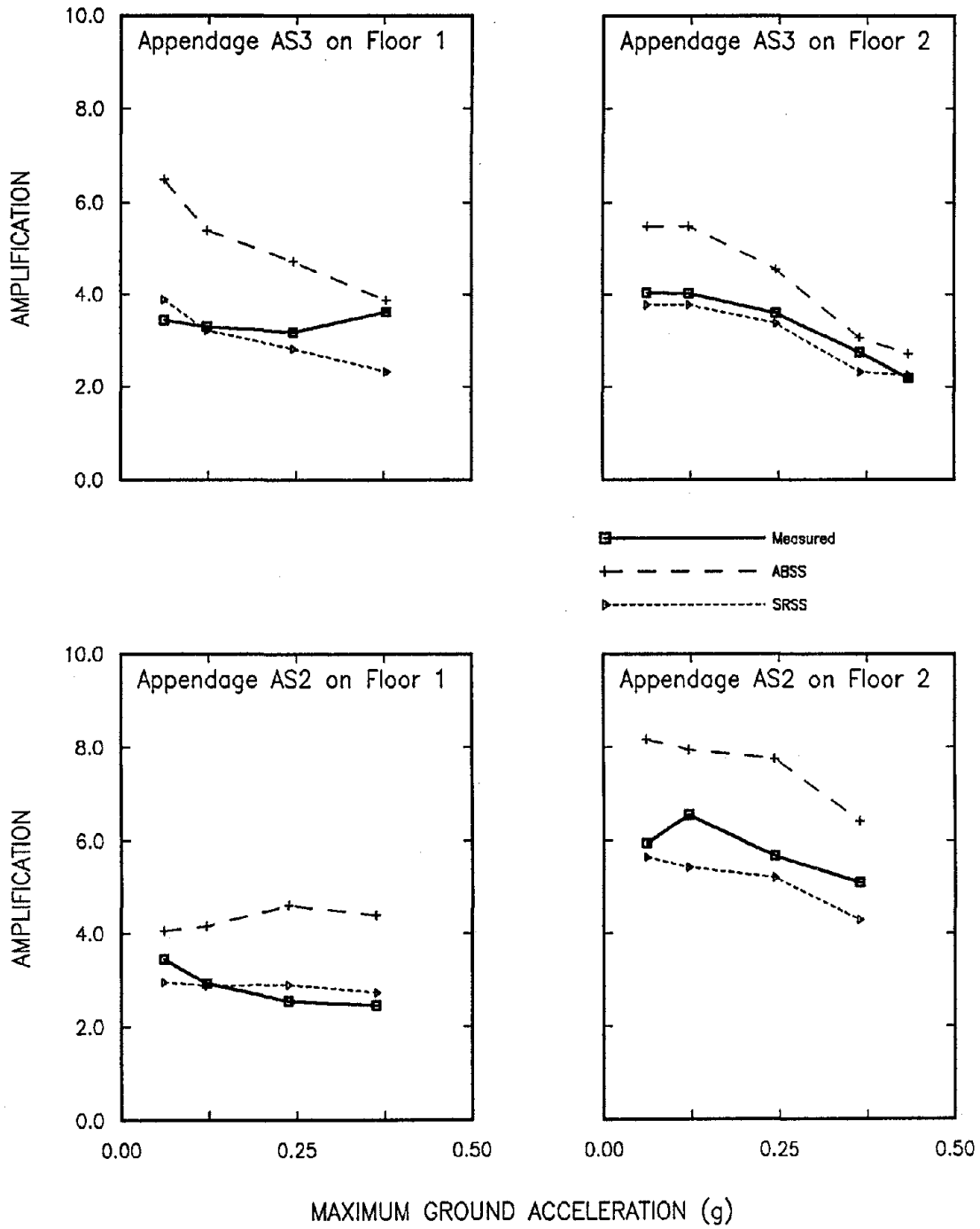


Figure 5.82 Comparison of Measured and Calculated Appendage Amplifications. Appendages on Two-Story Structure M1 Subjected to El Centro Earthquake

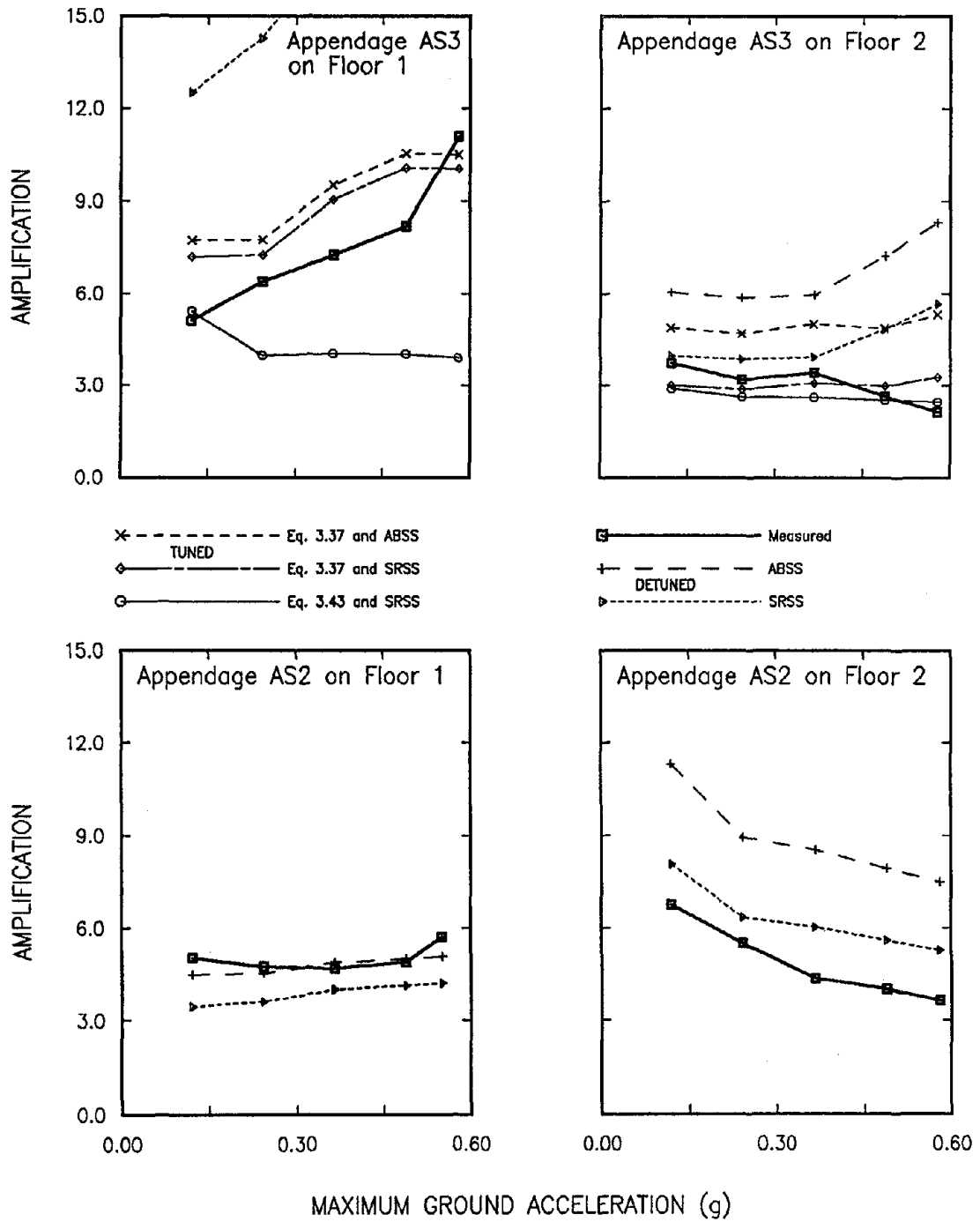


Figure 5.83 Comparison of Measured and Calculated Appendage Amplifications. Appendages on Two-Story Structure M2 Subjected to El Centro Earthquake

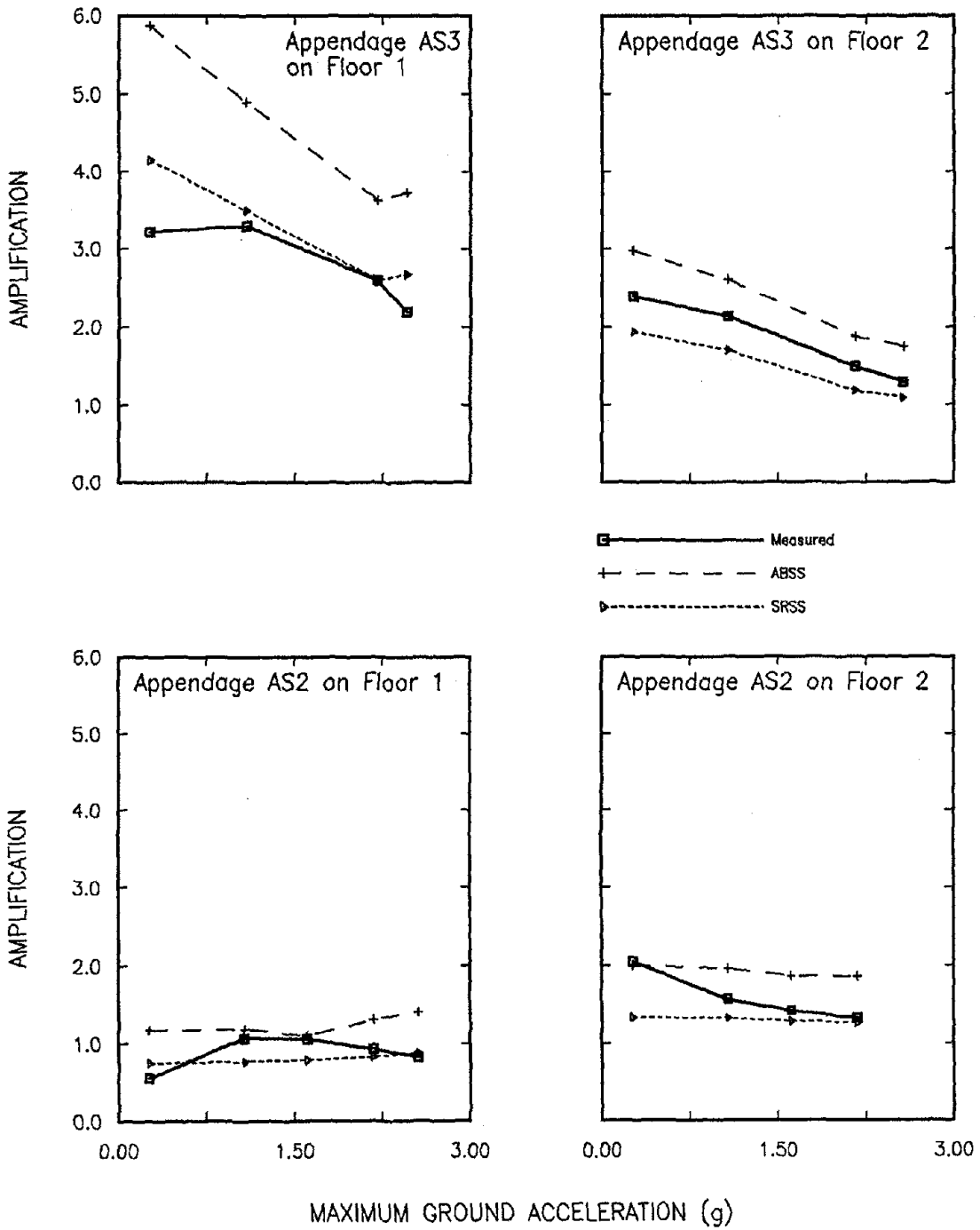


Figure 5.84 Comparison of Measured and Calculated Appendage Amplifications. Appendages on Two-Story Structure M1 Subjected to Melendy Earthquake

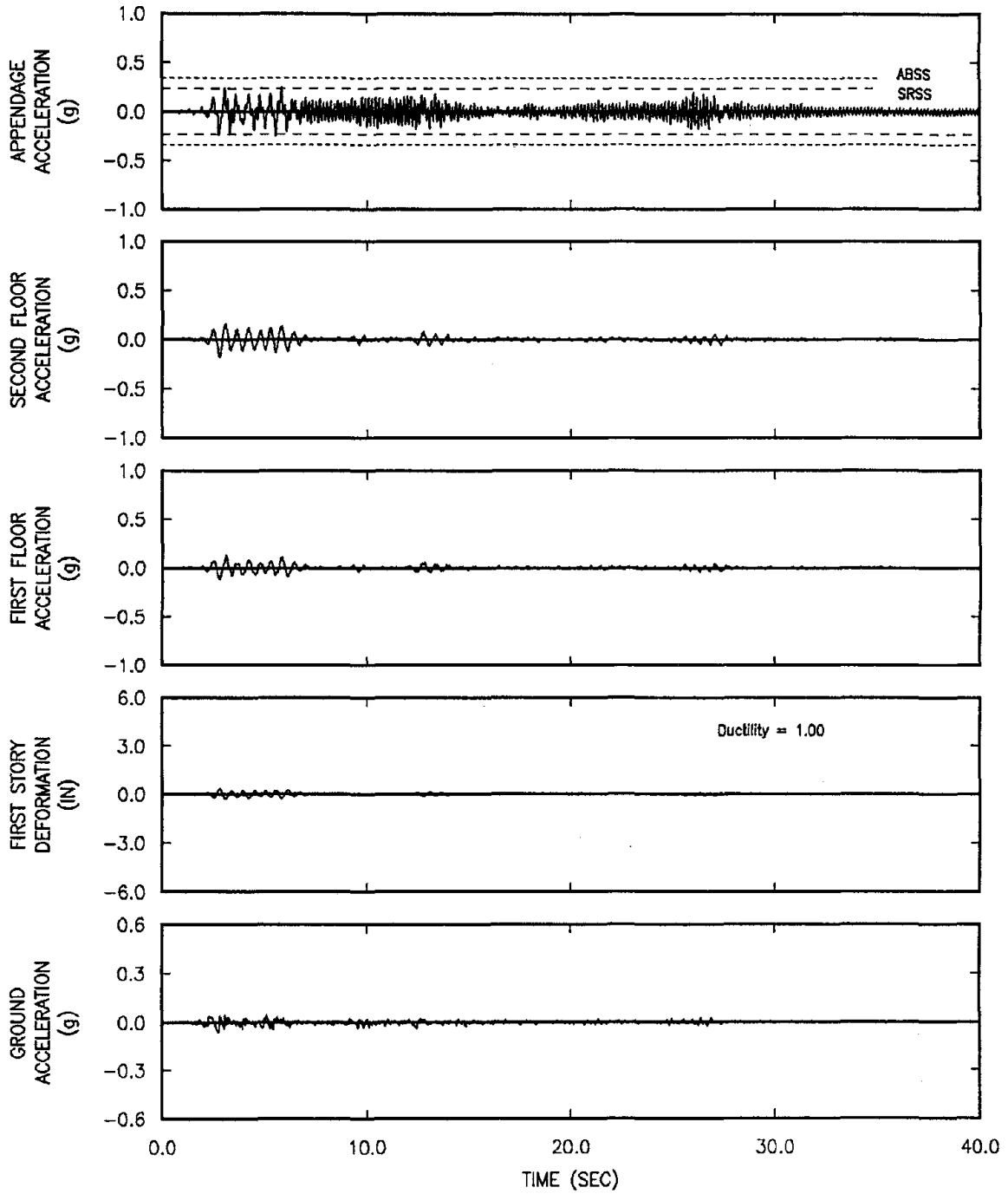


Figure 5.85 Measured Response of a Combined System. Appendage AS3 Mounted on the Second Floor of Structure M1 Subjected to El Centro Earthquake. First Story Ductility = 1.00

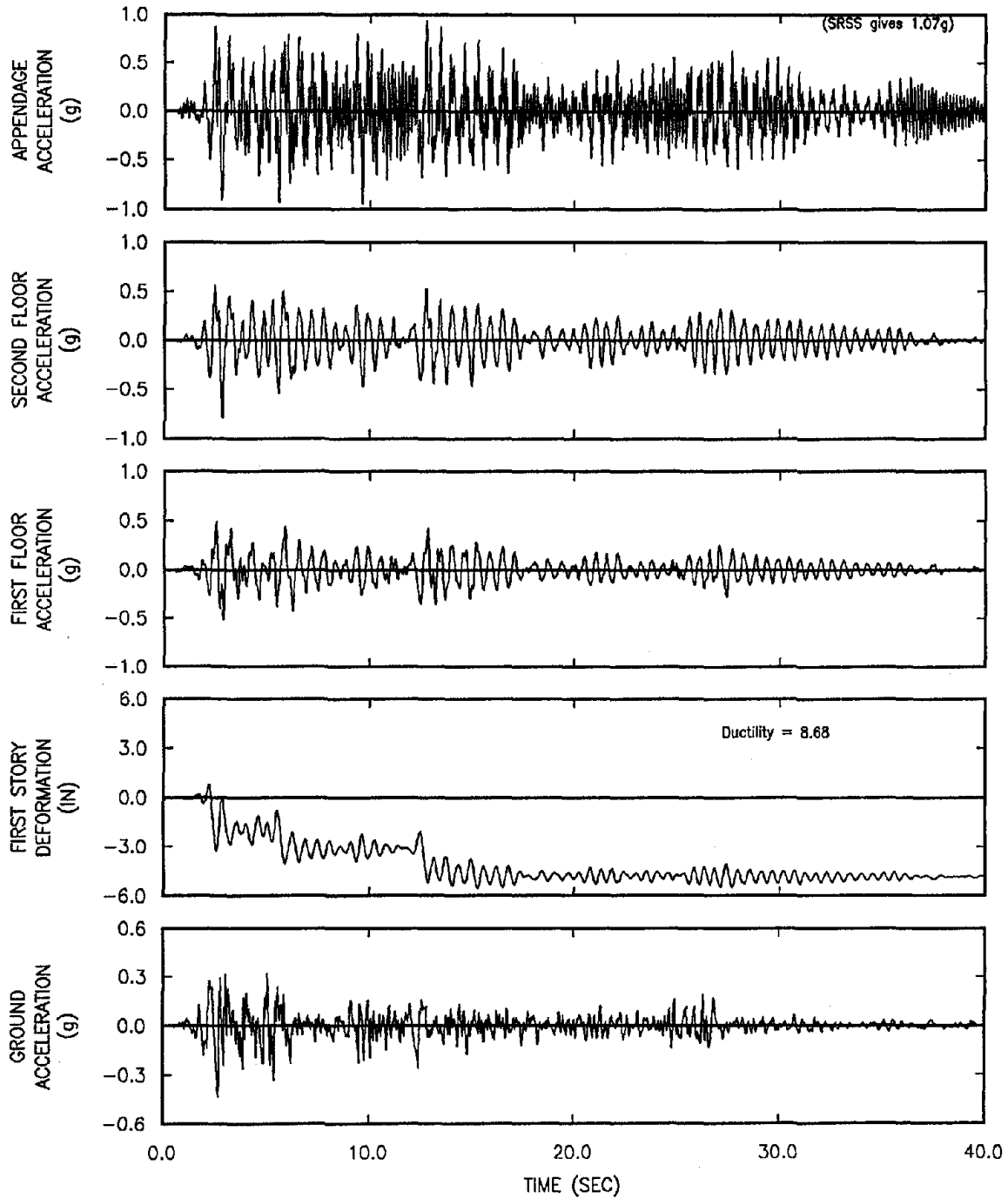


Figure 5.86 Measured Response of a Combined System. Appendage AS3 Mounted on the Second Floor of Structure M1 Subjected to El Centro Earthquake. First Floor Ductility = 8.68

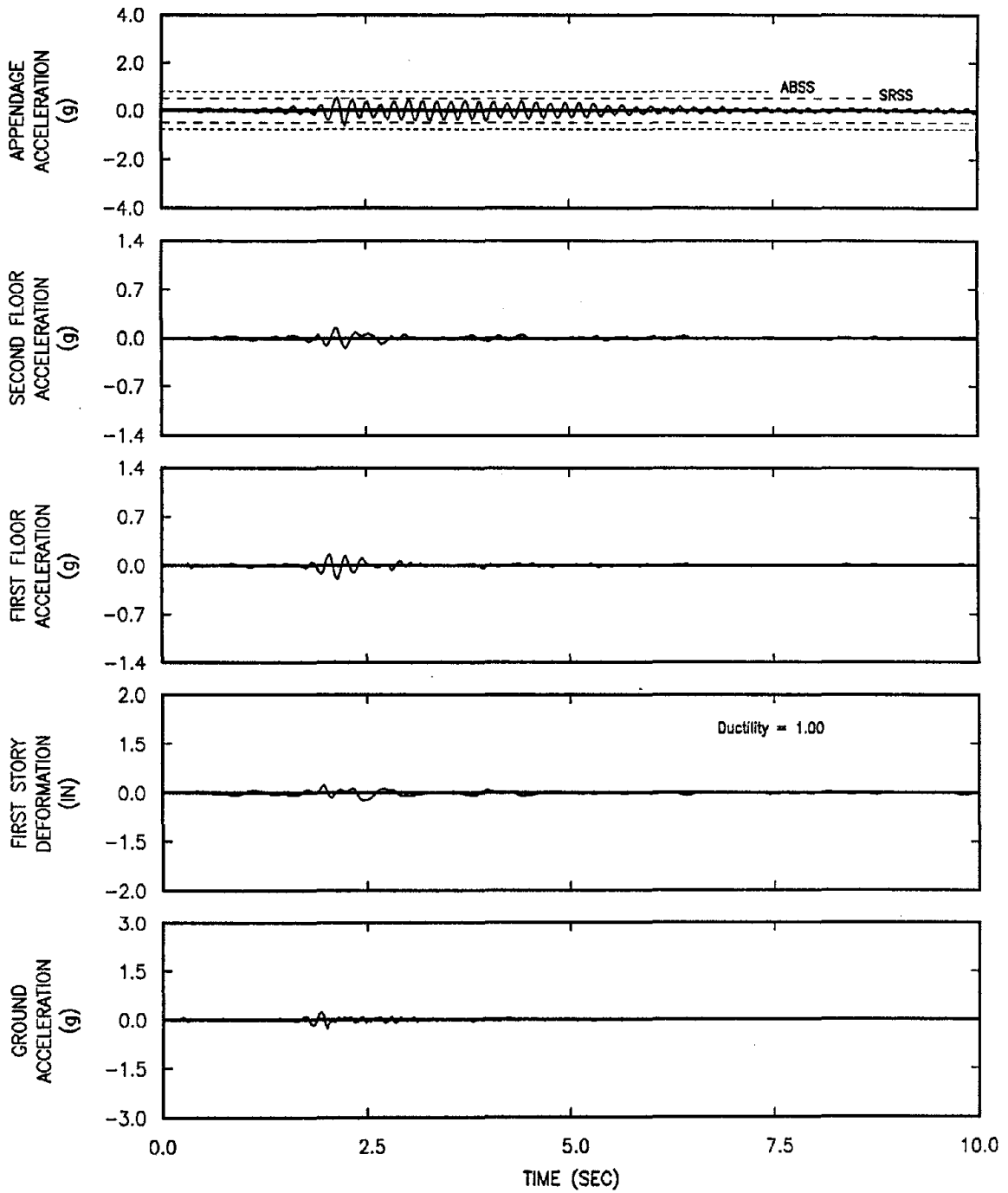


Figure 5.87 Measured Response of a Combined System. Appendage AS3 Mounted on the Second Floor of Structure M1 Subjected to Melendy Earthquake. First Floor Ductility = 1.00

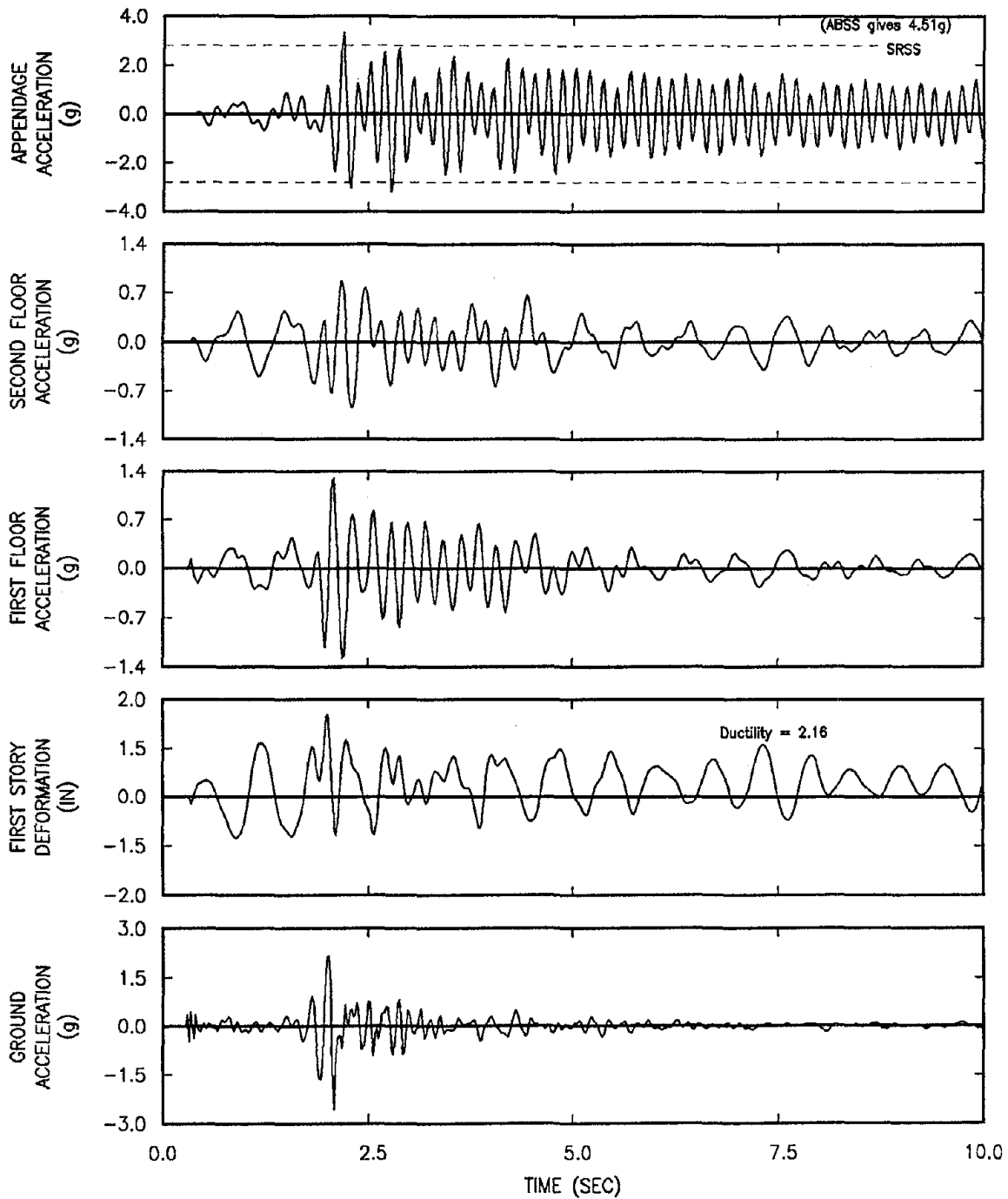


Figure 5.88 Measured Response of a Combined System. Appendage AS3 Mounted on the Second Floor of Structure M1 Subjected to Melendy Earthquake. First Floor Ductility = 2.16

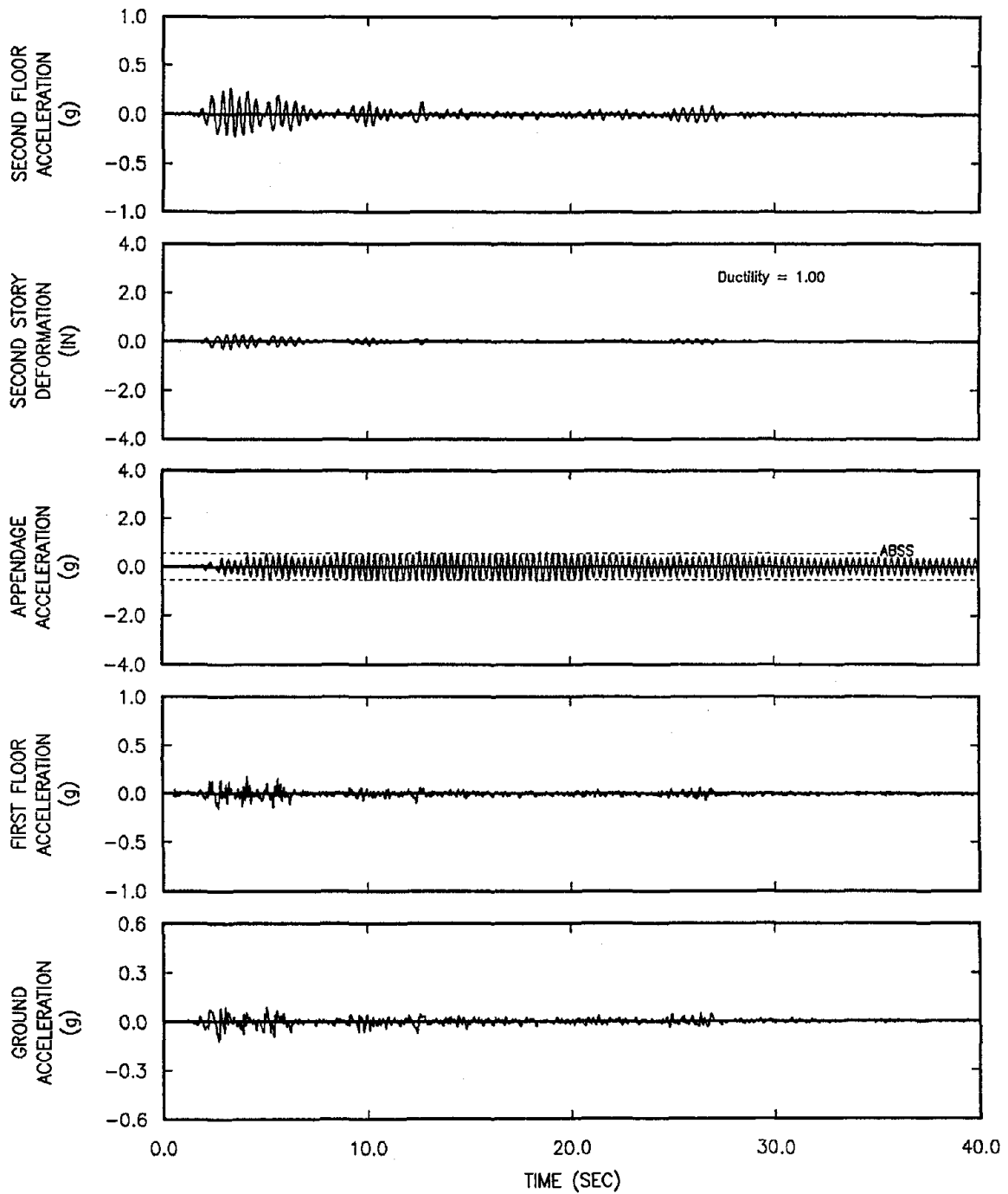


Figure 5.89 Measured Response of a Combined System. Appendage AS2 Mounted on the First Floor of Structure M2 Subjected to E1 Centro Earthquake. Second Floor Ductility = 1.00

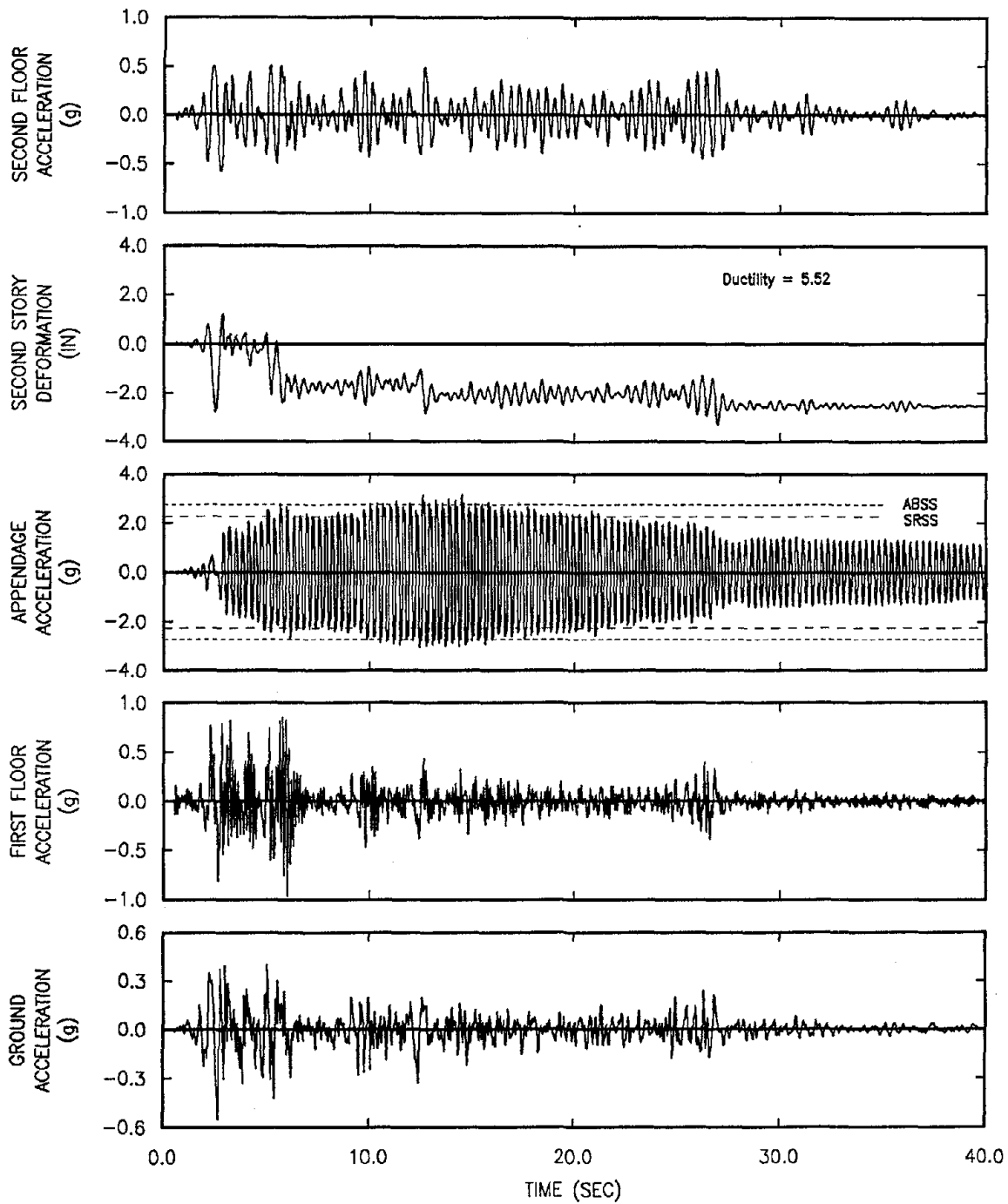


Figure 5.90 Measured Response of a Combined System. Appendage AS2 Mounted on the First Floor of Structure M2 Subjected to El Centro Earthquake. Second Floor Ductility = 5.52

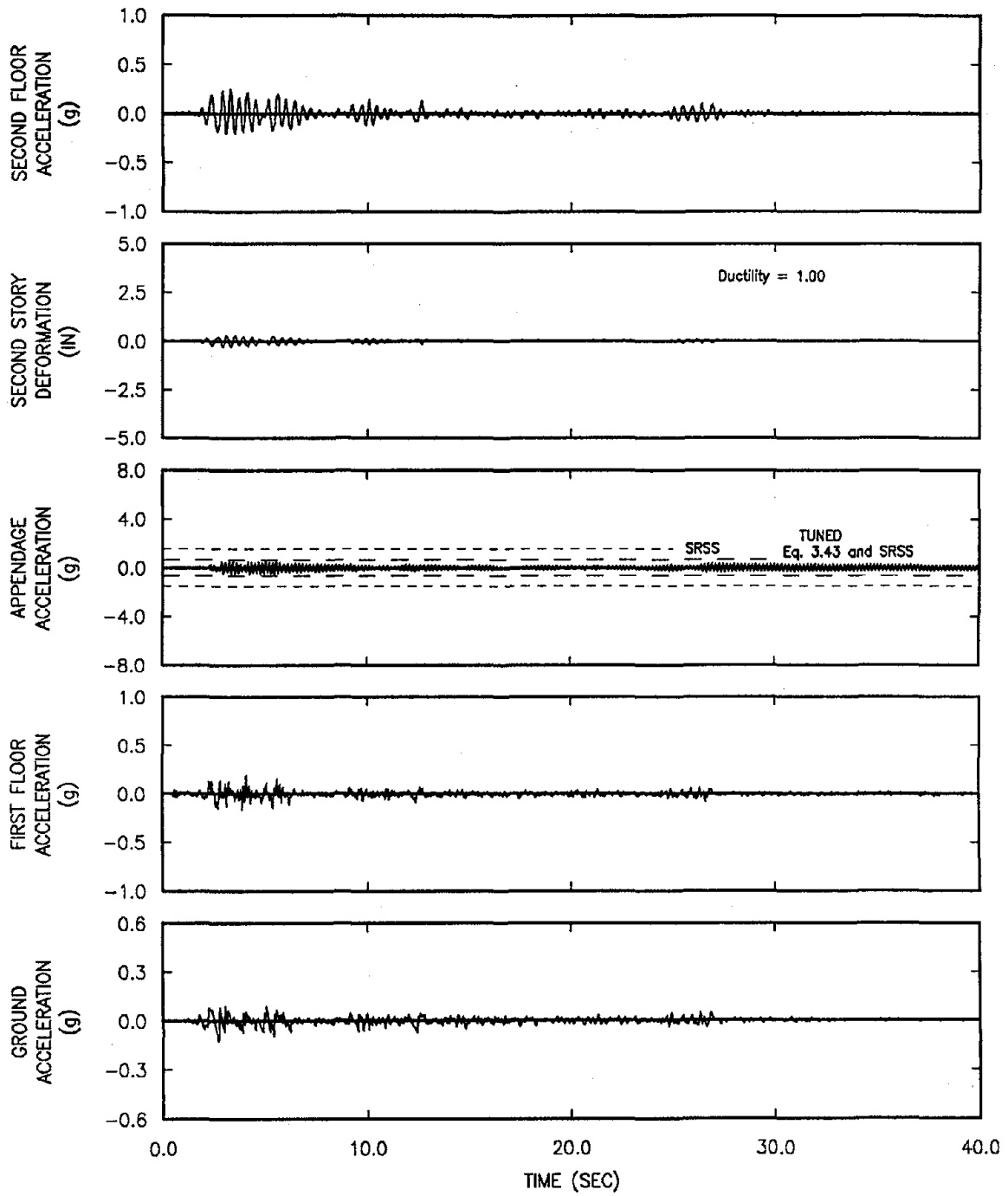


Figure 5.91 Measured Response of a Combined System. Appendage AS3 Mounted on the First Floor of Structure M2 Subjected to El Centro Earthquake. Second Floor Ductility = 1.00

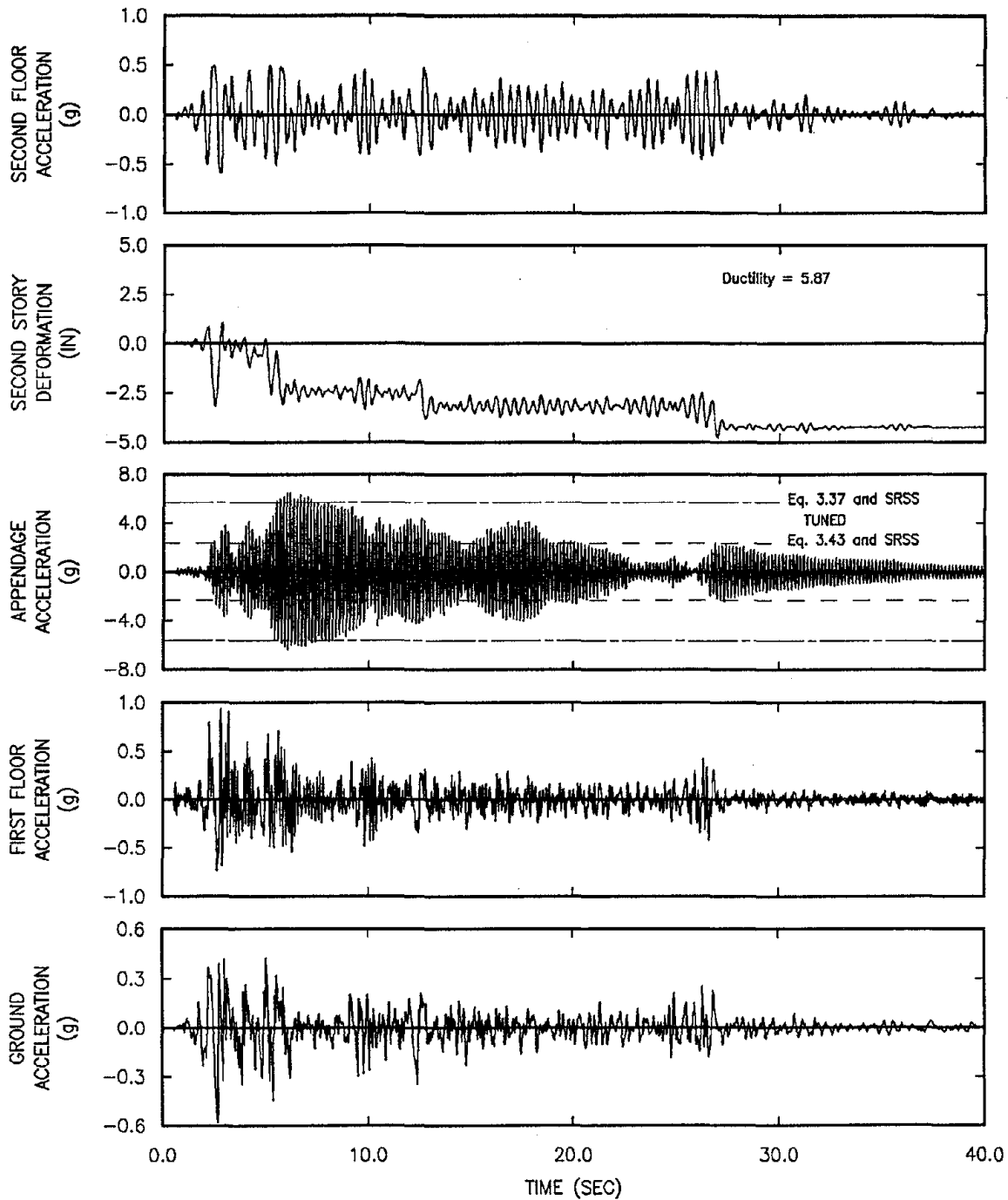


Figure 5.92 Measured Response of a Combined System. Appendage AS3 Mounted on the First Floor of Structure M2 Subjected to El Centro Earthquake. Second Floor Ductility = 5.87

LIST OF REFERENCES

1. ASCE, "Structural Analysis and Design of Nuclear Plant Facilities," ASCE Manuals and Reports on Engineering Practice - No. 58, 1980.
2. ASCE Standard, "Seismic Analysis of Safety-Related Nuclear Structures and Commentary on Standard for Seismic Analysis of Safety-Related Nuclear Structures," ASCE 4-86, September 1986.
3. Asfura A. and Der Kiureghian A., "A New Floor Response Spectrum Method for Seismic Analysis of Multiply Supported Secondary Systems," Report No. UCB/EERC-84/04, University of California, Berkeley, Ca., June. 1984.
4. Biggs J. M., "Seismic Response Spectra for Equipment Design in Nuclear Power Plants," Proceeding of the 1st International Conference on Structural Mechanics in Reactor Technology, Berlin, Germany, Sept. 1971.
5. Biggs J. M. and Roesset J. M., "Seismic Analysis of Equipment Mounted on a Massive Structure," in Seismic Design for Nuclear Power Plants, R.J. Hansen editor, M.I.T. Press, Cambridge 1970.
6. Clough R. W. and Penzien J., Dynamics of Structures, McGraw-Hill Book Co., 1975.
7. Coats D. W., "Recommended Revisions to Nuclear Regulatory Commission Seismic Design Criteria" Lawrence Livermore Laboratory Report NUREG/CR-1161 RD prepared for the U.S.N.R.C., May 1980.
8. Der Kiureghian A. Sackman J. L. and Kelly J. M., "Seismic Response of Multiply Supported Piping Systems," Transactions of the 5th International Conference on Structural Mechanics in Reactor Technology, Chicago Il., Aug. 1983.
9. Der Kiureghian A., Sackman J. L. and Nour-Omid B., "Dynamic Response of Light Equipment in Structures," Report No. UCB/EERC-81/05, University of California, Berkeley, Ca., April 1981.
10. Gupta A. K., "New Developments in Seismic Analysis of Primary and Secondary Systems," Proceeding of the Conference on Structural Engineering in Nuclear Facilities, ASCE, Raleigh, N.C., Sept. 1984.
11. Hadjian A. H., "a Reevaluation of Equivalent Linear Models for Simple Yielding structures," Earthquake Engineering & Structural Dynamics, Vol. 10, No.6, 1982.
12. Anagnostopoulos S. A., Haviland R. W. and Biggs J. M., "Use of Inelastic Spectra in Aseismic Design," Journal of the Structural Division, ASCE, Vol. 104, ST1, 1978.

13. Housner G. W., "Design Spectrum" in Earthquake Engineering, R.L. Wiegel editor, Prentice Hall 1970.
14. Igusa T. and Der Kiureghian A., "Dynamic Response of Multiply Supported Secondary Systems," Journal of the Engineering Mechanics Division, ASCE, 111, 1985.
15. Igusa T. and Der Kiureghian A., "Generation of Floor Response Spectra Including Oscillator-Structure Interaction," Earthquake Engineering & Structural Dynamics, Vol. 13, No.5, 1985.
16. Iwan W. D., "Estimating Inelastic Response Spectra from Elastic Response Spectra," Earthquake Engineering & Structural Dynamics, Vol. 8, No.4, 1980.
17. Kapur K. and Shao L. C., "Generation of Floor Response Spectra for Equipment Design," Proceedings of ASCE Specialty Conference on Structural Design of Nuclear Plant Facilities, Chicago, Il., December 1973.
18. Kawakatsu T., Kitade K., Takemori T., Kuwabara Y. and Ogiwara Y., "Floor Response Spectra Considering Elasto-Plastic Behavior of Nuclear Power Facilities," Proceedings of the 5th International Conference on Structural Mechanics in Reactor Technology, Volume K(b), Berlin, Germany, Aug. 1979.
19. Kelly M. J., "The Influence of Base Isolation on the Seismic Response of Light Equipment," Report No. UCB/EERC-81/17, University of California, Berkeley, Ca., February 1982.
20. Kennedy R. P., Short S. A., Kipp T. R., Bannon H., Tokarz F. J. and Merz K. I., "Engineering Characterization of Ground Motion - Task I: Effects of Characteristics of Free-Field Motion on Structural Response," Report SMA 12702.01, Structural Mechanics Associates, Newport Beach, Ca., February 1984.
21. Krawinkler H., Zohrei M., Lashkari-Irvani B., Cofie N. G. and Hadidi-Tamjed H., "Recommendations for Experimental Studies on the Seismic Behavior of Steel Components and Materials," Report No. 61, The John A. Blume Earthquake Engineering Center, Stanford University, Stanford, Ca., September 1983.
22. Kusainov A. A. and Clough R. W., "Alternatives to Standard Mode Superposition for Analysis of Non-Classically Damped Systems," Report No. UCB/EERC-88/09, University of California, Berkeley, Ca., June 1988.
23. Lai S. P., Biggs J. M. and Vanmarcke E. M., "On Inelastic Response Spectra for Aseismic Design," Publication No. R78-18, Department of Civil Engineering, MIT, Cambridge, Massachusetts, July 1978.

24. Lin J. and Mahin S. A., "Response of Subsystems on Inelastic Structures," Proceeding of the Conference on Structural Engineering in Nuclear Facilities, ASCE, Raleigh, N.C., Sept. 1984.
25. Lin J. and Mahin S., "Effect of Inelastic Behavior on the Analysis and Design of Earthquake Resistant Structures," Report No. UCB/EERC-85/08, University of California, Berkeley, Ca., June 1985.
26. Mahin S. and Lin J., "Construction of Inelastic Response Spectra for Single Degree of Freedom Systems," Report No. UCB/EERC-83/17, University of California, Berkeley, Ca., July 1983.
27. Manolis G. D., Juhn G. and Reinhorn A. M., "Experimental Investigation of Primary-Secondary System Interaction," Technical Report NCEER-88-0019, State University of New York at Buffalo, NY, May 27, 1988.
28. McCabe S. L. and Hall W. J., "Evaluation of Structural Response and Damage Resulting from Earthquake Ground Motion," Structural Research Series No. 538, University of Illinois, Urbana, Il., September 1987.
29. Nakhata T., Newmark N. M. and Hall W. J., "Approximate Dynamic Response of Light Secondary Systems," Structural Research Series No. 396, University of Illinois, Urbana, Il., March 1973.
30. Nelson F. C. and Greif R., "On the Incorporation of Damping in Large, General-Purpose Computer Programs," in Methods for Dynamic Structural Analysis, Compiled by T. A. Jaeger. International Seminar on Extreme Load Conditions and Limit Analysis Procedures for Structural Reactor Safeguards and Containment Structures, Berlin, September 1975.
31. Newmark N. M., "Current Trends in the Seismic Analysis and Design of High Rise Structures" in Earthquake Engineering, R.L. Wiegel editor, Prentice Hall 1970.
32. Newmark N. M., "Earthquake Response Analysis of Reactor Structures," Nuclear Engineering and Design 20 (1972).
33. Newmark N. M. and Hall W. J., "Development of Criteria for Seismic Review of Selected Nuclear Power Plants," NUREG-CR 0098, Sept. 1977.
34. Peters K. A., Schmitz D. and Wagner U., "Determination of Floor Response Spectra on the Basis of the Response Spectrum Method," Nuclear Engineering and Design, 44, 1977.
35. Roesset J., Whitman R. V. and Dobry R., "Modal Analysis for Structures with Foundation Interaction," Journal of the Structural Division, ASCE, Vol.99, No. ST3, March 1973.

36. Rothe D. H. and Sozen M. A., "A SDOF Model to Study Nonlinear Dynamic Response of Large and Small Scale R/C Test Structures," Structural Research Series No. 512, University of Illinois, Urbana, Il., Nov. 1983.
37. Ruzicka G. C. and Robinson A. R., "Dynamic Response of Tuned Secondary Systems," Structural Research Series No. 485, University of Illinois, Urbana, Il., Nov. 1980.
38. Sackman J. L. and Kelly J. M., "Rational Design Methods for Light Equipment in Structures Subjected to Ground Motion," Report No. UCB/EERC-78/19, University of California, Berkeley, Ca., Sept. 1978.
39. Sackman J. L. and Kelly J. M., "Equipment Response Spectra for Nuclear Power Plants Systems," Nuclear Engineering and Design 57 (1980).
40. Saïdi M. and Sozen M. A., "Simple and Complex Models for Nonlinear Seismic Response of Reinforced Concrete Structures," Structural Research Series No. 465, University of Illinois, Urbana, Il., Aug. 1979.
41. Sewell R. T., Cornell C. A., Toro G. R. and McGuire R. K., "A Study of Factors Influencing Floor Response Spectra in Nonlinear Multi-Degree-of-Freedom Structures," Department of Civil Engineering, Stanford University, Stanford Ca., Report No. 82, November 1986.
42. Shibata A. and Sozen M. A., "The Substitute-Structure Method for Earthquake-Resistant Design of Reinforced Concrete Frames," Structural Research Series No. 412, University of Illinois, Urbana, Il., Oct. 1974.
43. Singh M. P., "Generation of Seismic Floor Spectra," Journal of the Engineering Mechanics Division, ASCE, Vol.101, No. EM5, Oct. 1975.
44. Singh M. P., "Seismic Design Input for Secondary Systems," Journal of the Structural Division, ASCE, Vol.106, No. ST2, Febr. 1980.
45. Singh M. P. and Sharma A. M., "Floor Spectra for Nonclassically Damped Structures," Proceedings of the 5th Engineering Mechanics Division Specialty Conference, Laramie, Wy., Aug. 1984.
46. Singh M. P. and Wen Y. K., "Nonstationary Seismic Response of Light Equipment," Journal of the Engineering Mechanics Division, ASCE, Vol.103, No. EM6, Dec. 1977.
47. Srivastan S. and Nau J. M., "Seismic Analysis of Elastoplastic MDOF Structures," Journal of the Structural Engineering, ASCE, Vol. 114, No. 6, June 1988.

48. Tansirikongkol V. and Pecknold D. A., "Approximate Modal Analysis of Bilinear MDF Systems Subjected to Earthquake Motions," Structural Research Series No. 449, University of Illinois, Urbana, Il., Aug. 1978.
49. Thomson W. T., "Theory of Vibration with Applications," Prentice Hall Inc., Englewood Cliffs, N.J. 07632, 1981.
50. Thomson W. T., Calskin T. and Caravani P., "A Numerical Study of Damping," Earthquake Engineering & Structural Dynamics, Vol. 3, No. 1, 1974.
51. Tsushima Y., Jido J. and Mizuno N., "Analysis of Equations of Motion with Complex Stiffness Mode Superposition Method Applied to Systems with Many Degrees of Freedom," in Methods for Dynamic Structural Analysis, Compiled by T. A. Jaeger. International Seminar on Extreme Load Conditions and Limit Analysis Procedures for Structural Reactor Safeguards and Containment Structures, Berlin, September 1975.
52. Veletsos A. S. and Ventura C. E., "Modal Analysis of Non-Classically Damped linear Systems," Earthquake Engineering & Structural Dynamics, Vol. 14, No. 2, 1986.
53. Villaverde R. and Newmark N. M., "Seismic Response of Light Attachments to Buildings," Structural Research Series No. 469, University of Illinois, Urbana, Il., Febr. 1980.
54. Villaverde R., "Response Spectrum Method for the Analysis of Nonlinear Multistory Structures," Proceedings of the Eighth World Conference on Earthquake Engineering, San Francisco, Ca., July 1984.
55. Whitman R. V., "Soil Structure Interaction," in Seismic Design for Nuclear Power Plants, R.J. Hansen editor, M.I.T. Press, Cambridge 1970.
56. Whitman R. V., Christian J. T. and Biggs J. M., "Parametric Analysis of Soil Structure Interaction for a Reactor Building," Proceedings of the 1th International Conference on Structural Mechanics in Reactor Technology, Berlin, Germany, September 1971.
57. Yang J. N., Sarkani S. and Long F. X., "Modal Analysis of Nonclassically Damped Structural Systems Using Canonical Transformation," Technical Report NCEER-87-0019, State University of New York at Buffalo, NY, Sept. 1987.
58. Zahrah T. F. and Hall W. J., "Seismic Energy Absorption in Simple Structures," Structural Research Series No. 501, University of Illinois, Urbana, Il., Febr. 1982.

